DEVELOPMENT AND APPLICATION OF COLORIMETRIC ASSAYS AND ELECTROCHEMICAL BIOSENSORS IN SEAFOOD SAFETY

Sandra Leonardo Benet

UNIVERSITAT ROVIRA i VIRGILI

Development and Application of Colorimetric Assays and Electrochemical Biosensors in Seafood Safety

SANDRA LEONARDO BENET

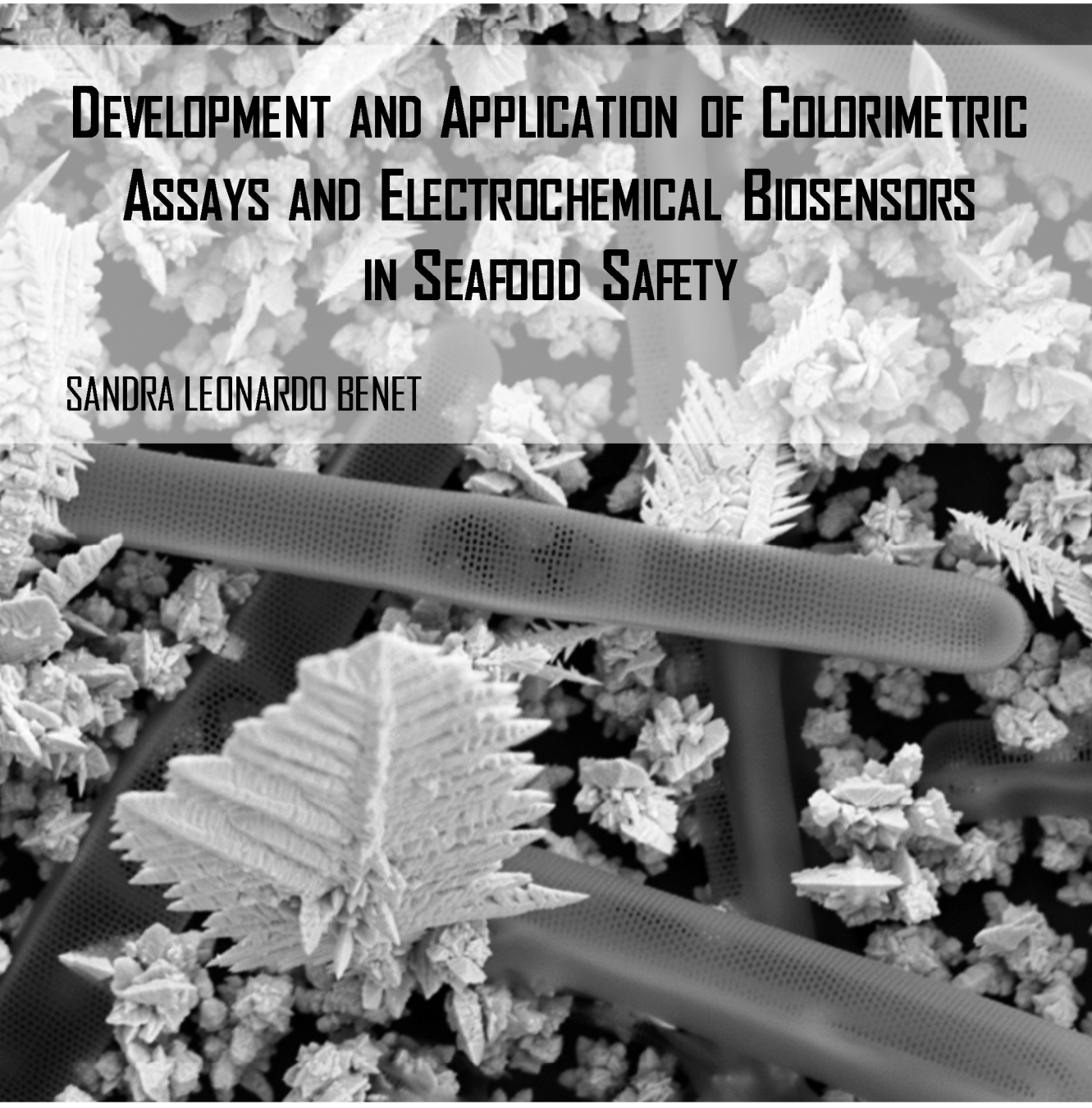

DOCTORAL THESIS 2018

Sandra Leonardo Benet

DEVELOPMENT AND APPLICATION OF COLORIMETRIC ASSAYS AND ELECTROCHEMICAL BIOSENSORS IN SEAFOOD SAFETY

DOCTORAL THESIS

Supervised by: Dr. Mònica Campàs

Co-supervised by: Dr. Ciara K. O'Sullivan

IRTA / Departament d'Enginyeria Química (URV)

Tarragona
2018

UNIVERSITAT ROVIRA i VIRGILI

I STATE that the present study, entitled **"Development and Appilcation of Colorimetric Assays and Electrochemical Biosensors in Seafood Safety"**, presented by **Sandra Leonardo Benet** for the award of the degree of Doctor, has been carried out under my supervision at the Department Chemical Engineernig of this university, and that it fulfils all the requirements to be eligible for the International Doctore Award.

Tarragona, 7th February 2018,

Dr. Mònica Campàs **Dr. Ciara K. O'Sullivan**

Acknowledgments

Abans de començar, agrair a la Universitat Rovira i Virgili i el Programa Martí i Franqués, a l'IRTA i Banc Santander per la beca otorgada per a la realització d'aquesta tesi.

Mai m'hagués imaginat que aquesta part fos de les més difícil d'escriure de tota la tesi, però no volia deixar passar l'oportunitat d'agrair a algunes de les persones que han fet que, directa o indirectament, avui pugui estar escrivint aquestes línies.

I no em queda altra que començar per **Mònica**. Perquè tot i que aquest treball porti el meu nom, tots sabem que res hagués estat possible sense tu. Perquè he aprés tan de tu... Gràcies per la teva confiança, la teva sinceritat, la teva guia constant, per buscar i sempre trobar les paraules més adequades en cada moment, per sentir i viure el que fas, per transmetre-ho en tantes ganes i alegria que ningú es pot quedar indiferent. De veritat, mil gràcies per aquesta oportunitat. M'han quedat moltes coses encara per aprendre, però m'emporto un sac ben ple gràcies a tu! (i l'esperança de que el temps em deixi omplir-ne molts més).

Agrair també a **Ciara**, la meva altra directora de tesi des d'una mica més a la distància. Gracias por tu apoyo, por encontrar siempre unas palabras agradables y celebrar todos los logros (¡te debo un brindis!). Gràcies a tota la gent de l'**IRTA**, sempre disposada a gaudir d'un bon esmorzar. Al grup de la **SMM**, pels vostres "quan acabes?" i per ajudar-me quan ha fet falta per a que pugui acabar, però també per les xerradetes pels passadissos que sempre fan la feina més alegre i agradable. A **Vane**, perquè he trobat a faltar el teu nervi i la teva alegria característica, gràcies per sempre preocupar-te de com anava tot. A **Jorge**, pels viatges de congressos i reunions, i perquè tot i que parli poc, tinc que agrair-te pel teu interès, les oportunitats brindades i la teva visió més "one health" de les coses. Gràcies, de veritat.

Com no, a les **Biosensors Girls**! A **Diana**, porque tu recibimiento fue tan bueno que ya no me quise marchar. Por la herencia que me dejaste, ya ves que las diatomeas me han hecho luchar pero también disfrutar mucho. Y porque ahora me toca desearte a mi lo mejor en esta nueva aventura que empiezas. A **Laia**, un altre pilar indispensable en aquesta etapa, que m'has acompanyat des del principi fins al final, i tot i que no et perdonaré mai que deixessis la taula de detràs buida, estic molt feliç de que tinguis un bon motiu per fer-ho! Saps que no trobaré les paraules per agrair-te per sempre estar allí, per ajudar-me tant i compartir molts bons moments. M'emporto una gran amiga, i això no té preu. ROC is loading... i tenim moltes ganes de coneixe'l!! I a **Anna**, sento molt dir-t'ho però a partir d'ara ja passaràs a ser la següent... és dur, però es supera, i tu ho faràs més que bé! Disfruta del que et queda, perquè ara ve el millor. Gràcies simplement per ser com ets. Puc dir ben orgullosa i contenta que he tingut el millor grup de treball que qualsevol pugui tenir!

A les meves altres companyes de despatx... per les converses i bons moments, per aguantar les vibracions freqüents del mòbil sense queixar-vos i per estar sempre allí per

desfogar-mos o celebrar qualsevol cosa. A **Olga**, per estar sempre "on fire max" i ensenyar-me a cuidar les diatomees quan jo pràcticament no sabia ni que eren. A **Elvira**, per tenir sempre a punt alguna paraula subtil per fer-nos riure. A **Àngels**, per deixar-me envair la teva taula i compartir la meva última etapa de la tesi i la teva primera... (tot i que la teva ràpida desesperació de vegades podria haver semblat al revés!). Ànims i calma, que encara queda temps! Ah! I a **Carme**, que tot i la paret al mig, ha estat una més del despatx! Gràcies pels teus massatgets, entre moltes altres coses.

A **Bea**, per donar-me la oportunitat de conèixer un altre centre, un altre grup de treball i un altre país, tot ben diferent del que havia vist abans. Moltes, moltes gràcies! A **Marc**, pels teus dibuixos tan bonics, però també per ensenyar Adelaida a Òscar i fer-nos riure tant amb les teves explicacions i traduccions com la de "Barcelona Little". A **Sandra** i **Xavi**, per acollir-nos tan i tan bé! Ara que ja esteu de volta, no teniu excusa per venir a fer una paelleta!

A la meua **maitasuna**, perquè som molt difícils de vore, però sempre estàs a prop. Gràcies per compartir les nostres il·lusions. A **Maria**, gràcies per perdonar les meves absències, però sobretot gràcies pels teus "caferets" i soparets, que encara que no hagin estat tots els que hagués volgut, han estat sempre acompanyats d'unes molt bones converses. I a **Cinta** i a **Gerard**, per les escapadetes i sopars, i per deixar-me dormir al vostre sofà!

A **Iván**, **Núria**, **Biel** i **Júlia**. A **Francisco** i **Margarita**, gràcies per estar sempre. A **JJ**, pels teus: "éts un crek". A mi **amatxu**, por cuidarme tanto y estar siempre orgullosa de mi, incluso sin entender lo que hago. I a **Òscar**, perquè només tu pots saber perquè.

Table of contents

Summary

In recent years, the increased consumption of seafood products has put great pressure on efficient monitoring and management programs to protect consumer's health and avoid economic losses to the shellfish industry. This thesis aims to contribute to both the development and applicability of colorimetric assays and electrochemical biosensors for the detection of marine toxins and biogenic amines, paving the way towards the implementation of low-cost, simple and reliable devices for seafood safety purposes. Since the immobilisation of the biorecognition molecule or antigen on the support plays a crucial role in the development of biochemical devices, different immobilisation strategies are explored. Thus, self-assembled monolayers (SAMs) are used as building blocks in the development of colorimetric immunoassays for the detection of okadaic acid-group toxins and tetrodotoxins. The SAM-based immunoassays for the detection of okadaic acid are applied to the analysis of seawater samples for monitoring purposes, while the immunoassays for the detection of tetrodotoxins are used in the analysis of shellfish and human urine samples derived from a puffer fish poisoning incident. Colorimetric and electrochemical immunoassays as well as immunosensors for the detection of azaspiracids are achieved by the immobilisation of the antibody by means of bioaffinity interactions on electrodes or using magnetic beads as immobilisation supports. Their use as powerful screening tools to monitor the presence of these toxins in mussels is demonstrated. Magnetic beads are also exploited as immobilisation supports in the development of electrochemical biosensors for the detection of biogenic amines. In this case, magnetic beads are used as enzyme immobilisation supports and the enzyme biosensors are applied to the determination of biogenic amines in naturally spoiled fish. Furthermore, the use of diatoms as natural nanostructured supports in the development of biosensors is also explored. With respect to this, biofunctionalised diatoms are immobilised on electrodes in an addressed way by means of gold electrodeposition, providing low-cost and eco-sustainable platforms and arrays with potential application in biosensing devices. The analytical devices developed in this thesis as well as the experimental steps presented throughout the different works (study of matrix effects, establishment of cross-reactivity factors, optimisation of the electrochemical detection, comparison between different analytical techniques, etc.) and the different examples provided regarding the application of the colorimetric assays and electrochemical biosensors, should facilitate the implementation of these powerful analytical approaches to routine seafood monitoring programs as well as to the agri-food, medical or environmental sectors in general.

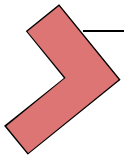

CHAPTER 1

Introduction

General Introduction

Fisheries and aquaculture are important sources of food, nutrition, income and livelihoods for hundreds of millions of people around the world. World per capita seafood supply reached a new record high of 20 kg in 2014, thanks to vigorous growth in aquaculture, which now provides half of all seafood for human consumption, and to a slight improvement in the state of certain fishery products stocks due to better fisheries management [1]. Moreover, seafood is one of the most traded food commodities worldwide with more than half of fishery products exports by value originating in developing countries. Fish and shellfish provide about 17% of global animal proteins and essential micronutrients (including fatty acids, vitamins A, B and D, and minerals including calcium, iodine, zinc, iron and selenium), whose health benefits are extensively recognised. However, seafood products are obtained from a constantly changing aquatic media, which is not free of risks. Thus, food safety remains a major concern facing the seafood industry, and is a critical component in ensuring food and nutrition security worldwide.

Fish and shellfish are one of the main sources of foodborne disease outbreaks worldwide [2], in many cases related to contaminated harvesting sites or mishandling along the processing chain [3]. Like other food, seafood may be a cause for concern if negligence or malpractice occurs in the different processes of production, harvesting, transformation, distribution and consumption. This is the case for the presence of histamine in some species of fish (also described as scombroid food poisoning) due to the transformation of histidine, naturally occurring in fish, to histamine, by exogenous decarboxylases released by microorganisms that grow rapidly at high temperatures.

Nonetheless, it is known that some seafood may be at risk due to the nature of the species itself. Some species are poisonous due to the presence of potent toxins produced within the organisms themselves. This is the case of the puffer fish (Tetraodontidae), whose meat is also known as fugu. In such circumstances, interdiction or strict restrictions are usually imposed by international or local administrations, and poisoning in humans may occur when the rules are not followed or when misinformation exists. As an example, severe cases of poisoning due to consumption of puffer fish have been reported in the eastern Mediterranean (Turkey and Grece). Although the European Union (EU) has regulated that species of the family Tetraodontidae cannot be put on the market, misinformation or negligence has given rise to severe intoxications by consumers who had access to these fishes (*Lagocephalus sceleratus*) and have been poisoned [4]. In this particular

case, *L. sceleratus* was a recently introduced species in the eastern Mediterranean Sea through the Suez channel, and misleading information regarding the risk that these fishes represented may have been an additional factor that favoured these poisonings.

Other sources of risk related to consumption of seafood arise from the marine environment itself and the quality of surrounding waters. The fact that seafood is obtained from marine organisms living in coastal, open or circulating waters for marine or estuarine ecosystems implies that their quality will depend to a certain extent on the environment they inhabit (i.e. the quality of the surrounding water and the food they eat). In addition to the abundances of microorganisms (bacteria and virus) or the presence of contaminants derived from human activities (e.g., metals, polycyclic aromatic hydrocarbons (PAHs), polychlorinated biphenyls (PCBS), dioxins, dioxin-like PCBS, microplastics and pharmaceuticals), which are not addressed in this thesis, an important group of organisms that have to be considered when focusing on seafood risk associated with consumption are microalgae that form harmful algal blooms (HABs). Different species of microalgae that produce toxins may naturally proliferate and increase their densities, resulting in the possible transfer, accumulation and transformation of the toxins they produce throughout the marine food webs.

Bearing in mind the existence of these natural and anthropogenic hazards that may explain the potential toxicity of seafood, food regulatory agencies have established control programs to prevent food contaminants from entering the supply chain at the source or at least to reduce its likelihood to acceptable levels. Currently, fish and shellfish are regularly controlled by efficient monitoring programs for some seafood hazards, which provide data for management and risk assessment purposes. However, for some of them, no maximum permitted levels have been set because of the lack of extensive information available. Research institutions aim to respond to the limitations of the legislation, providing more information regarding emerging risks and developing new detection tools to make the assessment of the presence of contaminants in seafood products easier and faster.

1. The role of biochemical assays and biosensors in seafood safety

The requirement and justification for easy-to-handle, low-cost and reliable methods for the rapid detection of seafood-related hazards is clear, even moreso considering that the globalisation of food industry and climate change can contribute to the rapid spread of food-related hazards in the food chain. Currently, chromatographic techniques coupled to different instrumentation for the detection are the most commonly used analytical methods for the monitoring of priority contaminants.

These analytical methods are highly specific and sensitive, but they require expensive and large equipment, are time-consuming and need highly trained personnel.

Biochemical assays and biosensors have been proposed as powerful screening methods, complementary or alternative to standard analytical methods, to allow the detection of the analytes of interest at the required levels in a rapid, inexpensive and user-friendly manner. Biochemical assays are based on the interaction of the analyte and a biorecognition molecule, such as enzymes, antibodies or aptamers, usually providing high sensitivities and resulting in low limits of detection. The integration of the biorecognition element in intimate contact with a physicochemical transducer leads to the development of biosensors. While the bioreceptor recognises the target analyte, the transducer converts the biorecognition event into a measurable signal, which can be electrochemical, optical, piezoelectric or thermal. Hence, biosensors combine the high affinity of the biochemical interactions with the possible miniaturisation, automation and portability of the devices. Moreover, among the different types of biosensors, electrochemical biosensors stand out for several reasons: their inherently high sensitivities, low cost and miniaturisation of electrodes and potentiostats, compatibility with microfluidics systems and the simplification of the protocols, which make them interesting for *in situ* monitoring [5].

Biochemical assays and biosensors for the detection of marine toxins: Marine toxins constitute a heterogeneous group of complex chemical compounds, some of them produced as secondary metabolites by microalgae of the groups of dinoflagellates and diatoms. Although not fully understood, specific environmental conditions and biological cycles can modulate microalgal population dynamics and may cause the appearance of HABs and their toxins, which may affect the ecosystems. Among other organisms, fish or shellfish can accumulate marine toxins produced by microalgae, thus entering in the food webs and potentially posing a threat to human consumers. Other routes of human exposure to marine toxins, apart from oral consumption of contaminated seafood, are respiration and skin contact. In contrast, tetrodotoxin (TTX) production is thought to be produced by bacteria of the genera *Pseudomonas*, *Shewanella*, *Alternomonas* or *Vibrio* [6], in symbiosis with certain animals such as the puffer fish, which has been presented previously.

Some marine toxins are quite well described according to their structure, mechanism of action, potency and geographical distribution. This is the case for Amnesic Shellfish Poisoning (ASP, e.g., domoic acid), Diarrhetic Shellfish Poisoning (DSP, e.g., okadaic acid) and Paralytic Shellfish Poisoning (PSP, e.g., saxitoxin) toxins

for which international regulations exist, which set up maximum permitted levels in food and define the official methodologies to detect them [7]. Nonetheless, many marine toxins are presently considered, with a certain degree of subjectivity, as "emerging" toxins, including those recently discovered (e.g. pinnatoxins), those that may have recently appeared in certain areas (e.g. ciguatoxins and TTXs), those that are not yet regulated because not enough information is available regarding their toxicity or distribution (e.g., palytoxins, brevetoxins and cyclic imines), and those for which regulation exists but additional toxicological information is required (e.g., azaspiracids) [8].

Due to the benefits presented, biochemical assays and biosensors have been developed for a large range of analytes of interest in food safety. However, in the field of marine toxins, the structural complexity, the scarcity of standards and the lack of extensive information and data available for some of them have compromised the development of methodologies for their detection. In some cases, biorecognition molecules for marine toxins have not been produced and this has limited the number of bioassays and biosensors developed. Nevertheless, marine toxins are nowadays awaking interest in the biosensor world, due to their importance in food safety and environmental monitoring, and this opens new applicability fields for biosensors. A review of the biosensors developed for the detection of emerging marine toxins is presented in the Annex.

Most of the biochemical assays and biosensors for food analysis, and especially for the detection of marine toxins, are based on the use of antibodies as biorecognition molecules, due to the major availability of antibodies for the detection of these analytes in comparison with enzymes or aptamers. Immunoassays and immunosensors are highly selective and sensitive, and offer a wide range of possibilities as they can be formatted to fit into different configurations. Moreover, antibodies may have the ability to detect different toxin analogues or derivatives if they share a structurally similar fragment. Most immunoassays and immunosensors for marine toxins have been reported for okadaic acid and dinophysistoxins, one of the three most important groups of toxins [9]. Nonetheless, some immunoassays and immunosensors for domoic acid, saxitoxin, brevetoxins, palytoxins and tetrodotoxins have also been reported, as well as, few immunoassays for the detection of ciguatoxins [6] and azaspiracids [10-13]. In Chapter 3, a review of the electrochemical biosensors for the detection of marine toxins is presented to provide an overview of the state of the art.

In contrast, a broad number of biochemical assays and biosensors have been developed for the detection of biogenic amines, especially for the detection of histamine [14]. Biogenic amines are low-molecular-weight organic bases mainly produced by microbial carboxylation of amino acids. Histamine is the only biogenic

amine with regulatory limits set by European Legislation, up to a maximum of 200 mg/kg in fresh fish and 400 mg/kg in fishery products treated by enzyme maturation in brine [15]. Nonetheless, the toxic effects of histamine are enhanced by the presence of other biogenic amines such as putrescine and cadaverine [16]. Although immunoassays and immunosensors have been explored for the detection of histamine, many assays and biosensors developed are based on an enzymatic reaction between amine oxidases and biogenic amines, which leads to the production of hydrogen peroxide. Hydrogen peroxide is subsequently monitored directly, through redox mediators or combined with a second enzyme, horseradish peroxidase (HRP), which converts hydrogen peroxide to oxygen and water. Concurrent to this reaction is the oxidation of a substrate that, for example, can produce a change of colour, leading to colorimetric measurements, or can be measured electrochemically. A wide variety of colorimetric enzymatic assays, as well as immunoassays, are currently commercially available [17-20]. Going a step further, an enzyme electrochemical biosensor for the detection of histamine has been recently commercialised by a Spanish company [21]. Nevertheless, some improvements regarding enzyme activity and enzyme immobilisation on the transducer should be accomplished for a better biosensor performance.

2. Key factors in the development of biochemical assays and biosensors

It is well known that the availability of sensitive enough biorecognition molecules able to recognise the analyte of interest in a specific way is a crucial factor in the development of biochemical assays and biosensors. Nonetheless, there are other many decisive points in the development of these type of assays based on biorecognition molecules.

For instance, when developing an immunoassay or immunosensor, the size and structure of the antigen play an important role in the format to be adopted for the immunoaproach development. While in competitive assays, free and immobilised or labelled antigens compete for an antibody, in sandwich assays the target analyte is sandwiched between two antibodies: a capture antibody, which is immobilised and recognises the analyte of the interest, and a detector antibody, which also recognises the antigen but not through the same antigenic site. Consequently, in the development of sandwich immunoassays, only large molecules with different antigenic epitopes can be targeted. This is of major importance in the development of immunoapproaches for the detection of marine toxins, considering the small size of some of them. Likewise, the way in which an antigen is tethered on a solid support to perform a competitive assay is also relevant: the antigenic site of the immobilised antigen has to remain accessible after immobilisation. In the case of

small molecules such as TTXs (319 Da), with a structure consisting of a cage-like polar molecule, steric impediments should be avoided to enable the antigen-antibody affinity interaction. Okadaic acid-group toxins and azaspiracids are polyether lipophilic compounds with molecular weights around 805 and 842 Da, respectively, both containing a terminal carboxylic group but presenting different structures (while okadaic acid is a linear polyether toxin, azaspiracids adopt a globular structure). Although being larger than TTX molecules, they are still very small molecules compared with other analytes in the field of food safety, and this does not allow using them in sandwich configurations. Figure 1 shows the structures of tetrodotoxin, okadaic acid and azaspiracid-1. When immobilising the antibody on the support, the conformation of the antibodies should not be altered and their binding sites should be sterically accessible.

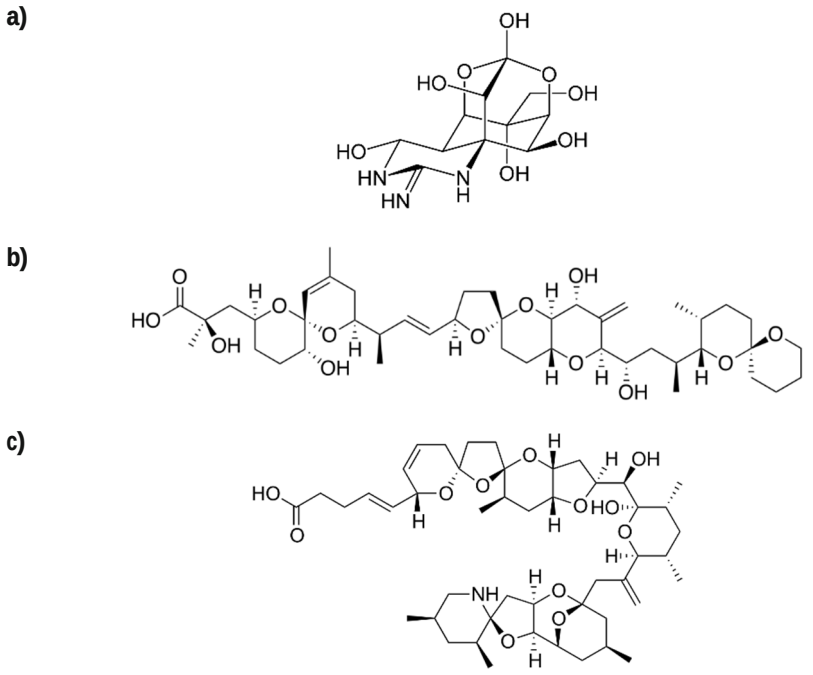

Figure 1. Structures of **(a)** tetrodotoxin, **(b)** okadaic acid and **(c)** azaspiracid-1.

The immobilisation step is also of importance in the development of enzyme biosensors since it may result in enzyme inactivation and compromise the sensitivity of the assay. Moreover, a stable binding that avoids leakage of the biorecognition

molecule should be assured and the active site of the enzyme should remain accessible to the analyte. In the development of electrochemical biosensors, the immobilisation procedure should also ensure a close proximity between the biological component and the transducer in order to obtain an efficient electron transfer. Thus, the choice of the immobilisation technique affects a wide range of parameters, including sensitivity, stability, repeatability, response time and shelf-life of the biosensors. Immobilisation supports should be selected according to the immobilisation strategy and the detection principle, and should favour biocompatibility.

2.1. Immobilisation methods

Among the different immobilisation methods, the most commonly used are adsorption, entrapment or copolymerisation within a polymeric matrix, cross-linking, covalent binding, and non-covalent coupling via electrostatic and affinity interactions [22]. While adsorption, entrapment or electrostatic interactions provide randomly immobilised molecules, sometimes partially hindering their biological activity, covalent binding and affinity interactions enable a controlled and stable immobilisation of the biomolecule.

Covalent binding is performed between a previously activated surface and functional groups of the molecule (amino, hydroxyl, carboxylic, thiol, etc.) that should not be essential for its functional activity. Despite the robustness, the stability of the immobilisation and consequently the absence of molecule leakage, the reduced non-specific adsorption and the high surface coverage, this immobilisation technique involves laborious and tedious protocols and possible loss of activity of the biorecognition molecule, due to the chemical reactions involved.

Further different immobilisation methods can be combined to allow linkage of molecules. Self-assembling is widely used for the immobilisation of molecules on gold, or alternatively to maleimide-modified surfaces, taking benefit of the dative binding between gold or maleimide and thiolated molecules. In addition to the thiol group, thiolated molecules can incorporate other functional groups for the subsequent covalent binding of molecules. The use of self-assembled monolayers (SAMs) as building blocks enables to control the orientation, distribution and spacing of the immobilised molecules, while reducing non-specific interactions [23]. In the development of biosensors, the self-assembling technique may suffer from diffusional impediments, but it is widely used due to the mildness and simplicity of the protocol, and the stability of the monolayers.

On the other hand, affinity interactions between recognition pairs, such as antigen-antibody, (strept)avidin–biotin and some glycoproteins-lectins, are also commonly used as immobilisation strategies in biochemical assays and biosensors due to the high-affinity constants. These non-covalent approaches are based on rapid and facile protocols and provide oriented configurations. Such is the case of the antibody immobilisation through affinity interactions with binding proteins (protein A or G), that bind to the Fc region of immunoglobulins (IgGs) or avidin–biotin interactions, commonly used due to the wide range of molecules that can be easily biotinylated using commercially available reagents.

2.2. Immobilisation supports

As previously mentioned, many factors can affect biomolecule or antigen immobilisation, necessary for the development of biochemical assays and biosensors. While some of these factors cannot be modified to any great extent, a wide range of supports can be used to tailor biochemical assays and biosensors according to the final application. Microtitre plates, usually made of polystyrene, are the gold standard in the development of most conventional colorimetric assays. Other materials such as polypropylene, polycarbonate and nylon are occasionally used. Pre-activated plates are also available for surface-tethering of the biomolecule, such as plates pre-coated with Protein A, Protein G or streptavidin or modified with maleic-anhydride or maleimide for group-specific attachment of molecules.

Regarding electrochemical biosensors, a wide variety of electrodes of different material, size, geometry and obtained by different fabrication methods can be used. Screen-printed electrodes are widely used as a consequence of their simple and low-cost fabrication as well as easy mass production. Due to the benefits presented by carbonaceous materials in terms of cost, potential window, electrical conductivity and electrocatalytic activity for a variety of redox mediators, most screen-printed electrodes are based on carbon materials [24]. Gold and other metallic surfaces are also explored because of their high conductivity and ease of modification through the formation of SAMs.

Over the past decade, the interest of nanotechnology in the development of biosensors has exponentially increased. Nanomaterials have unique optical and electrical characteristics that make their incorporation in biosensor configurations particularly interesting due to inherent advantages such as high sensitivity, low limits of detection (LODs) and reduced matrix effects [8]. The use of nanostructured materials as immobilisation supports provides larger surface areas able to carry high amounts of biomolecules. Magnetic beads, both in the micro- and the nanometre

range, have also received great attention, since they can act as switches, retaining and removing the bioreceptor onto and from magnetised supports.

Magnetic beads as immobilisation supports: Magnetic beads offer several attractive properties in food analysis since they can be coated with biological molecules and manipulated by an external magnetic field gradient. As such, the recognition molecule can be selectively bound to the magnetic beads and then separated from its biological media by applying an external magnetic field. Moreover, magnetic beads of a variety of materials, sizes and modified with different surface functional groups are now commercially available. It is believed that the combination of magnetic beads and electrochemical biosensing strategies improves analytical performance. Instead of direct surface modification of the electrode, both the biological reactions and the washing steps can be performed on magnetic beads, reducing matrix effects and improving assay kinetics. Following modification, the magnetic beads are easily captured by applying a magnetic field on the bottom of the electrode surface using magnets. This procedure constitutes a versatile platform for the analysis of complex food matrices [5].

Porous silicon nanostructured supports: Porous silicon (pSi) has been extensively researched due to its remarkable optical and morphological properties (including tuneable pore size and porosity), large internal surface and versatile surface chemistry. Therefore, it is not surprising that the past decade has seen a range of successful applications of pSi as an immobilisation platform for biomolecules [25]. Nevertheless, as far as pSi is concerned, electrochemical transducers have been overshadowed by optical sensors. The incorporation of pSi into electrochemical devices offers the advantages of a substantially larger sensing area compared with flat electrodes, but this is not the only advantage. In fact, depending on the transduction mechanisms, several issues like modulation of electric fields through the pores and its interface with the biomolecules and ions of the analytes or the orientation of the molecules within the pores can have a significant impact on the electrochemical biosensor performance. However, despite the well-known advantages of pSi, several challenges still need to be overcome to make biosensors based on pSi a reality, and the most important one relies on its fabrication. pSi is a relatively expensive sensing material and, to be cost effective, relatively small areas of thin silicon wafer need to be used. The machine assembly of fragile components into test devices poses a handling and fabrication challenge. Moreover, the safe handling of harsh and dangerous chemical solvents such as hydrofluoric acid required for silicon etching and the reproducibility of the nanostructures are other questions to be addressed.

Diatoms as natural three-dimensional nanostructures: Biological materials are a promising alternative to existing fabrication technologies, and diatoms, one of the most abundant unicellular microalgae found in aquatic environments, are among the most remarkable examples. Diatoms have rigid cell walls made of silica, called frustules, which possess a micro/nanoporous pattern of unparalleled diversity far beyond the possibilities of current micro- and nanofabrication techniques. Because of their large surface area, high and ordered pore and channel density, thermal and mechanical stability, optical properties and biocompatibility, diatoms have recently attracted extensive attention in a wide range of nanotechnology applications [26]. Additionally, diatoms present reactive Si-OH groups that coat the frustules, facilitating their chemical modification through well-established chemistries, which makes them promising as nanostructured supports in biosensing platforms. A review about the incipient use of diatoms as building blocks in biosensing systems is presented in Chapter 5.

3. Towards the implementation of biochemical assays and biosensors for marine toxins and biogenic amines

Seafood regulatory agencies have increased emphasis on preventive measures to control the introduction of contamination at source and have moved to food-chain approaches that encompass the whole food chain from primary production to final consumption, namely from sea to table. The implementation of analytical devices such as biochemical assays and especially biosensors can clearly contribute to the execution of these food management programs. Many countries rely on marine toxins monitoring programmes to protect public health. This involves monitoring the presence of naturally occurring marine toxins in shellfish and analysing seawater for the presence of toxin producing phytoplankton. The detection of marine toxins before the contamination of shellfish occurs is highly needed to avoid economic losses in the shellfish industry and protect consumers' health. However, toxic events are still very difficult to prevent and alternative rapid, low-cost and reliable early warning tools are required. Other marine toxins, such as TTXs, are believed to be produced by endosymbiotic bacteria, but the mechanism of production remains unclear. TTX has been responsible for many human fatalities, most commonly following the consumption of puffer fish originating from warm waters, especially of the Indian and Pacific Oceans. During the last decade, however, the presence of TTX and its analogues is increasingly reported from different marine species – including bivalve molluscs – in European waters, raising serious concerns regarding public health protection, taking into account that TTX is not a regulated toxin in the EU legislation [27]. The availability of new analytical methods for their detection in

different matrices would help further investigations for management and risk assessment purposes, and to confirm intoxication cases after undesired poisoning incidents.

Histamine and other biogenic amines are mainly produced as a consequence of inappropriate processing and storage conditions and subsequent microbial contamination. The implementation of bioanalytical devices during the food supply chain could help to prevent poisoning cases such as that reported on May 2017, in which hundreds of people of different European countries were struck by a histamine outbreak caused by the consumption of adulterated Spanish tuna [28].

In the past few years, most of the advances have been made on the development of bioanalytical systems but not on their implementation and validation. In bioanalysis, matrix components present in biological samples can affect the response from the biorecognition event. Matrix effects are complex and system-specific, and should be addressed prior to the application of biochemical assays and biosensors to the analysis of naturally contaminated samples. Furthermore, the results obtained in the analysis of samples need to be compared with current reference analysis methods. The different recognition principles between techniques and the different affinity of the biorecognition molecule towards the different analogues structurally similar to the target compound should be considered to understand the correlation between techniques in the analysis of samples with multiple analogues.

References

[1] Food and Agriculture Organization of the United Nations (FAO). The State of World Fisheries and Aquaculture 2016. Contributing to food security and nutrition for all, Rome, 2016.

[2] Center for Science in the Public Interest (CSPI). Outbreak Alert! 2015, Washington, 2015.

[3] C. Rodgers and J. Diogène. Microbiological and Toxin Outbreaks in Seafood, In: J.M. Soon, L. Manning, .C.A. Wallace (eds) Foodborne Diseases. Case Studies of Outbreaks in the Agri-food Industries, CRC Press, Boca Raton (20146) 189-239.

[4] P. Katikou, D. Georgantelis, N. Sinouris, A. Petsi, T. Fotaras. First report on toxicity assessment of the Lessepsian migrant pufferfish *Lagocephalus sceleratus* (Gmelin, 1789) from European waters (Aegean Sea, Greece). Toxicon 54 (2009) 50-55.

[5] M.I. Pividori, S. Alegret, Electrochemical biosensors for food safety, Contributions to Science 6 (2010) 173-191.

[6] V. Pratheepa, V. Vasconcelos, Microbial diversity associated with tetrodotoxin production in marine organisms, Environmental Toxicology and Pharmacology 36 (2013) 1046-1054.

[7] European Union Commission Regulation EC 854/2004. Office of the European Union L226:83–127.

[8] L. Reverté, L. Soliño, O. Carnicer. J. Diogène, M. Campàs, Alternative methods for the detection of emerging marine toxins: biosensors, biochemical assays and cell-based assays, Marine Drugs 12 (2014) 5719-5763.

[9] L. Reverté, B. Prieto-Simón, M. Campàs, New advances in electrochemical biosensors for the detection of toxins: Nanomaterials, magnetic beads and microfluidics systems. A review, Analytica Chimica Acta 908 (2016) 8-21.

[10] M.O. Frederick, S.D.L. Marin, K.D. Janda, K.C. Nicolaou, T.J. Dickerson, Monoclonal antibodies with orthogonal azaspiracid epitopes, Chembiochem 10 (2009) 1625-1629.

[11] C.J. Forsyth, J. Xu, S.T. Nguyen, I.A. Samdal, L.R. Briggs, T. Rundberget, M. Sanvik, C.O. Miles, Antibodies with broad specificity to azaspiracids by use of synthetic haptens, Journal of the American Chemical Society 128 (2006) 15114-15116.

[12] L.P. Rodríguez, N. Vilariño, M.C. Louzao, T.J. Dickerson, K.C. Nicolaou, M.O. Frederick, L.M. Botana, Microsphere-based immunoassay for the detection of azaspiracids, Analyitcal Biochemistry 447 (2014) 58-63.

[13] I.A. Samdal, K.E. Lovberg, L.R. Briggs, J. Kilcoyne, J. Xu, C.J. Forsyth, Development of an ELISA for the detection of azaspiracids, Journal of Agricultural and Food Chemistry 63 (2015) 7855-61.

[14] K. Kivirand, T. Rinken, Biosensors for biogenic amines: The present state of art mini-review, Analytical Letters 44 (2011) 2821-2833.

[15] European Union Commission Regulation EC 1441/2007. Office of the European Union L139:11-82.

[16]J.E. Stratton, R.W. Hutkins, S.L. Taylor, Biogenic amines in cheese and other fermented foods – a Review, Journal of Food Protection 54 (1991) 460-470.

[17] J. Hungerford, W.H. Wu, Comparison study of three rapid test kits for histamine in fish: BiooScientific MaxSignal enzymatic assay, Neogen Veratox ELISA, and the Neogen Reveal Histamine Screening test, Food Control 25 (2012) 448-457.

[18] Bioo Scientific Histamine Test Kits.http://www.biooscientific.com/Histamine-Test-Kits. Accessed 1 February 2018.

[19] Abraxis Histamine ELISA kit. https://www.abraxiskits.com/products/veterinary-residues-additives/. Accessed 1 February 2018.

[20] Rocky Mountain Diagnostics Histamine ELISA. https://rmdiagnostics.com/category/histamine-ELISA-Kits. Accessed 1 February 2018.

[21] Biolan Biofish. http://www.biolanmb.com/sectors/biofish-fish-product-sensors/biofish-700-fish-product-sensor#sectores. Accessed 1 February 2018.

[22] B. Prieto-Simón, M. Campàs, J.L. Marty, Biomolecule immobilization in biosensor development: Tailored strategies based on affinity interactions, Protein & Peptide Letters 15 (2008) 757-763.

[23] A. Fragoso, N. Laboria, D. Latta, C.K. O'Sullivan, Electron permeable self-assembled monolayers of dithiolatedaromatic scaffolds on gold for biosensor applications, Analytical Chemistry 80 (2008) 2556-2563.

[24] R.L. McCreery, Advanced carbon electrode materials for molecular electrochemistry, Chemical Reviews 108 (2008) 2646-2687.

[25] A. Jane, R. Dronov, A. Hodghes, N.H. Voelcker, Porous silicon biosensors on the advance, Trends in Biotechnology 27 (2009) 230-239.

[26] D. Losic (ed): Diatom Nanotechnology: Progress and Emerging Applications, RSC Nanoscience & Nanotechnology series 44, 2017.

[27] P. Katikou, A. Vlamis, Tetrodotoxins: recent advances in analysis method and prevalence in European waters, Current Opinion in Food Science 18 (2017) 1-6.

[28] Food Quality News. https://www.foodqualitynews.com/Article/2017/08/08/Multiple-EU-countries-report-outbreaks-caused-by-histamine. Accessed 1 February 2018.

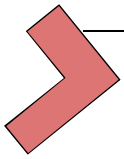

CHAPTER 2

Objectives and personal contribution

Which are the objectives of this thesis?

This thesis aims to contribute to both the development and the applicability of colorimetric assays and electrochemical biosensors for the detection of marine toxins and biogenic amines, paving the way towards the implementation of low-cost, simple and reliable devices for seafood safety purposes. The application of these devices aims to cover the entire food chain from sea to final consumption, thus using the bioanalytical approaches from early warning to the detection of contaminants in seafood or even in humans after an unfortunate intoxication event.

Different immobilisation strategies and supports for the development of immunoassays and electrochemical biosensors are explored according to the final purpose. Accordingly, this thesis has been divided into four different sections:

(1) Chapter 3 is focused on the use of SAMs as building blocks for the development of colorimetric immunoassays for the detection of marine toxins, specifically okadaic acid and its analogues and tetrodotoxins. The SAM-based immunoassays for the detection of okadaic acid are applied to the analysis of seawater samples as alternative monitoring tools, while the immunoassays for the detection of tetrodotoxins are used for the analysis of contaminated shellfish samples and for the detection of tetrodotoxins in human body fluids after a fatal puffer fish poisoning incident.

(2) In Chapter 4, the development and use of electrochemical biosensors is explored. A review regarding the trends and prospects on their use in the detection of marine toxins is included. Due to the lack of biosensors for the detection of azaspiracids and their presence in an increasing number of countries, the development of electrochemical biosensors for the detection of this group of marine toxins in mussels is pursued. Magnetic beads are explored as antibody immobilisation supports. Affinity biointeractions are also used for the immobilisation of the antibody on the electrodes.

(3) Enzyme electrochemical biosensors for the detection of biogenic amines in fish are presented in Chapter 5. In this case, magnetic beads are used as enzyme immobilisation supports.

(4) Finally, in Chapter 6, diatoms are proposed as natural nanostructured supports for the development of biosensors. A review highlighting the potential role of diatoms in biosensing is presented. The biofunctionalisation and immobilisation of diatoms on electrodes are addressed to rationally use them as building blocks in the development of electrochemical biosensors.

This thesis aims to demonstrate the development of useful and powerful analytical tools for seafood safety purposes, providing new approaches that will clearly make an important breakthrough in achieving low-cost and sustainable bioanalytical devices. This work should contribute to the implementation of biochemical assays and biosensors in the routine analysis of the food industry and monitoring programs.

Scientific publications and personal contribution

The development of this thesis has led to the publication of seven scientific publications. To achieve this, different institutions and researchers have collaborated. The aim of this section is to provide a statement of the personal contribution to the different experimental work performed in each one of the articles.

1. S. Leonardo, A. Toldrà, M. Rambla-Alegre, M. Fernández-Tejedor, K.B. Andree, L. Ferreres, K. Campbell, C.T. Elliott, C.K. O'Sullivan, Y. Pazos, J. Diogène, M. Campàs, **Self-assembled monolayer-based immunoassays for okadaic acid detection in seawater as monitoring tools**, Marine Environmental Research 133 (2018) 6-14.

   Personal contribution:

   - Development, optimisation and characterisation of the immunoassays for the detection of okadaic acid.
   - Establishment of cross-reactivity factors for dinophysistoxin-1 and dinophsysistoxin-2.
   - Preparation of seawater and mussel extracts.
   - Study of matrix effects.
   - Analysis of seawater and mussel samples by the immunoassays.

2. L. Reverté, M. Rambla-Alegre, S. Leonardo, C. Bellés, K. Campbell, C.T. Elliott, A. Gerssen, M.D. Klijnstra, J. Diogène, M. Campàs, **Development and validation of a maleimide-based enzyme-linked immunosorbent assay for the detection of tetrodotoxin in oysters and mussels**, Talanta 176 (2018) 659-666.

   Personal contribution:

   - Study of the storage stability of TTX-coated maleimide plates.
   - Study of interferences.
   - Analysis of shellfish samples by the immunoassay.

3. M. Rambla-Alegre, S. Leonardo, Y. Barguil, C. Flores, J. Caixach, K. Campbell, C.T. Elliott, C. Maillaud, M.J. Boundy, D.T. Harwood, M. Campàs, J. Diogène, **Rapid screening and multi-toxin profile confirmation of tetrodotoxins and analogues**

in human body fluids derived from a puffer fish poisoning incident in New Caledonia, Food and Chemical Toxicology 112 (2018) 188-193.

Personal contribution:

- Study of urine, serum and plasma matrix effects on the immunoassay.
- Analysis and quantification of TTX content in urine samples by the immunoassay.

4. S. Leonardo, M. Rambla-Alegre, I.A. Samdal, C.O. Miles, J. Kilcoyne, J. Diogène, C.K. O'Sullivan, M. Campàs, **Immunorecognition magnetic supports for the development of an electrochemical immunoassay for azaspiracid detection in mussels**, Biosensors and Bioelectronics 92 (2017) 200-206.

Personal contribution:

- Conjugation of the polyclonal antibody (PAb) to magnetic beads (MBs).
- Study of the storage stability of the PAb-MB conjugates.
- Development, optimisation and characterisation of the colorimetric and electrochemical immunoassays for the detection of azaspiracid-1 (AZA-1).
- Establishment of cross-reactivity factors for AZA-1–10.
- Study of interferences and mussel matrix effects.
- Analysis of mussel samples by the colorimetric and electrochemical immunoassays.

5. S. Leonardo, J. Kilcoyne, I.A. Samdal, C.O. Miles, C.K O'Sullivan, J. Diogène, M. Campàs, **Detection of azaspiracids in mussels using electrochemical immunosensors for fast screening in monitoring programs**, Sensors and Actuators B 262 (2018) 818-827.

Personal contribution:

- Development, optimisation and characterisation of the colorimetric immunoassays and electrochemical immunosensors.
- Study of mussel matrix effects.
- Analysis of naturally contaminated mussel samples using the developed colorimetric immunoassays and electrochemical immunosensors.

6. S. Leonardo, M. Campàs, **Electrochemical enzyme sensor arrays for the detection of the biogenic amines histamine, putrescine and cadaverine using magnetic beads as immobilisation supports**, Microchimica Acta 183 (2016) 1881-1890.

Personal contribution:

- Conjugation of diamine oxidase (DAO) to MBs.
- Study of the storage stability of DAO-MB conjugates.
- Development, optimisation and characterisation of the electrochemical biosensors for the detection of histamine, putrescine and cadaverine.
- Development of the colorimetric enzyme assay.
- Study of interferences.
- Biogenic amines extraction in fish samples.
- Analysis of fish samples by the developed electrochemical biosensors and the colorimetric enzyme assay.

7. S. Leonardo, D. Garibo, M. Fernández-Tejedor, C.K. O'Sullivan, M. Campàs, **Addressed immobilization of biofunctionalized diatoms on electrodes by gold electrodeposition**, Biofabrication 9 (2017) 015027.

Personal contribution:

- Diatom cultures, harvesting and removal of the organic matter.
- Diatom immobilisation by gold electrodeposition.
- Morphological characterisation by optical microscopy and scanning electron microscopy (SEM).
- Electrochemical characterisation of gold deposits and study of the electrocatalytical activity.
- Addressed diatom immobilisation on interdigitated electrodes.
- Biofunctionalisation of diatoms and colorimetric characterisation.
- Immobilisation of biofunctionalised diatoms and electrochemical characterisation.

Moreover, one review and two book chapters have also been published, which provide a wider overview of the different topics presented in this thesis.

1. S. Leonardo, A. Toldrà, M. Campàs, **Trends and prospects on electrochemical biosensors for the detection of marine toxins**, In: Diogène, J., Campàs, M. (eds) Recent Advances in the Analysis of Marine Toxins 78 (2017) 303-341.

2. S. Leonardo, B. Prieto-Simón, M. Campàs, **Past, present and future of diatoms in biosensing**, Trends in Analytical Chemistry 79 (2016) 276-285.

3. S. Leonardo, L. Reverté, J. Diogène, M. Campàs, **Biosensors for the Detection of Emerging Marine Toxins**, In: Nikolelis D., Nikoleli GP. (eds) Biosensors for Security and Bioterrorism Applications. Advances Sciences and Technologies for Security Applications (2013) 231-248.

The different works presented in what follows maintain the structure and format required by the journals or editorials where they have been published.

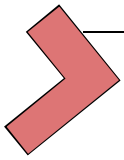

CHAPTER 3

Colorimetric immunoassays for the detection of marine toxins

Self-assembled monolayer-based immunoassays for okadaic acid detection in seawater as monitoring tools

Sandra Leonardo[a], Anna Toldrà[a], Maria Rambla-Alegre[a], Margarita Fernández-Tejedor[a], Karl B. Andree[a], Laura Ferreres[a], Katrina Campbell[b], Christopher T. Elliott[b], Ciara K. O'Sullivan[c,d], Yolanda Pazos[e], Jorge Diogène[a], Mònica Campàs[a]

[a]*IRTA, Ctra. Poble Nou, km. 5.5, 43540 Sant Carles de la Ràpita, Spain*

[b]*Institute for Global Food Security, School of Biological Sciences, Queen's University, Stranmillis Road, Belfast, Northern Ireland, BT9 5AG*

[c]*Departament d'Enginyeria Química, Universitat Rovira i Virgili, Av. Països Catalans, 26, 43007 Tarragona, Spain*

[d]*Institució Catalana de Recerca i Estudis Avançats, Pg. Lluís Companys, 23, 08010 Barcelona, Spain*

[e]*INTECMAR, Peirao de Vilaxoán, s/n, 36611 Vilagarcía de Arousa, Spain*

Abstract

Rapid and cost-effective methods to monitor the presence of diarrhetic shellfish poisoning (DSP) toxins in seawater samples in an easy and reliable manner are required to protect human health and avoid economic losses to shellfish industry. Immunoassays for the detection of okadaic acid (OA) and dinophysistoxin-1 and dinophysistoxin-2 are developed by immobilising OA on self-assembled monothiols or dithiols in an ordered and oriented way, providing an effective limit of detection of ~1 ng OA equiv./mL seawater. The immunoassays are applied to the analysis of the particulate fraction of seawater samples from two Catalan harbours (NW Mediterranean) and samples collected periodically from the Galician Rias (E Atlantic), as well as a reference mussel sample. Results are in agreement with LC-MS/MS and the certified values. OA concentration in seawater correlates with *Dinophysis* cell abundance, with a 1-2 weeks lag. The immunoassays provide powerful high-throughput analytical methods potentially applicable as alternative monitoring tools.

1. Introduction

Harmful algal blooms (HABs), which may result in accumulation of marine toxins in shellfish, are a growing human health and economic concern in many coastal regions. Among the several illnesses caused by contaminated bivalve molluscs, diarrhetic shellfish poisoning (DSP) is the most significant problem in regions with

well-developed aquaculture activities in temperate seas, e.g. Europe, USA, Chile, Japan and New Zeland (Eberhart et al., 2013; MacKenzie et al., 2005; Reguera et al., 2014). The DSP toxin group includes okadaic acid (OA) and analogues such as dinophysistoxin-1 (DTX-1) and dinophysistoxin-2 (DTX-2), which are produced by dinoflagellates of the *Dinophysis* (and potentially by *Phalacroma rotundatum*, formerly *D. rotundata*) and *Prorocentrum* genera.

Current monitoring programs are based on the quantification of toxicity of shellfish tissue by LC-MS/MS as the reference method (European Comission, 2011), being 160 µg OA equiv./kg shellfish meat the maximum permitted level established by the European Commission (European Comission, 2004). The identification and quantification of microalgae in water as an early warning parameter is also performed on routine bases by monitoring programs, but DSP events are still very difficult to predict, among other reasons, because of the high variability of the toxin content in phytoplankton cells. Alternative monitoring methods have also emerged, for example, those based on molecular analysis, notable omics approaches such as trancriptomics and epigenomics, to monitor the presence of marine toxins in shellfish (González-Romero et al., 2017; Suárez-Ulloa, et al, 2015; Suárez-Ulloa, et al., 2013a; Suárez-Ulloa, et al., 2013b). However, other alternative strategies that facilitate the detection of DSP toxins before contamination of shellfish occurs are highly needed.

The product of *Dinophysis* abundance and cell toxin content have been demonstrated to be decisive for DSP toxicity in filter feeders such as mussels (Lindahl et al., 2007). Therefore, the measurement of toxin concentration in the particulate fraction of seawater provides a good indicator of mussel toxicity since both cell abundance and toxin content are included in the analysis (García-Altares et al., 2016). The ability to monitor the presence of marine toxins in seawater samples in a rapid, easy, robust and cost-effective manner would provide a powerful strategy within monitoring programs, facilitating important decisions to be taken prior to contamination of shellfish above legal limits occurs. Moreover, the development of these methods would clearly play a key role in understanding, among others, the relationship between phytoplankton population dynamics during a bloom and the presence of marine toxins, the toxin transfer within food webs, the definition of areas at risk according to time series studies and the prevalence of toxins, and the identification of the possible impacts of climate change on the presence of marine toxins.

Immunoassays are promising sensitive rapid screening tools because, among other reasons, highly qualified personnel and expensive instrumentation are not required, in contrast to current analytical chemistry reference methods. Enzyme-linked immunosorbent assays (ELISAs) have been described for the detection of OA and its

analogues, some of them being adapted for the development of immnosensors (Campàs et al., 2012, 2007; Leonardo et al., 2017b; Reverté et al., 2016; Sassolas et al., 2013b). It is well known that a key point in the development of immunoassays and immunosensors is the immobilisation of the antibody or antigen onto the surface. Most of the reported immunoassays require the conjugation of OA to protein carriers such as bovine serum albumin (BSA) or ovalbumin (OVA), but this strategy results in a random antigen immobilisation (Campàs et al., 2008; Dubois et al., 2010; Kreuzer et al., 1999; Kreuzer et al., 2002; Sassolas et al., 2013a). Thus, a new self-assembled monolayer (SAM)-based immunoassay for OA detection is proposed (Figure 1). The use of SAMs as building blocks in immunoassays enables to control the orientation, distribution and spacing of the immunospecies while reducing non-specific interactions (Fragoso et al., 2008). In this work, OA was immobilised on maleimide plates using monothiols (cysteamine) or dithiols (dithiol-alkane aromatic PEG6-$NHNH_2$) to covalently immobilise OA through their amine or hydrazide groups, respectively. OA calibration curves were obtained and cross-reactivity factors (CRFs) for DTX-1 and DTX-2 established. Both SAM strategies were applied to the analysis of the particulate fraction of seawater samples collected from different points of two Catalan harbours (NW Mediterranean) and seawater samples collected periodically from the Galician Rias (E Atlantic Ocean). In addition, DSP toxins were analysed in certified reference material of DSP-contaminated mussel. The correlation between the OA concentration and presence of *Dinophysis* in seawater samples was investigated. The potential application of the SAM-based immunoassays as a highly valuable tool in monitoring programs as well as research purposes was thus demonstrated.

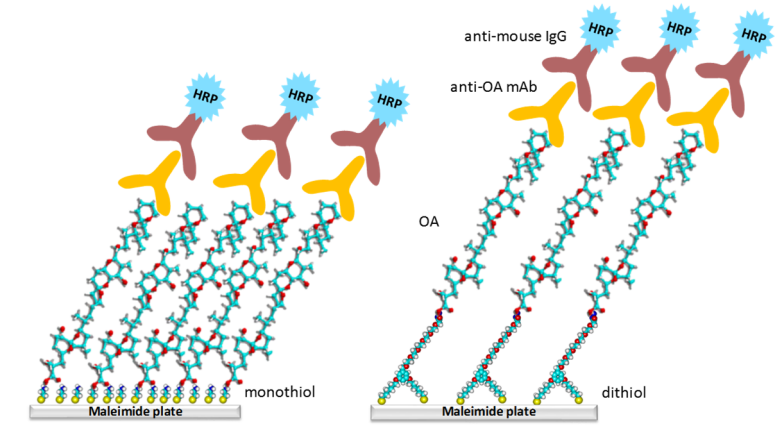

Figure 1. Schematic representation of the SAM-based immunoassays for the detection of OA.

2. Experimental

2.1. Reagents and Materials

Pierce maleimide-activated plates were obtained from Thermo Fisher Scientific (Madrid, Spain). Dithiol-alkane aromatic PEG6-$NHNH_2$ (dithiol) was purchased from Sensopath Technologies (Bozeman, USA). Cysteamine hydrochloride, okadaic acid potassium salt (OA) from *Prorocentrum concavum* (for immobilisation on maleimide plates), potassium phosphate monobasic, potassium chloride, Tween®-20, ethylenediaminetetraacetic acid (EDTA**),** 2-(N-morpholino)ethanesulfonic acid hydrate (MES), N-(3-dimethylaminopropyl)-N'-ethylcarbodiimide hydrochloride (EDC), N-hydroxysuccinimide (NHS), bovine serum albumin (BSA), anti-mouse IgG (whole molecule)–horseradish peroxidase antibody produced in rabbit (IgG-HRP) and 3,3',5,5'-tetramethylbenzidine (TMB) liquid substrate were supplied by Sigma–Aldrich (Madrid, Spain).

To perform calibration curves and LC-MS/MS analysis, certified reference materials (CRMs) of okadaic acid (OA), dinophysistoxin-1 (DTX-1), dinophysistoxin-2 (DTX-2), yessotoxin (YTX), homoyessotoxin (hYTX), pectenotoxin-2 (PTX-2), azaspiracid-1 (AZA-1), azaspiracid-2 (AZA-2), azaspiracid-3 (AZA-3), 13-desmethylspirolide C (SPX-1), gymnodimine A (GYM-A) and pinnatoxin G (PnTX-G) were obtained from the National Research Council of Canada (NRC, Halifax, NS, Canada).

The anti-OA monoclonal antibody (mAb) OUB-OA-7 was produced and characterised for cross-reactivity in surface plasmon resonance assay development as described in Stewart et al. (2009a, 2009b).

2.2. Seawater and mussel samples

Seawater samples (n=14) from Sitges and Masnou harbours (NW Mediterranean Sea) were collected from 4 different sites at 3 different depths (surface, medium depth, between 1–2 m, and bottom, maximum depth = 2–4 m) in March and April 2016, respectively, coinciding with the presence of *Dynophysis* blooms (Figure 2). Seawater samples (1.5 L) were filtered under low vacuum onto 0.45-µm nylon filters. Particulate matter retained by the filter, which included phytoplankton, was analysed.

Seawater samples (n=20) from the Galician Rías (E Atlantic Ocean) were obtained weekly over a 5-month period (March to July 2015) as part of the Galician HAB monitoring program conducted by INTECMAR from a single sampling station located in Bueu (Figure 2). Seawater samples were collected from the water column using a PVC hose divided into 3 sections: 0-5, 5-10 and 10-15 m. An integrated water sample

(0 to 15-m depth) was obtained by mixing equal volumes from each hose section. Seawater samples (1.5 L) obtained from the integrated profile were filtered through 47 mm diameter Whatman 2.7-µm GF/D and 0.7-µm GF/F filters. Phytoplankton passing through a GF/D, but retained onto GF/F filters was considered to represent the picoplankton fraction.

All filters were stored at -20 °C prior to extraction. Additionally, 50 mL of each sample were preserved with Lugol's iodine solution for phytoplankton identification and quantification. An additional subsample was retained from the Masnou and Sitges seawater samples for *Dinophysis* isolation.

Mussel tissue certified reference material for DSP toxins (CRM-DSP-Mus-c) and blank mussel tissue certified reference material (CRM-Zero-Mus) were obtained from the NRC (Halifax, NS, Canada). CRM-DSP-Mus-c contained certified values of OA (1.07 ± 0.08 mg/kg), DTX-1 (1.07 ± 0.11 mg/kg), DTX-2 (0.86 ± 0.08 mg/kg) and domoic acid (DA) and epiDA (11.8 ± 0.60 mg/kg), as well as non-certified values of fatty acid acyl esters of OA (2.4 mg/kg), DTX-1 (1.1 mg/kg) and DTX-2 (2.2 mg/kg).

Figure 2. Map of the Iberian Peninsula with sampling stations from the Catalan harbours (Sitges and Masnou) and from the Galician Rías (Bueu). Sampling stations are: P1B: 42°21'24.0"N 8°46'25.2"W; P1M: 41°28'32.9"N 2°18'31.0"E; P2M: 41°28'29.2"N 2°18'40.1"E; P3M: 41°28'33.7"N 2°18'50.2"E; P3M: 41°28'35.1"N 2°19'00.0"E; P1S: 41°14'03.6"N 1°49'17.6"E; P2S: 41°14'00.5"N 1°49'26.5"E; P3S: 41°13'57.8"N 1°49'30.8"E; P4S: 41°14'01.3"N 1°49'36.2"E.

2.3. Preparation of sample extracts

Filters retaining phytoplankton cells were extracted with 7 mL of methanol, vortex-mixed for 30 s and sonicated with a Vibra-Cell sonicator (Sonics & Materials Inc, Newton, USA) for 5 min at 37% amplitude with 3-s pulse cycles. The mixture was centrifuged at 3,000 rpm for 10 min and the supernatant was decanted and then filtered through 0.22-µm nylon membrane syringe filters. This extraction protocol was repeated twice. The extracts were combined, evaporated under nitrogen flow and reconstituted in 1 mL with methanol.

For mussel samples, a triple-step extraction with methanol (10 mL) was performed on whole homogenised tissues (1 g), according to the procedure proposed by Gerssen et al. (2009), which followed intra-laboratory validation by our group (García-Altares et al., 2013). The alkaline hydrolysis of the samples was performed according to the EURLMB Standard Operating Procedure (SOP) (EURLMB, 2011), based on the protocol developed by Mounfort et al. (2001).

2.4. Colorimetric self-assembled monolayer-based immunoassays

Cysteamine (monothiol) or dithiol-alkane aromatic PEG6-$NHNH_2$ (dithiol) were used for OA immobilisation on maleimide plates. The protocol was as follows: (1) maleimide-activated plates were rinsed three times with 200 µL of washing buffer (0.1 M potassium phosphate, 0.05% v/v Tween-20, pH 7.2); (2) 50 µL of 10 mM monothiol or 0.1 mM dithiol in binding buffer (0.1 M potassium phosphate, 10 mM EDTA, pH 7.2) were then added and incubated overnight at 4 °C for self-assembling; (3) previous to OA immobilisation, 2 µM OA in 0.1 M MES buffer, pH 5.0, was incubated with 20 mg/mL EDC and NHS (1:1) for 15 min to activate the OA carboxylic groups; (4) 50 µL of different concentrations (from 0.25 µM to 2 µM for protocol optimisation and 0.5 µM for the final competition assay) of the activated OA in 0.1 M MES buffer, pH 5.0, were added and incubated for 45 min to allow OA immobilisation through amine-carboxylic (monothiol approach) or hydrazide-carboxylic (dithiol approach) cross-linking reactions.

After OA immobilisation, (5) 25 µL of mAb diluted in binding buffer containing 2% w/v BSA (from 1/500 to 1/4,000 for protocol optimisation and 1/2,000 for the final competition assay) and 25 µL of OA, DTX-1 or DTX-2 standard solutions or samples, all diluted in binding buffer, were incubated for 45 min; (6) 50 µL of IgG-HRP dilution (1/1,000 and 1/2,000 for protocol optimisation and 1/2,000 for the final competition assay) in binding buffer containing 1% w/v BSA were added to wells for 45 min; (7) finally, 100 µL of TMB liquid substrate were added and incubated, after

10 min absorbance was read at 620 nm with a Microplate Reader KC4 from BIO-TEK Instruments, Inc. (Vermont, USA).

After each step, wells were rinsed three times with 200 µL of washing buffer and during incubations microtiter plates were placed on a plate shaker for mixing. With the exception of the thiol self-assembling step, which was performed at 4 °C, all steps were conducted at room temperature.

2.5. Liquid Chromatography-Tandem Mass Spectrometry (LC-MS/MS) analysis

For LC-MS/MS analysis of lipophilic marine toxins, our in-house validated method to determine lipophilic toxins in shellfish samples, described in García-Altares et al. (2013) was applied. Toxins were separated on a XBridge BEH C8 2.5µm 2.1x50mm column (Waters, Milford, MA, USA). A binary gradient was programmed with ultrapure Milli-Q water (mobile phase A) and 90:10 v:v acetonitrile/water (mobile phase B), both containing 6.7 mM of ammonium hydroxide. Mobile phases were filtrated through 0.2 µm nylon membrane filters (Whatman, Springfield Mill, UK).

Chromatographic separation was performed on an Agilent 1200 LC system (Agilent Technologies, Santa Clara, CA). All runs were carried out at 30 °C using a flow rate of 500 µL/min. The injection volume was 10 µL and the auto-sampler was set at 4 °C. A triple quadrupole 3200 QTRAPmass spectrometer (MS) equipped with a TurboV electrospray ion source (Apllied Biosystems, Foster City, CA) was used to perform mass spectrometry. All regulated lipohilic toxins were analysed in both negative (-ESI) and positive polarity (+ESI) (García-Altares et al., 2013), selecting two product ions per toxin to allow quantification (the most intense transition) and confirmation; identification was supported by toxin retention time and the MRM ion ratios. Table S1 shows the MRM list used for DSP toxins quantification and for screening of the rest of regulated lipophilic toxins.

The quality control criteria stated by the EURLMB SOP (EURLMB, 2011) regarding resolution, limits of quantification (LOQs) and linearity was checked in every batch. Resolution (*Rs*) between the isomers OA and DTX-2 was calculated according to the following equation:

$$R_s = 2\,(t_{R(DTX\text{-}2)} - t_{R(OA)})/(W_{(OA)} + W_{(DTX\text{-}2)})$$

where t_R means retention time and W means peak width (both in min). The EURLMB request resolution between OA and DTX-2 to be greater than one (EURLMB, 2011).

Phytoplankton concentrates and the certified mussel sample were injected in duplicate. A preliminary screening was perfomed before accurate quantification. An external standard calibration curve was prepared with a six level curve (from 4 to

40 ng toxin/mL for OA, DTX-1 and DTX-2 and from 5-50 ng toxin/mL for PTX-2) to quantify samples with estimated OA, DTX-1, DTX-2 and/or PTX-2 below 40 ng/mL. Samples with concentrations above 40 ng toxin/mL for OA, DTX-1 and DTX-2 and above 50 ng PTX-2/mL were diluted to fall into the calibration range.

The correlation coefficients (r^2) of the quantification curves had to be greater than 0.98 to ensure linearity and the deviation of the slopes between consecutive calibration curves has to be lower than 25% to be considered as acceptable. The intermediate precision was expressed as the relative standard deviation (RSD in %) and could not exceed 25% among the injection replicates.

2.6. Phytoplankton identification and quantification

The taxonomic identification of phytoplankton according to morphology was performed by light microscopy. Phytoplankton cells were counted according to the Utermöhl method with a Nikon or Leica DMIL inverted microscope settling 50 mL in Hydrobios chambers (Utermöhl, 1931). The entire surface of the chamber was counted at 100-200x magnification to quantify microalgae cell abundance (cells/L).

2.7. Single-cell isolation, PCR amplification and DNA sequencing

Single cells of *Dinophysis* were isolated from seawater samples collected in Masnou (Catalonia) using a microcapillary pipette under an inverted microscope (Leica DMIL) and washed by repeatedly transferring to drops of sterile filtered seawater, following the procedure of Ki et al. (2004). Afterwards, DNA extraction based on proteinase K was performed using the Arcturus™ PicoPure™ DNA Extraction Kit (Applied Biosystems, CA, USA). Following the manufacturer's instructions, 10 µL of Extraction Solution were added to the samples, which were incubated at 65 °C for 3 hours, followed by 10 min at 95 °C to inactivate proteinase K.

The mitochondrial cytochrome oxidase (mt *cox1*) gene was amplified from all cells using the Dinocox1F/Dinocox1R (5-AAAAATTGTAATCATAAACGCTTAGG-3/5-TGTTGAGCCACCTATAGTAAACATTA-3) pair of primers (Raho et al., 2013). Each 25 µL reaction mixture contained 1mM dNTP, 3 mM $MgCl_2$, 1 µM of each primer, 1 U of Taq polymerase and 2 µL of template DNA. Amplifications were carried out in an Eppendorf Mastercycler nexus gradient as follows: an initial denaturation step of 5 min at 94 °C, 40 cycles of 1 min at 94 °C, 1 min at 55 °C and 3 min at 72 °C, and a final extension step of 10 min at 72 °C. Each PCR reaction was checked by agarose gel electrophoresis visualised with ethidium bromide. PCR products were purified with QIAquick PCR Purification Kit and bidirectionally sequenced (Sistemas

Genómicos, LLC, Valencia, Spain), using the same primers as those applied in the amplification. Consensus sequences obtained from both reads for each strain were manually edited using BioEdit v7.0.5.2 to remove primer sequences and terminal artefacts (Hall, 1999). The mt *cox1* sequences obtained in this study were deposited in GenBank under accession numbers: KY849911-KY849921.

2.8. Phylogenetic analysis

Consensus sequences (mt *cox1*) were compared to those available in GenBank (NCBI) using the Basic Local Alignment Search Tool (BLAST) algorithm to compare similarity of sequences collected in this study to known sequences with a high similarity from GenBank for phylogenetic analysis. To obtain the phylogenetic tree, the obtained sequences were aligned using the ClustalW algorithm in BioEdit v7.0.5.2 with validated *Dinophysis* sequences from GenBank. Evolutionary analyses were conducted in MEGA v5 (Tamura et al., 2011). All codon positions were included and all ambiguous positions were removed for each sequence pair, using a final dataset of 864 nucleotide positions. The evolutionary history was inferred using the Maximum-Likelihood method (Felsenstein, 1981). The percentage of replicate trees in which the associated taxa clustered together in the bootstrap test (1,000 replicates) was calculated (Felsenstein, 1985). The evolutionary distances were computed using the Kimura 2-parameter model and are in the units of the number of base substitutions per site (Kimura, 1980).

2.9. Data analysis

Measurements were performed in triplicate in immunoassay approaches and in duplicate in LC-MS/MS analysis. The immunoassay calibration curves were fitted using a sigmoidal logistic four-parameter equation. The linear regression model was used to evaluate the correlation between OA equiv. content in the particulate fraction of seawater samples determined with the monothiol and dithiol SAM-based immunoassays and the values obtained from the LC-MS/MS analysis, and to study the correlation between *Dinophysis* cell abundance and OA equiv. content. To evaluate differences between quantifications provided by the monothiol SAM-based immunoassay, the dithiol SAM-based immunoassay and LC-MS/MS analysis, a one-way analysis of variance was conducted. Prior to the analysis, normality and equal variance tests were performed. Differences in the results were considered statistically significant at the 0.05 level. SigmaStat software package 3.1 was used for statistical analysis.

3. Results and discussion

3.1. Monothiol and dithiol SAM-based immunoassay calibration curves

A competitive indirect immunoassay for OA was performed on maleimide plates, modifying the format reported by Reverté et al. for tetrodotoxin (Reverté et al., 2015). At a pH of 6.5-7.5, maleimides react with free sulfhydryl groups forming stable thioether linkages. Thus, monothiol or dithiol were used to covalently immobilise OA in an ordered and well-oriented manner through the formation of SAMs. Whereas the short monothiol provided a packed monolayer, the longer dithiol generated a spaced and more stable monolayer due to its multivalent mechanism of interaction (Fragoso et al., 2008). Checkerboard titrations and competitive immunoassays were first carried out to optimise the concentrations of OA, mAb and IgG-HRP in monothiol and dithiol approaches. The absorbance values obtained showed expected trends according to antigen and primary and secondary antibody concentrations. Dithiols provided higher absorbance values than monothiols, which can be explained by a higher spacing of the immobilised OA and a better recognition by the mAb. In both approaches, the lowest secondary antibody concentration tested provided the lowest non-specific adsorption values (e.g., 20 *vs.* 28% in the monothiol approach, and 10 *vs.* 25% in the dithiol SAM-based immunoassay) while maintaining reasonable absorbance values. Thus, 1/2,000 IgG-HRP dilution was selected for subsequent experiments. Under these conditions, although both approaches provided acceptable values of non-specific adsorption from the secondary antibody, the formation of long-chain SAMs and the incorporation of the polyethylene glycol molecules in the dithiol molecules clearly reduced the non-specific binding as compared with the monothiols (Frederix et al., 2004).

To select OA and mAb concentrations, competitive immunoassays were performed using different immobilised OA/mAb ratios. Calibration curves demonstrated that the competition between free and immobilised OA for mAb binding sites was successful. The curves were corrected with respect to the controls with no mAb and fitted to sigmoidal logistic four-parameter equations ($R = 0.999$ in the monothiol approach and $R = 1.000$ in the dithiol immunoassay). Whereas the amount of immobilised antigen had a small effect on the competition assay, slightly decreasing the sensitivity with lower OA concentrations (e.g. half maximal inhibitory concentration (IC_{50}) values of 7.9 *vs.* 10.9 ng/mL for 1 and 0.25 µM OA, respectively), lower mAb concentrations provided higher sensitivity (e.g. IC_{50} values of 49.9, 26.0 and 13.9 ng/mL for 1/500, 1/1,000 and 1/2,000 mAb dilution, respectively). Optimal performance was achieved using 0.5 µM OA and a 1/4,000 mAb dilution, with the monothiol and dithiol approaches providing equal analytical performance (Figure

3). Standard deviations (SD) were always lower than 10%. Limits of detection (LODs) of 2.4 ± 0.3 and 2.1 ± 0.2 ng/mL OA equiv. and working ranges up to 17.1 ± 0.6 and 16.6 ± 1.4 ng/mL OA equiv. were achieved for the monothiol and dithiol SAM-based immunoassays, respectively. Results were in the same order of magnitude as other OA immunoassays previously reported (Campàs et al., 2008; Chin et al., 1995; Dubois et al., 2010; Hayat et al., 2011; Kreuzer et al., 1999; Sassolas et al., 2013a; Shestowsky et al., 1992). The SAM-based strategy provides an oriented, ordered and specific OA sensing platform, avoiding the need to conjugate the toxin to protein carriers, whilst favouring the antigen-antibody recognition.

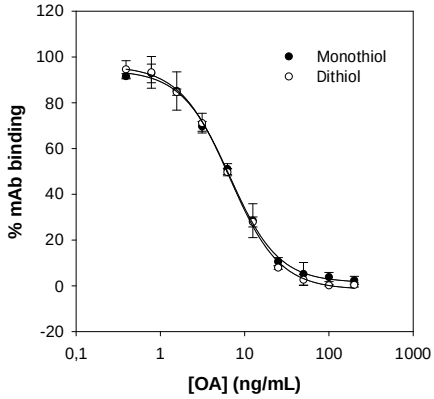

Figure 3. Calibration curves obtained using the monothiol and dithiol SAM-based immunoassays for OA detection. Inhibition is expressed as percentage of the control (no OA).

Besides detecting OA, an immunoassay for the detection of DSP toxins should also have the capability of recognising other OA group toxins that can also contribute to major contamination episodes. For this reason, the response to DTX-1 and DTX-2 with respect to OA was also evaluated. Cross-reactivity factors (CRFs) were calculated as the ratio of the IC_{50} value of the OA standard curve to the IC_{50} value of each analogue expressed in percentage. Although CRFs are mainly dependent on the intrinsic affinity of the antibody to recognise the different analogues, the immunospecies immobilisation strategy can also play an important role in the antigen-antibody interaction (Leonardo et al., 2017a). CRFs for DTX-1 and DTX-2 were 54% and 52% in the monothiol approach and 53% and 50% in the dithiol SAM-based immunoassay, respectively. It is important to take in mind that the reduction in immunoassay signal indicates competition, but does not indicate which toxin analogues are present in the samples. Thus, a global quantification of the sample

relative to OA is provided by the immunoassays. The establishment of CRFs contributes to better understand the comparisons between the quantifications provided by the immunochemical tools and those obtained by other analytical methods based on different recognition principles.

3.2. Seawater sample analysis

3.2.1. Seawater matrix effects

Prior to the analysis of seawater samples, OA calibration curves using extracts of filtered seawater (phytoplankton free) were performed to evaluate matrix effects on the immunoassays. Calibration curves were performed with pure seawater extracts and with 1/2, 1/4 and 1/8 dilutions in buffer. Matrix effects (mAb binding inhibition) were observed with pure seawater extracts, but they decreased as the matrix dilution increased, and were negligible for 1/4 extract dilutions or lower. Correction factors (CFs) were established as the ratio of the IC_{50} value of the OA standard curve in each extract dilution to the IC_{50} value of the OA standard curve in buffer. CFs for pure, 1/2 and 1/4 matrix dilutions were 0.42, 0.71 and 0.92 for the monothiol SAM-based immunoassay, and 0.43, 0.81 and 0.96, for the dithiol configuration. Taking into account the CFs, the effective LOD (eLOD) was calculated to be 1.0 and 0.9 ng/mL OA equiv. for monothiol and dithiol SAM-based immunoassays, respectively.

3.2.2. Analysis of seawater samples from Catalan harbours (Masnou and Sitges)

Toxin content. The OA equiv. content in the particulate fraction of seawater samples collected at different depths in different points of Sitges and Masnou harbours was determined by the SAM-based immunoassays as well as by LC-MS/MS analysis. LC-MS/MS analysis revealed that OA was the only DSP toxin present in the samples (limit of quantification (LOQ) = 4 ng/mL). Quantifications provided by the immunoassays —after applying the CFs— were compared with those provided by the LC-MS/MS reference method. Both immunoassays showed good correlation with the LC-MS/MS method ($y_{monothiol} = 1.056\,x - 2.276$, $R^2 = 0.992$, $y_{dithiol} = 0.995\,x - 1.632$, $R^2 = 0.991$) (Figure 4). OA was detected in all samples by the three approaches, reaching values up to 38 ng/mL in Sitges and 45 ng/mL in Masnou.

The presence of other lipophilic toxins outside of the OA group of toxins was also evaluated by LC-MS/MS. YTX, hYTX, AZAs, SPX-1, GYM-A and PnTX-G were not present in the particulate fraction of seawater samples. However, all samples from

Masnou and Sitges harbours contained high levels of PTX-2 in the particulate matter of seawater, in some cases more than 12-fold higher compared with OA concentration. Since no significant differences were observed in the OA quantifications of the samples determined by the monothiol SAM-based immunoassay, the dithiol SAM-based immunoassay and LC-MS/MS analysis (P = 0.358), it is safe to affirm the lack of interferences from other non-DSP lipophilic toxins, as expected from previous works (Stewart et al., 2009b).

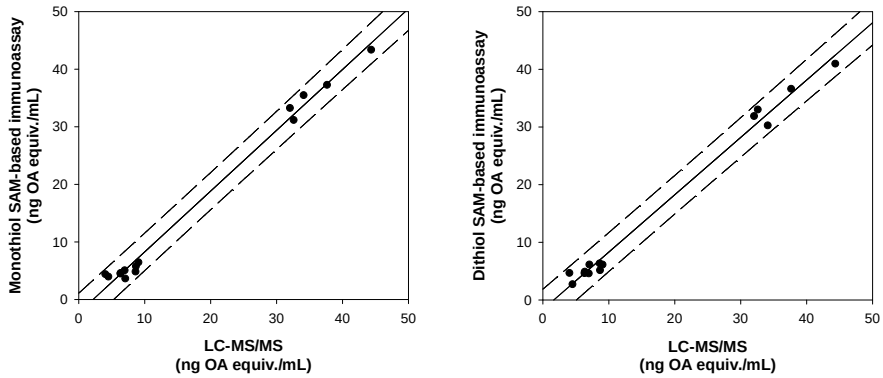

Figure 4. Linear regressions for the correlations between OA quantifications by the monothiol and dithiol SAM-based immunoassays and by LC-MS/MS analysis of seawater samples from the Catalan harbours. Dashed lines represent the 95% prediction intervals.

Phytoplankton identification. Cell contour –the size and shape of their large hypothecal plates– and the shape of the left sulcal lists and the ribs were the morphological features used for the taxonomic identification of *Dinophysis* species. Nevertheless, the morphological variability of *Dinophysis* species as a result of their polymorphic life cycle can lead to uncertain identification and quantification of phytoplankton samples, especially in those where two close species of *Dinophysis*, such as the pair *D. acuminata* and *D. sacculus*, co-occur (Reguera et al., 2012). On the Western Mediterranean coast, DSP events have been mainly related to blooms of *D. sacculus* (Giacobbe et al., 2000). Although no evidence of co-occurrence of *D. sacculus* with *D. accuminata* has been previously reported in the NW Mediterranean coast, *Dinophysis* cells with a wide range of different sizes and shapes were observed when analysing samples from Sitges and Masnou harbours. Most cells were attributed to *D. sacculus* by the comparison of morphologic formulae but some cells showed morphological characteristics close to *D.*

acuminata species. Thus, genetic information was required to provide a reliable identification.

Dinophysis cells labelled as *D.* cf. *acuminata* (5 cells) and as *D.* cf. *sacculus* (6 cells) were isolated from samples from the Catalan coast. To date, most molecular markers for dinoflagellates are based on ribosomal DNA (rDNA) genes and their ITS regions. However, due to the low variability of rDNA genes among *Dinophysis* species, mt *cox1* mitochondrial marker was used to discriminate among *Dinophysis* species within the "*D. acuminata* complex", which includes *D. acuminata* (and its small cell *D. skagi*) (Escalera and Reguera, 2008), *D. sacculus* and *D. ovum*. The mt *cox1* sequences isolated from the 11 *Dinophysis* cells showed high similarity. BLAST analyses showed that the sequences had a high degree of correlation with *D. sacculus* described in GenBank. The optimal mt *cox1* tree, including 19 nucleotide sequences, with the highest log likelihood (-1459.3415), is shown in Figure S1. The phylogenetic results confirm that the 11 isolated *Dinophysis* cells were clustered into a well-supported group, which corresponds to *D. sacculus*. Thus, *Dinophysis* cells initially labelled as *D.* cf. *acuminata* were actually *D. sacculus*, although intra-specific differences in morphology were identified by light microscopy.

From all samples, only one contained levels below the *Dinophysis* spp. abundance threshold of 500 cells/L established in the monitoring program of the Catalan coast as an early warning parameter. Whilst in Masnou values ranged from 280 cells/L to 5,160 cells/L of *D. sacculus*, in Sitges values ranged from 560 cells/L to 8,600 cells/L.

The dinoflagellate *Alexandrium minutum* was also detected in seawater samples from both harbours, with concentrations up to 687 cells/L in Sitges and from 238,980 cells/L to 3,785,000 cells/L in Masnou. *Pseudo-nitzchia* spp. cells were observed in high amounts, reaching values up to 53,703 cells/L in Masnou and 2,977 cells/L in Sitges.

Correlation between toxin content and cell abundance. OA concentration in the particulate fraction of seawater increased as the number of *D. sacculus* cells increased in seawater samples. Although *A. minutum* and diatom cells were in some cases detected at concentrations even higher than *D. sacculus*, the presence of these microalgae did not affect the OA detection (no significant differences were observed between the quantifications provided by the imunoassays and LC-MS/MS analysis). Strong correlations between the OA equiv. content determined by the monothiol ($R = 0.914$, $p < 0.0001$) and the dithiol ($R = 0.933$, $p < 0.0001$) immunoassays and *D. sacculus* cell abundance were observed (Figure S2). Concentrations of OA per cell during the *D. sacculus* bloom ranged from 1 to 11 pg OA/cell. A strong linear correlation between PTX-2 concentration (determined by

LC-MS/MS) and the presence of *D. sacculus* was also observed (R = 0.940, $p < 0.0001$), with concentrations ranging from 20 to 96 pg PTX-2/cell. Results are in agreement with previous studies about toxin profiles of *D. sacculus* in the NW Mediterranean (García-Altares et al., 2016).

3.2.3. Analysis of seawater samples from the Galician Rias

Toxin content. The particulate fraction of seawater samples collected once a week from March to July 2015 in Bueu (Galicia) were analysed by the SAM-based immunoassays and LC-MS/MS to determine the concentration of OA in phytoplankton. The Galician Northern Rias are one of the largest mussel production areas in the world that suffers from high incidences of DSP toxins, leading to lengthy closures that affect shellfish producers and have a high economic impact. Thus, it was not surprising that OA equiv. were detected in all samples analysed, from trace amounts (~1 ng OA equiv./mL) to approximately 500 ng OA equiv./mL. Two OA equiv. content peaks were clearly observed, the biggest one coinciding with samples collected from mid-April to mid-May (and reaching 500 ng/mL of OA equiv. the 5th of May) and a smaller peak starting at the end of June 2015 and reaching its maximum level of 114 ng/mL the 6th of July 2015. LC-MS/MS analysis revealed that OA was the only regulated lipophilic toxin present in the sample. Excellent correlations of the quantifications provided by the monothiol ($y_{\text{monothiol}} = 1.03\,x - 0.983$, $R^2 = 0.999$) and the dithiol ($y_{\text{dithiol}} = 0.951\,x - 1.193$, $R^2 = 0.997$) SAM-based immunoassays with LC-MS/MS analysis were obtained (Figure 5). No significant differences were observed between the three strategies (P = 0.970).

SAM-based immunoassays were also applied to the analysis of the picoplankton fraction (0.7-2.7 µm) of seawater samples. It is interesting to note that OA equiv. were detected in 5 out of the 20 samples analysed, coinciding with the two peaks observed in the analysis of phytoplankton particulate fraction (>2.7 µm), and representing up to 20% of the total OA equiv. content. Results were validated with LC-MS/MS analysis, showing non-significant differences with the results obtained by the monothiol and dithiol SAM-based immunoassays (P = 0.997), and confirming the presence of OA (and none of its analogues or other lipophilic toxins). These results highlight the possible presence of OA associated with picoplankton and/or organic aggregates, making evident its contribution in the total DSP toxins content in seawater (Pizarro et al., 2013).

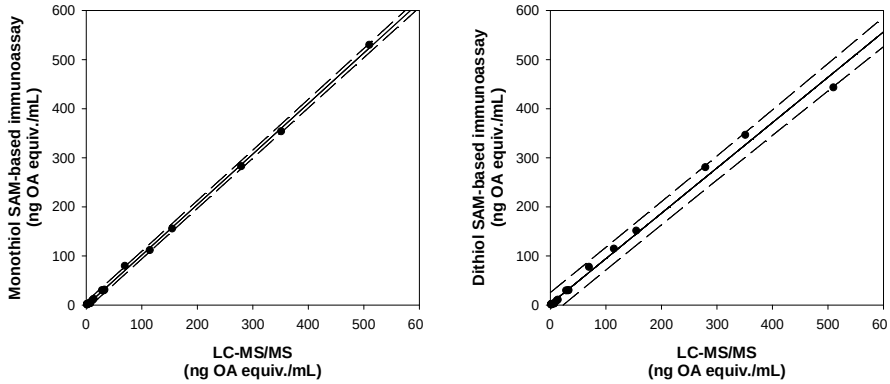

Figure 5. Linear regressions for the correlations between OA quantifications by the monothiol and dithiol SAM-based immunoassays and by LC-MS/MS analysis of seawater samples from the Galician Rías. Dashed lines represent the 95 % prediction intervals.

Phytoplanckton identification. As expected, *D. acuminata*, the main agent of DSP events on European Atlantic coasts (Reguera et al., 2014), was the principal phytoplankton species found in seawater samples from Galicia. Two main *D. acuminata* blooms were clearly evidenced, the largest one starting in mid-April to mid-May and reaching 10,760 cells/L the 27th of April, and the second bloom that lasted from mid to end of June and reached a maximum cell content of 3,080 cells/L. *D. skagi* and *P. rotundatum* were also detected in low abundance in a few samples. High amounts of other dinoflagellates (from 1,705 cells/L to 81,175 cells/L) and diatom cells (from 8,950 cells/L to 2,793,718 cells/L) were observed in all seawater samples.

Correlation between toxin content and cell abundance. In general, the OA concentration in the particulate fraction of sewater increased as total *Dinophysis* cell abundance in seawater samples increased. Appropriate correlations between OA content determined by the monothiol ($R = 0.874$, $p < 0.0001$) and the dithiol ($R = 0.879$, $p < 0.0001$) SAM-based immunoassays and total *Dinophysis* cells were obtained (Figure S3). When toxin content per cell was calculated, concentrations of OA ranged from less than 1 pg/cell to 466 pg/cell. The temporal representation of total *Dinophysis* cell abundance and OA content showed that OA peaks appeared 1-2 weeks later than *Dinophysis* blooms (Figure 6), explaining the variability in the OA content per cell (García-Altares et al., 2016). It is important to keep in mind that toxins are secondary metabolites that result from a balance between rates of toxin production, toxin excretion and division of *Dinophsysis* cells. Imbalances between these processes may lead to a very low accumulation rate of toxins (if either division

or toxin release rates are high) or high accumulation rates (if division stops and toxin production continues).

Although setting *Dinophysis* alert levels could be efficient enough to warn against the presence of OA, it has been demonstrated that the risk of shellfish toxicity can persist even when cell abundance is below the threshold. Hence, OA detection in seawater samples provides an alternative in monitoring programs for early warning of DSP toxins.

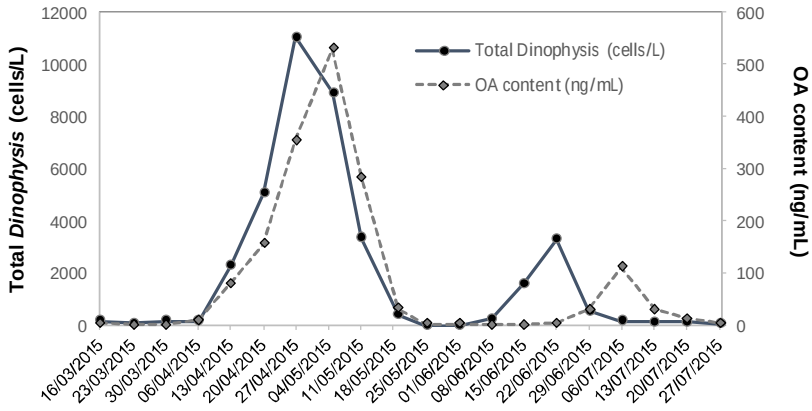

Figure 6. Temporal representation of total *Dinophysis* cell abundance and OA content in seawater samples from the Galician Rías.

3.3. Analysis of mussel samples

A certified reference material (CRM) from naturally contaminated mussel tissues containing certified contents of OA, DTX-1 and DTX-2 was analysed. The influence of matrix effects on the response was evaluated using 2.5 mg/mL mussel tissue certified to contain no DSP toxins, and the effect was observed to be negligible. Thus, the CRM-DSP-Mus-c extract was diluted to 2.5 mg/mL to obtain toxin values that fall into the calibration curve for its quantification. Taking into account the presence of DTX-1 and DTX-2 in the mussel sample in addition to the OA content, CRFs for both analogues were applied to the concentrations provided by the NRC certificate and LC-MS/MS analysis (Table 1). Following the application of the corresponding CRFs to DTX-1 and DTX-2 individual concentrations, correlations between OA equiv. content obtained by the monothiol and dithiol SAM-based immunoassays and the values provided by NRC were 97% and 99%, respectively. When comparing the quantifications of the monothiol and dithiol approaches with

those obtained in LC-MS/MS analysis, correlations were 104% and 106%, respectively.

Additionally to OA, DTX-1 and DTX-2, bivalve molluscs may contain esterified forms of the OA-group toxins (DTX-3), which are believed to be produced by the acylation of OA and analogues in the bivalves (Reguera et al., 2014). Thus, an alkaline reaction was performed on mussel extracts to hydrolyse the OA-group acyl esters and thus detect their possible presence. The hydrolysed sample was also diluted to 2.5 mg/mL. The prior analysis of the hydrolysed negative control discarded possible solvent effects. Again, CRFs were applied to post-hydrolysis NRC and LC-MS/MS values, and results were compared with those provided by the immunoassays (Table 1). In this case, correlations were 105 % and 107 % for the monothiol and dithiol SAM-based immunoassays, respectively, compared with NRC values, and 99 % and 100 % when comparing with LC-MS/MS analysis.

Both SAM-based immunoassays provided OA equiv. contents in good agreement with the certified and LC-MS/MS values, both before and after sample hydrolysis. Thus, the lack of interference from other marine toxins such as domoic acid (DA) or epiDA, also present in the mussel tissues, was again demonstrated.

Table 1. DSP toxins concentrations (µg toxin/kg mussel) of a mussel tissue certified reference material for okadaic acid and dinophysistoxins (CRM-DSP-Mus-c) and comparison between the reference values (NRC values), the quantifications provided by LC-MS/MS and those obtained by the dithiol and monothiol SAM-based immunoassays.

	NRC values					**LC-MS/MS**					**SAM-based immunoassays**	
	OA	DTX-1	DTX-2	OA equiv. *(applying CRFs)*		OA	DTX-1	DTX-2	OA equiv. *(applying CRFs)*		OA equiv.	
				Monothiol	Dithiol				Monothiol	Dithiol	Monothiol	Dithiol
Before hydrolisis	1,070	1,070	860	**2,095**	**2,067**	992	1,026	776	**1,950**	**1,924**	**2,024**	**2,042**
Post-hydrolisis	2,400	1,100	2,200	**4,138**	**4,083**	2,655	927	2,384	**4,396**	**4,338**	**4,350**	**4,357**

4. Conclusions

The self-assembling of both monothiols and dithiols on maleimide plates allows an ordered and optimally-oriented immobilisation of OA, providing colorimetric immunoassays with similar analytical performance. Whilst the use of dithiols enables a higher spacing of the immobilised immunospecies and reduces non-specific binding compared with monothiols, the use of monothiols such as cysteamine decreases the cost of the assay. The application of both immunoassays to the analysis of seawater samples and also contaminated shellfish samples has been successfully demonstrated. The SAM-based immunoassays provide powerful analytical tools that accomplish the major requirements to be implemented in monitoring programs as they are reliable, easy to perform and cost-effective methods that allow the detection of all DSP toxins in a selective way. Moreover, their high-throughput design allows multiple samples to be analysed in a matter of hours.

Although a good correlation between *Dinophysis* cell abundance and OA detection has been observed, it has been demonstrated that the poisoning risk can persist even when cell abundance is low. Thus, OA detection in the particulate fraction of seawater by SAM-based immunoassays constitutes a viable alternative to the monitoring of *Dinophysis* levels. The implementation of the SAM-based immunoassays to research programs will clearly contribute to set the basis for further investigation aimed to improve the allocation of monitoring efforts to protect the marine environment in production areas and guarantee seafood safety.

Acknowledgements

The authors acknowledge financial support from the Ministerio de Economía, Industria y Competitividad through the SEASENSING (BIO2014-56024-C2-2-R) project and the Instituto Nacional de Investigación y Tecnología Agraria y Alimentaria (INIA) through the PROMAQUA project (RTA2013-00096-00-00). The authors also acknowledge support from CERCA Programme / Generalitat de Catalunya and Pol Picón and Charlotte Steiner for their help in the preparation and analysis of seawater sample extracts. Sandra Leonardo and Anna Toldrà acknowledge IRTA – Universitat Rovira i Virgili – Banco Santander for their PhD grants (2013PIPF URV-IRTA-BS-01 and 2015PMF-PIPF-67).

References

Campàs, M., de la Iglesia, P., Le Berre, M., Kane, M., Diogène, J., Marty, J.-L., 2008. Enzymatic recycling-based amperometric immunosensor for the ultrasensitive detection of okadaic acid in shellfish. Biosensors & Bioelectronics 24, 716-722.

Campàs, M., Garibo, D., Prieto-Simón, B., 2012. Novel nanobiotechnological concepts in electrochemical biosensors for the analysis of toxins. Analyst 137, 1055-1067.

Campàs, M., Prieto-Simón, B., Marty, J.L., 2007. Biosensors to detect marine toxins: Assessing seafood safety. Talanta 72, 884-895.

Chin, J.D., Quilliam, M.A., Fremy, J.M., Mohapatra, S.K., Sikorska, H.M., 1995. Screening for okadaic acid by immunoassay. Journal of Aoac International 78, 508-513.

Dubois, M., Demoulin, L., Charlier, C., Singh, G., Godefroy, S.B., Campbell, K., Elliott, C.T., Delahaut, P., 2010. Development of ELISAs for detecting domoic acid, okadaic acid, and saxitoxin and their applicability for the detection of marine toxins in samples collected in Belgium. Food Additives and Contaminants Part a-Chemistry Analysis Control Exposure & Risk Assessment 27, 859-868.

Eberhart, B.-T.L., Moore, L.K., Harrington, N., Adams, N.G., Borchert, J., Trainer, V.L., 2013. Screening tests for the rapid detection of diarrhetic shellfish toxins in Washington State. Marine Drugs 11, 3718-3734.

Escalera, L., Reguera, B., 2008. Planozygote division and other observations on the sexual cycle of several species of Dinophysis (Dinophyceae, Dinophysiales). Journal of Phycology 44, 1425-1436.

EURLMB, 2011. European Union Reference Laboratory for Marine Biotoxins. Interlaboratory Validation Study of the EU-Harmonised SOP-LIPO-LC-MS/MS.

European Commission, 2004. Regulation (EC) No 853/2004. Off. J. Eur. Union L 226 (22).

European Comission, 2011. Regulation (EC) No 15/2011. Off. J. Eur. Union L 6 (3).

Felsenstein, J., 1981. Evolutionary trees from DNA sequences: a maximum likelihood approach. J. Mol. Evol. 17, 368-379.

Felsenstein, J., 1985. Confidence-limits on phylogenies - An approach using the Bootstrap. Evolution 39, 783-791.

Fragoso, A., Laboria, N., Latta, D., O'Sullivan, C.K., 2008. Electron permeable self-assembled monolayers of dithiolatedaromatic scaffolds on gold for biosensor applications. Analytical Chemistry 80, 2556-2563.

Frederix, F., Bonroy, K., Reekmans, G., Laureyn, W., Campitelli, A., Abramov, M.A., Dehaen, W., Maes, G., 2004. Reduced nonspecific adsorption on covalently immobilized protein surfaces using poly(ethylene oxide) containing blocking agents. Journal of Biochemical and Biophysical Methods 58, 67-74.

García-Altares, M., Casanova, A., Fernández-Tejedor, M., Diogène, J., de la Iglesia, P., 2016. Bloom of Dinophysis spp. dominated by D. sacculus and its related diarrhetic shellfish poisoning (DSP) outbreak in Alfacs Bay (Catalonia, NW Mediterranean Sea): Identification of

DSP toxins in phytoplankton, shellfish and passive samplers. Regional Studies in Marine Science 6, 19-28.

García-Altares, M., Diogène, J., de la Iglesia, P., 2013. The implementation of liquid chromatography tandem mass spectrometry for the official control of lipophilic toxins in seafood: Single-laboratory validation under four chromatographic conditions. Journal of Chromatography A 1275, 48-60.

Gerssen, A., Mulder, P.P.J., McElhinney, M.A., de Boer, J., 2009. Liquid chromatography-tandem mass spectrometry method for the detection of marine lipophilic toxins under alkaline conditions. Journal of Chromatography A 1216, 1421-1430.

Giacobbe, M.G., Penna, A., Ceredi, A., Milandri, A., Poletti, R., Yang, X., 2000. Toxicity and ribosomal DNA of the dinoflagellate Dinophysis sacculus (Dinophyta). Phycologia 39, 177-182.

Gonzalez-Romero, R., Suarez-Ulloa, V., Rodriguez-Casariego, J., Garcia-Souto, D., Diaz, G., Smith, A., Pasantes, J.J., Rand, G., Eirin-Lopez, J.M.., 2017. Effects of Florida Red Tides on histone variant expression and DNA methylation in the Eastern oyster *Crassostrea virginica*. Aquatic Toxicology 186, 196-204.

Hall, T.A., 1999. BioEdit: a user-friendly biological sequence alignment editor and analysis program for windows 95/98/NT. Nucleic Acids Symposium Series 41, 95-98.

Hayat, A., Barthelmebs, L., Marty, J.-L., 2011. Enzyme-linked immunosensor based on super paramagnetic nanobeads for easy and rapid detection of okadaic acid. Analytica Chimica Acta 690, 248-252.

Ki, J.S., Jang, G.Y., Han, M.S., 2004. Integrated method for single-cell DNA extraction, PCR amplification, and sequencing of ribosomal DNA from harmful dinoflagellates Cochlodinium polykrikoides and Alexandrium catenella. Marine Biotechnology 6, 587-593.

Kimura, M., 1980. A simple method for estimating evolutionary rates of base substitutions through comparative studies of nucleotide-sequences. Journal of Molecular Evolution 16, 111-120.

Kreuzer, M.P., O'Sullivan, C.K., Guilbault, G.G., 1999. Development of an ultrasensitive immunoassay for rapid measurement of okadaic acid and its isomers. Analytical Chemistry 71, 4198-4202.

Kreuzer, M.P., Pravda, M., O'Sullivan, C.K., Guilbault, G.G., 2002. Novel electrochemical immunosensors for seafood toxin analysis. Toxicon 40, 1267-1274.

Lindahl, O., Lundve, B., Johansen, M., 2007. Toxicity of Dinophysis spp. in relation to population density and environmental conditions of the Swedish west coast. Harmful Algae 6 (2), 218-231.Leonardo, S., Rambla-Alegre, M., Samdal, I.A., Miles, C.O., Kilcoyne, J., Diogène, J., O'Sullivan, C.K., Campàs, M., 2017a. Immunorecognition magnetic supports for the development of an electrochemical immunoassay for azaspiracid detection in mussels. Biosensors and Bioelectronics 92, 200-206.

Leonardo, S., Toldrà, A., Campàs, M., 2017b. Trends and prospects on electrochemical biosensors for the detection of marine toxins. Comprehensive Analytical Chemistry.

MacKenzie, L., Beuzenberg, V., Holland, P., McNabb, P., Suzuki, T., Selwood, A., 2005. Pectenotoxin and okadaic acid-based toxin profiles in Dinophysis acuta and Dinophysis acuminata from New Zealand. Harmful Algae 4, 75-85.

Mountfort, D.O., Suzuki, T., Truman, P., 2001. Protein phosphatase inhibition assay adapted for determination of total DSP in contaminated mussels. Toxicon 39, 383-390.

Pizarro, G., Morono, A., Paz, B., Franco, J.M., Pazos, Y., Reguera, B., 2013. Evaluation of passive samplers as a monitoring tool for early warning of dinophysis toxins in shellfish. Marine Drugs 11, 3823-3845.

Raho, N., Rodríguez, F., Reguera, B., Marín, I., 2013. Are the mitochondrial cox1 and cob genes suitable markers for species of Dinophysis Ehrenberg? Harmful Algae 28, 64-70.

Reguera, B., Riobó, P., Rodríguez, F., Díaz, P., Pizarro, G., Paz, B., Franco, J., Blanco, J., 2014. Dinophysis toxins: Causative organisms, distribution and fate in shellfish. Marine Drugs 12, 394.

Reguera, B., Velo-Suárez, L., Raine, R., Park, M.G., 2012. Harmful Dinophysis species: A review. Harmful Algae 14, 87-106.

Reverté, L., de la Iglesia, P., del Rio, V., Campbell, K., Elliott, C.T., Kawatsu, K., Katikou, P., Diogène, J., Campas, M., 2015. Detection of tetrodotoxins in puffer fish by a self-assembled mono layer-based immunoassay and comparison with surface plasmon resonance, LC-MS/MS, and mouse bioassay. Analytical Chemistry 87, 10839-10847.

Reverté, L., Prieto-Simón, B., Campàs, M., 2016. New advances in electrochemical biosensors for the detection of toxins: Nanomaterials, magnetic beads and microfluidics systems. A review. Analytica Chimica Acta 908, 8-21.

Sassolas, A., Catanante, G., Hayat, A., Stewart, L.D., Elliott, C.T., Marty, J.L., 2013a. Improvement of the efficiency and simplification of ELISA tests for rapid and ultrasensitive detection of okadaic acid in shellfish. Food Control 30, 144-149.

Sassolas, A., Hayat, A., Catanante, G., Marty, J.-L., 2013b. Detection of the marine toxin okadaic acid: Assessing seafood safety. Talanta 105, 306-316.

Shestowsky, W.S., Quilliam, M.A., Sikorska, H.M., 1992. An idiotypic antiidiotypic competitive immunoassay for quantitation of okadaic acid. Toxicon 30, 1441-1448.

Stewart, L.D., Elliott, C.T., Walker, A.D., Curran, R.M., Connolly, L., 2009a. Development of a monoclonal antibody binding okadaic acid and dinophysistoxins-1, -2 in proportion to their toxicity equivalence factors. Toxicon 54, 491-498.

Stewart, L.D., Hess, P., Connolly, L., Elliott, C.T., 2009b. Development and single-laboratory validation of a pseudofunctional biosensor Immunoassay for the detection of the okadaic acid group of toxins. Analytical Chemistry 81, 10208-10214.

Suarez-Ulloa, V., Gonzalez-Romero, R., Eirin-Lopez, J.M., 2015. Environmental epigenetics: A promising venue for developing next-generation pollution biomonitoring tools in marine invertebrates. Marine Pollution Bulletin 98, 5-13.

Suarez-Ulloa, V., Fernandez-Tajes, J., Aguiar-Pulido, V., Rivera-Casas, C., Gonzalez-Romero, R., Ausio, J., Mendez, J., Dorado, J., Eirin-Lopez, J.M., 2013a. The CHROMEVALOA database: a resource for the evaluation of Okadaic Acid contamination in the marine enviornment based

on the chromatin-associated transcriptome of the mussel Mytilus galloprovinciales. Marine Drugs 11, 830-841.

Suarez-Ulloa, V., Fernandez-Tajes, J., Manfrin, C., Gerdol, M., Venier, P., Eirin-Lopez, J.M., 2013b. Bivalve omics: state of the art and potential applications for the biomonitoring of harmful marine compounds. Marine Drugs 11, 4370-4389.

Tamura, K., Peterson, D., Peterson, N., Stecher, G., Nei, M., Kumar, S., 2011. MEGA5: Molecular evolutionary genetics analysis using maximum likelihood, evolutionary distance, and maximum parsimony methods. Molecular Biology and Evolution 28, 2731-2739.

Utermöhl, V.H., 1931. Neue Wege in der quantitativen Erfassung des Planktons. (Mit besondere Beriicksichtigung des Ultraplanktons). Verhandlungen der Internationalen Vereinigung für Theoretische und Angewandte Limnologie 5, 567-595.

Supplementary Information

Table S1. Transitions monitored, dwell times, declustering potentials (DP), entrance potentials (EP), collision cell entrance potentials (CEP) and collision energies (CE) for the detection of lipophilic marine toxins.

Toxin	Transitions (m/z)	Time (ms)	DP(V)	EP(V)	CEP (V)	CE(V)	CXP(V)	Precursor ion
OA and DTX-2	803.5 > 255.2 (MRM1)	100.0	-125.0	-10.5	-38.0	-64.0	-4.0	**$[M-H]^-$**
	803.5 > 113.1 (MRM2)	60.0	-115.0	-12.0	-40.0	-82.0	-2.0	
DTX-1	817.5 > 255.2 (MRM1)	100.0	-135.0	-9.0	-42.0	-68.0	-4.0	**$[M-H]^-$**
	817.5 > 113.1 (MRM2)	60.0	-130.0	-12.0	-40.0	-84.0	-2.0	
YTX	570.4 > 467.4 (MRM1)	100.0	-75.0	-4.0	-34.0	-40.0	-6.0	**$[M-2H]^{2-}$**
	570.4 > 396.4 (MRM2)	60.0	-80.0	-8.5	-40.0	-42.0	-4.0	
45-OHYTX	578.4 > 467.4 (MRM1)	100.0	-75.0	-4.0	-34.0	-40.0	-6.0	**$[M-2H]^{2-}$**
	578.4 > 396.4 (MRM2)	60.0	-80.0	-8.5	-40.0	-42.0	-4.0	
homoYTX	577.4 > 474.4 (MRM1)	100.0	-75.0	-11.0	-36.0	-38.0	-6.0	**$[M-2H]^{2-}$**
	577.4 > 403.4 (MRM2)	60.0	-85.0	-7.0	-50.0	-44.0	-4.0	
45-OH homoYTX	585.4 > 474.4 (MRM1)	100.0	-75.0	-11.0	-36.0	-38.0	-6.0	**$[M-2H]^{2-}$**
	585.4 > 403.4 (MRM2)	60.0	-85.0	-7.0	-50.0	-44.0	-4.0	

(Continued)

Toxin	Transitions (m/z)	Time (ms)	DP(V)	EP(V)	CEP (V)	CE(V)	CXP(V)	Precursor ion
SPX-1	692.5 > 444.2 (MRM1)	75.0	111.0	7.0	36.0	51.0	6.0	**$[M+H]^+$**
	692.5 > 426.3 (MRM2)	50.0	106.0	7.5	38.0	51.0	4.0	
PnTX-G	694.5 > 676.4 (MRM1)	75.0	111.0	7.5	32.0	43.0	4.0	**$[M+H]^+$**
	694.5 > 164.5 (MRM2)	50.0	116.0	8.5	32.0	65.0	4.0	
GYM-A	508.4 > 490.4 (MRM1)	75.0	71.0	9.0	26.0	33.0	6.0	**$[M+H]^+$**
	508.4 > 392.4 (MRM2)	50.0	71.0	8.0	28.0	45.0	4.0	
PTX-2	876.5 > 213.3 (MRM1)	75.0	71.0	7.0	48.0	53.0	4.0	**$[M+NH_4]^+$**
	876.5 > 823.5 (MRM2)	50.0	76.0	9.5	52.0	39.0	4.0	
PTX-1	892.5 > 213.3 (MRM1)	75.0	71.0	7.0	48.0	53.0	4.0	**$[M+NH_4]^+$**
	892.5 > 821.5 (MRM2)	50.0	76.0	9.5	52.0	39.0	4.0	
AZA-1	842.5 > 362.3 (MRM1)	75.0	91.0	10.0	46.0	73.0	4.0	**$[M+H]^+$**
	842.5 > 462.5 (MRM2)	50.0	96.0	8.5	44.0	59.0	6.0	
AZA-2	856.5 > 362.3 (MRM1)	75.0	76.0	12.0	48.0	67.0	4.0	**$[M+H]^+$**
	856.5 > 462.5 (MRM2)	50.0	86.0	10.0	44.0	59.0	6.0	

(Continued)

Toxin	Transitions (m/z)	Time (ms)	DP(V)	EP(V)	CEP (V)	CE(V)	CXP(V)	Precursor ion
AZA-3	828.5 > 362.3 (MRM1)	75.0	91.0	9.0	46.0	65.0	4.0	**$[M+H]^+$**
	828.5 > 448.5 (MRM2)	50.0	91.0	8.0	44.0	55.0	4.0	

Figure S1. Phylogenetic analysis of mitochondrial cytochrome oxidase (mt *cox1*) gene showing the relationship between *Dinophysis* sequences from this study (in bold) and other *Dinophysis* sequences from GenBank. Values at nodes are bootstrap values obtained by the Maximun-Likelihood method. Bootstrap values less than 30% are not shown. Scale bar is substitution per site.

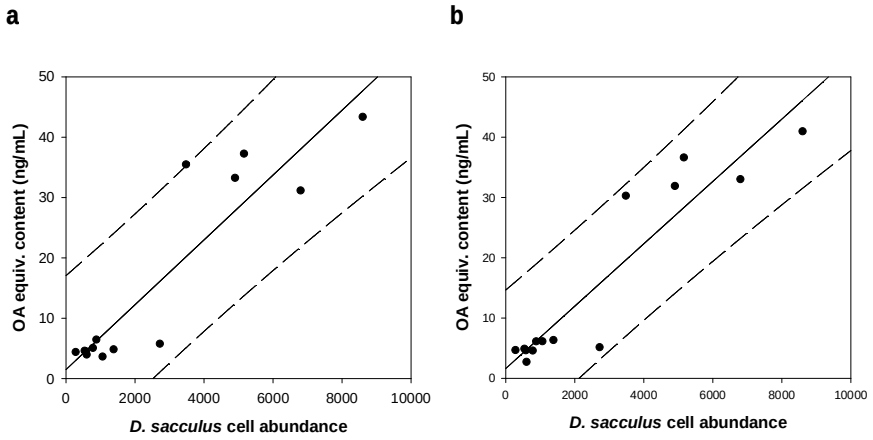

Figure S2. Linear regressions for the correlations between OA quantifications by the monothiol **(a)** and dithiol **(b)** SAM-based immunoassays and *D. sacculus* cell abundance in seawater samples from the Catalan harbours. Dashed lines represent the prediction intervals of 95%.

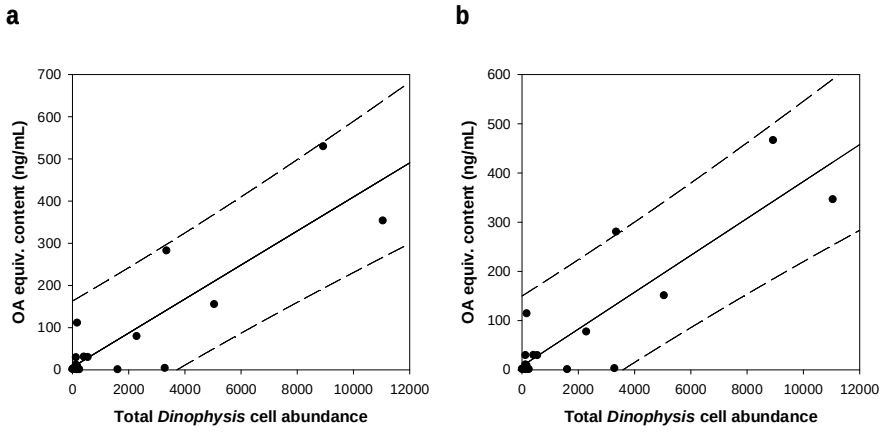

Figure S3. Linear regressions for the correlations between OA quantifications by the monothiol **(a)** and dithiol **(b)** SAM-based immunoassays and total *Dinophysis* cell abundance in seawater samples from the Galician Rías. Dashed lines represent the prediction intervals of 95%.

Development and validation of a maleimide-based enzyme-linked immunosorbent assay for the detection of tetrodotoxin in oysters and mussels

Laia Reverté[a], Maria Rambla-Alegre[a], Sandra Leonardo[a], Carlos Bellés[a], Katrina Campbell[b], Christopher T. Elliott[b], Arjen Gerssen[c], Mirjam D. Klijnstra[c], Jorge Diogène[a], Mònica Campàs[a]

[a]*IRTA, Carretera Poble Nou km 5.5, 43540 Sant Carles de la Ràpita, Tarragona, Spain*
[b]*Institute for Global Food Security, School of Biological Sciences, Queen's University, Stranmillis Road, Belfast BT9 5AG, Northern Ireland*
[c]*RIKILT (Institute of Food Safety) - Wageningen University and Research, 6700 AE, Wageningen, The Netherlands*

Abstract

The recent detection of tetrodotoxins (TTXs) in puffer fish and shellfish in Europe highlights the necessity to monitor the levels of TTXs in seafood by rapid, specific, sensitive and reliable methods in order to protect human consumers. A previous immunoassay for TTX detection in puffer fish, based on the use of self-assembled monolayers (SAMs) for the immobilization of TTX on maleimide plates (mELISA), has been modified and adapted to the analysis of oyster and mussel samples. Changing dithiol for cysteamine-based SAMs enabled reductions in the assay time and cost, while maintaining the sensitivity of the assay. The mELISA showed high selectivity for TTX since the antibody did not cross-react with co-occurring paralytic shellfish poisoning (PSP) toxins and no interferences were observed from arginine (Arg). Moreover, TTX-coated maleimide plates stored for 3 months at -20 °C and 4 °C were stable, thus when pre-prepared, the time to perform the assay is reduced. When analyzing shellfish samples, matrix effects and toxin recovery values strongly depended on the shellfish type and the sample treatment. Blank oyster extracts could be directly analyzed without solid-phase extraction (SPE) clean-up, whereas blank mussel extracts showed strong matrix effects and SPE and subsequent solvent evaporation were required for removal. However, the SPE clean-up and evaporation resulted in toxin loss. Toxin recovery values were taken as correction factors (CFs) and were applied to the quantification of TTX contents in the analysis of naturally contaminated shellfish samples by mELISA. The lowest effective limits of detection (eLODs) were about 20 and 50 µg/kg for oyster extracts without and with SPE clean-up, respectively, and about 30 µg/kg for mussel extracts with both protocols, all of

them substantially below the eLOD attained in the previous mELISA for puffer fish (230 µg/kg). Analysis of naturally contaminated samples by mELISA and comparison with LC-MS/MS quantifications demonstrated the viability of the approach. This mELISA is a selective and sensitive tool for the rapid detection of TTX in oyster and mussel samples showing promise to be implemented in routine monitoring programs to protect human health.

1. Introduction

Tetrodotoxin (TTX) is a potent low-molecular-weight (319 Da) marine neurotoxin, named for the family of fish Tetraodontidae [1]. Tetrodotoxin possesses a unique structure, consisting of a positively charged guanidine group connected to a highly oxygenated carbon backbone [1-3]. Although TTX was originally found in the ovaries of puffer fish [4], several marine organisms have been shown to contain the toxin such as blue-ring octopus, ribbon worms, starfish and xanthid crabs [5], as well as terrestrial animals such as frogs and newts [6]. Unlike many other marine toxins, which are of microalgal origin, TTX production is thought to be produced by bacteria of the genera *Pseudomonas, Shewanella, Alteromonas* or *Vibrio* [7], in symbiosis with certain animals [8]. Recently, the marine dinoflagellate *Prorocentrum minimum* has been described to produce TTXs in cultures, with possible implication of endosymbiotic bacteria [9]. Tetrodotoxin has the ability to selectively bind to voltage-gated sodium channels (VGSCs), blocking the influx of sodium ions into the nerve cells, affecting neuromuscular transmission [10]. The consumption of puffer fish contaminated with TTX may result in mild gastrointestinal effects, numbness, respiratory failure, and even in death [11]. Human intoxication has been reported worldwide, mainly caused by the ingestion of contaminated puffer fish, served in Japan as a delicacy known as “fugu” [8, 11]. A toxic species of puffer fish, *Lagocephalus sceleratus*, recently reached the Mediterranean through the Suez channel [12], resulting in new reports of food poisoning in the Western Mediterranean and further migration towards eastern waters [13-15]. In Europe, the first toxicity report related with TTX-contaminated shellfish occurred in Spain in 2007 and it was caused by the ingestion of contaminated trumpet shells, although the shellfish was bought in Portugal [16]. Since then, TTXs have been detected in bivalve shellfish in different parts of Europe, including England [17], Greece [18] and the Netherlands [19]. In humans, according to case studies, between 0.18 and 0.2 mg of TTX have been reported to cause severe symptoms, and a fatality was reported after ingestion of around 2 mg of TTX [20]. Despite the fact that TTX is a toxin with a high fatality rate and worldwide distribution, neither a reference method nor regulatory limits have been specifically set for TTX. Nevertheless, in

Japan a value of 2 mg TTX equiv./kg edible portion has been used as the acceptance criterion to consider puffer fish safe for consumption [21]. Moreover, in Europe, the Regulation (EC) no. 854/2004 stipulates that "fishery products derived from poisonous fish of the following families must not be placed on the market: Tetraodontidae, Molidae, Diodontidae and Canthigasteridae" [22]. Concern for TTX in Europe has been increasing, and just recently, the European Food Safety Authority has concluded that a concentration below 44 µg TTX equiv./kg shellfish meat, based on a large portion size of 400 g, is considered not to result in adverse effects in humans [19].

Given the occurrence of TTXs in European bivalve shellfish and the threat that this hazardous toxin poses to human health, the development of rapid, specific, sensitive, reliable and easy-to-use methods for their detection is a matter of utmost importance. Accordingly, several methods have been reported for the detection of TTXs, including immunoassays [23-33] and immunosensors [23, 34-41]. Although some of these immunochemical approaches have been applied to the analysis of puffer fish [32, 33, 36, 38, 40-41], newts [26], caddisflies [27], terrestrial flatworms [29], sea snails [38], urine [36] and milk/apple juice [37], none of them has been applied to the analysis of bivalve mollusks. Indeed, up to date only the LC-MS/MS method has been applied to the detection of TTXs in mussels and oysters [42, 43]. However, this technique requires trained personnel, sample pre-treatment and expensive equipment. Taking as a starting point an immunoassay previously developed for the determination of TTXs in puffer fish samples [33], the aim of this research was to illustrate the development of an improved bioanalytical tool for the analysis of oyster and mussel samples (Figure 1).

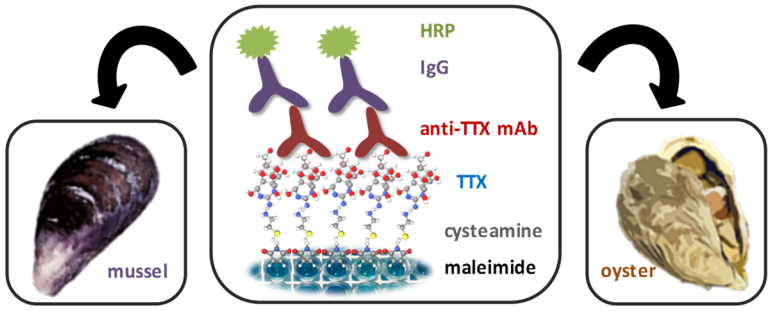

Figure 1. Scheme of the mELISA strategy developed for the detection of TTXs in oyster and mussels

2. Materials and methods

2.1. Reagents and solutions

For mELISA, pure TTX standard was purchased from Tocris Bioscience (Bristol, UK) and standard solutions were prepared at 1 mg/mL in 10 mM acetic acid (AA). For LC-MS/MS analysis, pure TTX standard was purchased from Latoxan (Valence, France) and standard solutions were prepared at 1 mg/mL in 350 mM AA. Certified reference materials (CRMs), specifically gonyautoxin 1&4 (GTX1&4), gonyautoxin 2&3 (GTX2&3), decarbamoyl gonyautoxin 2&3 (dcGTX2&3), gonyautoxin 5 (GTX5), neosaxitoxin (NEO), decarbamoyl neosaxitoxin (dcNEO), saxitoxin (STX), decarbamoyl saxitoxin (dcSTX) and N-sulfocarbamoyl gonyautoxin 2&3 (C1&2), were obtained from the National Research Council of Canada (NRC, Halifax, NS, Canada). The anti-TTX monoclonal antibody (mAb) TX-7F was produced as described in Kawatsu et al. [25]. Pierce maleimide-activated plates were obtained from Thermo Fisher Scientific (Madrid, Spain). Ammonium hydroxide solution (NH_4OH, 25%), amorphous graphitized polymer carbon Supelco ENVI-Carb 250 mg/3 mL cartridges, anti-mouse IgG (whole molecule)-horseradish peroxidase antibody produced in rabbit (IgG-HRP), L-arginine (Arg), bovine serum albumin (BSA), cysteamine hydrochloride, ethylenediaminetetraacetic acid (EDTA), formaldehyde solution, 4-morpholineethanesulfonic acid (MES) hydrate, potassium phosphate dibasic, potassium phosphate monobasic and 3,3',5,5'-tetramethylbenzidine (TMB) liquid substrate were all supplied by Sigma-Aldrich (Tres Cantos, Spain). HPLC-grade acetonitrile (ACN), glacial AA and methanol (MeOH) were obtained from Chem-lab (Zedelgem, Belgium). Formic acid (FA) (98-100%) was purchased from Merck (Darmstadt, Germany). Ultra LC-MS ACN, Ultra LC-MS MeOH and Ultra LC-MS H_2O were purchased from Actu-All (Oss, The Netherlands). Ultrapure Milli-Q water (18.2 $M\Omega/cm^2$) was used for the preparation of solutions (Millipore, Bedford, MA, USA).

2.2. Instrumentation

For toxin extraction, a water bath (model 6000138 600 W) purchased from J. P. Selecta S. A. (Barcelona, Spain), an Alegra X-15R centrifuge provided by Beckman Coulter (Barcelona, Spain) and a DVX-2500 multi-tube vortex mixer acquired at VWR International Eurolab S. L. (Barcelona, Spain) were used.

Extraction clean-up was performed with a Rapid Trace SPE workstation supplied by Caliper Life Sciences (Waltham, MA, USA).

Colorimetric measurements were performed with a Microplate Reader KC4 from BIO-TEK Instruments, Inc. with GEN 2.09 software (Winooski, VT, USA).

For LC-MS/MS analysis, the separation was performed on a Waters Acquity I-Class UPLC system (Waters, Milford, MA, USA) and mass spectrometric analysis on a Waters Xevo TQ-S (Waters, Milford, MA, USA).

2.3. Shellfish samples

For the evaluation of matrix effects and toxin recovery, Pacific oyster (*Crassostrea gigas*) and mussel (*Mytilus galloprovincialis)* samples from the Ebro Delta (Alfacs Bay, NW Mediterranean Sea) were used. These shellfish samples were determined as TTXs negative by LC-MS/MS analysis. For the analysis of naturally contaminated shellfish, three oyster (*Crassostrea gigas*) and three mussel (*Mytilus edulis*) samples were obtained from production sites at the Oosterschelde in The Netherlands.

2.4. mELISA protocol

The protocol was similar to that previously described by our group [33], with some modifications regarding the TTX immobilization. The first step was the self-assembling of 1 mM cysteamine in phosphate buffer for 3h, followed by the direct immobilization of TTX (2 µg/mL) with formaldehyde (3.4 %) in the same buffer overnight. A competitive assay was then performed by incubating 50 µL of free TTX/shellfish extract and 50 µL of 1:3,200 anti-TTX mAb dilution in 1% BSA-phosphate buffer for 30 min. A blocking step was then performed with 200 µL of 1% BSA-phosphate buffer for 30 min and, finally, 100 µL of IgG-HRP at 1:1,000 dilution in 1% BSA-phosphate buffer was incubated for 30 min. Colorimetric response was measured at 620 nm after 10 min of TMB liquid substrate incubation.

2.5. Storage stability of TTX-coated maleimide plates

Tetrodotoxin was immobilized through cysteamine self-assembled on maleimide-activated plates as described in the section above, and TTX-coated maleimide plates were kept at 4 °C and -20 °C. Absorbance values of wells with mAb (maximum response) and without mAb (background) in the absence of free TTX were measured in triplicate at day 0 (reference value) and during several weeks up to 3 months.

2.6. Interference study

The selectivity of the mELISA was assessed by the analysis of the following Paralytic Shellfish Poisoning (PSP) toxins: GTX1&4, GTX2&3, dcGTX2&3, GTX5, NEO, dcNEO, STX, dcSTX and C1&2, as well as L-arginine (Arg). A concentration of 100 ng/mL was

chosen taking into account that TTX almost completely inhibits the mAb binding. The protocol was the same as that explained in the mELISA protocol section, but replacing free TTX by PSP toxins or Arg prepared in 1% BSA-phosphate buffer in the competition step. Percentage of mAb binding was calculated with respect to the response obtained without toxin (maximum response).

2.7. Toxin extraction and SPE clean-up

For the analysis of toxins in shellfish by mELISA, extracts were obtained following the single dispersive procedure described in the literature [43] for other paralytic shellfish toxins, adapted to the amount of sample available. In brief: 1 g ± 0.1 g of shucked shellfish homogenate was weighed into a 15-mL tube and 1 mL of AA/H_2O (1:100, v:v) was added. After shaking the tube for 90 s on a multi-tube vortex mixer, samples were boiled in a water bath for 5 min at 100 °C. Tubes were then cooled and shaken again with the multi-vortex mixer for 90 s. Finally, samples were centrifuged at 4,500 rpm for 10 min, and the supernatants were filtered through 0.2-µm nylon filters and kept at -20 °C until analysis. The resulting extracts contained fresh shellfish matrix at a concentration of 1,000 mg equiv./mL.

For the clean-up of shellfish sample extracts, SPE was performed using graphitized polymer carbon ENVI-carb cartridges by adapting the automated protocol described by Boundy et al. [43]. Briefly, a 0.5-mL aliquot of the AA extract was transferred to a polypropylene tube and 1.25 µL of NH_4OH solution was added. The cartridges were conditioned with 3 mL of ACN/H_2O/AA (20:80:1, v:v:v), followed by 3 mL of H_2O/NH_4OH (1000:1, v:v). Then, 400 µL of sample extracts were loaded onto the conditioned cartridges and were washed with 700 µL of deionized H_2O. Finally, the retained TTX was eluted with 2 mL of ACN/H_2O/AA (20:80:1, v:v:v) and stored at -20 °C until analysis. Resulting extracts were at a shellfish matrix concentration of 200 mg equiv./mL. Further dilutions for mELISA experiments were performed in phosphate buffer. When required, shellfish sample extracts were evaporated for solvent exchange (from ACN/H_2O/AA to phosphate buffer).

Blank, TTX-spiked and naturally-contaminated shellfish sample extracts were analyzed by mELISA at 3 different stages: (1) after SPE clean-up, (2) after SPE clean-up, evaporation and solvent exchange, and (3) directly after toxin extraction (without SPE clean-up nor evaporation and solvent exchange). The matrix effects of blank samples were evaluated and the TTX contents obtained in spiked and naturally contaminated samples at each stage were determined.

2.8. LC-MS/MS analysis

For the analysis by LC-MS/MS, naturally-contaminated shellfish sample extracts were obtained as follows: 1 g of shellfish homogenate was accurately weighed, and 2 mL of H_2O/MeOH (50:50, v:v) containing 15 mM AA solution was added. First, TTX was extracted by a 15-min head-over-head extraction. The sample was then centrifuged for 10 min at 5,200 g and the supernatant was transferred to a volumetric tube. A second extraction was performed by adding 1.5 mL of extraction solvent and vortex mixing during 1 min. After centrifugation, the total volume was brought to 4 mL with the same extraction solvent. The extract was diluted 1:9 with ACN/H_2O (70:20, v:v) containing 6.7 mM AA. Subsequently, the diluted extract was centrifuged at 16,200 g during 5 min and the supernatant was transferred to a vial. For the construction of calibration curves, matrix-matched standards were prepared by spiking blank shellfish material with known concentrations of TTX, respectively 0, 20, 50, 75, 150 µg/kg.

Chromatographic separation was achieved using a UPLC system. The system consisted of a binary solvent manager, a sample manager and a column manager. The column temperature was at room temperature and the temperature of the sample manager was kept at 10 °C. For the analysis of TTX, a 10-µL injection volume was used. Mobile phase A was H_2O and B was ACN, both containing 50 mM FA. The analytical column used was a Tosoh Bioscience TSKgel Amide-80 column (250x2 mm, 5-µm particles). A flow rate of 0.2 mL/min was used. A gradient started at 30% A and after 1 min it was linearly increased to 95% A in 7.5 min. This composition was kept for 5 min and returned to 30% A in 0.5 min. An equilibration time of 6 min was allowed prior to the next injection. The effluent was directly interfaced in the electrospray ionization (ESI) source of the triple quadrupole mass spectrometer. The mass spectrometer operated in ESI positive ionization mode and two transitions for TTX were measured, *m/z* 320.1 > 162.1 and *m/z* 320.1 > 302.1.

2.9. Data analyses and statistics

Measurements were performed in triplicate for the mELISA experiments and singular in LC-MS/MS analysis. In the mELISA, calibration curves were background-corrected with respect to the controls with no mAb and adjusted to sigmoidal logistic four-parameter equations using SigmaPlot software 12.0 (Systat Software Inc., San José, CA, USA). From the equations, inhibitory concentrations (ICs) were calculated. Specifically, the midpoint (IC_{50}), the limit of detection (LOD) established as the IC_{20}, and the working range (IC_{20}-IC_{80}), were determined. In this work, the limit of quantification (LOQ) has been considered equal to the LOD.

To evaluate differences in the quantifications provided by the three approaches (mELISA with SPE clean-up/evaporated samples, mELISA with no SPE clean-up/not evaporated samples and LC-MS/MS analysis), a one-way analysis of variance was conducted using SigmaStat 3.1 software (Systat Software Inc., San José, CA, USA). Prior to the analysis, a normality and equal variance test was performed. Differences in the results were considered statistically significant at the 0.05 level.

3. Results and discussion

3.1. mELISA performance

Rapidity, low-cost and simplicity are key parameters for the success of immunoassays. To this purpose, the mELISA described previously elsewhere [33] was improved by using reagents readily available, reducing the protocol time and cost. The carboxylate-dithiol used for TTX-coating of the microtiter plate was replaced by cysteamine, which simplifies the protocol by eliminating 3 steps and shortens the analysis time by 90 min. Cysteamine can be readily purchased from different companies and it costs about 1,000-fold less than carboxylate-dithiol.

To enable the substitution of carboxylate-dithiol by cysteamine, the amount of cysteamine required for the SAM formation had to be determined, and according to the solubility of cysteamine, the solvent was changed from ethanol into an aqueous (phosphate) buffer. Thus, concentrations of 1, 10, 50 and 100 mM of cysteamine were tested in competition assays, using 2 µg/mL of TTX, 1:3,200 mAb dilution and 1:1,000 IgG-HRP dilution. All competitive assays showed appropriate trends according to the free TTX concentrations and provided similar IC_{50} values. Moreover, similar absorbance values were obtained for the positive (without free TTX) and negative (without mAb) controls, altogether indicating that 1 mM of cysteamine is a saturated concentration. Therefore, subsequent experiments were performed with 1mM cysteamine. Under the selected conditions, an IC_{50} of 8 ng/mL, an LOD, established as the IC_{20}, of 2 ng/mL and a working range (IC_{20}-IC_{80}) between 2 and 43 ng/mL were attained (Figure 2), with an *R* from the sigmoidal adjustment of 0.996. The standard deviation (SD) values for the calibration points were lower than 8% of the mAb binding signal. The LOD attained with the mELISA described herein was similar to that obtained with the previous mELISA (using carboxylate-dithiol). In contrast, a narrower working range was obtained in the mELISA using cysteamine with respect to the previous mELISA using dithiol (2-43 *vs.* 2-95 ng/mL, respectively). This difference is attributed to the higher sensitivity of the cysteamine-based mELISA. The LOD provided by the mELISA described herein was in accordance with other immunoassays reported for TTX (~2 ng/mL [23, 25, 33]) and lower than others (5 ng/mL [32] and 10 ng/mL [28]).

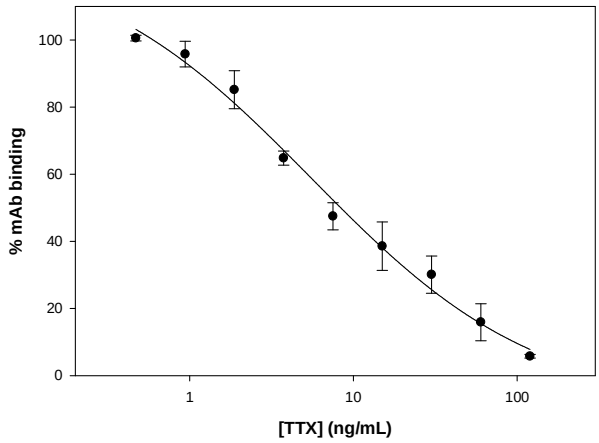

Figure 2. TTX calibration curve obtained by the improved mELISA. Response is expressed as mAb binding percentage, normalized to mAb signal when no TTX is present. Error bars represent the standard deviation values for 3 replicates.

Additionally, to investigate the possibility of further shortening the time of the mELISA protocol, the storage stability of TTX-coated maleimide plates at 4 and -20 °C was evaluated. The mAb binding signal was constant up to 3 months at both 4 °C and -20 °C, demonstrating the stability of the maleimide plates with immobilized TTX (Figure 3). The great stability of the TTX-coated plates significantly reduces the assay time, as multiple plates can be prepared on the same day and stored until use. Consequently, provided that TTX-coated plates are ready-to-use, the analysis of samples can be performed in less than 2 h on the same day, making a substantial improvement with respect to the previously reported mELISA [33]. Moreover, the preparation of multiple plates using the same solutions reduced the variability between assays, making the system more reproducible, particularly for a commercialization.

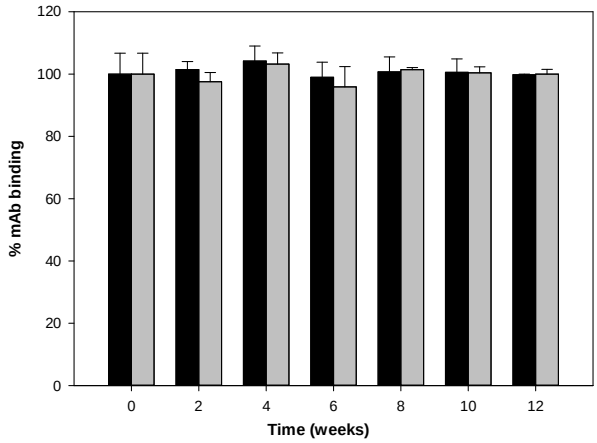

Figure 3. Storage stability of TTX-coated maleimide plates. Bars represent the % mAb binding obtained with plates stored at 4 °C (black bars) and at -20 °C (grey bars). Error bars represent the standard deviation values for 3 replicates.

3.2. Interference studies

The protocol applied for TTX extraction from shellfish is also adequate to extract PSP toxins. Therefore, the TTX extraction process may extract PSP toxins, if present. As a consequence, prior to the analysis of naturally-contaminated samples, it is necessary to ensure that potential PSP toxins will not interfere in the TTX immunoassay performance. With this aim, the possible recognition of several PSP toxins (GTX1&4, GTX2&3, dcGTX2&3, GTX5, NEO, dcNEO, STX, dcSTX and C1&2) by the anti-TTX antibody was evaluated. As the mAb binding obtained for all toxins analyzed was close to 100% (Figure 4), the cross-reactivity of the PSP toxins at a concentration of 100 ng/mL can be neglected, demonstrating the high specificity and selectivity of the mELISA. As a positive control, TTX tested at the same concentration resulted in a mAb binding decrease of more than 90% (Figure 2). This study illustrates that those PSP toxins, for which standards are available, that may co-exist with TTX in shellfish extracts will not interfere with the immunorecognition of TTX in the assay.

Additionally, since multiple reaction monitoring (MRM) transitions for Arg have been found to suppress TTX response in the mass spectrometer source [42], the possible interference of this amino acid in the mELISA was also evaluated. As can be seen in Figure 4, no significant effects of Arg on the mAb binding were observed.

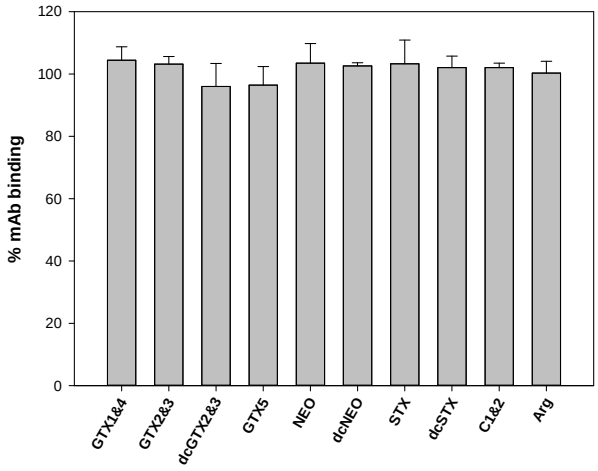

Figure 4. Percentage of mAb binding obtained by mELISA with 100 ng/mL of PSP toxins and Arg. Error bars represent the standard deviation values for 3 replicates.

3.3. Evaluation of matrix effects and establishment of matrix correction factors

Mussel and oyster matrix effects were studied by the analysis of blank shellfish extracts at different matrix concentrations (50, 75, 100 and/or 150 mg equiv./mL) at 3 different stages of the extraction protocol.

1) After SPE clean-up without solvent evaporation: Although SPE clean-up should reduce matrix effects, the highly acidic nature of the ACN/H_2O/AA solvent mixture used in the SPE protocol had a negative impact on the system, since mAb binding percentages obtained were not consistent with the shellfish matrix concentration used. The detrimental effects observed in the mELISA were assumed to be due to the solvent composition rather than to the shellfish matrix. Even decreasing the solvent mixture percentage by 4 times respect to the extract arising from the SPE column (i.e. 12.5% of the total volume of the well), the solvent effect could not be avoided.

2) After SPE clean-up, evaporation and solvent exchange: SPE cleaned-up extracts were evaporated until dryness, dissolved in phosphate buffer and analyzed by mELISA at the same matrix concentrations. mAb binding percentages were between 92 and 108% in either oyster or mussel extracts, regardless of the matrix concentration used (Table 1). Taking into consideration that the highest RSD value obtained was of 10%, negligible matrix effects are assumed when mAb binding percentages are between 90 and 110%. Thus, results obtained with this protocol

indicate that evaporation completely removes the previously observed undesirable effects. These results also reaffirm that when no evaporation was performed, the inhibition of the mAb binding was not due to the shellfish matrix, but to the solvent mixture presence, which could be harming the cysteamine and/or TTX immobilization. Therefore, mELISA enables loading up to 150 mg equiv./mL of shellfish matrix after SPE clean-up and evaporation.

3) Directly after toxin extraction (without SPE clean-up nor evaporation and solvent exchange): In order to evaluate if the SPE clean-up can be avoided to simplify the protocol or if, on the contrary, is a crucial step in the analysis of oyster and mussel extracts, extracts without SPE clean-up and not evaporated were tested. Under these conditions, differences between oyster and mussel extracts were observed (Table 1). In the case of oyster, no matrix effects were observed (i.e. mAb binding percentages were between 103 and108 %), indicating that the mELISA tolerates up to 150 mg equiv./mL of oyster matrix without SPE clean-up and with no need of solvent exchange. These results indicate that whereas solvent evaporation is crucial for the analysis of SPE cleaned-up oyster extracts, oyster extracts without SPE clean-up containing up to 7.5 % of the extraction solvent do not to interfere with the assay performance and, therefore, solvent evaporation is not required for the analysis of these extracts. However, in the analysis of mussel, pronounced matrix effects were obtained for all matrix concentrations tested. Although loading a lower matrix concentration could in principle remove remaining matrix effects, this would compromise the effective LOD (eLOD) of the assay. While the reason for the different behavior between mussel and oyster extracts remains unclear, it is evident that in the analysis of mussel extracts, SPE clean-up and subsequent solvent exchange are recommended to avoid non-desired matrix interferences.

3.4. Toxin recovery in oysters and mussel samples

From the experiments performed with blank oyster extracts, it was concluded that up to 150 mg equiv./mL of oyster extract can be loaded on the immunoassay without requiring a clean-up step nor solvent exchange. Nonetheless, solvent evaporation is required if the oyster extract undergoes a SPE clean-up step. Mussel extract after SPE clean-up also requires solvent evaporation prior to analysis to avoid solvent interference in the immunoassay. However, mussel extracts without SPE clean-up and with no evaporation suffer from undesirable matrix effects even at 50 mg equiv./mL of mussel matrix. Consequently, oyster and mussel tissue homogenates were spiked and extracted, and toxin recovery was evaluated without SPE clean-up/not evaporated and after SPE clean-up/evaporated. Taking into account the matrix concentrations of the resulting extracts and to fit into the TTX

calibration curves, extracts were spiked at 2 different levels of TTX in order to evaluate the toxin recovery.

1) After SPE clean-up, evaporation and solvent exchange: As SPE cleaned-up and evaporated extracts can be analyzed at 150 mg equiv./mL of shellfish matrix concentration, shellfish tissues were spiked at 75 µg TTX/kg (concentration that should provide about 50% of mAb binding inhibition when extract is analyzed at 150 mg equiv./mL of matrix concentration). Under these conditions, low toxin recovery values were obtained for both oyster and mussel tissue extracts (Table 2). These low recovery values can be attributed to toxin loss during the SPE clean-up and solvent exchange and/or interference of the shellfish matrix on the free toxin/antibody recognition. Nevertheless, these toxin recovery values can be taken as correction factors (CFs) and will be applied in the quantifications obtained in the subsequent analysis of naturally contaminated samples extracted and treated under these conditions.

2) Directly after toxin extraction (without SPE clean-up nor evaporation and solvent exchange): Mussel extracts with no SPE clean-up showed higher matrix effects and, therefore, samples had to be analyzed at lower matrix concentrations. Consequently, to test these conditions, a higher TTX concentration (250 µg TTX/kg) was spiked in mussels (also for oysters, although it was not a requirement). Under these conditions, toxin recovery values were higher than those obtained for SPE cleaned-up extracts. Regarding oyster samples, the lower the matrix concentration, the higher the toxin recovery. The excellent toxin recovery at 75 mg equiv./mL (96%) indicates that these extracts do not suffer from toxin loss during SPE or solvent exchange. Consequently, the inhibition of mAb binding at higher matrix concentrations can only be due to the effect of the matrix on the free toxin/antibody recognition, which obviously decreases as the matrix concentration decreases. Again, these toxin recovery values can be taken as CFs and will be applied in the quantifications obtained in the subsequent analysis of naturally contaminated oyster samples extracted and treated under these conditions. Regarding mussel samples, only one matrix concentration (50 mg equiv./mL) was analyzed (matrix effects at higher matrix concentrations were considered too high to conduct spiking trials), and the toxin recovery obtained was very high (166%). In this case, it is evident that the mussel matrix inhibits the response (as observed in the previous experiment where no TTX was present), causing an overestimation of the TTX content. Taking into account the toxin recovery value (166%) and the percentage of mAb binding obtained in the analysis of blank mussel tissue at 50 mg equiv./mL (74%), a CF of 123% is obtained, which will be used in the quantifications obtained in the subsequent analysis of naturally-contaminated mussel samples extracted and treated under these conditions.

Once obtained all toxin recovery values, eLODs in µg TTX/kg shellfish were calculated for each shellfish matrix and for both protocols. These eLODS were calculated as the ratio of the LOD obtained in buffer (2 ng/mL ± SD) to the shellfish matrix concentration used and applying the corresponding CF (Table 3).

Regarding oysters, eLOD obtained for extracts without SPE clean-up and not evaporated were lower than for SPE cleaned-up and evaporated extracts. Consequently, SPE clean-up is certainly not worth conducting as this additional step increases the analysis time. Regarding mussels, similar eLODs were obtained after SPE clean-up at 150 mg equiv./mL of matrix and without SPE clean-up at 50 mg equiv./mL. These results reaffirm that SPE clean-up is not a requirement for the analysis of oyster and mussel extract samples.

The eLOD values obtained for both shellfish matrices are higher than those previously reported for TTX by LC-MS/MS (5 µg/kg in this work, 3 µg/kg [17], 7.2 µg/kg [18] and 15 µg/kg [43]), but still very acceptable. Notably, they are substantially below from the eLOD obtained for puffer fish with the previous mELISA (230 µg/kg) [33]. Moreover, the eLODS values obtained herein proved the capability of the mELISA of detecting TTX below or only slightly above the concentration of 44 µg TTX equiv./kg shellfish meat, level that is considered not to result in adverse effects in humans [19]. Therefore, the mELISA described herein is absolutely appropriate for the screening as well as for the quantification of TTX contents in natural shellfish samples.

Table 1. Percentages of mAb binding obtained in the analysis of blank oyster and mussel tissues extracted under different conditions (n=4 replicates).

Shellfish tissue	Protocol	[Matrix] (mg equiv./mL)			
		150	**100**	**75**	**50**
Oyster	SPE clean-up / not evaporated	X	X	X	X
	SPE clean-up / evaporated	106	92	97	-
	no SPE clean-up / not evaporated	103	110	108	108
Mussel	SPE clean-up / not evaporated	X	X	X	X
	SPE clean-up / evaporated	105	96	108	-
	no SPE clean-up / not evaporated	57	63	71	74

X: not consistent; -: not tested

Table 2. Percentages of toxin recovery obtained in the analysis of TTX-spiked oyster and mussel tissues extracted under different conditions (n=4 replicates).

Shellfish tissue	Protocol	TTX level (µg/kg)	[Matrix] (mg equiv./mL)			
			150	100	75	50
Oyster	SPE clean-up / evaporated	75	29	-	-	-
	no SPE clean-up / not evaporated	250	71	83	96	-
Mussel	SPE clean-up / evaporated	75	50	-	-	-
	no SPE clean-up / not evaporated	250	-	-	-	166

-: not tested

Table 3. eLODs (µg TTX/kg shellfish) determined for SPE cleaned-up evaporated and no SPE cleaned-up not evaporated oyster and mussel extracts at different matrix concentrations.

Shellfish tissue	Protocol	[Matrix] (mg equiv./mL)			
		150	100	75	50
Oyster	SPE clean-up / evaporated	47 ± 17	-	-	-
	no SPE clean-up / not evaporated	19 ± 7	25 ± 9	28 ± 10	-
Mussel	SPE clean-up / evaporated	27 ± 10	-	-	-
	no SPE clean-up / not evaporated	-	-	-	33 ± 12

-: not tested

3.5. Analysis of oyster and mussel samples and comparison with LC-MS/MS analysis

After evaluating the matrix effects and establishing the CFs according to the toxin recovery values obtained, the mELISA was applied to the analysis of 3 oyster and 3 mussel samples from the Oosterschelde, The Netherlands. Oyster and mussel extracts were analyzed using the two different protocols (without SPE clean-up not evaporated and with SPE clean-up and evaporated). The corresponding CF values

were applied to the TTX content determined in each sample, and resulting quantifications were compared to those obtained by LC-MS/MS analysis (Table 4).

Although the number of samples was too low for statistical treatment (due to the limited availability of natural samples of shellfish containing TTX), no significant differences (P=0.702) were observed in the quantifications provided by the three approaches (mELISA with SPE clean-up/evaporated samples, mELISA with no SPE clean-up/not evaporated samples and LC-MS/MS analysis). In the analysis of samples by LC-MS/MS, only TTX was detected (other TTX analogues were not found at detectable levels). This toxin profile, with only TTX, contributes to the similarity between techniques, even though they are based on different recognition principles.

The TTX content in the shellfish samples ranged from slightly below 44 µg/kg up to 4- or 5-fold higher. Thus, we provide the first immunoassay capable of screening and quantifying TTX in shellfish samples at levels that may be considered of concern for human health.

Table 4. TTX content of 3 oyster and 3 mussel samples from the sanitary monitoring program of The Netherlands by the cysteamine-based mELISA under two different extraction protocols and comparison with LC-MS/MS analysis.

Method	Protocol	Oyster 1	Oyster 2	Oyster 3	Mussel 1	Mussel 2	Mussel 3
mELISA	SPE clean-up evaporated	82 ± 2	36 ± 6	67 ± 21	70 ± 11	146 ± 14	16 ± 4
(µg TTX equiv./kg shellfish)	no SPE clean-up not evaporated	61 ± 7	116 ± 16	86 ± 13	55 ± 1	227 ± 7	24 ± 5
LC-MS/MS* (µg TTX/kg shellfish)	-	113	51	79	93	172	41

*Samples were analyzed singular; during the intra laboratory validation of this method the repeatability error at 20 µg/kg was 15.7%.

4. Conclusions

A modified SAM-based immunoassay has been applied to the determination of TTX in mussel and oyster samples. The replacement of dithiols by cysteamine for the SAM formation allowed decreasing the required time and cost, while maintaining the sensitivity of the previously reported mELISA (LOD of 2 ng/mL). Storage at -20 °C and 4 °C of the TTX immobilization up to at least 3 months, provided ready-to-use microtiter plates, enabling a user to perform the assay in less than 2 h. Additionally, as proven by the absence of interferences from PSP toxins and Arg, the mELISA is highly selective for TTX, and certainly TTX analogues, as demonstrated in our previous work [33, 40, 41, 44].

In the analysis of blank shellfish, oyster extracts did not show matrix effects even without the SPE clean-up step. The SPE clean-up of mussel extracts removed the strong matrix effects observed when no SPE was used. However, the SPE clean-up and the required solvent evaporation resulted in low toxin recovery percentages when analyzing TTX-spiked samples, probably because of toxin lost in the column and during the evaporation step. Toxin recovery values were obtained for all protocols and shellfish types, and can be used as CFs to be applied to the quantification of TTX contents in naturally contaminated samples. Taking them into account, the lowest eLOD values obtained were about 20 and 50 µg TTX/kg for oyster extracts without and with SPE clean-up, respectively, and about 30 µg TTX/kg for mussel extracts with both protocols, substantially below the eLOD obtained by the previous mELISA for puffer fish (230 µg TTX/kg). This is in relatively good agreement with the level of 44 µg TTX equiv./kg shellfish meat, which is considered not to result in adverse effects in humans by the EFSA. Highly analogous results were determined on the comparison of the analysis of naturally contaminated shellfish by mELISA with LC-MS/MS analysis.

Overall, the mELISA developed herein meets the requirements in terms of selectivity and sensitivity. Although toxin recovery values, and thus CFs, were obtained for all protocols, shellfish samples can be rapidly processed and analyzed by mELISA without SPE clean-up, which is a clear advantage over LC-MS/MS methodologies, where SPE is required. Therefore, the implementation of the mELISA for the screening of TTXs in bivalve shellfish samples in routine monitoring programs could be straightforward, providing a complementary analytical technique suitable for ensuring food safety and consumer protection.

Acknowledgements

The research leading to these results has received funding from the the Instituto Nacional de Investigación y Tecnología Agraria y Alimentaria (INIA) through the PROMAQUA project (RTA2013-00096-00-00) and from CERCA/Generalitat de Catalunya program. Sandra Leonardo acknowledges scholarship from IRTA-Universitat Rovira i Virgili-Banco Santander (2013PIPF URV-IRTA-BS-01). Authors would like to thank Karla Barnés Albuera for drawing the mussel and oyster pictures of the graphical abstract.

References

[1] K. Tsuda, R. Tachikawa, C. Tamura, S. Ikuma, M. Kawamura, K. Sakai, O. Amakasu, On the structure of tetrodotoxin, Chem.Pharm. Bull., 12 (1964) 642-645.

[2] R.B. Woodward, J.Z. Gougouta, Structure of tetrodotoxin, J. Am. Chem. Soc., 86 (1964) 5030-5030.

[3] T. Goto, Y. Kishi, Takahash.S, Y. Hirata, Tetrodotoxin, Tetrahedron, 21 (1965) 2059-2088.

[4] Y. Tahara, Hirata, Y., Studies on the puffer fish toxin, J. Pharm. Soc. Jpn., 29 (1909) 587-625.

[5] T. Noguchi, O. Arakawa, T. Takatani, TTX accumulation in pufferfish, Comp. Biochem. Phys. D., 1 (2006) 145-152.

[6] V. Bane, M. Lehane, M. Dikshit, A. O'Riordan, and A. Furey, Tetrodotoxin: Chemistry, toxicity, source, distribution and detection, Toxins (2014), 6(2) 693-755.

[7] V. Pratheepa, V. Vasconcelos, Microbial diversity associated with tetrodotoxin production in marine organisms, Environ. Toxicol. Pharm., 36 (2013) 1046-1054.

[8] T. Noguchi, O. Arakawa, Tetrodotoxin - Distribution and accumulation in aquatic organisms, and cases of human intoxication, Mar. Drugs, 6 (2008) 220-242.

[9] I. Rodriguez, et al., The association of bacterial C-9-based TTX-like compounds with *Prorocentrum minimum* opens new uncertainties about shellfish seafood safety, Sci. Rep. (2017), 7.

[10] T. Narahashi, Tetrodotoxin - A brief history, Proc. Jpn. Acad. B-Phys. Biol. Sci., 84 (2008) 147-154.

[11] T. Noguchi, K. Onuki, O. Arakawa, Tetrodotoxin poisoning due to pufferfish and gastropods, and their intoxication mechanism, ISRN Toxicol., (2011) 276939-276939.

[12] Y. Bentur, J. Ashkar, Y. Lurie, Y. Levy, Z.S. Azzam, M. Litmanovich, M. Golik, B. Gurevych, D. Golani, A. Eisenman, Lessepsian migration and tetrodotoxin poisoning due to *Lagocephalus sceleratus* in the eastern Mediterranean, Toxicon, 52 (2008) 964-968.

[13] J. Kheifets, B. Rozhavsky, Z. Girsh Solomonovich, R. Marianna, A. Soroksky, Severe tetrodotoxin poisoning after consumption of *Lagocephalus sceleratus* (pufferfish, fugu) fished in Mediterranean Sea, treated with cholinesterase inhibitor, Case Reports in Critical Care, 2012 (2012) 782507.

[14] C. Acar, S. Ishizaki, Y. Nagashima, Toxicity of the Lessepsian pufferfish *Lagocephalus sceleratus* from eastern Mediterranean coasts of Turkey and species identification by rapid PCR amplification, Eur. Food Res. Technol., 243 (2017) 49-57.

[15] P. Katikou, D. Georgantelis, N. Sinouris, A. Petsi, T. Fotaras, First report on toxicity assessment of the Lessepsian migrant pufferfish *Lagocephalus sceleratus* (Gmelin, 1789) from European waters (Aegean Sea, Greece), Toxicon, 54 (2009) 50-55.

[16] P. Rodriguez, A. Alfonso, C. Vale, C. Alfonso, P. Vale, A. Tellez, L.M. Botana, First toxicity report of tetrodotoxin and 5,6,11-trideoxyTTX in the trumpet shell *Charonia lampas lampas* in Europe, Anal. Chem., 80 (2008) 5622-5629.

[17] A.D. Turner, A. Powell, A. Schofield, D.N. Lees, C. Baker-Austin, Detection of the pufferfish toxin tetrodotoxin in European bivalves, England, 2013 to 2014, Euro surveill., 20 (2015) 2-8.

[18] A. Vlamis, P. Katikou, I. Rodriguez, V. Rey, A. Alfonso, A. Papazachariou, T. Zacharaki, A.M. Botana, L.M. Botana, First detection of tetrodotoxin in Greek shellfish by UPLC-MS/MS potentially linked to the presence of the dinoflagellate *Prorocentrum minimum*, Toxins, 7 (2015) 1779-1807.

[19] EFSA (European Food Safety Authority), Risks for public health related to the presence of tetrodotoxin (TTX) and TTX analogues in marine bivalves and gastropods, EFSA J., 15:4 (2017): 4752.

[20] T. Noguchi, J.S.M. Ebesu, Puffer poisoning: Epidemiology and treatment, J. Toxicol.-Toxin Rev., 20 (2001) 1-10.

[21] Y. Mahmud, K. Yamamori, T. Noguchi, Occurrence of TTX in a brackish water puffer "midorifugu", *Tetraodon nigroviridis*, collected from Thailand, J. Food Hyg. Soc. Jpn., 40 (1999) 363-367.

[22] European Commission Regulation, (EC) No 854/2004 of the European Parliament and of the council of 29 April 2004 laying down specific rules for the organization of official controls on products of animal origin intended for human consumption. Off. J. Eur. Union. L226 (2004) 83-127.

[23] D. Neagu, L. Micheli, G. Palleschi, Study of a toxin-alkaline phosphatase conjugate for the development of an immunosensor for tetrodotoxin determination, Anal. Bioanal. Chem., 385 (2006) 1068-1074.

[24] T.J.G. Raybould, G.S. Bignami, L.K. Inouye, S.B. Simpson, J.B. Byrnes, P.G. Grothaus, D.C. Vann, A monoclonal antibody-based immunoassay for detecting tetrodotoxin in biological samples, J. Clin. Lab. Anal., 6 (1992) 65-72.

[25] K. Kawatsu, Y. Hamano, T. Yoda, Y. Terano, T. Shibata, Rapid and highly sensitive enzyme immunoassay for quantitative determination of tetrodotoxin, Jpn. J. Med. Sci. Biol., 50 (1997) 133-150.

[26] B.G. Gall, A.N. Stokes, S.S. French, E.A. Schlepphorst, E.D.III. Brodie, E.D.Jr. Brodie, Tetrodotoxin levels in larval and metamorphosed newts (*Taricha granulosa*) and palatability to predatory dragonflies, Toxicon, 57 (2011) 978-983.

[27] B.G. Gall, A.N. Stokes, S.S. French, E.D.III. Brodie, E.D.Jr. Brodie, Predatory caddisfly larvae sequester tetrodotoxin from their prey, eggs of the rough-skinned newt (*Taricha granulosa*), J. Chem. Ecol., 38 (2011) 1351-1357.

[28] A.N. Stokes, B.L. Williams, S.S. French, An improved competitive inhibition enzymatic immunoassay method for tetrodotoxin quantification, Biol. Proced. Online 14:3 (2012).

[29] A.N. Stokes, P.K. Ducey, L. Neuman-Lee, C.T. Hanifin, S.S. French, M.E. Pfrender, E.D.III Brodie, E.D.Jr. Brodie, Confirmation and distribution of tetrodotoxin for the first time in terrestrial invertebrates: two terrestrial flatworm species (*Bipalium adventitium* and *Bipalium kewense*), Plos One, 9 (2014) e100718.

[30] Y. Zhou, Y.S. Li, F.G. Pan, Z.S. Liu, Z. Wang, Identification of tetrodotoxin antigens and a monoclonal antibody, Food Chem., 112 (2009) 582-586.

[31] R. Wang, A. Huang, L. Liu, S. Xiang, X. Li, S. Ling, L. Wang, T. Lu, S. Wang, Construction of a single chain variable fragment antibody (scFv) against tetrodotoxin (TTX) and its interaction with TTX, Toxicon, 83 (2014) 22-34.

[32] J. Tao, W.J. Wei, L. Nan, L.H. Lei, H.C. Hui, G.X. Fen, L.Y. Jun, Z. Jing, J. Rong, Development of competitive indirect ELISA for the detection of tetrodotoxin and a survey of the distribution of tetrodotoxin in the tissues of wild puffer fish in the waters of south-east China, Food Addit. Contam. A, 27 (2010) 1589-1597.

[33] L. Reverté, P. de la Iglesia, V. del Río, K. Campbell, C.T. Elliott, K. Kawatsu, P. Katikou, J. Diogène, M. Campàs, Detection of tetrodotoxins in puffer fish by a self-assembled monolayer-based immunoassay and comparison with surface plasmon resonance, LC-MS/MS, and mouse bioassay, Anal. Chem., 87 (2015) 10839-10847.

[34] M.P. Kreuzer, M. Pravda, C.K. O'Sullivan, G.G. Guilbault, Novel electrochemical immunosensors for seafood toxin analysis, Toxicon, 40 (2002) 1267-1274.

[35] A.D. Taylor, J. Ladd, S. Etheridge, J. Deeds, S. Hall, S.Y. Jiang, Quantitative detection of tetrodotoxin (TTX) by a surface plasmon resonance (SPR) sensor, Sensor. Actuat. B-Chem., 130 (2008) 120-128.

[36] A.D. Taylor, H. Vaisocherova, J. Deeds, S. DeGrasse, S. Jiang, Tetrodotoxin detection by a surface plasmon resonance sensor in pufferfish matrices and urine, J. Sensors, (2011) Article ID 601704, 10 pages.

[37] B.J. Yakes, J. Deeds, K. White, S.L. DeGrasse, Evaluation of surface Plasmon resonance biosensors for detection of tetrodotoxin in food matrices and comparison to analytical methods, J. Agric. Food Chem., 59 (2011) 839-846.

[38] K. Campbell, P. Barnes, S.A. Haughey, C. Higgins, K. Kawatsu, V. Vasconcelos, C.T. Elliott, Development and single laboratory validation of an optical biosensor assay for tetrodotoxin detection as a tool to combat emerging risks in European seafood, Anal. Bioanal. Chem., 405 (2013) 7753-7763.

[39] B.J. Yakes, K.M. Kanyuck, S.L. DeGrasse, First report of a direct surface Plasmon resonance immunosensor for a small molecule seafood toxin, Anal. Chem., 86 (2014) 9251-9255.

[40] L. Reverté, M. Campàs, B.J. Yakes, J. R. Deeds, P. Katikou, K. Kawatsu, M. Lochhead, C.T. Elliott, K. Campbell, Tetrodotoxin detection in puffer fish by a sensitive planar waveguide immunosensor, Sens. Actuators B-Chem., 253 (2017) 967-976.

[41] L. Reverté, K. Campbell, M. Rambla-Alegre, C.T. Elliott, J. Diogène, M. Campàs, Immunosensor array platforms based on self-assembled dithiols for the electrochemical detection of tetrodotoxins in puffer fish, Anal. Chim. Acta, 989 (2017) 95-103.

[42] A.D. Turner, M.J. Boundy, M.D. Rapkova, Development and single-laboratory validation of a liquid chromatography tandem mass spectrometry method for quantitation of tetrodotoxin in mussels and oysters, J. AOAC Int., 100 (2017) doi: 10.5740/jaoacint.17-0017.

[43] M.J. Boundy, A.I. Selwood, D.T. Harwood, P.S. McNabb, A.D. Turner, Development of a sensitive and selective liquid chromatography-mass spectrometry method for high throughput analysis of paralytic shellfish toxins using graphitised carbon solid phase extraction, J. Chromatogr. A, 1387 (2015) 1-12.

[44] M. Rambla-Alegre, L. Reverté, V. Del Río, P. de la Iglesia, O. Palacios, C. Flores, J. Caixach., K. Campbell, C. T. Elliott, A. Izquierdo-Muñoz, M. Campàs, J. Diogène, Evaluation of tetrodotoxins in puffer fish caught along the Mediterranean coast of Spain. Toxin profile of *Lagocephalus sceleratus*, Environ. Res., 158 (2017) 1-6.

Rapid screening and multi-toxin profile confirmation of tetrodotoxins and analogues in human body fluids derived from a puffer fish poisoning incident in New Caledonia

Maria Rambla-Alegre[a], Sandra Leonardo[a], Yann Barguil[b], Cintia Flores[c], Josep Caixach[c], Katrina Campbell[d], Christopher T. Elliott[d], Claude Maillaud[e], Michael J. Boundy[f], D. Tim Harwood[f], Mònica Campàs[a], Jorge Diogène[a]

[a]*IRTA, Ctra, Poble Nou, km 5.5, 43540 Sant Carles de la Ràpita, Tarragona, Spain*
[b]*Service of Biochemistry, Territorial Hospital Center of New Caledonia, BP J5, 98849 Nouméa cedex, New Caledonia, France*
[c]*Mass Spectrometry Laboratory/Organic Pollutants, IDAEA-CSIC, Jordi Girona 18, 08034 Barcelona, Spain*
[d]*Institute for Global Food Security, School of Biological Sciences, Queen's University, Stranmillis Road, Belfast BT9 5AG, Northern Ireland*
[e]*Lacave Laplagne Street, Noumea 98800, New Caledonia, France*
[f]*Cawthron Institute – 98 Halifax ST, Nelson 7010, New Zealand*

Abstract

In August 2014, a puffer fish poisoning incidence resulting in one fatality was reported in New Caledonia. Although tetrodotoxin (TTX) intoxication was established from the patients' signs and symptoms, the determination of TTX in the patient's urine, serum or plasma is essential to confirm the clinical diagnosis. To provide a simple cost-effective rapid screening tool for clinical analysis, a maleimide-based enzyme-linked immunosorbent assay (mELISA) adapted for the determination of TTX contents in human body fluids was assessed. The mELISA was applied to the analysis of urine samples from two patients and a response for the presence of TTX and/or structurally similar analogues was detected in all samples. The analysis by LC-MS/MS confirmed the presence of TTX but also TTX analogues (4-*epi*TTX, 4,9-anhydroTTX and 5,6,11-trideoxyTTX) in the urine. A change in the multi-toxin profile in the urine based on time following consumption was observed. LC-MS/MS analysis of serum and plasma samples also revealed the presence of TTX (32.9 ng/mL) and 5,6,11-trideoxyTTX (374.6 ng/mL) in the post-mortem plasma. The results provide for the first time the TTX multi-toxin profile of human samples from a puffer fish intoxication and clearly demonstrate the implication of TTX as the causative agent of the reported intoxication case.

1. Introduction

Tetrodotoxin (TTX) is one of the most potent low-molecular-weight marine neurotoxin, well-known for its distribution in puffer fish, but also present in many other organisms, including amphibians, echinoderms, cephalopods and bivalve molluscs (Noguchi et al., 2008; Turner et al. 2017). It is believed to be primarily produced by certain marine endosymbiotic bacteria and to accumulate through the food webs and enter into other organisms, eventually reaching humans (Pratheepa and Vasconcelos, 2013). TTX and TTX analogues selectively bind to site one of voltage-gated sodium channels, blocking the influx of sodium ions into the nerve cells and affecting neuromuscular transmission, causing progressive paralysis and even death due to a failure of the respiratory system (Lee and Ruben, 2008).

Puffer fish food poisoning cases have been reported worldwide. A poisoning incidence reported by the Territorial Hospital of New Caledonia in August 2014 resulting from the ingestion of an *Arothron nigropunctatus* puffer fish (Maillaud et al., 2015) is addressed in this work to demonstrate the implication of TTX in this intoxication. At around 6 pm on the 27th of August, four men aged 33, 34, 37 and 38 years old, with no known medical history, consumed a boiled fish that the oldest man had captured whilst fishing. The older fisherman ate most of the liver and the gonads in their totality. One of the other men consumed, the flesh in great quantity and, the other man consumed, a small portion of the liver. The fourth and youngest man only ingested a small part of the flesh. Rapidly, the first three consumers presented with gastrointestinal signs such as nausea, vomiting and diffuse abdominal pain, together with neurological signs such as peribuccal, facial and extremal paraesthesia and ataxia-like sensations. The three men lay down and fell asleep. On the morning of the 28th of August, the fisherman was found deceased in his bed and the other two men showed regressed digestive signs and appearance of tetraparesis. The fourth consumer returned home with no signs of intoxication. The two men that presented with neurological signs were hospitalised, one patient in the intensive care unit (Pt#1) and the other one (Pt#2) in the short stay hospitalization unit of the Territorial Hospital of New Caledonia. The neurological symptoms with associating tetraparesis, tetraparesthesis, ataxia and deep sensitivity disturbance dissipated after 48 hours and disappeared in a few days.

Although the causative agent of the food poisoning was established from the patients' symptoms and the identification of the species responsible through the photos of the fish provided by the medical team to one of the patients, the puffer fish could not be analysed for the identification of the toxin involved in this intoxication case. Thus, the detection of TTXs in clinical samples of the poisoned patients can be essential to confirm TTX intoxication. As TTXs are very polar

compounds, the ingested toxins are mainly eliminated in urine. Previous studies have indicated that TTXs only remain in blood for a matter of hours (less than 24 h), but they can be found in urine even on day 4 after ingestion (O'Leary et al., 2004).

Chromatography-based methods have been to date the most widely used techniques for the determination of TTXs in the urine and blood of patients from poisoning incidents. However, determining TTX intoxication from body fluids faces certain challenges. First, unlike in food, the amount of toxin in the urine and blood of a patient who has been intoxicated is typically low; therefore, a sensitive method is required. Secondly, because TTXs are very polar compounds, there will be low retention on conventional reverse-phase columns; thus, the use of another type of analytical column or modification of the mobile phase composition is needed. Third, endogenous metabolites of the biological samples may lead to matrix effects. Ion suppression is a big challenge in mass spectrometry (MS) analysis, requiring efficient clean-up procedures before sample analysis (Leung et al., 2011).

Enzyme-linked immunosorbent assays (ELISAs) are rapid, sensitive, cost-efficient and easy-to-use methods of analysis that do not require sophisticated instrumentation and highly trained personnel. The use of ELISAs as alternative or complementary to conventional methods for the determination of TTXs in biological samples can provide expedient solutions for rapid and reliable diagnosis in food poisoning incidences, and favours their implementation at hospitals where patients are treated. A maleimide-based ELISA (mELISA) for the detection of TTXs in mussels and oysters was recently developed at IRTA (Reverté et al., 2017). The TTX was immobilised on self-assembled cysteamine in a stable, ordered and optimally-oriented way that provided a long-term stability for storage of the modified microtiter plates, allowing the assay to be performed in less than 2 hours with the use of these pre-coated plates. To the best of our knowledge, only one work has used an immunoassay for the analysis of human body fluids for TTX monitoring, but no details are provided on the method or its performance (Islam et al., 2011). Here, the application of the mELISA to the screening of TTXs in clinical samples was assessed and fully characterised by the analysis of blank and TTX-spiked samples. Moreover, urine samples from the two intoxicated patients were analysed and the multi-toxin profile (TTX and TTX analogues) in urine, serum and plasma samples was evaluated by liquid chromatography-tandem mass spectrometry (LC-MS/MS) analysis. The results obtained by both techniques were compared, demonstrating the applicability of the immunoassay and the complementarity of the techniques based on different recognition principles.

2. Materials and methods

2.1. Reagents and materials

Pure TTX standard was purchased from Tocris Bioscience (Bristol, UK) and standard solutions were prepared at 1 mg/mL in 10 mM acetic acid (AA). The anti-TTX monoclonal antibody (mAb) TX-7F was produced as described in Kawatsu et al. (1997). Pierce maleimide-activated plates were obtained from Thermo Fisher Scientific (Madrid, Spain). Cysteamine hydrochloride, formaldehyde solution, anti-mouse IgG (whole molecule)-horseradish peroxidase antibody produced in rabbit (IgG-HRP), bovine serum albumin (BSA), ethylenediaminetetraacetic acid (EDTA), 4-morpholineethanesulfonic acid (MES) hydrate, potassium phosphate dibasic, potassium phosphate monobasic and 3,3',5,5'-tetramethylbenzidine (TMB) liquid substrate, ammonium hydroxide solution (NH_4OH, 25%), ammonium acetate and amorphous graphitized polymer carbon Supelco ENVI-Carb 250 mg/3 mL cartridges were supplied by Sigma-Aldrich (Tres Cantos, Spain). HPLC-grade acetonitrile (ACN), glacial acetic acid (AA) and methanol (MeOH) were obtained from Chem-lab (Zedelgem, Belgium). Ultrapure Milli-Q water (18.2 MΩ/cm^2) was used for the preparation of solutions (Millipore Iberica Ltd., Madrid, Spain).

2.2. Human samples

Urine, serum and plasma samples were collected and stored at -20 °C until their analysis (Table 1). Urine and serum samples from patient 1 (Pt#1) were collected the 28th and 29th of August 2014**,** coinciding with ~17 h and ~45 h after the ingestion of the boiled puffer fish; urine and serum samples from patient 2 (Pt#2) were taken only the second day of hospitalisation, approximately 42 h after the ingestion of the fish. Three plasma samples were collected from Pt#1: the first one was collected at the moment of hospitalisation, ~17 h after the puffer fish consumption; two additional samples were collected ~38 and ~43 h after the ingestion; only one plasma sample was collected from Pt#2, ~23 h after the fish consumption. A post-mortem plasma sample was collected from the fisherman, ~17 h after the puffer fish ingestion.

The creatinine concentration in urine samples was determined by Echevarne Laboratory (Barcelona, Spain) using Jaffe's reaction.

Table 1. Human body fluid samples collected from the two hospitalised patients and the deceased fisherman**.**

	Date	Time (hours after ingestion)	Samples
Pt#1	28/08/14	17 h	Urine, serum and heparinized plasma
	29/08/14	38 h	Heparinized plasma
	29/08/14	43 h	Heparinized plasma
	29/08/14	45h	Urine and serum
Pt#2	28/08/14	23 h	Heparinized plasma
	29/08/14	42 h	Urine and serum
Fisherman	28/08/14	17 h	Post-mortem plasma (with fluoride)

2.3. Colorimetric maleimide-based enzyme-linked immunosorbent assay (mELISA)

Urine samples were analysed by mELISA, using the protocol previously developed by our group for the determination of TTX in shellfish (Reverté et al., 2018). Briefly, 100 µL of 1 mM cysteamine in binding buffer (0.1 M potassium phosphate, 10 mM EDTA, pH 7.2) was added to the maleimide plates and incubated for 3 h, followed by the direct immobilization of TTX (2 µg/mL) with formaldehyde (3.4%) in the same buffer overnight. A competitive assay was then performed by incubating 50 µL of free TTX/sample dilution and 50 µL of 1:1,600 anti-TTX monoclonal antibody (mAb) dilution in 1% BSA-phosphate buffer for 30 min. A blocking step was then performed with 200 µL of 1% BSA-phosphate buffer for 30 min and, finally, 100 µL of IgG- HRP at 1:1,000 dilution in 1% BSA-phosphate buffer was incubated for 30 min. The colorimetric response was measured at 620 nm after 10 min of TMB liquid substrate incubation.

2.4. Solid-phase extraction (SPE) clean-up

Solid-phase extraction (SPE) clean-up was used before LC-MS/MS analysis, adapting the protocol described by Boundy et al. (2015) for shellfish samples. In this work, the addition of NH_4OH to the crude extract is avoided. Briefly, graphitized polymer carbon ENVI-carb cartridges were conditioned with 3 mL of ACN/H_2O/AA (20:80:1, v:v:v), followed by 3 mL of H_2O/NH_4OH (1000:1, v:v). Then, 400 µL of sample was loaded onto the conditioned cartridges and washed with 700 µL of deionized H_2O. Finally, the retained TTXs were eluted with 2 mL of ACN/H_2O/AA (20:80:1, v:v:v). The eluent was diluted by transferring 100 µL to an insert and adding 100 µL of ACN. Sample vials could be stored at -20 °C until analysis.

2.5. Liquid chromatography-tandem mass spectrometry (LC-MS/MS) analysis

Urine, serum and plasma samples were analysed by LC-MS/MS, using the protocol previously developed by our group for the analysis of puffer fish (Rambla-Alegre et al., 2017). Briefly, a TSQ Quantum system (Thermo Fisher Scientific, Bremen, Germany) and a HILIC XBridge Amide column were used; a binary gradient elution was programmed with H_2O (mobile phase A) and ACN/H_2O (mobile phase B), both containing ammonium acetate and adjusted to pH 5.8 with acetic acid. Extracts were analysed by electrospray ionisation (ESI) operating in positive mode, $[M+H]^+$; multiple reaction monitoring (MRM) transitions were monitored for the following TTX analogues (precursor ion > product ion): 320.1 > 302.1 / 162.2 for TTX and 4-*epi*TTX, 302.1 > 256.1 / 162.2 for 4,9-anhydroTTX, 304.1 > 286.1 / 162.2 for 5-deoxyTTX and 11-deoxyTTX, 288.1 > 270.1 / 224.0 for 5,11-dideoxyTTX and 6,11-dideoxyTTX, 272.1 > 254.1 / 162.2 for 5,6,11-trideoxyTTX, 290.1 > 272.1 / 162.2 for 11-norTTX-6(*S*)-ol and 11-norTTX-6(*R*)-ol; identification was supported by the toxin retention time and MRM ion ratios. ESI parameters and voltages were optimised to: spray voltage of 3.5 kV, capillary temperature of 300 °C, sheath gas flow rate of 40 (arbitrary units) and auxiliary gas flow rate of 10 (arbitrary units), capillary voltage of 30.0 V, tube lens voltage of 130 V and skimmer voltage of 28 V. Data was processed with Xcalibur 2.0.7 SP1 software (ThermoFisher Scientific, Bremen, Germany).

Quantification was calculated through an external calibration using TTX standard as a reference. Six level calibration curves between 1- 250 ng/mL showed good intra-batch performance and linear adjustment (r^2) ≥ 0.9990. According to the recoveries and dilution factor of the samples, the working ranges of the method in urine, plasma and serum were 12-2,909 ng/mL, 25-6,361 ng/mL and 22-5,447 ng/mL, respectively.

3. Results and discussion

3.1. Detection of TTX equivalent content in human samples by mELISA

3.1.1. Matrix effects and TTX recovery

When performing an immunoassay, the functionality of the antibodies can be strongly affected by the presence of matrix compounds other than the target analyte, thus, the effect of each type of matrix on the assay should be evaluated prior to the analysis of naturally contaminated samples. To test urine matrix effects, pure and diluted blank and spiked (5 ng/mL TTX) urine samples were analysed. The mAb binding percentages obtained ranged between 95 and 104% for pure blank urine samples and all dilutions tested, indicating the lack of interference from urine

matrix in the recognition of the immobilised TTX by the mAb. In contrast, urine matrix effects on the recognition of free TTX by the mAb were observed in the analysis of TTX-spiked urine samples, obtaining toxin recoveries of 27±4% in pure urine samples. Toxin recoveries increased with sample dilutions, reaching 101±2% recovery at ¼-diluted samples. Thus, it was clearly demonstrated that ¼ dilution of urine in buffer is an effective way to overcome matrix effects, avoiding sample pre-treatment. Considering ¼ urine dilution and the limit of detection (LOD) obtained in the standard calibration curve in buffer (IC_{10}=0.9 ng/mL), an effective LOD (eLOD) of 3.6 ng TTX/mL urine was calculated, with a working range (IC_{20}–IC_{80}) between 6.1 and 184.0 ng TTX/mL urine. However, urine is a fluid with a large variation in matrix components and concentrations, differing both among people and within the same person depending on the status of dehydration of the patient. Thus, when the analysis is not compromised by analyte concentrations below the LOD, additional sample dilutions are encouraged to validate that the matrix effect has been completely removed and TTX equiv. content is not being underestimated.

In regards to the serum and plasma samples, the preliminary studies revealed high non-specific absorption values from the secondary antibody in blank serum and plasma samples –from pure samples to ⅛ sample dilutions in binding buffer–. Due to the high interference of the matrix components in serum and plasma, the analysis of these clinical samples by mELISA was not fulfilled. Since mELISA is proposed as a rapid screening tool, the clean-up of serum and plasma samples to reduce the matrix effects was not approached. Determination of TTX in urine by mELISA is an appropriate strategy for clinical laboratory diagnosis due to the low matrix effects but also the long duration of TTX in urine compared with plasma and serum.

3.1.2. Quantification of TTX equivalent content in urine samples

Urine samples were analysed by mELISA to determine the TTX equiv. contents (Table 2). TTX equiv. were detected in all urine samples. To eliminate the effect of dehydration and variations in urinary output of the patients, urine creatinine adjustment of the TTX concentrations was made (Yu et al., 2010; Fong et al., 2011) expressing the concentration of TTX equiv. in relation to creatinine concentrations (ng TTX equiv./µmol creatinine). It was found that urine creatinine-adjusted TTX (UC-TTX) concentrations agree well with the degree of poisoning, as observed from clinical symptoms, and with the expected TTX excretion rates. In Pt#1, the urine sample collected ~17 h after fish ingestion presented the highest UC-TTX concentration. The UC-TTX content decreased in the urine sampled from the same patient ~45 h after fish ingestion. Urine sample from Pt#2, collected ~42 h after fish ingestion, showed the lowest UC-TTX levels. TTX equiv. contents found in urine are

consistent with previous TTX intoxication episodes reported (Yu et al., 2010). However, in many cases the results are difficult to compare due to differences in the urine collection time and differences in the hydration state of patients and no adjustment with creatinine levels.

3.2. Detection of TTXs in human samples by LC-MS/MS analysis

3.2.1. TTX recovery

Urine, serum and plasma matrix effects were studied by the analysis of blank and TTX-spiked matrices. After SPE clean-up of the samples, toxin recoveries of 43%, 23% and 20% were obtained for urine, serum and plasma samples, respectively. The low recovery values achieved in the analysis of the clinical samples can be attributed to toxin loss during SPE clean-up and/or ion suppression. Nevertheless, these toxin recovery values are taken as correction factors (CFs) and will be applied in the quantifications obtained in the subsequent analysis of naturally contaminated samples extracted and treated under these conditions.

After applying the corresponding CFs, LODs of 5.9, 10.9 and 12.7 ng TTX/mL and limits of quantification (LOQs) of 11.6, 21.8 and 25.4 ng TTX/mL were calculated for urine, serum and plasma samples, respectively.

3.2.2. Identification and quantification of TTXs

TTX content in urine, serum and plasma samples was evaluated by LC-MS/MS. As expected from the previous results obtained by mELISA, TTX was detected in all urine samples. Figure 1 shows the chromatograms obtained after the analysis of the urine sample of Pt#2, as an example. The analysis revealed a multi-toxin profile in all urine samples, with the presence of TTX but also 4- *epi*TTX, 4,9-anhydroTTX and 5,6,11-trideoxyTTX analogues (Table 2, Figure 2). It is interesting to mention that whereas 5,6,11-trideoxyTTX was the major analogue found in urine from Pt#1 collected ~17 h after the puffer fish ingestion, TTX was the major compound found in urine from the same patient collected ~45 h after the fish ingestion. Urine sample from Pt#2, collected ~42 h after the fish ingestion, also presented TTX as the major compound. Concentrations of TTX and TTX analogues obtained could suggest the metabolism of 5,6,11-trideoxyTTX to TTX and its equivalent analogues 4-*epi*TTX and 4,9-anhydroTTX, a pathway already predicted by Yotsu-Yamashita et al. (2013). After adjusting TTX and TTX analogues values to creatinine concentration to correct the effect of dehydration and variations in urinary output, as performed in the quantifications by mELISA (section 3.1.2), a decrease of TTX and all the analogue

concentrations was observed with time (hours after fish consumption). Consequently, the TTX metabolic pathway cannot be concluded from these results since differences in the metabolic profile could also be explained by the different stability of TTX analogues.

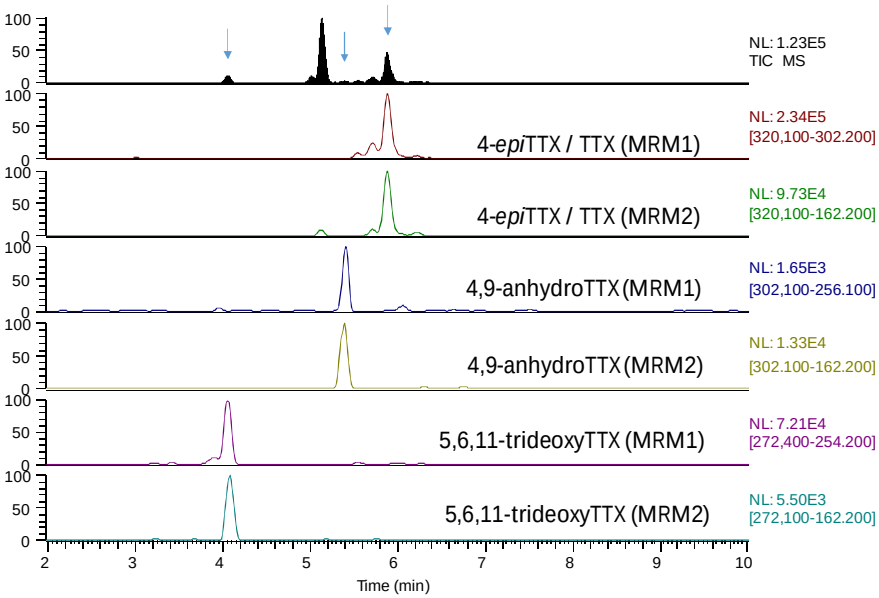

Figure 1. Total ion chromatogram (TIC) and MRM chromatogram of transitions monitored obtained following the analysis of TTX and its analogues in urine from Pt#2 by LC-MS/MS. Arrows indicate TTX and TTX analogues peaks identified.

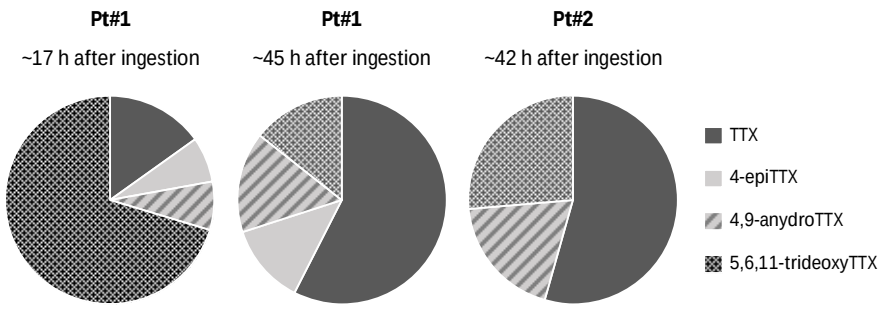

Figure 2. Graphical representation of the multi-toxin profile of the urine samples.

To obtain an estimation of the total TTX content of a sample in terms of toxicity (expressed in TTX equiv.), the application of the toxicity equivalency factors (TEFs) of each analogue to the individual quantifications provided by LC-MS/MS is necessary. TEFs express the toxicity of each individual analogue in relation to TTX toxicity used as a reference. Thus, TEFs for 4-*epi*TTX ($TEF_{4\text{-}epiTTX}$=0.156), 4,9-anhydroTTX ($TEF_{4,9\text{-}anhydroTTX}$=0.019) and 5,6,11-trideoxyTTX ($TEF_{5,6,11\text{-}trideoxyTTX}$=0.011) previously established in the literature (Nakamura and Yasumoto 1985; Yotsu-Yamashita et al. 1995) were applied to each TTX analogue concentration in urine samples, obtaining TTX equiv. concentrations, which were afterwards adjusted according to creatinine concentrations. A correspondence between the adjusted values and the clinical symptoms of the patients was again observed.

Regarding serum and plasma samples from the hospitalised patients, neither TTX nor TTX analogues were detected above the LODs, which indicates the rapid elimination of TTX into urine. In contrast, TTX and 5,6,11-trideoxyTTX were detected in the post-mortem plasma sample from the fisherman at concentrations of 32.9 ng/mL and 374.6 ng/mL, respectively (Figure 3). Although 5,6,11-trideoxyTTX was clearly the major compound detected in the plasma, its low toxicity compared with TTX points out TTX to be the main causative agent of this fatal case. It is important to take into consideration that blood TTX concentrations greater than 9 ng/mL have been suggested to be potentially lethal (Islam et al., 2011). The detection of TTX in the post-mortem plasma at this high concentration clearly reflects the high amount of TTX ingested by the fisherman, probably due to the consumption of liver and gonads, the most toxic parts of puffer fish species (Noguchi et al., 2008).

Table 2. TTX and creatinine concentrations in urine samples of two patients with TTX poisoning and comparison between TTX quantifications provided by LC-MS/MS analysis and mELISA.

		TTX (ng/mL)							**Creatinine (µmol/L)**	**UC-TTX (ng/µmol creatinine)**		
		LC-MS/MS						mELISA		LC-MS/MS		mELISA
	Hours after ingestion	TTX	4-*epi*TTX	4,9-anhydro TTX	5,6,11-trideoxy TTX	TTX equiv. (applying TEFs)	TTX equiv. (applying CRFs)	TTX equiv.		TTX equiv. (applying TEFs)	TTX equiv. (applying CRFs)	TTX equiv.
Pt#1	17	217.4	101.2	108.3	1008.2	246.3	217.4–318.6	211.1	3,890	63.3	55.9–81.9	54.3
Pt#1	45	683.9	149.0	184.7	171.6	712.6	683.9–833.9	561.4	20,774	34.3	32.9–40.1	27.0
Pt#2	42	65.4	n.d.*	23.0	31.8	66.2	65.4	32.0	2,829	23.4	23.1	11.3

*n.d.: not detected

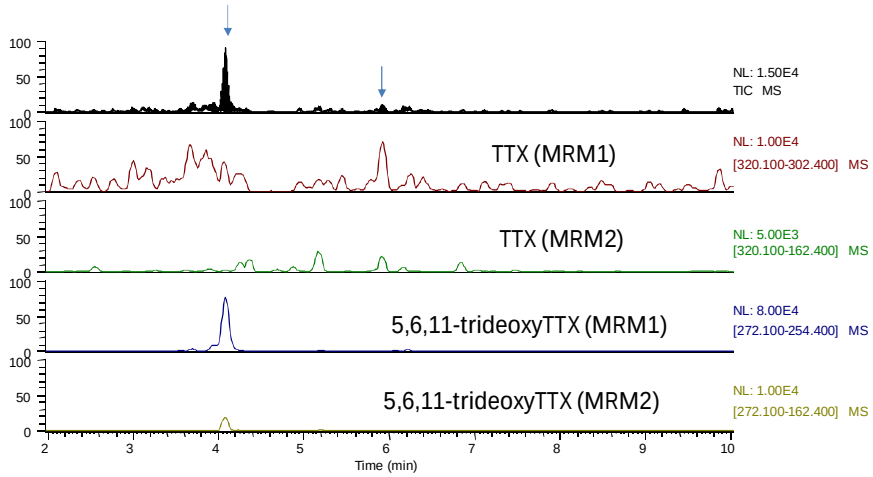

Figure 3. TIC and MRM chromatogram of transitions monitored obtained following the analysis of TTX and its analogues in post-mortem plasma from the fisherman by LC-MS/MS. Arrows indicate TTX and TTX analogues peaks identified.

3.3. Comparison between TTX quantifications provided by mELISA and by LC-MS/MS analysis

The application of cross-reactivity factors (CRFs) of TTX analogues to the individual contents determined by LC-MS/MS to obtain the total TTX content of a sample in terms of immunochemical recognition (expressed in TTX equiv.), is crucial when comparing results between immunochemical and physicochemical approaches. CRFs depend on the affinity of the antibody for the different analogues, but also on the immunological approach and the manner in which antibodies/antigens are immobilised (Reverté et al., 2015; Leonardo et al., 2017). CRFs for 4,9- anhydroTTX and 5,6,11-trideoxyTTX analogues were previously established by mELISA, being 10^{-4} and 10^{-6}, respectively. Unfortunately, the CRF for 4-*epi*TTX could not be established due to the lack of standard. The total TTX equiv. content by LC-MS/MS was calculated by adding up the contents of TTX and TTX analogues after applying the corresponding CRFs to each analogue (Table 2). The low CRFs of 4,9-anhydroTTX and 5,6,11-trideoxyTTX certainly makes the contribution of these analogues to the total sum to be very low. Since CRF for 4-*epi*TTX was not available, the CRF values of 0 and 1 were assumed for this analogue to provide a content range that should include the real values (this affects to samples from Pt#1, as 4-*epi*TTX was not quantified in sample from Pt#2). After creatinine adjustment, appropriate correlations between the C-TTX quantifications provided by mELISA and LC-MS/MS

analysis were obtained, regardless of whether 4-*epi*TTX CRF was considered to be 0 (y = 1.288 x – 17.2, R^2 = 0.995) or 1 (y = 0.717 x – 3.8, R^2 = 0.993). Due to the small amount of 4-*epi*TTX in relation to the total TTX content of the sample, no significant differences were observed either when the CRF applied was 0 (t=0.405, p=0.706) or 1 (t=0.813, p=0.462). Nevertheless, p-values obtained suggest that the real value should be closer to 0, the affinity of the antibody to recognise 4-*epi*TTX in the mELISA probably being very low in comparison with TTX.

The interaction of toxins with antibodies is based on a structural recognition that is not necessary related to the toxicity. Ideally, an immunoassay should be able not only to recognise all toxic analogues that contribute to the intoxication case, but also to provide a quantification equivalent to the total toxicity. Thus, quantifications provided by mELISA were also compared with total TTX equiv. concentrations calculated after LC-MS/MS analysis. Good correlations were obtained (y = 1.050 x – 11.5, R^2 = 0.990) with results showing no significant differences (t=0.547, p=0.614). The lower affinity of the mAb towards less toxic TTX analogues in comparison with TTX makes the mELISA an ideal tool for preliminary screening of the toxicity of urine samples. Since only three urine samples were available in this study, additional samples should be analysed to fully validate this method. Nevertheless, the obtained results clearly demonstrate the applicability of the mELISA to both fast screening and quantification of TTX in urine samples in a simple and reliable way.

4. Conclusions

The implication of TTX as the responsible agent of the reported intoxication case in New Caledonia following consumption of puffer fish has been proven.

The applicability of the mELISA to the analysis of urine samples has been demonstrated, confirming the presence of TTX equiv. in all urine samples from the hospitalised patients. The results were in good correlation with LC-MS/MS analysis, that revealed a multi-toxin profile, with the presence of TTX and three TTX analogues (4-*epi*TTX, 4,9-anhydroTTX and 5,6,11-trideoxyTTX). No TTXs were detected in plasma and serum of these patients by LC-MS/MS analysis, but TTX and 5,6,11-trideoxyTTX were detected in the post-mortem plasma of the fisherman at a lethal concentration of 37.0 ng/mL, after applying the TEFs.

The results obtained herein show the mELISA as a powerful tool for the fast screening of TTXs in urine samples, surpassing some of the challenges associated with LC-MS/MS analysis (e.g. lack of retention on conventional reverse-phase columns or significant ion suppression due to endogenous substances in urine). The analysis of urine samples by mELISA is a reliable, simple and cost-effective strategy

to estimate the degree of TTX poisoning in humans. The complementary analysis by LC-MS/MS performed in parallel confirms the causative intoxication agent and provide a full characterisation of the multi-toxin profile of the sample. This work constitutes the first report that describes the multi-toxin profile in urine and post-mortem plasma samples after puffer fish consumption, and complements the previous information on TTX present in human samples.

Acknowledgments

The research leading to these results has received funding from the Instituto Nacional de Investigación y Tecnología Agraria y Alimentaria (INIA) through the PROMAQUA project (RTA2013-00096-00-00) and from CERCA/Generalitat de Catalunya program. Sandra Leonardo acknowledges scholarship from IRTA-Universitat Rovira i Virgili-Banco Santander (2013PIPF URV-IRTA-BS-01).

References

Boundy M.J., Selwood A.I., Harwood D.T., McNabb P.S., Turner A.D., 2015. Development of a sensitive and selective liquid chromatography-mass spectrometry method for high throughput analysis of paralytic shellfish toxins using graphitised carbon solid phase extraction. J. Chromatogr. A 1387, 1-12.

Fong B. M.-W., Tam S., Tsui K.-H., Leung S.-Y. K., 2011. Development and validation of a high-throughput double solid phase extraction-liquid chromatography-tandem mass spectrometry for the determination of tetrodotoxin in human urine and plasma. Talanta 83, 1030-1036.

Islam Q.T., Razzak M.A., Islam M.A., Bari M.I., Basher A., Chowdhury F.R., Sayeduzzaman A.B.M., Ahasan H.A.M.N., Faiz M.A., Arakawa O., Yotsu-Yamashita M., Kuch U., Mebs D., 2011. Puffer fish poisoning in Bangladesh: clinical and toxicological results from large outbreaks in 2008. Trans. R. Soc. Trop. Med. Hyg. 105, 74-80.

Kawatsu K., Hamano Y., Yoda T., Terano Y., Shibata T., 1997. Rapid and highly sensitive enzyme immunoassay for quantitative determination of tetrodotoxin, Jpn. J. Med. Sci. Biol. 50, 133-150.

Lee C.H., Ruben P.C., 2008. Interaction between voltage-gated sodium channels and the neurotoxin, tetrodotoxin. Channels 2, 407e412.

Leonardo S., Rambla M., Samdal I.A., Miles C.O., Kilcoyne J., Diogène J., O'Sullivan C.K., Campàs M., 2017. Immunorecognition magnetic supports for the development of an electrochemical immunoassay for azaspiracid detection in mussels. Biosens. Bioelectron. 97, 200-206

Leung K. S.-Y., Fong M.-W. B., Tsoi Y.-K., 2011. Analytical challenges: Determination of tetrodotoxin in human urine and plasma by LC-MS/MS. Mar. Drugs 9, 2291-2303.

Nakamura M., Yasumoto T., 1985. Tetrodotoxin derivatives in puffer fish. Toxicon 23, 271-279.

Noguchi T., Arakawa O., 2008. Tetrodotoxin – Distribution and accumulation in aquatic organisms, and cases of human intoxication. Mar. Drugs 6, 220-242.

O'Leary M.A., Schneider J.J., Isbister G.K., 2004. Use of high performance liquid chromatography to measure tetrodotoxin in serum and urine of poisoned patients. Toxicon 44, 549-553.

Pratheepa V., Vasconcelos V., 2013. Microbial diversity associated with tetrodotoxin production in marine organisms. Environ. Toxicol. Pharm. 36, 1046-1054.

Maillaud C., Barguil Y., Le Coq Saint-Gilles H., Mikulski M., Guittonneau-Leroy A.L., Pérès H., Nour M., 2015. Puffer fish poisoning in New Caledonia. Case reports. Toxicologie Analytique et Clinique 28, 57-63.

Rambla-Alegre M., Reverté L., del Río V., de la Iglesia P., Palacios O., Flores C., Caixach J., Campbell K., Elliott C.T., Izquierdo-Muñoz A., Campàs M., Diogène J., 2017. Evaluation of tetrodotoxins in puffer fish caught along the Mediterranean coast of Spain. Toxin profile of *Lagocephalus sceleratus*. Environ. Res. 158, 1-6.

Reverté L., de la Iglesia P., del Río V., Campbell K., Elliott C.T., Kawatsu K., Katikou P., Diogène J., Campàs M., 2015. Detection of tetrodotoxins in puffer fish by a self-assembled monolayer-based immunoassay and comparison with surface plasmon resonance, LC-MS/MS and mouse bioassay. Anal. Chem. 87, 10839-10847.

Reverté L., Rambla-Alegre M., Leonardo S., Bellés C., Campbell K., Elliott C.T., Gerssen A., Klijnstra M.D., Diogène J., Campàs M., 2018. Development and validation of a maleimide-based enzyme-linked immunosorbent assay for the detection of tetrodotoxins in oysters and mussels. Talanta 176, 659-666.

Turner A.D., Boundy M.J., Dhanji Rapkova M, 2017. Development and single-laboratory validation of a liquid chromatography tandem mass spectrometry method for quantitation of tetrodotoxin in mussels and oysters. JAOAC Int. 100 (5) 1-14.

Yotsu-Yamashita M., Abe Y., Kudo Y., Ritson-Williams R., Paul V.J., Konoki K., Cho Y., Adachi M., Imazu T., Nishikawa T., Isobe M., 2013. First identification of 5,11-dideoxytetrodotoxin in marine animals, and characterization of major fragment ions of tetrodotoxin and its analogs by high resolution ESI-MS/MS. Mar. Drugs 11, 2799-2813.

Yotsu-Yamashita M., Yamagishi Y., Yasumoto T., 1995. 5,6,11-Trideoxytetrodotoxin from the puffer fish, *Fugu poecilonotus*. Tetrahedron Lett. 36, 9329-9332.

Yu C.H., Yu C.F., Tam S., Yu P.H.F., 2010. Rapid screening of tetrodotoxin in urine and plasma of patients with puffer fish poisoning by HPLC with creatinine correction. Food Addit. Contam. 27, 89-96.

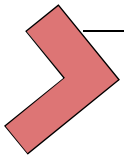

CHAPTER 4

Electrochemical biosensors for the detection of marine toxins

Trends and prospects on electrochemical biosensors for the detection of marine toxins

Sandra Leonardo, Anna Toldrà, Mònica Campàs

IRTA, Carretera de Poble Nou, km 5.5, 43540 Sant Carles de la Ràpita, Spain

Abstract

The need for rapid, sensitive and reliable methods able to guarantee seafood safety and to protect consumers has favoured the development of electrochemical biosensors for the detection of marine toxins. Thanks to their ability to analyse complex samples, ease of use, portability and low cost, electrochemical biosensors have recently emerged as promising bioanalytical tools in the marine toxin field. In the last years, several immunosensors, enzyme sensors, aptasensors and cell biosensors have been reported for the detection of marine toxins. The aim of this chapter is to critically analyse the existing electrochemical biosensors for marine toxins, while providing a general overview of the basic principles and types of electrochemical biosensors. Although the use of biosensors to detect and quantify marine toxins is being accomplished, the implementation of such devices in daily life still requires a lot of effort. Nonetheless, biotechnology and nanotechnology are revolutionising their development and improving their performance. Progress in these areas is so fast that biosensors for marine toxins could be implemented in routine analysis soon.

1. Introduction

Biosensors are compact bioanalytical tools that incorporate a biorecognition element in intimate contact with a physio-chemical transducer. While the bioreceptor recognises the target analyte, the transducer converts the biorecognition event into a measurable signal, which can be electrochemical, optical, piezoelectric or thermal. Ideally, for a biosensor to be useful, it should be sensitive, selective, precise, fast, cheap, miniaturised and automated, allow *in situ* analysis, and be able to deal with small sample volumes. Among the different transduction techniques, electrochemistry stands out because of the inherent high sensitivities, low cost and possible miniaturisation of electrodes and potentiostats, compatibility with microfluidics systems, and automation and subsequent simplicity

of the protocols. It is not surprising, then, that many electrochemical biosensors have been developed for a large range of analytes and applications such as the medical field, food analysis, defence/bioterrorism and environmental surveillance in the last years.

Electrochemical biosensors for the detection of marine toxins emerged no more than 25 years ago. Although not for all marine toxins, several immunosensors, enzyme sensors, aptasensors and cell biosensors have been reported [1]. Obviously, such biosensors do not fulfil all requirements mentioned above, but they pave the way towards their broad implementation. In fact, biosensors for the detection of marine toxins are nowadays experiencing a boom time thanks to the recent advances in biotechnology and nanotechnology, which contribute to their modernisation and improvement of their applicability [2, 3]. Table 1 summarises the electrochemical biosensors that have been developed for the detection of marine toxins, which are described in the following sections.

2. Immunosensors

Specific affinity interaction between antibodies (Abs) and antigens constitutes the keystone of immunoassays and immunosensors. Enzyme-linked immunosorbent assays (ELISAs), which rely on the use of specific Abs against target analytes and enzymes as labels (usually horseradish peroxidase (HRP) or alkaline phosphatase (ALP)), are the most common immunoassay approaches. ELISA formats have been adapted for the development of immunosensors, differing from the ELISA tests in the immunospecies immobilisation surface and the detection technique. Nowadays, immunosensors are the most widely used type of biosensors for the screening and precise quantification of marine toxins, because of their high selectivity and sensitivity, as well as the availability of specific Abs compared to enzymes and aptamers.

Nonetheless, obtaining Abs for the development of immunoassays and immunosensors for marine toxins is sometimes challenging. Abs are not always commercially available and they can be difficult to produce due to the small size of some marine toxins or the scarcity of purified toxin standards. The size and structure of the toxin also play an important role in the format adopted for the immunosensor development. While in competitive assays free and immobilised or labelled toxins compete for a capture Ab, in sandwich assays the target analyte is sandwiched between two Abs: a capture Ab, which is usually immobilised and recognises the analyte of interest, and a detector Ab, which also recognises the antigen but not through the same antigenic site. Consequently, in the development of sandwich

immunoassays, only large molecules with different antigenic epitopes can be targeted.

It is important to keep in mind that the interaction of toxins with Abs is based on a structural recognition, thus not necessarily related to their toxicity. Abs may have the ability to detect different toxin analogues or derivatives if they share a structurally similar fragment. This cross-reactivity may be advantageous or not, depending on whether the purpose is to detect the whole family of toxins (not all of them necessarily having the same toxicological potency) or just a specific one. Nevertheless, Abs are robust biorecognition molecules, with high affinity and sensitivity towards their analytes. Together with their easy handling and manipulation, the use of Abs in the development of electrochemical biosensors offers a wide range of possibilities.

Despite being beyond the scope of this chapter, it is worth mentioning the strategy based on the combination of immunoassays with capillary electrophoresis and subsequent electrochemical detection, which has been applied to the detection of some marine toxins [4-10]. In those works, immunocomplexes are formed in solution and subsequently introduced into capillaries for separation and detection of the product from the enzyme label reaction into a detection cell. Consequently, since in these cases there is no intimate contact between the biorecognition element and the transducer, these bioanalytical systems cannot be considered as electrochemical biosensors in the strict sense.

In this section, we provide a detailed overview of the electrochemical immunosensors that have been developed for the detection of okadaic acid (OA), dinophysistoxin-1 (DTX-1), azaspiracids (AZAs), domoic acid (DA), saxitoxin (STX), brevetoxins (PbTXs), palytoxin (PlTX) and tetrodotoxins (TTXs). Ciguatoxins (CTXs) and cyclic imines (CIs) (spirolides, gymnodimines, pinnatoxins and pteriatoxins), although also of concern, have not been included since no electrochemical immunosensors have been reported to date.

2.1. Okadaic acid

The accumulation of okadaic acid (OA) and its derivatives dinophysistoxin-1 (DTX-1) and dinophysistoxin-2 (DTX-2) in shellfish during *Dinophysis* blooms poses a serious threat to consumers and an enormous economic problem for shellfish producers. With apparently no harmful effect on shellfish, the consumption of OA-contaminated shellfish by humans results in symptoms such as diarrhoea, nausea, vomiting and abdominal pain. This clinical profile is known as diarrheic shellfish

poisoning (DSP). OA immunosensors have been one of the most explored electrochemical biosensors among marine toxins.

The selection of the immunospecies immobilisation technique on the transducer surface is the key point in the design of an immunosensor. In many cases, bovine serum album (BSA) or ovalbumin (OVA) have been used as carriers to immobilise the toxin on the electrode surface. The first immunosensors for OA were based on this approach [11, 12]. OA-BSA and OA-OVA conjugates were prepared following a carbodiimide reaction that allowed binding the OA to the protein through its carboxylic group. OA conjugates were immobilised on screen-printed carbon electrodes and competed with free toxin for an anti-OA Ab. A direct immunosensor was developed using an ALP-labelled anti-OA Ab, providing a limit of detection (LOD) of 1.5 ng/mL [11]. Campàs and collaborators developed an indirect OA immunosensor using secondary Abs labelled with ALP or HRP for signal generation (Figure 1) [12]. LODs of 1.07 and 1.98 ng/mL were obtained by the detection of *p*-aminophenol produced by the reaction of *p*-aminophenyl phosphate with ALP, and by the detection of 5-methyl-phenazinium methyl sulphate redox mediator in the HRP bioelectrocatalysis, respectively. An electrochemical signal amplification system based on diaphorase recycling was integrated into the ALP-based immunosensor, which enabled to decrease the LOD to 0.03 ng/mL and enlarge the working range by two orders of magnitude. Mussel and oyster samples were analysed and results compared with those obtained by the colorimetric immunoassay, the protein phosphatase inhibition assay (PPIA) and liquid chromatography coupled to tandem mass spectrometry (LC-MS/MS), demonstrating the viability of the approach.

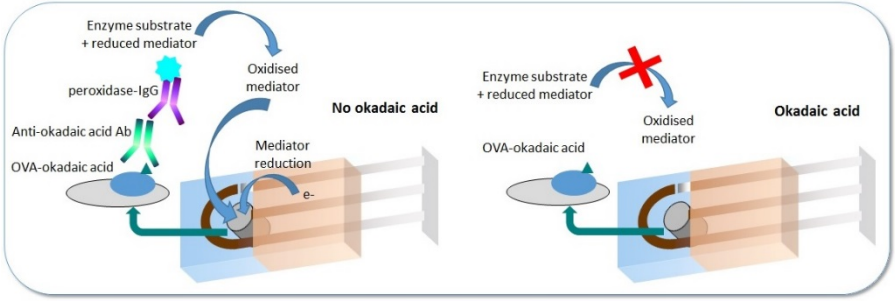

Figure 1. Electrochemical immunosensor for okadaic acid (OA) detection based on a competitive indirect assay.

To avoid the coating of electrodes with protein carriers that would reduce electron transfer and decrease the sensitivity of electrochemical immunosensors, the direct immobilisation of OA on the electrode surface was explored. An electrochemical method based on the diazonium-coupling reaction mechanism (electrografting) was exploited by Hayat and collaborators for the immobilisation of OA on screen-printed carbon electrodes [13]. Electrochemical reduction of diazonium species *via* one-electron process lead to the formation of 4-carboxyphenyl radicals covalently attached to the electrode surface. The terminal carboxylic group of 4-carboxyphenyl was then activated to bind hexamethyldiamine. OA was immobilised to the second terminal amine group of hexamethyldiamine *via* its activated carboxylic group. After OA immobilisation, an indirect competitive immunoassay step was used to detect the free toxin. The immunosensor provided an LOD of 1.44 pg/mL in buffer and of 2.4 ng/kg in mussel samples, a concentration extremely lower than the agreed maximum permitted level set by several institutions such as the European Commission (160 µg of OA equivalents/kg shellfish) [14].

The use of magnetic beads (MBs) as immobilisation supports or carriers provides wide advantages in the development of immunosensors: increase of the surface area, easy and fast functionalisation and manipulation, and decrease of the matrix effects. Streptavidin-coated MBs were used to immobilise biotinylated OA and to perform a competitive indirect assay [15], which attained an LOD of 0.38 ng/mL. The good toxin recovery percentage obtained in the analysis of spiked mussel samples (96%) demonstrated the lack of matrix effects and interferences, and highlighted the usefulness of MBs in the development of immunosensors. MBs also allowed the integration of the immunosensor into an automated flow system, decreasing the LOD to 0.15 ng/mL [16]. Flow injection analysis provides rapidity and accuracy to the systems due to the high degree of control and the constancy of analytical parameters. Furthermore, automation makes routine tasks easier and less cumbersome. The use of MBs in flow injection analysis systems is a first step towards miniaturised and portable analysis devices.

Instead of OA immobilisation on the electrode surface, other approaches have proposed the immobilisation of the Ab and, if possible, in an oriented way. Tang and collaborators immobilised the anti-OA Ab by adsorption, which clearly did not allow an oriented immobilisation of the Ab [17]. A competition step between OA and OA-ALP conjugate was performed, which provided an LOD of 2 ng/mL by the detection of *p*-aminophenol resulting from the reaction catalysed by the OA-ALP tracer. To provide an oriented Ab immobilisation and avoid possible steric effects, protein G-coated MBs were explored as Ab immobilisation supports [18]. Electrografting of diazonium species was also used to immobilise the anti-OA Ab through the terminal carboxylic groups on screen-printed [19] or graphene-modified [20] carbon

electrodes. These approaches provided a label-free format. The blocking effect of the OA (when performing a direct assay) [18-19] or OA-OVA conjugate (when performing a competitive assay) [20] and the subsequent decrease of electrode transfer was used to detect OA by differential pulse voltammetry (DPV) [18], electrochemical impedance spectroscopy (EIS) [19] or square wave voltammetry (SWV) [20]. LODs of 0.5 ng/mL and 0.3 ng/mL were obtained in the direct assays based on the use of MBs and electrografting, respectively. Due to the higher blocking effects and the overall negative charge of OA-OVA conjugate, a lower LOD of 19 pg/mL was obtained in the competitive approach [20]. The good recovery percentages obtained in the analysis of spiked-mussel samples (95%) demonstrate the feasibility of the different approaches.

2.2. Azaspiracids

Azaspiracids (AZAs) are lipophilic marine toxins that originate from the microalgae of the genera *Azadinium* and *Amphidoma*, which can accumulate in shellfish and also be metabolised into other AZA analogues. The consumption of AZA-contaminated shellfish can lead to AZA shellfish poisoning (AZP). Although more than 30 different analogues have been identified, the European Commission has set a maximum level of 160 μg of AZA equivalents/kg shellfish only for AZA-1, AZA-2 and AZA-3, the most important analogues based on occurrence and toxicity [14]. To date, only a polyclonal Ab (PAb) raised using a synthetic fragment of AZA [21] and a monoclonal Ab (mAb) raised using AZA-1 [22] have been reported. Recently, the anti-AZA PAb has been used in the development of an MB-based direct immunoassay for AZA detection [23]. The Ab was immobilised on protein G-coated MBs and a competitive step using HRP-labelled AZA was performed. A colorimetric approach was first developed to optimise the experimental parameters and establish the cross-reactivity factors (CRFs) for AZA-1–10. The subsequent combination of the immunorecognition MBs with 8-electrode arrays enabled the multiple electrochemical detection of AZAs. However, it is necessary to mention that the immobilisation of the MBs on the electrode surface by the use of a magnet to provide the corresponding electrochemical immunosensor produced a change in the slope of the calibration curve that increased the LOD (3.7 ng/mL) compared with the colorimetric immunoassay (1.1 ng/mL). This difference could be due to mass transfer limitations of the enzyme kinetics due to its packed distribution on the electrode. For this reason, in a second approach, the enzyme reaction was performed in suspension and the resulting product was transferred to the electrodes for the corresponding amperometric measurement. Naturally-contaminated mussel samples were analysed and the results showed an excellent correlation with LC-MS/MS analysis. The electrochemical MB-based immunoassay

allowed the quantification of a wide range of AZA concentrations (120-2,875 µg AZA-1 equivalent/kg), with an LOD (63 µg AZA-1 equivalent/kg) below the regulatory threshold, using a protocol that requires very few steps and a very short analysis time (~15 min). The high specificity of the assay provided a tool able to recognise all regulated AZAs but also a broad range of other toxic AZA analogues, which is complementary to the LC-MS/MS official method.

2.3. Domoic acid

Domoic acid (DA) is a potent neurotoxin produced by several diatom species of the genus *Pseudo-nitzschia.* Ingestion of DA-contaminated shellfish leads to amnesic shellfish poisoning (ASP), which is characterised by both gastrointestinal and neurological symptoms. To protect consumers from ASP, the European Commission has set a regulatory limit for DA in shellfish of 20 mg/kg [14]. For the development of electrochemical immunosensors, DA-BSA conjugates were obtained and immobilised on screen-printed carbon electrodes. Anti-DA PAbs were used to perform a competition assay between free and immobilised DA [11, 24, 25]. Secondary Abs labelled with ALP were used for the detection of *p*-aminophenol (by amperometry) [11, 24] or α-naphthol (by DPV) [25], electroactive products produced by ALP after addition of the corresponding enzyme substrate. LODs attained ranged from 0.1 to 5 ng/mL. Micheli and collaborators applied the electrochemical immunosensor to the analysis of spiked mussel samples, obtaining an effective LOD of 20 mg/kg mussel, equal to the maximum permitted level [25].

2.4. Saxitoxin

Paralytic shellfish poisoning (PSP) toxins arise from dinoflagellates belonging to the genera *Alexandrium*, *Gymnodinium* and *Pyrodinium* and certain cyanobacteria (including *Anabaena*, *Cylindrospermopsis*, *Aphanizomenon*, *Planktothrix* and *Lyngbya*). These toxins, including neosaxitoxin (neoSTX), gonyautoxins (GTXs), decarbamoylsaxitoxin (dcSTX) and saxitoxin (STX) as the parent toxin, cause PSP in humans upon consumption of contaminated seafood, producing numbness in the face and extremities, respiratory paralysis, and potentially death when PSP toxins block neuron transmission upon binding to voltage-gated sodium channels. As PSP toxins are present worldwide, have no known antidote, and have potencies that do not decrease by food preparation (e.g., heating, freezing, treatment with acid), there is the need for monitoring coastal waters and detecting PSP toxins in seafood to ensure public safety. The European Commission has set a maximum permitted level of 800 µg STX equivalents/kg shellfish [14]. To the best of our knowledge, only

one STX electrochemical immunosensor has been reported, which was published in 1993, being probably the first electrochemical immunosensor for a marine toxin ever developed [26]. The work also included the development of an electrochemical immunosensor for PbTX. Both immunosensors were based on the immobilisation of toxin-BSA conjugates on a membrane through the lysine moiety of BSA and the subsequent competition for glucose oxidase (GOx)-labelled primary Ab. When glucose was added, GOx produced H_2O_2, which was subsequently detected by amperometry.

2.5. Brevetoxins

Brevetoxins (PbTXs) are primarily produced by the dinoflagellate *Karenia brevis* and can accumulate in shellfish and fish, being the causative agent of neurotoxic shellfish poisoning (NSP). The toxicological information for PbTXs is limited. Maximum permitted levels have been established in the USA (20 mouse units (MU)/100 g or 0.8 mg PbTX-2 equivalents/kg fish) [27], New Zealand [28] and Australia [29] (20 MU/100 g). Currently there are no regulatory limits for PbTX-group toxins in shellfish or fish in Europe. The discovery of new PbTX-group toxin-producing algae and the apparent trend towards expansion of algal blooms distribution suggest that PbTXs could emerge in Europe and their analysis in shellfish and fish should be considered. PbTXs are low-molecular weight toxins (~900 g/mol) usually with only one hydroxyl group available for cross-linking, which hinders its immobilisation to develop immunosensors. Some years after the development of the first electrochemical immunosensor for STX and PbTX previously reported [26], Kreuzer and co-workers, following the same procedure used to develop the immunosensors for OA, DA and TTX, obtained a PbTX-3-BSA conjugate that was immobilised on the screen-printed electrode surface to perform a competitive assay, using an ALP-labelled secondary Ab for the measurement [11]. An LOD of 6 ng/mL was obtained, although the authors reported a sensitivity problem attributed to the difficulties encountered in the conjugate synthesis and the low amount of toxin available.

The sensitivity of immunosensors can usually be improved by the control of the amount and orientation of antigens/Abs immobilised on the electrode surface, which have to retain their biological activity. Dendrimers are hyperbranched polymers precisely engineered to carry molecules encapsulated in their interior void spaces or attached to their surface, providing high immunospecies immobilisation yields. A sensitive electrochemical immunosensor for PbTX-2 was developed exploiting dendrimers as toxin immobilisation nanostructured supports [30]. Due to the low conductivity of dendrimers, gold nanoparticles (AuNPs) were synthesised

and encapsulated into amine-terminated poly(amidoamine), providing conjugates with good conductivity that were afterwards adsorbed on ester-modified gold electrodes. PbTX-2-BSA conjugates were then immobilised on the nanostructured surface. Free and immobilised PbTX-2 competed for the HRP-labelled anti-PbTX-2 mAb and the immunosensor response was measured using *o*-phenylendiamine and H_2O_2. An LOD of 0.01 ng/mL was obtained, which is much lower than the LOD for the immunosensor without AuNPs or dendrimers (0.5 ng/mL and 0.1 ng/mL, respectively). As demonstrated, the use of the 3D-network of AuNP-dendrimer conjugates greatly increased the amount of immobilised PbTX-2-BSA. Moreover, the higher conductivity of the immunosensing interface, achieved by the use of AuNPs, enhanced the sensitivity of the electrochemical immunosensor.

Although enzyme labels are widely used and well-explored in the development of immunosensors, they require enzyme substrates and their bioactivity can decrease when they are exposed to harsh reaction conditions. To tackle this issue, other electroactive species such as thionine or guanine/adenine nucleobases can be used as indicators, as well as various nanomaterials, including quantum dots, metal nanoparticles and metal ions. Chen's research group explored the use of MBs to covalently immobilise anti-PbTX-2 mAb and act as immunosensing probes for the capture of PbTX-2 [31]. PbTX-2-BSA conjugates were chemically modified with guanine-assembled graphene nanoribbons. Guanine, which can be oxidised in the presence of $Ru(bpy)_2^{3+}$, was used as a label. The catalytic oxidation of guanine was electrochemically detected after the competition step and entrapment of the magnetic immunocomplex on the electrode. The LOD of the magneto-controlled electrochemical immunoassay was 1 pg/mL of PbTX-2 and its applicability was demonstrated by the analysis of spiked mussel, clam and cockle samples, which provided similar results to those obtained with a commercial ELISA. The same research group also explored the use of metal nanoclusters as labels [32]. MBs were used to co-immobilise anti-PbTX-2 and anti-DTX-1 mAbs by epoxy-amine reaction. Cadmium nanoclusters and copper nanoclusters were linked to PbTX-2-BSA and DTX-1-BSA, respectively, and used as distinguishable signal tags. On the basis of the competitive immunoassay format, the immunocomplexes were collected onto a magnetic detection cell and the electrochemical signals were simultaneously recorded at different potentials using square wave anodic stripping voltammetry (SWASV). The multiplexed immunosensor was able to discriminate between PbTX-2 and DTX-1 without any interference. The LODs obtained were 1.8 ng/mL and 2.2 ng/mL for PbTX-2 and DTX-1, respectively. The method featured unbiased identification of negative and positive samples, as it was demonstrated by the analysis of spiked mussel, clam and cockle samples containing both marine toxins and comparison with a commercial ELISA.

Other enzyme-free electrochemical immunosensors for PbTX-2 exploring mesoporous structures have also been described [33-34]. A competitive immunoassay was developed using a mesoporous carbon-enriched palladium nanostructure (MSC-PdNS) as a label due to its peroxidase mimic activity [33]. In this configuration, PbTX-2-BSA was immobilised onto a nanogold-functionalised carbon electrode through affinity interactions between cysteine or lysine residues of BSA and gold. Afterwards, free PbTX-2 present in the sample competed with immobilised PbTX-2-BSA for the MSC-PdNS-labelled mAb, and the resulting catalytic current in the presence of H_20_2 and thionine mediator was recorded. The electrochemical immunosensor showed an LOD of 5 pg/mL and was successfully applied to the analysis of spiked mussel samples, providing results in good correlation with the commercial ELISA. Mesoporous silica structures also allow the encapsulation of substrates in their pores, as they possess tuneable pore size and chemically modifiable surfaces, which makes possible their use as nanocontainers. An electrochemical immunoassay for PbTX-2 detection was developed that exploits these mesoporous silica nanocontainers (MSNs) [34]. Methylene blue was loaded into the pores of anti-PbTX-2 Ab-functionalised mesoporous silica, and the pores were capped with aminated polystyrene microspheres *via* electrostatic interaction. Upon addition of target PbTX-2, the positively charged microspheres were displaced from the negatively charged mAb-MSNs because of the specific antigen-Ab interaction. Thereafter, the molecular gate was opened and the trapped methylene blue was released from the pores and was monitored by SWV, obtaining an LOD for PbTX-2 of 6 pg/mL. Spiked seafood samples were analysed, which were in good accordance with the results obtained by a commercial ELISA.

2.6. Palytoxins

Palytoxins (PlTXs) are complex polyhydroxylated compounds with lipophilic and hydrophilic parts. The potential routes of human exposure to PITXs are seafood consumption and dermal and inhalation exposure to aerosols from *Ostreopsis* blooms. Additionally, clupeotoxism is a rarely occurring highly fatal form of human intoxication in tropical areas due to the ingestion of clupeoid fish (some species of sardines and herrings) in which PlTxs are involved. However, the available toxicological information of PITX is still limited and no regulations on PITX-group toxins in shellfish are currently available. Nevertheless, in a meeting of the working group of Toxicology of the National Reference Laboratories for Marine Biotoxins, a provisional limit of 250 µg/kg in shellfish was proposed [35].

The relatively large size of PITX (2,680 g/mol) makes the production of Abs *via* animal immunisation easy and allows the development of sandwich immunoassays,

as different antigenic epitopes can be targeted. Zamolo and collaborators developed an electrochemical immunosensor for the detection of PlTX based on a sandwich format and electrochemiluminescence detection [36]. The immunosensor incorporated double carboxyl-functionalised multi-walled carbon nanotubes (MWCNTs), the groups on the sidewalls being used to conjugate capture anti-PlTX mAb and those on the tips being used to immobilise it on the surface of an optically transparent electrode coated by an electrochemical polymer layer. The electrochemiluminescence detection was performed by labelling the detection anti-PlTX PAb with a ruthenium complex. The use of MWCNTs increased the amount of immobilised mAb and favoured the electron transfer, providing an LOD of 0.07 ng/mL. The applicability of the immunosensor was demonstrated by the analysis of spiked mussels and microalgae samples. Low matrix effects were observed due to the modification of the electrode with MWCNTs, which minimised the non-specific adsorption, and the electrochemiluminescent transduction strategy.

2.7. Tetrodotoxins

Tetrodotoxin (TTX) is one of the most potent low-molecular-weight (319 g/mol) marine toxins. Unlike other marine toxins, TTX may not be produced by microalgae but by certain endo-symbiotic bacteria. Recently, the marine dinoflagellate *Prorocentrum minimum*, has been described to produce TTXs in cultures, with possible implication of endosimbiotic bacteria [37]. Although TTX was originally discovered in puffer fish, its presence has been reported in many other organism, including amphibians, echinoderms, cephalopods and even bivalve molluscs [38]. In Japan, a value of 2 mg of TTX equivalents/kg of edible portion has been used as a criterion to judge the acceptability of puffer fish as food [39]. In Europe, the current legislative requirements establish that poisonous fish of the family Tetraodontidae and products derived from them must not be placed on the European markets [14]. The occurrence of puffer fish from the species *Lagocephalus sceleratus* in the Mediterranean coast (Turkey [40], Greece [41], Israel [42, 43], Lebanon [44], Lybia [45], Cyprus [46], Italy [47] and Spain [48]) in the last decade, in some cases related to human intoxications, as well as the recent detection of shellfish contaminated by TTX in England [49], Greece [50] and the Netherlands [51], have led to an increasing concern about the risk that this toxin may pose in Europe. Our group, in collaboration with Queen's University of Belfast, has recently developed an electrochemical biosensor for the detection of TTXs in the frame of the ECsafeSEAFOOD project. This immunosensor was based on the immobilisation of TTX to carboxylated polyethylene glycol-dithiols self-assembled on gold electrode arrays and a subsequent competition step. Compared to the previous electrochemical immunosensors [11, 52], this strategy results in an ordered and

oriented antigen immobilisation, with antigens spaced enough to favour interaction with the Ab, and with low matrix effects because of the protecting effect from the polyethylene glycol chains. Prior to immunosensor development, the strategy was checked by colorimetry on microtiter plates [53]. Colorimetric immunoassays demonstrated the feasibility of the approach, which provided an LOD of TTX of 2.28 ng/mL in buffer, which would correspond to 0.23 mg/kg when analysing puffer fish. Colorimetric immunoassays also allowed establishing correction factors for the different puffer fish matrices (intestinal tract, muscle, skin, liver and gonads) and CRFs for several TTX analogues (5,6,11-trideoxy-TTX, 5-deoxy-TTX and 11-deoxy-TTX, 11-nor-TTX-6-ol, and 4,9-anhydro-TTX). Once the colorimetric immunoassay was fully characterised, the electrochemical detection was investigated by using a precipitating redox mediator for the HRP label, which favours the electron transfer. The immunosensor attained an LOD of 2.6 ng/mL in buffer, being 0.07 mg/kg when analysing puffer fish (lower than in the colorimetric immunoassay because of the ability of the immunosensor to operate under puffer fish matrix loadings of 40 mg/mL).

3. Enzyme sensors

Enzyme assays and sensors are usually based on the ability of enzymes to convert a substrate into a product, or to be inhibited or activated by an analyte. Very few enzyme sensors have been developed for the detection of marine toxins, the main reason being the scarcity of enzymes specific for these analytes. To date, only two enzymes, protein phosphatase (PP) and phosphodiesterase (PDE), have been identified as biorecognition molecules for specific marine toxins. The principle of detection is the inhibitory effect that DSP toxins and yessotoxins (YTXs) cause on the activity of PPs and PDEs, respectively. The recognition principle in enzyme assays and sensors is based on a functional recognition, and this recognition may not be related to toxicity. Consequently, similarly to the CRFs in immunoassays and immunosensors, the elucidation of inhibition equivalency factors (IEFs) for the toxins from a same family respect to the parent toxin is of high interest.

3.1. Okadaic acid and dinophysistoxins

DSP toxins are known to inhibit the activity of several serine/threonine PPs (e.g. PP2A and PP1) when binding the hydrophobic region near the active site [54]. The consequence of the blocking of PP enzyme activity is hyperphosphorylation of the proteins that control sodium secretion by intestinal cells and of cytoskeletal or

junctional elements that regulate permeability, with the subsequent loss of fluids probably responsible for diarrheic symptoms.

The inhibitory effect of DSP toxins on PP activity has been exploited to develop enzyme-based assays for the detection of these toxins [55-63]. One of the main challenges to overcome is the inherent instability of PP. Immobilisation of PPs on microtiter plates by entrapment into polymers and gels has been proven to increase enzyme stability [64-66]. Another important issue is the effect that sample matrices may cause on the enzyme activity. It is important to keep in mind that the biorecognition event between the toxin and the enzyme takes place at the same moment than the enzyme substrate development, and therefore sample matrices are of utmost concern. A careful and appropriate establishment of matrix loading limits (according to the shellfish matrix and to the specific PP) is crucial to avoid false positives and to provide accurate toxin determinations [62]. A sample clean-up step using solid-phase extraction (SPE) fractioning also decreases the matrix effects and allows loading higher matrix concentrations in order to attain lower LODs. This strategy has been useful to detect trace amounts of OA in a culture of *Prorocentrum rhathymum* from Malaysia [61] and also to screen the presence of DSP toxins in mussel samples [60].

Like CRFs in immunoassays and toxicity equivalency factors (TEFs) in cell-based assays (CBAs), the establishment of IEFs for OA analogues is crucial to characterise the performance of PP inhibition-based assays and sensors, as well as to understand the correlation with the reference LC-MS/MS method. IEFs have been established for DTX-1 and DTX-2 [63], and have been observed to differ depending on the enzyme type and nature (e.g. PP1 versus PP2A, wild versus recombinant) and, if pertinent, on the immobilisation method [63, 65, 67-68]. Although in general terms PP2A is more sensitive to DSP marine toxins than PP1, and DTX-2 inhibits less the enzymatic activity than DTX-1, the type and nature of the enzyme used and the experimental conditions may result in different inhibitory potencies from the different analogues. Consequently, we suggest to perform a full characterisation of the bioanalytical system prior to its implementation. Another issue worth to mention is the effect from DSP toxin esters, since they do not inhibit PPs or inhibit them at a much lower extent than parent toxins [59, 60, 63]. Nevertheless, hydrolysis is also required in LC-MS/MS analysis.

Whereas a wide variety of assays has been reported, the number of biosensors based on PP inhibition is much lower. The first work appeared in 2004, but it was not exactly a biosensor since PP was not immobilised on an electrode [69]. The authors combined the PP inhibition by OA with the phosphate ion consumption by pyruvate oxidase (PyOx) in a flow injection analysis system. Only PyOx, which is not the biorecognition enzyme, was immobilised. An LOD of 0.1 ng/mL was attained,

50-fold lower than in the colorimetric immunoassay. In a similar way, Volpe and collaborators combined the PP inhibition by OA with the PP activity towards glycogen phosphorylase a, enzyme that catalyses the conversion of glycogen to glucose-1-phosphate, in a flow injection analysis system [70]. These two enzymes were used off-line and in solution. Glucose-1-phosphate was then converted into glucose by ALP, and glucose was converted into H_2O_2 by GOx, which was electrochemically oxidised at a platinum electrode. Only ALP and GOx were co-immobilised on the electrode. Following this strategy, an LOD of 30 pg/mL was attained.

In 2007, PP was first immobilised on an electrode for the development of the corresponding electrochemical biosensor (Figure 2, left) [71]. The authors entrapped the enzyme with poly(vinyl alcohol) azide-unit pendant water-soluble photopolymer on screen-printed carbon electrodes and measured the enzyme activity with a novel substrate, catechyl monophosphate. Only when OA was not present, PP showed enzyme activity towards its phosphorylated substrate and thus, an amperometric current from the oxidation of the corresponding dephosphorylated substrate was obtained. The biosensor attained an LOD as low as 6.42 ng/mL and its applicability was demonstrated by the analysis of *Prorocentrum* spp. dinoflagellate extracts and the good agreement found with the contents obtained by the colorimetric assay and LC-MS/MS analysis. Although this immobilisation method provides stability to the enzyme, it creates a barrier that may limit its accessibility to the toxin and the substrate. With the purpose of avoiding this limitation, genetically engineered PPs containing a hexa-His tail have been obtained in order to immobilise them on Ni-modified MBs [68]. This immobilisation method, based on the affinity interaction between amino acid residues and metals, not only avoids the use of polymer matrices but also provides an oriented enzyme immobilisation. However, it has been observed that high enzyme amounts are required to achieve high enough electrochemical signals, which compromises the sensitivity of the biosensor.

Very recently, a biosensor that incorporates MWCNTs on the electrode surface by electropolymerisation of *p*-nitrophenol has been described [72]. Although PP was simply physically adsorbed, the immobilisation was stable probably because of the hydrogen bonding interactions and the π-π stacking interaction between the sidewalls of MWCNTs and the aromatic rings of the enzyme. An LOD of 0.55 ng/mL, corresponding to 2.75 µg/kg in mussels, was achieved.

Although PP stability is an important technological limitation, the main concern of PP inhibition-based biosensors is that only lipophilic DSP toxins can be addressed. Consequently, they should be restricted to geographical areas with outbreaks caused only by these toxins. Nevertheless, they can be applied as screening tools in

monitoring programs and save time and economic resources. For example, they can be used to analyse hydrolysed extracts (to date, hydrolysis is only required for DSP toxins), which means a reduction by half in the number of samples to analyse by LC-MS/MS. In case of positive results, preventive closures would be recommended, and the sample should be analysed by LC-MS/MS for confirmation. Additionally, the use of PP inhibition-based biosensors in research is unquestionable.

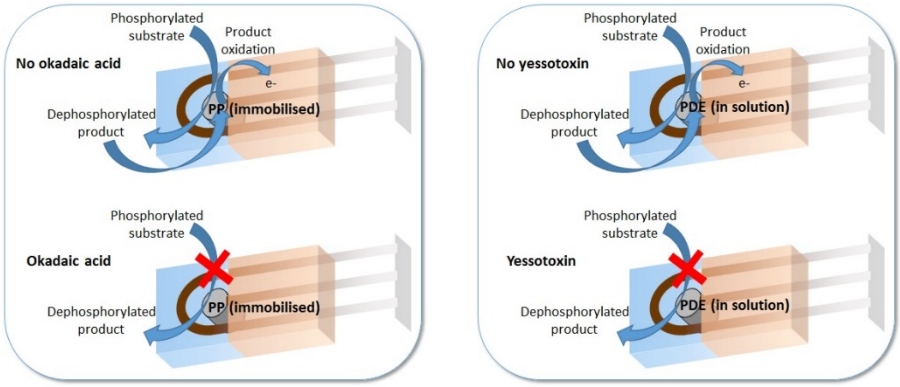

Figure 2. Electrochemical enzyme sensors for okadaic acid (OA) *(left)* and yessotoxin (YTX) *(right)* detection based on protein phosphatase (PP) and phosphodiesterase (PDE) inhibition, respectively.

3.2. Yessotoxins

Yessotoxin (YTX) is a lipophilic polycyclic ether toxin mainly produced by the dinoflagellates *Protoceratium reticulatum*, *Lingulodinium polyedrum* and *Gonyaulax spinifera*. Although YTX was initially included in the DSP toxin group, a lack of diarrheic effect was demonstrated in mice, an observation that led to no longer including YTX and its analogues within the DSP group. The presence of YTXs in shellfish is still regulated in Europe and other countries, despite the regulatory limit has already been increased from 1,000 µg of YTX equivalents/kg of shellfish meat to 3,750 µg/kg [73].

Only one strategy has been described for the electrochemical detection of YTX with enzymes and it is not exactly an enzyme sensor [74]. The strategy is based on the interaction between YTX and PDE, the corresponding enzyme inhibition and the electrochemical measurement of the enzyme activity. However, PDE was not immobilised on the electrode surface but used in solution in a drop configuration (Figure 2, right). The main challenge was to find an appropriate enzyme substrate, electrochemically active only after hydrolysis by PDE and at an appropriate working

potential. Best results were achieved with α-naphthyl phosphate, which provided an LOD of 0.69 µg/mL. The applicability of the electrochemical assay to the quantification of YTX in natural samples was evaluated by the analysis of cultures from different *Protoceratium reticulatum* strains (using *Prorocentrum micans* as a negative control). The study not only allowed the determination of YTXs contents in those cultures, but it also resulted in the identification of a strain that produces a YTX congener in high amounts. This result evidences that although this biosensor may not be very interesting in monitoring programs (because the possible YTX deregulation), its applicability to research purposes can be very useful.

4. Aptasensors

Aptasensors are based on the specificity of aptamers towards their targets. Aptamers are single stranded DNA (ssDNA) or RNA oligonucleotides that bind to a specific molecule with high affinity and specificity. They are selected from a random oligonucleotide library *via* an iterative process known as Systematic Evolution of Ligands by Exponential Enrichment (SELEX) that involves target binding, separation between bound and unbound sequences, elution of aptamers and PCR amplification. Aptamers have emerged as excellent recognition receptors since they offer attractive features: 1) their *in vitro* selection process avoids animal experimentation and leads to a low-cost and straightforward production, 2) they are highly stable, which provides long term-storage, 3) they can be easily modified with functional groups, and 4) their conformational change upon binding with the analyte can be exploited in the design of direct detection strategies [75-77].

Several aptamers against marine toxins have been produced in the last years [78-84], but only four electrochemical aptasensors have been reported [79, 82, 85, 86]. The aptamers have been produced to recognise TTX [78], OA [79, 80], STX [81], PbTX-2 [82], GTX-1&4 [83] and PITX [84], with dissociation constants in the nanomolar range. Most of the SELEX processes require the immobilisation of the toxin on a solid substrate, such as agarose [79] and sepharose [82] or, more recently, MBs [81, 84], which may change the original target conformation and/or restrict the affinity interaction (at least, towards a specific side of the target analyte). Nevertheless, a recent SELEX method has been developed to overcome this limitation [80, 83, 87] and has been applied to the SELEX for OA [80] and GTX-1&4 [83]. The method exploits the affinity interaction between graphene oxide (GO) and unbound oligonucleotide sequences, and separates them from the aptamers bound to the toxin. As a result, aptamers may be more effective in the analysis of natural samples containing toxins in their native conformation. The SELEX process can also be improved in order to increase the specificity of the resulting aptamers [88]. A

negative selection step without immobilised toxin can be added to the process to discard those sequences that may adsorb non-specifically on the solid substrates, as reported for STX [81] and PbTX-2 [82] aptamers. The addition of a counter selection step may increase even more the specificity. This counter SELEX consists on introducing toxins that have structural similarity to the target or are likely to coexist in the target environment. In this regard, counter-toxins have been used to generate highly specific aptamers against OA [80], GTX-1&4 [83] and PITX [84]. Biosensors using these aptamers showed no cross-reactivity against the marine toxins used in the counter selection step. Ideally, for applications in monitoring programs, an aptamer should be specific towards the whole family of toxins and, if possible, should show the same affinity for each toxin analogue. Consequently, the different selection steps of the SELEX process have to be carefully and rationally designed according to the final purpose. Finally, a post-SELEX optimisation can be performed to improve the affinity of the selected aptamers [88]. As an example, an optimised STX aptamer was generated through rational site-directed mutagenesis and truncation [89], achieving a 30-fold higher affinity compared with the parent aptamer [81].

4.1. Okadaic acid

A label-free impedimetric aptasensor was developed for the detection of OA [79]. The aptamer was immobilised on a gold electrode and the biorecognition event was monitored by the impedimetric signal variation caused by the change of the aptamer conformation upon toxin binging (Figure 3) without the need of any label. In the absence of OA, the negative charge of the DNA aptamer repeals the negatively charged $[Fe(CN)_6]^{3-/4-}$ anions, inhibiting the electron transfer. In the presence of OA, the aptamer changes its configuration thereby favouring the access of the redox indicator to the sensor surface and promoting electron transfer. The aptasensor attained an LOD of 70 pg/mL and did not show cross-reactivity towards DTX-1 and DTX-2. A preliminary application of the aptasensor to the analysis of OA-spiked shellfish samples was examined, achieving a toxin recovery of 92%.

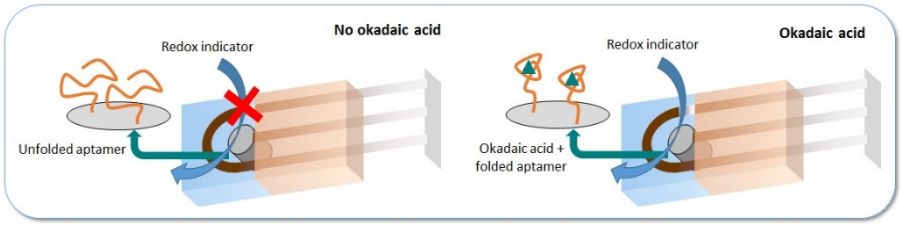

Figure 3. Electrochemical aptasensor for okadaic acid (OA) detection based on label-free target-induced folding of the aptamer.

4.2. Brevetoxin-2

The aptasensor described for the detection of PbTX-2 is also label free and uses EIS measurements, but it is based on a competitive format [82]. Gold electrodes were modified with a cysteamine self-assembled monolayer (SAM) for the subsequent covalent attachment of PbTX-2 *via* its hydroxyl group. The competition was established between immobilised PbTX-2 and free PbTX-2 in solution in the presence of a fixed amount of the aptamer. In the absence of free PbTX-2, the aptamer binds to the immobilized PbTX-2, blocking the electron transfer from $[Fe(CN)_6]^{3-/4-}$. As the concentration of free PbTX-2 in solution increases, the amount of free aptamer available for binding to the immobilised PbTX-2 on the gold surface decreases. As a consequence, $[Fe(CN)_6]^{3-/4-}$ is able to reach the electrode surface and transfer electrons. An LOD of 0.11 ng/mL was attained, and a high degree of cross-reactivity was observed towards PbTX-3. Moreover, no cross-reactivity with OA and microcystin-LR (MC-LR) was detected, which indicates the high selectivity of the aptasensor. The aptasensor was applied to the detection of PbTX-2 in spiked shellfish extracts showing a very high recovery percentage (between 102 and 110%).

4.3. Saxitoxin

A label-free aptasensor based on DPV measurements has been recently proposed for the detection of STX [85]. Gold electrodes were modified with an octadecanethiol SAM and then coated with a film of MWCNTs to which the amino-terminated aptamer was covalently immobilised. Methylene blue was electrostatically anchored on the MWCNTs and used as a redox indicator. The detection strategy of the aptasensor is based on a target-induced structure switching. In the absence of STX, the aptamer shows a flexible conformation which allows the methylene blue to bind to guanine bases. In the presence of STX, the aptamer changes its configuration from a flexible to a rigid structure, which prevents the exposure of the bases and restricts the electron transfer from the

redox indicator to the electrode surface, resulting in a lower electrochemical signal. So, as STX concentration increases, the DPV current from methylene blue decreases. The aptasensor attained an LOD of 0.11 ng/mL and demonstrated no cross-reactivity towards toxins that may be present along with STX or structurally similar, including OA, neoSTX and GTX-1&4. The assay was applied to the determination of STX in spiked mussel samples and the recovery was found to be between 63 and 121%.

4.4. Tetrodotoxin

The aptasensor developed for the detection of TTX was also label free and based on EIS measurements, and it did not even require the presence of a redox mediator in solution [86]. Glassy carbon electrodes were modified with poly(4-styrenesolfonic acid)-doped polyaniline films (PSSA/PANI) by electropolymerisation. Afterwards, the amino-terminated aptamer against TTX was covalently immobilised on the PSSA/PANI films *via* glutaraldehyde cross-linking. The detection of TTX was assessed by the change in impedance upon target binding. In the absence of TTX, electron transfer of the PSSA/PANI film occurs, whereas when TTX is present the electron transfer decreases. The low LOD attained, 19.9 pg/mL, was certainly due to the ordered monolayer of conductive PSSA/PANI films, which improved the electron transfer. Cross-reactivity experiments towards other toxins as well as studies in natural samples were not assessed.

5. Cell biosensors

CBAs give an indication of the overall toxicity of a sample and therefore are extremely useful for the identification of unknown toxic compounds, not targeted in chemical analysis. Cell biosensors (which also include tissue-based sensors) are well behind biosensors based on Abs, enzymes or aptamers. The limited progress in the field may be related to the difficulty to immobilise cells without affecting their functionalities, as well as the multiple and complex processes that simultaneously take place into the cells and that may hinder the interpretation of the obtained results. It is difficult to classify the cell biosensors for marine toxins, as some of them usually detect more than one toxin family. A multi-toxin section has been preferred, although the electrochemical assay for PITX based on its haemolytic activity has deserved a separate section.

5.1. Multi-toxin

The first cell biosensors for the detection of marine toxins were developed around 20 years ago and thus, they show technical limitations such as the use of tissue as a biorecognition element. In these first works, a Na^+ electrode was covered with a frog bladder membrane, rich in Na^+ channels, and integrated into a flow cell [90-92]. Since TTX, STX and GTX are all Na^+ channel blockers, toxin levels correlated with Na^+ ions detected on the electrode. Good agreements were found with mouse bioassay when analysing puffer fish samples, and even lower LODs.

More sophisticated are the recent works from Wang's research group [93-95]. The authors cultured cells (cardiomyocytes and neuroblastoma) on electrodes and used EIS to detect cell growth and/or beating status of cells, i.e. relaxation and contraction due to STX and TTX effect in the presence of veratridine (which causes the persistent inflow of Na^+) and ouabain (which inhibits the activity of Na^+/K^+-ATPases) [93, 94]. The system did not recognise PbTx-2, a Na^+ channel opener [94]. This technique is non-invasive, label-free and provides real-time measurements. Additionally, when exploited in a 96-well sensor plate format, the biosensor offers high throughput detection [93]. In order to improve this methodology, the authors developed another biosensor based on the measurement of extracellular field potential signals from cells cultured on a SAM-modified electrode array. In this case, the system was able to recognise not only STX, but also PbTX-2, and discriminate them because of their different responses in spike amplitude, firing rate and spike potential duration. In this work, marine toxins induced changes within 5 min of exposure, instead of the 24 h required in the EIS-based cell biosensors, and the biosensor had a working life of 60 h in front of 24 or 32 h of the previous ones, improvements that could accelerate their implementation [95].

If the purpose of a cell biosensor is to detect as many marine toxins as possible, the work performed by Nicolas and collaborators is highly promising [96]. The authors seeded rat cortical neurons on a gold microelectrode array and measured local field potentials to assess the presence of a wide range of neurotoxic marine toxins (STX, TTX, PbTX-3, P-CTX-1, PITX and DA). These toxic compounds produce different effects on cells: STX and TTX are Na^+ channel blockers, PbTX-3 and CTX are Na^+ channel activators, PITX is a Na^+/K^+-ATPase blocker, and DA is a glutamate receptor agonist. Nevertheless, the biosensor was able to successfully detect them all, at different degrees but at a higher sensitivity than the *in vitro* neuroblastoma Neuro-2a assay, and it is expected to be able to detect other marine toxins, such as AZAs. The key is the measured parameter, the local field potential, which responds to a wide variety of neurotoxic effects. This cell biosensor was applied to the analysis of mussels contaminated with STX and fish flesh contaminated with TTX, and the curves correlated well with those obtained with pure marine toxins. As a conclusion,

this biosensor could be a highly valuable screening tool for seafood safety monitoring, but since primary cells are used, availability and variability issues can compromise the exploitation.

5.2. Palytoxin

Although not a biosensor because cells are not immobilised, a CBA where an enzyme activity is measured by amperometric detection has been described for the detection of PlTX [97]. This system is quite different from those previously described. It is based on the release of lactate dehydrogenase (LDH) from erythrocytes to the medium due to the haemolytic activity of PlTX. Two approaches were used for the electrochemical detection, both based on the use of phenazine methosulfate (PMS^+), which reacts with the NADH remaining from the reaction between LDH and its substrate pyruvate, and produces PMSH. Whereas in the first one, PMSH reacts with O_2 to produce H_2O_2, which is measured at a Prussian blue-modified screen-printed electrode, in the second one PMSH reacts with hexacyanoferrate(III) producing hexacyanoferrate(II), which is measured at a graphite screen-printed electrode. Under the best conditions, the LODs were 0.007 and 0.16 ng/mL for 24 and 4 h of cells exposure to PlTX, respectively. No interferences were observed from OA and YTX, not even from STX, PbTX and TTX, which also act on Na^+/K^+ channels. The applicability of the assay was evaluated by the analysis of spiked mussels, result that indicated the necessity to use a matrix-matched calibration curve for accurate analysis. The main limitation of this biosensor was probably the assay time, since at least 4 h were required to incubate the cells with PlTX.

Table 1. Electrochemical biosensors for the detection of marine toxins.

Biosensor type	Marine toxin	Immobilisation method	Format	Electrochemical technique	LOD	Matrix	Ref.
Immunosensors	OA	OA conjugation to a protein for subsequent electrode coating	Competitive direct assay	Amperometry	1.5 ng/mL	-	[11]
	OA	OA conjugation to a protein for subsequent electrode coating	Competitive indirect assay with enzyme recycling for signal amplification	Amperometry	0.03 ng/mL	Mussel Oyster	[12]
	OA	OA electrografting on screen-printed carbon electrodes	Competitive indirect assay	Differential pulse voltammetry	1.44 pg/mL	Mussel	[13]
	OA	Biotinylated OA immobilisation on streptavidin-coated MBs	Competitive indirect assay	Differential pulse voltammetry	0.38 ng/mL (batch) 0.15 ng/mL (flow)	Mussel	[15] [16]
	OA	Ab immobilisation on protein G-coated MBs	Label-free assay	Differential pulse voltammetry	0.5 ng/mL	Mussel	[18]
	OA	Ab electrografting on screen-printed carbon electrodes	Label-free assay	Electrochemical impedance spectroscopy	0.3 ng/mL	Mussel	[19]
	OA	Ab electrografting on screen-printed graphene-modified carbon electrodes	Label-free competitive assay	Square wave voltammetry	19 pg/mL	Mussel	[20]

(Continued)

Biosensor type	Marine toxin	Immobilisation method	Format	Electrochemical technique	LOD	Matrix	Ref.
	AZA	Ab immobilisation on protein G-coated MBs	Competitive direct assay with AZA-HRP as a tracer	Amperometry	1.1 ng/mL	Mussel	[23]
	DA	DA conjugation to protein for subsequent electrode coating	Competitive indirect assay	Amperometry	2 ng/mL 0.1 ng/mL	-	[11] [24]
	DA	DA conjugation to protein for subsequent electrode coating	Competitive indirect assay	Differential pulse voltammetry	5 ng/mL	Mussel	[25]
	STX	STX conjugation to a protein for subsequent electrode coating through a membrane	Competitive direct assay with GOx as a label	Amperometry	-	-	[26]
	PbTX-3	PbTX-3 conjugation to a protein for subsequent electrode coating through a membrane	Competitive direct assay with GOx as a label	Amperometry	-	-	[26]
	PbTX-3	PbTX-3 conjugation to a protein for subsequent electrode coating	Competitive direct assay	Amperometry	6 ng/mL	-	[11]

(Continued)

Biosensor type	Marine toxin	Immobilisation method	Format	Electrochemical technique	LOD	Matrix	Ref.
	PbTX-2	PbTX-2 conjugation to dendrimers for subsequent absorption on ester-modified gold electrodes	Competitive direct assay	Differential pulse voltammetry	0.01 ng/mL	Mussel Clam Cockle	[30]
	PbTX-2	Ab immobilisation to epoxy-modified MBs	Competitive direct assay with guanine-assembled graphene nanoribbons as a label	Square wave voltammetry	1 pg/mL	Mussel Clam Cockle	[31]
	PbTX-2 DTX-1	Ab immobilisation to epoxy-modified MBs	Competitive direct assay with metal nanoclusters as labels	Square wave anodic stripping voltammetry	1.8 ng/mL PbTX-2 2.2 ng/mL DTX-1	Mussel Clam Cockle	[32]
	PbTX-2	PbTX-2 conjugation to a protein for subsequent electrode coating	Competitive direct assay with mesoporous carbon-enriched palladium nanostructure as a label	Differential pulse voltammetry	5 pg/mL	Mussel	[33]

(Continued)

Biosensor type	Marine toxin	Immobilisation method	Format	Electrochemical technique	LOD	Matrix	Ref.
	PbTX-2	Ab immobilisation on mesoporous silica nanocontainers	Displacement of the microspheres that capped the silica pores of nanocontainers by the antigen-Ab interaction and release of the redox mediator	Square wave voltammetry	6 pg/mL	Mussel Clam Cockle	[34]
	PlTX	Ab immobilisation on MWCNTs	Sandwich with detector Ab labelled with a ruthenium complex	Electrochemilumi-nescence	0.07 ng/mL	Mussel Microalgae	[36]
	TTX	TTX conjugation to a protein for subsequent electrode coating	Competitive direct assay	Amperometry	16 pg/mL	-	[11]
	TTX	Ab immobilisation on protein G-modified electrodes	Competitive assay with TTX-ALP as a tracer	Differential pulse voltammetry	1 ng/mL	-	[52]
	TTX	TTX immobilisation to carboxylated polyethylene glycol-dithiols SAM-modified gold electrode arrays	Competitive indirect assay	Amperometry	2.6 ng/mL	Puffer fish	[53]

(Continued)

Biosensor type	Marine toxin	Immobilisation method	Format	Electrochemical technique	LOD	Matrix	Ref.
Enzyme sensors	OA	PP not immobilised; PyOx entrapment into a polymeric matrix	Phosphoprotein dephosphorylation by PP, pyruvic acid oxidation by PyOx and O_2 consumption measurement	Amperometry	0.1 ng/mL	-	[69]
	OA	PP and glycogen phosphorylase a not immobilised; ALP and GOx covalent immobilisation to a nylon net membrane	PP binding to glycogen phosphorylase a, glycogen phosphorylation by glycogen phosphorylase a, glucose-1-phosphate dephosphorylation by ALP, glucose oxidation by GOx and H_2O_2 oxidation	Amperometry	30 pg/mL	-	[70]
	OA	PP entrapment into a polymeric matrix	Catechyl monophosphate dephosphorylation by PP and catechol oxidation	Amperometry	6.42 ng/mL	*Prorocentrum* spp. dinoflagellates	[71]

(Continued)

Biosensor type	Marine toxin	Immobilisation method	Format	Electrochemical technique	LOD	Matrix	Ref.
	OA	PP adsorption on carbon nanotube-modified electrodes	*p*-Nitrophenyl phosphate dephosphorylation by PP and *p*-nitrophenol oxidation	Differential pulse voltammetry	0.55 ng/mL	Mussel	[72]
	YTX	PDE not immobilised, but placed on a screen-printed carbon electrodes	α-Naphthyl phosphate dephosphorylation by PDE and α-naphthol oxidation	Differential pulse voltammetry	0.69 µg/mL	*Protoceratium reticulatum* dinoflagellates	[74]
Aptasensors	OA	Aptamer SAM on gold electrodes	Label-free assay based on aptamer folding	Electrochemical impedance spectroscopy	70 pg/mL	Shellfish	[79]
	PbTX-2	PbTX-2 immobilisation to cysteamine SAM-modified gold electrodes	Label-free competitive assay	Electrochemical impedance spectroscopy	0.11 ng/mL	Shellfish	[82]
	STX	Aptamer immobilisation to MWCNT-octadecanethiol SAM-modified gold electrodes	Label-free assay based on aptamer folding and methylene blue bound to guanine bases and accumulated on the MWCNT-SAM	Differential pulse voltammetry	0.11 ng/mL	Mussel	[85]

(Continued)

Biosensor type	Marine toxin	Immobilisation method	Format	Electrochemical technique	LOD	Matrix	Ref.
	TTX	Aptamer immobilisation to PSSA/PANI-modified glassy carbon electrodes	Label-free assay based on TTX interaction	Electrochemical impedance spectroscopy	19.9 pg/mL	-	[86]
Cell biosensors	TTX STX	Na^+ electrode coating with frog bladder membrane	Effect of toxin on Na^+ channels and Na^+ ions detection	Amperometry	1.72 pg/mL (TTX)	*Takifugu niphobles* and *Takifugu parudale* swellfish (TTX)	[90]
	TTX STX GTX	Na^+ electrode coating with frog bladder membrane	Effect of toxin on Na^+ channels and Na^+ ions detection	Amperometry	1.72 pg/mL (TTX) 0.1 pg/mL (STX)	*Takifugu niphobles* and *Takifugu parudale* swellfish (TTX) *Zosimus aeneus* crab (STX)	[91]
	TTX STX	Na^+ electrode coating with frog bladder membrane	Effect of toxin on Na^+ channels and Na^+ ions detection	Amperometry	-	Shellfish Swellfish	[92]
	STX TTX	Cardiomyocyte cell seeding on a gold microelectrode array	Cell growth and/or beating status monitoring	Electrochemical impedance spectroscopy	87 pg/mL (STX) 89 ng/mL (TTX)	-	[93]
	STX	Neuro-2a cell seeding on interdigitated gold electrodes	Cell growth monitoring	Electrochemical impedance spectroscopy	31 pg/mL	Mussel	[94]

(Continued)

Biosensor type	Marine toxin	Immobilisation method	Format	Electrochemical technique	LOD	Matrix	Ref.
	STX PbTX-2	Cardiomyocyte cell culture on a SAM-modified gold microelectrode array	Electrical activity monitoring of cells	Extracellular field potential	0.35 ng/mL (STX) 1.55 ng/mL (PbTX-2)	-	[95]
	STX TTX PbTX-3 P-CTX-1 PITX DA	Rat neonatal cortical cell seeding on a poly-L-lysine-coated gold microelectrode array	Electrical activity monitoring of cells	Local field potential	<0.15 ng/mL (STX) 0.32 ng/mL (TTX) 0.90 ng/mL (PbTX-3) 1.11 pg/mL (P-CTX-1) 2.68 pg/mL (PITX) 31 ng/mL (DA)	Mussel (STX) Fish (TTX)	[96]
	PITX	Erythrocytes not immobilised	LDH released from erythrocytes and measured using PMS^+	Amperometry	7 pg/mL (24 h) 0.16 ng/mL (4 h)	Mussel	[97]

6. Conclusions and perspectives

The impact of the biosensing technology is increasing in many sectors such as pharmaceutical, healthcare, environment and food. In the field of marine toxins, electrochemical biosensors for the detection of OA and DTXs, AZAs, DA, PlTXs, PbTXs, TTXs, YTXs, CTX and STX have been described in the past years, although their repercussion in food safety applications has been moderate. In order to promote their implementation and take the leap from the bench to the market, efforts should be made on 1) simplifying their handling, 2) applying them to the analysis of a high number of naturally-contaminated samples and, if necessary, improving their performance, and 3) performing validation and inter-laboratory studies.

Immunosensors are the main type of electrochemical biosensors developed for marine toxins, probably because several antibodies are already available. Many fewer aptasensors can be found, but it is necessary to say that the aptamer field is much more recent. Nevertheless, aptamers are gaining ground because of their easier synthesis and lower cost compared to antibodies. Both immunosensors and aptasensors have been able to attain detection limits at the level of nano to picogram per millilitre, which, in general, are below the maximum permitted levels established for marine toxins. However, most works have analysed only spiked seafood samples and the applicability to naturally-contaminated samples has not been studied in detail.

Nowadays, a trending topic in the field of biosensors is the development of multiplexed assays, which allow the determination and discrimination of multiple analytes in the same sample. In this regard, antibodies and aptamers can be produced against different families of marine toxins and integrated into array platforms for multiplexed detection. Labelling antibodies, antigens or aptamers with different electroactive molecules or metal nanoparticles (which can be detected at different redox potentials) or, when using enzyme labels, even with the same enzyme but controlling the diffusion of electroactive products from one site of the array to the adjacent one, can lead to multiplexed detection. Another valuable attribute of immunosensors and aptasensors is the ability to operate in a label-free mode. Label-free detection in impedimetric biosensors simplifies the assay protocols, but it is limited to specific targets (the small size of many marine toxins going against).

An added advantage of aptamers is that they have a great degree of flexibility, i.e. they can be formatted to fit into different configurations, offering a wide range of possibilities. Apart from competitive or sandwich assays, commonly found when using antibodies, aptamers can be exploited in target-induced structure switching designs, which take advantage of the conformational change that the aptamer itself

undergoes when binding to the toxin. This structural change has been used in label-free impedimetric aptasensors, but it can also be accompanied by the direct detection of a redox moiety previously incorporated in one extreme of the aptamer (electrochemical molecular beacon aptamer), which avoids the use of a redox mediator in solution and provides a reagentless configuration. The exceptional properties of aptamers make them compelling for biosensor development and they are expected to be increasingly exploited in the coming years.

Regarding enzyme sensors, apart from one example on PDE inhibition by YTX, all the rest are based on the PP inhibition. It would be very useful to identify enzymes able to recognise marine toxins other than the DSP toxins. But for this discovery to be a fact, the involvement of other disciplines, such as cell and molecular biology, is crucial in order to understand the mechanisms of action of marine toxins, not always fully elucidated. The knowledge on marine toxin production and their implication on cell processes may help to find novel enzymes or other biorecognition molecules for the detection of these analytes.

When using cells as biorecognition elements, a wide variety of channels, receptors, enzymes and other signalling proteins may provide measurable responses to the physiological effects of marine toxins. The issues that are limiting the progress of cell biosensors are the weak robustness and stability of cells. Nevertheless, efforts are being made to develop new cell preservation techniques and to provide cells with extended shelf life. Specificity should not be considered as a limitation; on the contrary, the main advantage of some cell biosensors is the ability to provide indication of an overall toxic effect. In fact, cell biosensors could give a positive response when different toxins at levels below the regulatory limits are combined in a same sample, in the case of synergistic effects, or in the presence of unknown toxins, which is of utmost importance for food safety and human health protection. Additionally, they could help to reduce animal experimentation.

Nanobiotechnology is revolutionising the development of electrochemical biosensors: tailor-made biorecognition molecules, such as recombinant enzymes or aptamers, may provide better specificity, higher sensitivity, specific sites for their oriented immobilisation and versatility of the signal transduction designs; the use of nanostructured electrodes as immobilisation supports (e.g. with metallic nanoparticles, graphene, dendrimers or porous materials) results in higher biomolecule immobilisation yields and enhanced electron transfer; MBs have been shown to improve specific affinity interactions in homogeneous/heterogeneous systems and reduce matrix effects when analysing natural samples; additionally, the easy integration of MBs into microfluidics systems paves the way towards the development of automated analysis devices. Although electrochemical biosensors

for marine toxins have only timidly benefited from nanobiotechnology, recent works demonstrate that progress in this field is assured.

Electrochemical biosensors can provide expedient solutions to the most contemporary demands of biochemical sensing of marine toxins, such as *in situ* measurements of minimally treated samples, ultra-sensitive multiplexed analysis of different targets and label-free detection. The easy miniaturisation of both the electrodes and the required instrumentation at a relatively low cost, and the subsequent portability, the ability of such micro- or nano-sized electrodes to operate with low sample volumes, and the compatibility with coloured or turbid solutions such as seafood matrixes, are examples of the advantages of electrochemical detection. Taking all this into account, it seems evident that electrochemical biosensors are a promising alternative or complementary method to conventional analytical techniques. However, since most advances have been made on the development of the bioanalytical systems but not on their validation, the implementation of such devices in daily life still requires more effort. Scientific community should focus their work on useful and powerful approaches rather than on sophisticated designs in order to really foster the use of electrochemical biosensors in the agro-food and environmental fields. Challenges such as biorecognition molecule stability, internal calibration, pre-concentration of samples, and avoidance of incubation and washing steps, still need to be overcome. Additionally, the integration of information and communication technologies into biosensing systems will definitively mark a milestone in the deployment of electrochemical biosensor for marine toxins. We will not take long to see automated and wireless electrochemical biosensing platforms able to provide information in real time from the sea to our mobile phones.

Acknowledgments

The authors acknowledge financial support from the European Union Seventh Framework Programme (FP7/2007-2013) through the ECsafeSEAFOOD project (grant agreement n° 311820) and from the Ministerio de Economía, Industria y Competitividad through the SEASENSING (BIO2014-56024-C2-2-R) project. The publication reflects the views only of the authors, and the European Union cannot be held responsible for any use which may be made of the information contained therein. The authors also acknowledge support from CERCA Programme / Generalitat de Catalunya. Sandra Leonardo and Anna Toldrà acknowledge IRTA – Universitat Rovira i Virgili – Banco Santander for their PhD grants (2013PIPF URV-IRTA-BS-01 and 2015PMF-PIPF-67).

References

[1] M. Campàs, B. Prieto-Simón, J.L. Marty, Biosensors to detect marine toxins: assessing seafood safety, Talanta 72 (2007) 884–895.

[2] M. Campàs, D. Garibo, B. Prieto-Simón, Novel nanobiotechnological concepts in electrochemical biosensors for the analysis of toxins, Analyst 137 (2012) 1055–1067.

[3] L. Reverté, B. Prieto-Simón, M. Campàs, New advances in electrochemical biosensors for the detection of toxins: nanomaterials, magnetic beads and microfluidics systems. A review, Anal. Chim. Acta 908 (2016) 8–21.

[4] X.W. Zhang, Z.X. Zhang, Development of a capillary electrophoresis-based enzyme immunoassay with electrochemical detection of the determination of okadaic acid and dinophysistoxin2 in shellfish samples, Anal. Lett. 45 (2012) 1365–1376.

[5] X.W. Zhang, Z.X. Zhang, Quantification of domoic acid in shellfish samples by capillary electrophoresis-based enzyme immunoassay with electrochemical detection, Toxicon 59 (2012) 626–632.

[6] X.W. Zhang, Z. X. Zhang, Capillary electrophoresis-based immunoassay with electrochemical detection as rapid method for determination of saxitoxin and decarbamoylsaxitoxin in shellfish samples, J. Food Compost. Anal. 28 (2012) 61–68.

[7] X.W. Zhang, Z. X. Zhang, Capillary electrophoresis-based immunoassay for the determination of brevetoxin-B in shellfish using electrochemical detection, J. Chromatogr. Sci. 51 (2013) 107–111.

[8] Z.X. Zhang, X.L. Li, A.Q. Ge, F. Zhang, X.M. Sun, X.M. Li, High selective and sensitive capillary electrophoresis-based electrochemical immunoassay enhanced by gold nanoparticles, Biosens. Bioelectron. 41 (2013) 452–458.

[9] Z.X. Zhang, Y. Liu, C.Y. Zhang, W.X. Luan, Horseradish peroxidase and antibody labelled gold nanoparticle probe for amplified immunoassay of ciguatoxin in fish samples based on capillary electrophoresis with electrochemical detection, Toxicon 96 (2015) 89–95.

[10] Z.X. Zhang, C.Y. Zhang, W.X. Luan, X.F. Li, Y. Liu, X.L. Luo, Ultrasensitive and accelerated detection of ciguatoxin by capillary electrophoresis via on-line sandwich immunoassay with rotating magnetic field and nanoparticles signal enhancement, Anal. Chim. Acta 888 (2015) 27–35.

[11] M.P. Kreuzer, M. Pravda, C.K. O'Sullivan, G.G. Guilbault, Novel electrochemical immunosensors for seafood toxin analysis, Toxicon 40 (2002) 1267–1274.

[12] M. Campàs, P. de la Iglesia, M. Le Berre, M. Kane, J. Diogène, J.L. Marty, Enzymatic recycling-based amperometric immunosensor for the ultrasensitive detection of okadaic acid in shellfish, Biosens. Bioelectron. 24 (2008) 716–722.

[13] A. Hayat, L. Barthelmebs, A. Sassolas, J.L. Marty, An electrochemical immunosensor based on covalent immobilization of okadaic acid onto screen printed carbon electrode via diazotization-coupling reaction, Talanta 85 (2011) 513–518.

[14] European Commission (EC) (2004) Regulation (EU) no 853/2004 of 29 April 2004 laying down specific hygiene rules for on the hygiene of foodstuffs, Off. J. Eur. Union L139, 55–205.

[15] A. Hayat, L. Barthelmebs, J.L. Marty, Enzyme-linked immunosensor based on super paramagnetic nanobeads for easy and rapid detection of okadaic acid, Anal. Chim. Acta 690 (2011) 248–252.

[16] R.B. Dominguez, A. Hayat, A. Sassolas, G.A. Alonso, R. Munoz, J.L. Marty, Automated flow-through amperometric immunosensor for highly sensitive and on-line detection of okadaic acid in mussel sample, Talanta 99 (2012) 232–237.

[17] A. Tang, M. Kreuzer, M. Lehane, M. Pravda, G.G. Guilbault, Immunosensor for the Determination of okadaic acid based on screen-printed electrode, Int. J. Environ. Anal. Chem. 83 (2003) 663–670.

[18] A. Hayat, L. Barthelmebs, A. Sassolas, J.L. Marty, Development of a novel label-free amperometric immunosensor for the detection of okadaic acid, Anal. Chim. Acta 724 (2012) 92–97.

[19] A. Hayat, L. Barthelmebs, J.L. Marty, Electrochemical impedimetric immunosensor for the detection of okadaic acid in mussel sample, Sensor. Actuat. B-Chem. 171–172 (2012) 810–815.

[20] S. Eissa, M. Zourob, A graphene-based electrochemical competitive immunosensor for the sensitive detection of okadaic acid in shellfish, Nanoscale 4 (2012) 7593–7599.

[21] C.J. Forsyth, J. Xu, S.T. Nguyen, I.A. Samdal, L.R. Briggs, T. Rundberget, M. Sandvik, C.O. Miles, Antibodies with broad specificity to azaspiracids by use of synthetic haptens, J. Am. Chem. Soc. 128 (2006) 15114–15116.

[22] M.O. Frederick, K.D. Janda, K.C. Nicolau, T.J. Dickerson, Monoclonal antibodies with orthogonal azaspiracid epitopes, Chembiochem. 10 (2009) 1625–1629.

[23] S. Leonardo, M. Rambla-Alegre, I.A. Samdal, C.O. Miles, J. Kilcoyne, J. Diogène, C.K. O'Sullivan, M. Campàs, Immunorecognition magnetic supports for the development of an electrochemical immunoassay for azaspiracid detection in mussels, Biosens. Bioelectron. 92 (2017) 200–206.

[24] M. Kania, M. Kreuzer, E. Moore, M. Pravda, B. Hock, G. Guilbault, Development of polyclonal antibodies against domoic acid for their use in electrochemical biosensors, Anal. Lett. 36 (2003) 1851–1863.

[25] L. Micheli, A. Radoi, R. Guarrina, R. Massaud, C. Bala, D. Moscone, G. Palleschi, Disposable immunosensor for the determination of domoic acid in shellfish, Biosens. Bioelectron. 20 (2004) 190–196.

[26] R.M. Carter, M.A. Poli, M. Pesavento, D.E.T. Sibley, G.J. Lubrano, G.G. Guilbault, Immunoelectrochemical biosensors for detection of saxitoxin and brevetoxin, Immunomethods 3 (1993) 128–133.

[27] United States Food and Drug Administration (US FDA) (2001) Fish ahd fisheries products hazards and controls guidance, 3rd ed. Appendix - FDA & EPA Safety levels in regulations and guidance.

[28] New Zealand Food Safety Authority (NZFSA) (2006) Animal products (specification for bivalve molluscan shellfish).

[29] Food Standards Australia New Zealand (FSANZ) (2010) Food standard code, incorporating amendments up to and including amendment 116, standard 4.1.1., primary production and processing standards, preliminary provisions, standard 1.4.1., contaminants and natural toxicants, issue 111.

[30] D. Tang, J. Tang, B. Su, G. Chen, Gold nanoparticles-decorated amine-terminated poly(amidoamine) dendrimer for sensitive electrochemical immunoassay of brevetoxins in food samples, Biosens. Bioelectron. 26 (2011) 2090–2096.

[31] J. Tang, L. Hou, D. Tang, J. Zhou, Z. Wang, K. Li, G. Chen, Magneto-controlled electrochemical immunoassay of brevetoxin B in seafood based on guanine-functionalized graphene nanoribbons, Biosens. Bioelectron. 38 (2012) 86–93.

[32] B. Zhang, L. Hou, D. Tang, B. Liu, J. Li, G. Chen, Simultaneous multiplexed stripping voltammetric monitoring of marine toxins in seafood based on distinguishable metal nanocluster-labeled molecular tags, J. Agr. Food Chem. 60 (2012) 8974–8982.

[33] Y. Lin, Q. Zhou, Y. Lin, M. Lu, D. Tang, Mesoporous carbon-enriched palladium nanostructures with redox activity for enzyme-free electrochemical immunoassay of brevetoxin B, Anal. Chim. Acta 887 (2015) 67–74.

[34] B. Zhang, B. Liu, J. Liao, G. Chen, D. Tang, Novel electrochemical immunoassay for quantitative monitoring of biotoxin using target-responsive cargo release from mesoporous silica nanocontainers, Anal. Chem. 85 (2013) 9245–9252

[35] CRLMB, Report on toxicology working group meeting, Cesenatico, Italy, 2005, 24–25.

[36] V.A. Zamolo, G. Valenti, E. Venturelli, O. Chaloin, M. Marcaccio, S. Boscolo, V. Castagnola, S. Sosa, F. Berti, G. Fontanive, M. Poli, A. Tubaro, A. Bianco, F. Paolucci, M. Prato, Highly sensitive electrochemiluminescent nanobiosensor for the detection of palytoxin, ACS Nano 6 (2012) 7989–7997.

[37] I. Rodriguez, A. Alfonso, E. Alonso, J.A. Rubiolo, M. Roel, A. Vlamis, P. Katikou, S.A. Jackson, M.L. Menon, A. Dobson, and L.M. Botana, The association of bacterial C-9-based TTX-like compounds with *Prorocentrum minimum* opens new uncertainties about shellfish seafood safety, Sci. Rep. 7 (2017) 40880.

[38] T. Noguchi, O. Arakawa, Tetrodotoxin – Distribution and accumulation in aquatic organisms, and cases of human intoxication, Mar. Drugs 6 (2008) 220–242.

[39] Y. Mahmud, K. Yamamori, T. Noguchi, Occurrence of TTX in a brackish water puffer "Midorifugu", *Tetraodon nigrovidiris*, collected from Thailand, J. Food Hyg. Soc. Japan 40 (1999) 363-367.

[40] M. Aydin, Growth, reproduction and diet of puffer fish (*Lagocephalus sceleratus* Gmelin, 1789) from Turkey's Mediterranean Sea coast, Turk. J. Fish. Aquat. Sc. 11 (2011) 589–596.

[41] P. Katikou, D. Georgantelis, N. Sinouris, A. Petsi, T. Fotaras, First report on toxicity assessment of the Lessepsian migrant pufferfish *Lagocephalus sceleratus* (Gmelin, 1789) from European waters (Aegean Sea, Greece), Toxicon 54 (2009) 50–55.

[42] Y. Bentur, J. Ashkar, Y. Lurie, Y. Levy, Z.S. Azzam, M. Litmanovich, M. Golik, B. Gurevych, D. Golani, A. Eisenman, Lessepsian migration and tetrodotoxin poisoning due to *Lagocephalus sceleratus* in the eastern Mediterranean, Toxicon 52 (2008) 964–968.

[43] J. Kheifets, B. Rozhavsky, Z.G. Solomonovich, R. Marianna, A. Soroksky, Severe tetrodotoxin poisoning after consumption of *Lagocephalus sceleratus* (pufferfish, fugu) fished in Mediterranean Sea, treated with cholinesterase inhibitor, Case Rep. Crit. Care 782507 (2012) 3 pp.

[44] P. Carpentieri, S. Lelli, F.C. Colloca, C. Mohanna, V. Bartolino, S. Moubayed, G.D. Ardizzone, Incidence of lessepsian migrants on landings of the artisanal fishery of South Lebanon, J. Mar. Biodivers. Rec. 2 (2009) 1–5.

[45] M. Milazzo, E. Azzurro, F. Badalamenti, On the occurrence of the silverstripe blaasop *Lagocephalus sceleratus* (Gmelin, 1789) along the Libyan coast, Bioinvasions Rec. 1 (2012) 125–127.

[46] S.P. Iglésias, L. Frotté, Alien marine fishes in Cyprus: update and new records, Aquat. Inv. 10 (2015) 425–438.

[47] E. Azzurro, L. Castriota, M. Falautano, F. Giardina, F. Andaloro, The silver-cheeked toadfish *Lagocephalus sceleratus* (Gmelin, 1789) reaches Italian waters, J. Appl. Ichthyol. 30 (2014) 1050–1052.

[48] M. Rambla-Alegre, L. Reverté, V. del Rio, P. de la Iglesia, O. Palacios, C. Flores, J. Caixach, K. Campbell, C.T. Elliott, A. Izquierdo-Muñoz, M. Campàs, J. Diogène, Evaluation of tetrodotoxins in puffer fish caught along the Mediterranean coast of Spain. Toxin profile of *Lagocephalus sceleratus*, Environ. Res., 158 (2017) 1–6.

[49] A.D. Turner, A. Powell, A. Schofield, D.N. Lees, C. Baker-Austin, Detection of the pufferfish toxin tetrodotoxin in European bivalves, England, 2013 to 2014, Euro surveill. 20 (2015) 2–8.

[50] A. Vlamis, P. Katikou, I. Rodriguez, V. Rey, A. Alfonso, A. Papazachariou, T. Zacharaki, A.M. Botana, L.M. Botana, First detection of tetrodotoxin in Greek shellfish by UPLC-MS/MS potentially linked to the presence of the dinoflagellate *Prorocentrum minimum*, Toxins 7 (2015) 1779–1807.

[51] RASFF Consumers Portal. Notification details - 2016.0845. Possible presence of tetrodotoxin in live oysters from the Netherlands. https://webgate.ec.europa.eu/rasff-window/consumers/?event=notificationDetail&NOTIF_REFERENCE=2016.0845&country=NL. Accessed by May 2017.

[52] D. Neagu, L. Micheli, G. Palleschi, Study of a toxin-alkaline phosphatase conjugate for the development of an immunosensor for tetrodotoxin determination, Anal. Bioanal. Chem. 385 (2006) 1068–1074.

[53] L. Reverté, P. de la Iglesia, V. del Río, K. Campbell, C.T. Elliott, K. Kawatsu, P. Katikou, J. Diogène, M. Campàs, Detection of tetrodotoxins in puffer fish by a self-assembled monolayer-based immunoassay and comparison with surface Plasmon resonance, LC-MS/MS, and mouse bioassay, Anal. Chem. 87 (2015) 10839–10847.

[54] C. Bialojan, A. Takai, Inhibitory effect of a marine sponge toxin, okadaic acid, on protein phosphatases, Biochem. J. 256 (1988) 283–290.

[55] A. Tubaro, C. Florio, E. Luxich, S. Sosa, R. Della Loggia, T. Yasumoto, A protein phosphatase 2A inhibition assay for a fast and sensitive assessment of okadaic acid contamination in mussels, Toxicon 34 (1996) 743–752.

[56] M.R. Vieytes, O.I. Fontal, F. Leira, J.M. Baptista de Sousa, L.M. Botana, A fluorescent microplate assay for diarrheic shellfish toxins, Anal. Biochem. 248 (1997) 258–264.

[57] R. Della Loggia, S. Sosa, A. Tubaro, Methodological improvement of the protein phosphatase inhibition assay for the detection of okadaic acid in mussels, Nat. Toxins 7 (1999) 387–391.

[58] D.O. Mountfort, G. Kennedy, I. Garthwaite, M.A. Quilliam, P. Truman, D.J. Hannah, Evaluation of the fluorometric protein phosphatase inhibition assay in the determination of okadaic acid in mussels, Toxicon 37 (1999) 909–922.

[59] D.O. Mountfort, T. Suzuki, P. Truman, Protein phosphatase inhibition assay adapted for determination of total DSP in contaminated mussels, Toxicon 39 (2001) 383–390.

[60] E. Cañete, M. Campàs, P. de la Iglesia, J. Diogène, NG108-15 cell-based and protein phosphatase inhibition assays as alternative semiquantitative tools for the screening of lipophilic toxins in mussels. Okadaic acid detection, Toxicol. in vitro 24 (2010) 611–619.

[61] A. Caillaud, P. de la Iglesia, M. Campàs, L. Elandaloussi, M. Fernández, N. Mohammad-Noor, K. Andree, J. Diogène, Evidence of okadaic acid production in a cultured strain of the marine dinoflagellate *Prorocentrum rhathymum* from Malaysia, Toxicon 55 (2010) 633–637.

[62] D. Garibo, E. Dàmaso, H. Eixarch, P. de la Iglesia, M. Fernández-Tejedor, J. Diogène, Y. Pazos, M. Campàs, Protein phosphatase inhibition assays for okadaic acid detection in shellfish: Matrix effects, applicability and comparison with LC–MS/MS analysis, Harmful Algae 19 (2012) 68–75.

[63] D. Garibo, P. de la Iglesia, J. Diogène, M. Campàs, Inhibition equivalency factors for dinophysistoxin-1 and dinophysistoxin-2 in protein phosphatase assays, applicability to the analysis of shellfish samples and comparison with LC-MS/MS, J. Agric. Food Chem. 61 (2013) 2572–2579.

[64] M. Campàs, D. Szydlowska, M. Trojanowicz, J.L. Marty, Towards the protein phosphatase-based biosensor for microcystin detection, Biosens. Bioelectron. 20 (2005) 1520–1530.

[65] A. Sassolas, G. Catanante, A. Hayat, J.L. Marty, Development of an efficient protein phosphatase-based colorimetric test for okadaic acid detection, Anal. Chim. Acta 702 (2011) 262–278.

[66] A. Hayat, L. Barthelmebs, J. L. Marty, A simple colorimetric enzymatic-assay for okadaic acid detection based on the immobilization of protein phosphatase 2A in sol-gel, Appl. Biochem. Biotechnol. 166 (2012) 47–56.

[67] T. Ikehara, S. Imamura, A. Yoshino, T. Yasumoto, PP2A inhibition assay using recombinant enzyme for rapid detection of okadaic acid and its analogs in shellfish, Toxins 2 (2010) 195–204.

[68] D. Garibo, E. Devic, J. L. Marty, J. Diogène, I. Unzueta, M.Blázquez, M. Campàs, Conjugation of genetically engineered protein phosphatases to magnetic particles for okadaic acid detection, J. Biotechnol. 157 (2012) 89–95.

[69] N. Hamada-Sato, N. Minamitani, Y. Inaba, Y. Nagashima, T. Kobayashi, C. Imada, E. Watanabe, Development of amperometric sensor system for measurement of diarrheic shellfish poisoning (DSP) toxin, okadaic acid (OA), Sensor Mater. 16 (2004) 99–107.

[70] G. Volpe, E. Cotroneo, D. Moscone, L. Croci, L. Cozzi, G. Ciccaglioni, G. Palleschi, A bienzyme electrochemical probe for flow injection analysis of okadaic acid based on protein phosphatase-2A inhibition: an optimization study, Anal. Biochem. 385 (2009) 50–56.

[71] M. Campàs, J. L. Marty, Enzyme sensor for the electrochemical detection of the marine toxin okadaic acid, Anal. Chim. Acta 605 (2007) 87–93.

[72] J. Zhou, X. Qiu, K. Su, G. Xu, P. Wang, Disposable poly (o-aminophenol)-carbon nanotubes modified screen print electrode-based enzyme sensor for electrochemical detection of marine toxin okadaic acid, Sensor. Actuat. B-Chem. 235 (2016) 170–178.

[73] European Commission (EC), 2013, Regulation (EU) no 786/2013 of August 2013 amending Annex III to Regulation (EC) No 853/2004 of the European Parliament and of the Council as regards the permitted limits of yessotoxins in live bivalve molluscs, Off. J. Eur. Union L220.

[74] M. Campàs, P. de la Iglesia, M. Fernández-Tejedor, J. Diogène, Colorimetric and electrochemical phosphodiesterase inhibition assays for yessotoxin detection: development and comparison with LC-MS/MS, Anal. Bioanal. Chem. 396 (2010) 2321–2330.

[75] A. Hayat, J.L. Marty, Aptamer based electrochemical sensors for emerging environmental pollutants, Front. Chem. 41 (2014) 1–9.

[76] I. Willner, M. Zayats, Electronic aptamer-based sensors, Angew. Chem. Int. Ed. 46 (2007) 6408–6418.

[77] Y. Xu, G. Cheng, P. He, Y. Fang, A Review: Electrochemical aptasensors with various detection strategies, Electroanalysis 21 (2009) 1251–1259.

[78] B. Shao, X. Gao, F. Yang, W. Chen, T. Miao, J. Peng, Screening and structure analysis of the aptamer against tetrodotoxin, Food Sci. Technol. 2 (2012) 347–351.

[79] S. Eissa, A. Ng, M. Siaj, A.C. Tavares, M. Zourob, Selection and identification of DNA aptamers against okadaic acid for biosensing application, Anal. Chem. 85 (2013) 11794–11801.

[80] H. Gu, N. Duan, S. Wu, L. Hao, Y. Xia, X. Ma, Z. Wang, Graphene oxide-assisted non-immobilized SELEX of okdaic acid aptamer and the analytical application of aptasensor, Nature Sci. Rep. 6 (2016) 2045–2322.

[81] S.M. Handy, B.J. Yakes, J.A. DeGrasse, K. Campbell, C.T. Elliott, K.M. Kanyuck, S.L. DeGrasse, First report of the use of a saxitoxin-protein conjugate to develop a DNA aptamer to a small molecule toxin, Toxicon 61 (2013) 30–37.

[82] S. Eissa, M. Siaj, M. Zourob, Aptamer-based competitive electrochemical biosensor for brevetoxin-2, Biosens. Bioelectron. 69 (2015) 148–154.

[83] S. Gao, B. Hu, X. Zheng, Y.Cao, D. Liu, M. Sun, B. Jiao, L. Wang, Gonyautoxin 1/4 aptamers with high-affinity and high-specificity: from efficient selection to aptasensor application, Biosens. Bioelectron. 79 (2016) 938–944.

[84] S. Gao, X. Zheng, B. Hu, M. Sun, J. Wu, B. Jiao, L. Wang, Enzyme-linked, aptamer-based, competitive biolayer interferometry biosensor for palytoxin, Biosens. Bioelectron. 89 (2017) 952–958.

[85] L. Hou, L. Jiang, Y. Song, Y. Ding, J. Zhang, X. Wu, D. Tang, Amperometric aptasensor for saxitoxin using a gold electrode modified with carbon nanotubes on a self-assembled monolayer, and methylene blue as an electrochemical indicator probe, Microchim. Acta. 183 (2016) 1971–1980.

[86] G. Fomo, T.T. Waryo, C.E. Sunday, A.A. Baleg, P.G. Baker, E.I. Iwuoha, Aptameric recognition modulated electroactivity of poly(4-styrenesolfonic acid)-doped polyaniline films for single-shot detection of tetrodotoxin, Sensors 15 (2015) 22547–22560.

[87] J.W. Park, R. Tatavarty, D.W. Kim, H.T. Jung, M.B. Gu, Immobilization-free screening of aptamers assisted by graphene oxide, Chem. Commun. 48 (2012) 2071–2073.

[88] K.L. Hong, L.J. Sooter, Single-stranded DNA aptamers against pathogens and toxins: identification and biosensing applications, Biomed. Res. Int. (2015) 1–31.

[89] X. Zheng, B. Hu, S.X. Gao, D.J. Liu, M.J. Sun, B.H. Jiao, L.H. Wang, A saxitoxin-binding aptamer with higher affinity and inhibitory activity optimized by rational site-directed mutagenesis and truncation, Toxicon 101 (2015) 41–47.

[90] B. Cheun, H. Endo, T. Hayashi, Y. Nagashima, E. Watanabe, Development of an ultra high sensitive tissue biosensor for determination of swellfish poisoning, tetrodotoxin, Biosens. Bioelectron. 11 (1996) 1185–1191.

[91] B. Cheun, M. Loughran, T. Hayashi, Y. Nagashima, E. Watanabe, Use of a channel biosensor for the assay of paralytic shellfish toxins, Toxicon 36 (1998) 1371–1381.

[92] B.S. Cheun, S. Takagi, T. Hayashi, Y. Nagashima, E. Watanabe, Determination of Na channel blockers in paralytic shellfish toxins and pufferfish toxins with a tissue biosensor, J. Nat. Toxins 7 (1998) 109–120.

[93] Q. Wang, K. Su, L. Hu, L. Zou, T. Wang, L. Zhuang, N. Hu, P. Wang, A novel and functional assay for pharmacological effects of marine toxins, saxitoxin and tetrodotoxin by cardiomyocyte-based impedance biosensor, Sensor. Actuat. B-Chem. 209 (2015) 828–837.

[94] L. Zou, C. Wu, Q. Wang, J. Zhou, K. Su, H. Li, N. Hu, P. Wang, An improved sensitive assay for the detection of PSP toxins with neuroblastoma cell-based impedance biosensor, Biosens. Bioelectron. 67 (2015) 458–464.

[95] Q. Wang, J. Fang, D. Cao, H. Li, K. Su, N. Hu, P. Wang, An improved functional assay for rapid detection of marine toxins, saxitoxin and brevetoxin using a portable cardiomyocyte-based potential biosensor, Biosens. Bioelectron. 72 (2015) 10–17.

[96] J. Nicolas, P.J. Hendriksen, R.G. van Kleef, A. de Groot, T.F. Bovee, I.M. Rietjens, R.H. Westerink, Detection of marine neurotoxins in food safety testing using a multielectrode array, Mol. Nutr. Food Res. 58 (2014) 2369–2378.

[97] G. Volpe, L. Cozzi, D. Migliorelli, L. Croci, G. Palleschi, Development of a haemolytic-enzymatic assay with mediated amperometric detection for palytoxin analysis: Application to mussels, Anal. Bioanal. Chem. 406 (2014) 2399–2410.

Immunorecognition magnetic supports for the development of an electrochemical immunoassay for azaspiracid detection in mussels

Sandra Leonardo[a], Maria Rambla-Alegre[a], Ingunn A. Samdal[b], Christopher O. Miles[b], Jane Kilcoyne[c], Jorge Diogène[a], Ciara K. O'Sullivan[d,e], Mònica Campàs[a]

[a]*IRTA, Ctra. Poble Nou, km. 5.5, 43540 Sant Carles de la Ràpita, Spain*
[b]*Norwegian Veterinary Institute, P.O. Box 750 Sentrum, N-0106 Oslo, Norway*
[c]*Marine Institute, Rinville, Oranmore, County Galway H91 R673, Ireland*
[d]*Departament d'Enginyeria Química, Universitat Rovira i Virgili, Av. Països Catalans, 26, 43007 Tarragona, Spain*
[e]*Institució Catalana de Recerca i Estudis Avançats, Pg. Lluís Companys, 23, 08010 Barcelona, Spain*

Abstract

As azaspiracids (AZAs) are being reported from the coastal waters of an increasing number of countries on a global scale, the need for rapid, simple and cost-effective methods to detect these marine toxins and protect seafood consumers' health is becoming evident. A magnetic bead (MB)-based direct immunoassay for the detection of AZAs, using protein G-coated MBs as supports for antibody immobilisation and peroxidase-labelled AZAas a tracer is detailed. A colorimetric approach was first developed to optimise the experimental parameters and establish the cross-reactivity factors for AZA-1–10. The subsequent combination of the immunorecognition MBs with 8-electrode arrays enabled the multiplexed electrochemical detection of AZAs. Naturally contaminated mussel samples were analysed and the results obtained showed an excellent correlation with LC-MS/MS analysis. The MB-based immunoassay facilitated the quantification of a wide range of AZA concentrations (120–2875 μg AZA-1 equiv./kg), with a limit of detection (63 μg AZA-1 equiv./kg) below the European regulatory threshold, using a protocol that requires very few steps and a short analysis time (~ 15 min). The simplicity, cost-effectiveness, rapidity, robustness, selectivity and precision of the assay provide a valuable tool for the detection of all regulated AZAs and other toxic AZA analogues, suitable for end users in the field of food safety.

1. Introduction

The identification of azaspiracids (AZAs) as a food safety issue is relatively recent, as the first human intoxication episodes were reported in 1995 in the Netherlands after the consumption of contaminated mussels imported from Ireland (McMahon and Silke, 1996). AZAs are lipophilic marine toxins that originate from the phytoplankton *Azadinium* spp. (Tillmann et al., 2009) and *Amphidoma* spp. (Krock et al., 2012) and can accumulate in shellfish, where metabolism of AZAs from microalgae into other AZAs analogues may occur. The consumption of AZA-contaminated shellfish can lead to azaspiracid shellfish poisoning (AZP), with the major symptoms in humans being nausea, vomiting, severe diarrhoea and stomach cramps (Twiner et al., 2008). While initially thought of as an Irish problem, it was soon reported globally following the identification of AZA in waters of other western European countries (James et al., 2002; Braña-Magdalena et al., 2013), Morocco, Canada, Japan and Chile (López-Rivera et al., 2010). The AZA group comprises a unique spiral ring assembly, a heterocyclic amine and an aliphatic carboxylic acid moiety, and includes more than 30 analogues that are either produced by phytoplankton, through biotransformation in shellfish, or as by-products formed as a result of storage or cooking of AZA-contaminated shellfish (Hess et al., 2014). However, only AZA-1–3 are currently regulated by the European Comission, with 160 µg AZA-1 equivalents/kg being the maximum permitted level in shellfish meat (European Commission Regulation (EC) No 853/2004). As with the other lipophilic marine toxins, LC-MS/MS is the reference method for the analysis of AZAs (European Commission Regulation (EC) No 15/2011).

Although chemical approaches are certainly good strategies for the detection of marine toxins in food, alternative user-friendly methods that can provide shorter analysis times and lower costs are needed to enable multiple sample analysis to be implemented by the food industry and monitoring programs. Immunoassays are well suited to rapid screening due to their high sensitivity and because highly qualified personnel and expensive instrumentation are not required. To date, only a polyclonal antibody raised using a synthetic fragment of AZA (Forsyth et al., 2006) and a monoclonal antibody raised using AZA-1 (Frederick et al., 2009) have been reported, which have recently been used in the development of an enzyme-linked immunosorbent assay (ELISA) (Samdal et al., 2015) and a flow fluorimetry-based immunoassay (Rodríguez et al., 2014) for AZA detection, respectively.

The application of electrochemical detection methods to immunoassays overcomes some of the problems associated with other modes of detection, such as radioactivity, fluorescence, luminescence or phosphorescence, and provides versatility, reliability and faster analysis times than conventional immunoassays

(Laschi et al., 2011). In an immunosensor strategy, the antigen or antibody is directly immobilised onto the electrode surface that will finally be used to measure the antibody-antigen affinity interaction. However, use of the electrode surface as both an immunosorbent support and an electrochemical transducer can present some drawbacks, e.g. hindrance of electron transfer caused by coating of the surface with immunoreagents, or high non-specific adsorption of lipophilic molecules such as AZAs. The use of magnetic beads (MBs) as an alternative immobilisation support overcomes these limitations and provides a broad range of other advantages, such as ease of manipulation, improved assay kinetics and reduction of matrix effects.

Here we report the development of an MB-based direct immunoassay for AZA detection (Figure 1). Anti-AZA polyclonal antibody (PAb) was immobilised on protein G-coated MBs and a competitive step using peroxidase-labelled AZA was performed. A colorimetric approach was first developed and used for protocol optimisation and assay characterisation, to demonstrate the high stability of the conjugates, and to establish the cross-reactivity factors (CRFs) for AZA-2–10 (with respect to AZA-1) necessary for the subsequent validation of the method by comparison with LC-MS/MS. PAb-MB conjugates were then combined with electrode arrays as transducer elements and amperometry as the electroanalytical detection method, with the aim of providing a high-throughput system with low assay cost and simple instrumentation that enables device miniaturisation and easy AZA determination. To the best of our knowledge, this work reports the first electrochemical immunoassay for the detection of AZAs, providing a powerful strategy for marine toxin detection in shellfish within food safety monitoring and research programs.

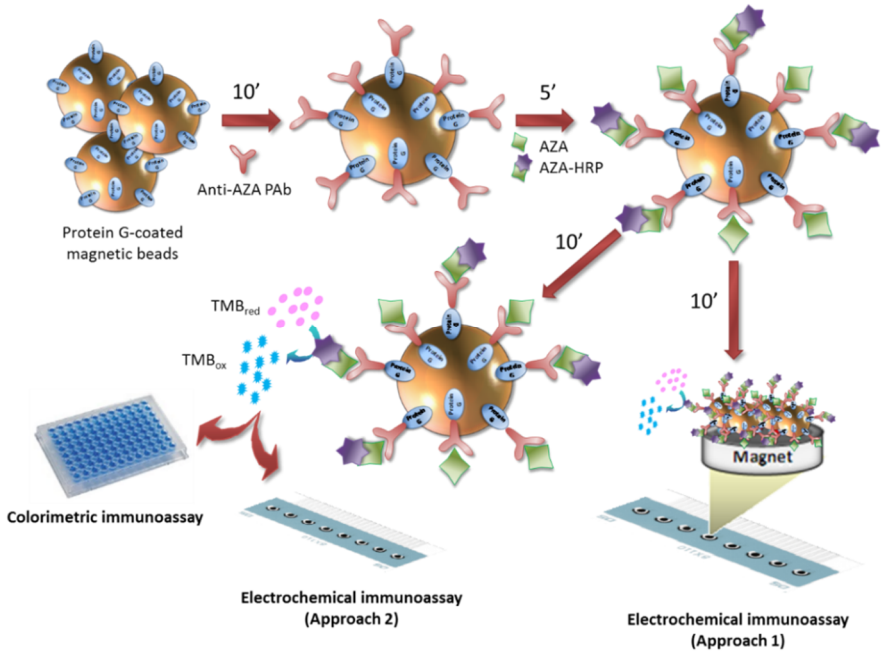

Figure 1. Schematic representation of the MB-based immunoassay and the different approaches developed for AZA detection by colorimetric and electrochemical detection methods.

2. Material and methods

2.1. Reagents and solutions

Dynabeads® Protein G-coated beads (30 mg /mL) were supplied by Invitrogen (Life Technologies, S.A., Alcobendas, Spain). Potassium phosphate monobasic, potassium chloride, Tween®-20, bovine serum albumin (BSA), 3,3',5,5'-tetramethylbenzidine (TMB) liquid substrate, ammonium formate (reagent grade) and formic acid (>98%) were purchased from Sigma–Aldrich (Steinheim, Germany). Acetonitrile (pesticide analysis grade) was obtained from J. T. Baker (Poland). Milli-Q water (Millipore, Bedford, USA) was used to prepare solutions. To perform LC-MS/MS analysis, distilled H_2O was further purified using a Barnstead nanopure diamond UV purification system (Thermo Scientific).

Certified reference materials (CRMs) of AZA-1–3, AZA-Mus, okadaic acid (OA), dinophysistoxin-1 (DTX-1), dinophysistoxin-2 (DTX-2), yessotoxin (YTX), homoyessotoxin (hYTX), pectenotoxin-2 (PTX-2), 13-desmethylspirolide C (SPX-1), gymnodimine A (GYM-A) and pinnatoxin G (PnTX-G) were obtained from the

National Research Council of Canada (NRC, Halifax, NS, Canada). Laboratory reference materials (LRMs) of AZA-4–AZA-10 were prepared as described by Kilcoyne et al. (2015a).

HRP (Type VI-A) from Sigma–Aldrich (Oslo, Norway) was conjugated to purified AZA-1 (Kilcoyne et al., 2012) using standard procedures for covalent linking of small molecules to enzymes (Hermanson, 2008). Antiserum AgR367-11b was obtained after 11 immunisations with two different haptens as described in Samdal et al. (2015).

2.2. Equipment

Magnetic separation was performed using a MagneSphere Technology Magnetic Separation Stand (for 12 0.5-mL or 1.5-mL tubes) and a PolyATtract System 1000 Magnetic Separation Stand (for one 15- or 30-mL tube) from Promega Corporation (Madison, WI, USA).

Colorimetric measurements were performed with a Microplate Reader KC4 from BIO-TEK Instruments, Inc. (Vermont, USA). Gen5 software was used to collect and evaluate data.

An array of eight screen-printed carbon electrodes (DRP-8X110), a boxed connector (DRP-CAST8X) and a magnetic support (DRP-MAGNET8X) were provided by Dropsens S.L. (Oviedo, Spain). The array consists of 8 carbon working electrodes of 2.5 mm in diameter, each with its own carbon counter electrode and silver reference electrode. Amperometric measurements were performed with a PalmSens potentiostat connected to an 8-channel multiplexer (MUX8) (Houte, the Netherlands). Data were collected and evaluated with PalmSens PC software.

2.3. Raw and heat-treated mussel tissues

AZA-Mus CRM prepared from naturally contaminated mussel tissues (*Mytilus edulis*) and AZA-contaminated raw mussel (*M. edulis*) samples from the routine monitoring program in Ireland, were selected for analysis. A blank raw mussel sample was analysed to perform matrix effect analysis.

Mussel samples were shucked and homogenised with an Ultra Turrax homogenizer. A triple step-extraction with methanol (10 mL) was performed on AZA-Mus and blank raw mussel homogenised tissues (1 g) according to Gerssen et al. (2009), protocol that was validated intra-laboratory by García-Altares et al. (2013). A vortex-mixer MS2 Minishaker (IKA Labortechnik, Staufen, Germany) and a centrifuge Jouan MR 23i (Thermo Fisher Scientific Inc., Waltham, MA, USA) were used. Crude extracts

were filtered through polytetrafluoroethylene (PTFE) 0.2-µm membrane syringe filters. Thus, AZA-Mus and blank raw mussel extracts at a matrix concentration of 100 mg/mL were obtained. Extraction of the Irish AZA-contaminated raw mussel samples was performed by a two-step extraction with methanol (25 mL). Homogenised tissue samples were weighed (2 g) into 50-mL centrifuge tubes and extracted by vortex mixing for 1 min with 9 mL of MeOH, centrifuged at 3,950 *g* (5 min), and the supernatants decanted into 25-mL volumetric flasks. The remaining pellet was further extracted using an Ultra Turrax (IKA) for 1 min with an additional 9 mL of MeOH, centrifuged at 3,950 *g* (5 min), and the supernatants decanted into the same 25-mL volumetric flasks, which were brought to volume with MeOH. A portion (10 mL) of each extract was transferred into sealed centrifuge tubes and placed in a water bath heated to 90 °C for 10 min to allow decarboxylation of the carboxylated AZAs (McCarron et al., 2009 and Kilcoyne et al., 2015b). The raw and heat-treated samples were then passed through Whatman 0.2 µm cellulose acetate filters into HPLC vials for analysis. Heated and raw mussel extracts were obtained at a matrix concentration of 80 mg/mL. All samples were stored at −20 °C until analysis.

2.4. PAb conjugation to MBs

PAb–MB conjugates were prepared as follows: (1) 50 µL of MB suspension were transferred to a tube and washed with PBS–Tween (0.1 M PBS, pH 7.2, with 0.05% Tween®-20), with vigorous mixing; for the washing steps, the tube was placed on the magnetic separation stand and the washing solution was removed; (2) 1 mL of anti-AZA PAb dilution (from 1/2,500 to 1/160,000 for the checkerboard and 1/10,000 dilution for the competition) in PBS–Tween, was added and incubated for 30 min (from 10 to 60 min in the conjugation-time optimisation) at room temperature with slow tilt-rotation; (3) the anti-AZA PAb–MB conjugates were washed three times and re-suspended in 1 mL of PBS–Tween. Where amounts of MB varied, volumes were adjusted proportionally.

2.5. Immunoassay protocol

Direct competition assays were performed in 0.5-mL plastic tubes coated with BSA by incubation of PBS–BSA overnight at 4 °C to avoid non-specific adsorption. The protocol was as follows: (1) 50 µL of anti-AZA PAb–MB conjugate were added to the BSA-coated tubes and placed on the magnetic separation stand to remove the supernatant; (2) 25 µL of standard or sample dilutions in PBS–Tween with 10-20% MeOH, and 25 µL of AZA–HRP (dilution from 1/100 to 1/3,200 for the checkerboard, and 1/800 for the competition) in PBS–Tween, were added to a tube and incubated

at room temperature for 30 min (from 5 to 30 min in the competition-time optimisation) with slow tilt-rotation; (3) three washing steps with PBS–Tween were performed and the content of each tube was re-suspended in 50 µL of PBS–Tween. Subsequent steps differed slightly for the different approaches and are described below.

For the colorimetric immunoassay: (5) 40 µL of immunocomplex were transferred to a new tube and the supernatant was removed; (6) 125 µL of TMB were incubated for 10 min; (7) tubes were placed on the magnetic separation stand and 100 µL of solution were taken for absorbance reading at 620 nm.

For the electrochemical immunoassay, two approaches were tested. In Approach 1, (5) 40 µL of immunocomplex were placed on each working electrode of an 8-electrode array with a magnetic support on the back, the magnetic immunocomplex was trapped and the supernatant was removed; (6) 40 µL of TMB were incubated for 10 min; (7) TMB oxidation was measured by amperometry, applying −0.2 V (vs. Ag) for 5 s, and the reduction current was recorded. In Approach 2, steps 5 and 6 were the same as in the colorimetric approach; (7) tubes were placed on the magnetic separation stand, 40 µL of solution were placed on each working electrode of an 8-electrode array and the reduction current was recorded by applying −0.2 V (vs. Ag) for 5 s.

2.6. Storage stability of PAb–MB conjugates

An anti-AZA-PAb–MB conjugate pool at 1/10,000 dilution was prepared and aliquots were stored at 4 °C and −20 °C. AZA–HRP aliquots at 1/800 dilution were also stored at −20 °C. The initial response (reference value) and the response after 1, 2, 3, 7, 15, 30, 60, 90, 120, 150 and 180 days was measured by addition of 25 µL of PBS–Tween with 10% MeOH and 25 µL of AZA–HRP tracer at 1/800 dilution. Responses were measured by colorimetry.

2.7. LC-MS/MS analysis

For LC-MS/MS analysis of AZA analogues, a Waters Acquity UPLC coupled to a Xevo G2-S QToF monitoring in MS^e mode (*m/z* 100–1200) was used using leucine enkephalin as the reference compound. The cone voltage was 40 V, collision energy was 50 V, the cone and desolvation gas flows were set at 100 and 1000 l/h, respectively, and the source temperature was 120 °C. Analytical separation was performed on an Acquity UPLC BEH C18 (50 × 2.1 mm, 1.7 µm) column (Waters). Binary gradient elution was used, with phase A consisting of H_2O and phase B of

CH_3CN (95%) in H_2O (both containing 2 mM ammonium formate and 50 mM formic acid). The gradient was from 30–90% B over 5 min at 0.3 mL/min, held for 0.5 min, and returned to the initial conditions and held for 1 min to equilibrate the system. The injection volume was 2 µL and the column and sample temperatures were 25 °C and 6 °C, respectively. AZA-1–3 were quantified using CRMs while AZA-4–10 were quantified with RMs (Kilcoyne et al., 2015a). Matrix interferences were assessed using single point matrix matched standards for AZA-1–6 and AZA-8, using a blank *M. edulis* tissue. An aliquot (2 g) of tissue was extracted as described above, this time making the solution up to a final volume of 20 mL. The matrix-matched standard was prepared by adding 1.25 mL of an AZA-1–6 and AZA-8 stock solution in MeOH to 1 mL of the filtered (Whatmann, 0.2 µm, cellulose acetate filter) blank tissue extract. In parallel, a MeOH standard was prepared by adding 1.25 mL of the same AZA-1–6 and AZA-8 stock solution to 1 mL of MeOH.

For LC-MS/MS analysis of lipophilic marine toxins other than AZA, a binary gradient was programmed with water (mobile phase A) and acetonitrile/water (mobile phase B), both containing 6.7 mM of ammonium hydroxide. All runs were carried out at 30 °C using a flow rate of 500 µL/min. The injection volume was 10 µL and the auto-sampler was set at 4 °C. These toxins were analysed in both negative (-ESI) and positive polarity (+ESI) (García-Altares et al., 2013), selecting two product ions per toxin to allow quantification (the most intense transition) and confirmation; identification was supported by toxin retention time andMRM ion ratios.

2.8. Data analysis

Measurements were performed in triplicate in immunoassay approaches and in duplicate in LC-MS/MS analysis. The calibration curves were fitted using a sigmoidal logistic four-parameter equation. The linear regression model was used to evaluate the correlation between AZA-1 equivalent content in naturally contaminated mussel samples determined with the colorimetric and electrochemical MB-based immunoassays and the values obtained from the LC-MS/MS analysis after application of the corresponding CRFs. To evaluate differences in the quantifications provided by the colorimetric and electrochemical MB-based immunoassays and the LC-MS/MS analysis, data were first tested for normality. The paired *t*-test was used for normally distributed data sets, while Wilcoxon matched-pairs signed-ranks was used for non-normally distributed data. Differences in the results were considered statistically significant at the 0.05 level. SigmaStat software package 3.1 was used for statistical analysis.

3. Results and discussion

3.1. Optimisation of the experimental parameters of the MB-based immunoassay protocol

The conjugation of PAb to MBs is based on the ability of the recombinant protein G to bind to the Fc region of the antibody, allowing a stable and oriented antibody immobilisation and thus avoiding possible steric effects. To determine whether conjugation was successful and to establish the optimum PAb and AZA–HRP concentrations to be used in the assay, colorimetric checkerboards were carried out. The absorbance values obtained showed appropriate trends according to PAb and AZA–HRP tracer dilutions, demonstrating both the PAb conjugation to the MBs and the successful synthesis of the AZA–HRP tracer, as well as the feasibility of the strategy. Very low absorbance values were obtained in the controls with no PAb, highlighting the benefits of magnetic separation, which improves washing steps and reduces non-specific phenomena.

Antibody and tracer concentrations need to be well established when performing a competitive immunoassay. Whilst decreasing concentrations of antibody and/or tracer usually provides greater sensitivity (Reverté et al., 2015), too low levels of antibody and/or tracer may result in low signal and poor precision. In this assay, 1/10,000 PAb and 1/800 AZA–HRP dilutions were selected as a compromise between sufficiently high response and low antibody/tracer loading.

The time required to perform the PAb–MB conjugation was also optimised. No significant differences in signals were observed in PAb-MB conjugations performed for 10, 20, 30, 45 and 60 min, demonstrating that in 10 min the conjugation of the antibody to the MB was complete. Furthermore, in order to investigate the possibility of storing PAb–MB conjugates until use, their stability at 4 °C and −20 °C was evaluated over 180 days. Absorbance values were constant with time, clearly demonstrating that PAb–MB conjugates were stable for at least 6 months, stored both at 4 °C or −20 °C, but also highlighting the stability of the AZA–HRP tracer stored at −20 °C (Figure S1). The excellent storage stability of the conjugates simplifies and further decreases the protocol assay time. Ready-to-use conjugates can be available at any time and provide a higher reproducibility to the system, as the same conjugate pool can be used for the analysis of different samples on different days.

Relative standard deviations (RSDs) were always below 5%, regardless of the number of replicates, the PAb–MB conjugation pool or the PAb–MB storage conditions tested. This low variability results in a highly repeatable, robust and reproducible system.

3.2. Colorimetric MB-based immunoassay

In the direct competition assay, the signal is reported as the AZA–HRP binding to PAb, where the amount of AZA–HRP bound depends on the tracer/antigen ratio, with increasing amounts of target AZA resulting in less binding of the AZA-HRP and a lower signal. Calibration curves demonstrated competition of free AZA-1 with AZA–HRP for PAb binding (Figure 2), achieving a half maximal inhibitory concentration (IC_{50}) of 9.2 ± 0.5 µg/L AZA-1, a limit of detection (LOD), established as the IC_{10}, of 1.1 ± 0.1 µg/L, and a working range (IC_{20}–IC_{80}) between 2.3 ± 0.1 and 46.7 ± 1.0 µg/L. IC values were obtained as the mean of the values from three different calibration curves and their standard deviations. Independent of the day or the person who performed the assay, RSD values were always lower than 7%, demonstrating the high reproducibility of the immunoassay. The results obtained are similar to the ELISA developed by Samdal et al. (2015), where an indirect competitive assay was performed by immobilising the antigen on a plate. That method required the use of higher amounts of antiserum and plate-coating antigen, and was a longer and more complex assay compared to the direct immunoassay described here.

The competition time for the immunoassay was also evaluated (5, 10, 20 and 30 min). Although absorbance values increased with time, absorbance values at 5 min were high enough to obtain calibration curves with the same analytical characteristics, highlighting the robustness of the assay and further decreasing the time required to perform the immunoassay.

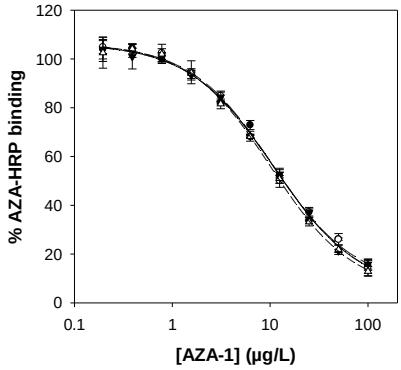

Figure 2. Colorimetric calibration curves for AZA-1 performed in buffer with 20% (△) and 10% (▼) MeOH and in 8 mg/mL (○) and 16 mg/mL (●) mussel matrix with 20% MeOH.

3.3. Establishment of cross-reactivity factors (CRFs)

The development of an immunoassay able to recognise all regulated AZAs but also other toxic AZA analogues was pursued. The reduction in the immunoassay signal indicates competition, but does not show which analytes bind to the antibody. For this reason, the response of the MB-based immunoassay to AZA-2–10 relative to AZA-1 was evaluated and the corresponding cross-reactivity factors (CRFs) were established by colorimetry. The establishment of CRFs would help to better understand the comparison between the quantifications provided by the immunochemical tools and those obtained by LC-MS/MS analysis in the determination of AZA content of shellfish samples. All AZA analogues caused concentration-dependent inhibition of antibody binding. CRFs for all analogues established on the basis of IC_{50} relative to AZA-1 are shown in Table 1. Cross-reactivity studies indicated that the recognition of analogues by antibodies in the magnetic-bead based immunoassay was slightly reduced for AZA-2 but increased for all the other AZA analogues tested. All values were corrected for the known impurities in the AZA-4–10 standards (Table S1), although this only resulted in minor changes due to the relatively low concentrations of impurities in the standards. In comparison with CRFs established in the ELISA developed by Samdal et al. (2015) — where the same PAb was used— the antibody recognised AZA-3–10 with significantly higher affinity. This clearly demonstrates that CRFs not only depend on the affinity of the antibody for the different analogues, but also on the immunological approach and the manner in which antibodies/antigens are immobilised, especially in the case of polyclonal antisera.

Table 1. Cross-reactivity factors (CRFs) for AZA analogues.

		AZA analogue									
		AZA-1	**AZA-2**	**AZA-3**	**AZA-4**	**AZA-5**	**AZA-6**	**AZA-7**	**AZA-8**	**AZA-9**	**AZA-10**
CRF (%)	*MB-based immunoassay*	100	76	273	383	139	270	200	185	269	217
	Samdal et al. (2015) immunoassay	100	75	140	145	100	144	72	95	114	128

3.4. Study of interferences and matrix effect

Standard methods for extraction of lipophilic marine toxins are performed using 100% MeOH. Previous optimisations of the MB-based immunoassay were performed with 10% MeOH in the sample dilutions to be compatible with extraction and analysis methods of lipophilic marine toxins. This compatibility involves a 10-fold dilution of the sample. Nevertheless, the influence of MeOH concentration on the immunoassay performance was evaluated using colorimetric detection to study the possibility of performing the immunoassay with a higher MeOH concentration, thus allowing a higher load of shellfish matrix while avoiding the evaporation of the sample and possible toxin loss. Results demonstrated that there were no significant differences between 10% and 20% MeOH concentration in samples, so samples can be diluted 5-fold instead of 10, decreasing the effective limit of detection 2-fold (Figure 2). Nonetheless, to ensure the applicability of the assay to the analysis of natural samples, the effect of mussel matrix was also evaluated. The study of the matrix effects is crucial in the development of biochemical assays, where the functionality of biorecognition molecules may be strongly affected by the presence of matrix compounds other than the target analyte. No matrix effects were observed with the highest matrix concentration tested (16 mg/mL), which was chosen according to the protocol for lipophilic toxins extraction in AZA-contaminated samples (80 mg mussel matrix in 1 mL of MeOH) and its subsequent dilution to 20% MeOH. With a 5-fold sample dilution, the LOD and the limit of quantification (LOQ, established as the IC_{20}) in mussel for the colorimetric MB-based immunoassay were 71 ± 6 µg AZA-1 equiv./kg and 141 ± 6 µg AZA-1 equiv./kg, respectively. Both values were below the European regulatory limit and in the same order of magnitude as the immunoassays previously reported (Samdal et al., 2015; Rodríguez et al., 2014). The MB-based immunoassay presented a broad working range that enabled the quantification up to 2,919 ± 63 µg AZA-1 equiv./kg of mussel matrix without requiring additional sample dilutions.

During the AZAs extraction process, all lipophilic marine toxins are extracted. In consequence, the specific detection of AZAs prior to the analysis of real samples has to be demonstrated. With this aim, the possible interference from all other lipophilic marine toxins (OA, DTX-1, DTX-2, YTX, hYTX, PTX-2, SPX-1, GYM-A, PnTX-G) was evaluated. Results showed that major lipophilic toxins apart from AZAs are not detected by the immunoassay at concentrations up to 100 µg/L (Fig. S2), demonstrating the high specificity of the assay.

3.5. Electrochemical MB-based immunoassay

In order to develop the electrochemical immunoassay, the magnetic immunocomplex or the resulting enzyme product was integrated on an 8-electrode array to carry out multiple electrochemical measurements (Figure 3). In Approach 1, the enzymatic reaction between AZA–HRP and the substrate (TMB) was performed on the electrode, and TMB reduction was subsequently measured by amperometry. In this case, the IC_{50} (21.5 ± 0.7 µg/L) and LOD (3.7 ± 0.1 µg/L) were higher than those obtained in the colorimetric immunoassay (IC_{50} = 9.2 ± 0.5 µg/L; LOD = 1.1 ± 0.1 µg/L). This difference could be due to mass transfer limitations of the enzyme kinetics due to its packed distribution on the electrode. To improve the electrochemical immunoassay, a second approach (Approach 2) was attempted by performing the enzyme reaction in suspension and transferring the resulting product to the electrodes for the corresponding electrochemical measurement. In this case, an IC_{50} of 8.7 ± 0.3 µg/L was achieved, with an LOD of 1.0 ± 0.1 µg/L and a working range between 1.9 ± 0.1 and 46.1 ± 4.0 µg/L. Matrix effects and interferences were assumed to be negligible since the competition step takes place away from the electrode surface in the same way as in the colorimetric approach. Consequently, an efficient LOD of 63 ± 6 µg AZA-1 equiv./kg and a working range between 120 ± 6 and 2,881 ± 250 µg AZA-1 equiv./kg in mussel tissue were obtained.

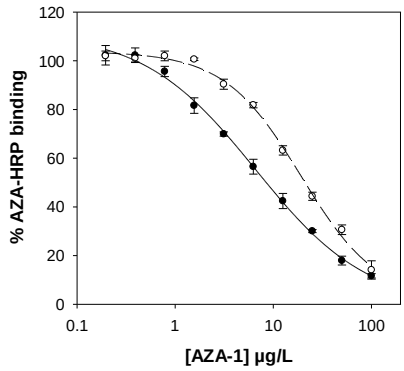

Figure 3. Electrochemical calibration curves for AZA-1 obtained by two different approaches. In Approach 1 (○), the enzymatic reaction between AZA–HRP and TMB substrate was performed on the electrode by magnetic entrapment of the immunocomplex. In Approach 2 (●), the enzymatic reaction was performed in suspension and the resulting product was transferred to the electrode.

The use of MBs as antibody immobilisation supports facilitates the performance of all reactions in suspension, improving the assay kinetics and allowing the detection of lower toxin levels. On the other hand, the use of electrode arrays allows multiple measurements to be performed in a compact and fast way, making the assay suitable for high-throughput analysis of AZAs.

3.6. Analysis of mussel samples

The utility of the MB-based immunoassay for the analysis of real samples was demonstrated by the determination of AZAs content in naturally contaminated mussel (*M. edulis*) samples. A CRM containing certified contents of AZA-1–3 as well as other AZA-4–10 analogues was analysed both by the colorimetric and the electrochemical immunoassays. The application of the CRFs of the AZA analogues to the individual contents is crucial to compare the results between the NRC values and the quantifications of our assays. After the application of the corresponding CRFs to the quantifications provided by NRC, the correlations between NRC values and the quantifications achieved by the MB-based colorimetric and electrochemical (Approach 2) immunoassays were 100.6 % and 99.1 %, respectively.

The AZA content of 11 contaminated raw mussel samples from the routine monitoring program in Ireland was also determined by the immunoassay approaches. The samples analysed contained a wide range of AZA concentrations, from well below the regulatory limit to far in excess of the permitted threshold. As expected, quantifications provided by the colorimetric and the electrochemical (Approach 2) MB-based immunoassay were in good agreement (y = 1.047 x - 93, R^2 = 0.988). Although samples 1 and 2 gave a response of less than 20% of inhibition of AZA–HRP binding in both approaches –values below the LOQ–, AZA-1 equiv. content was quantified using the sigmoidal logistic regression equation. Quantifications provided by the MB-based immunoassay were compared with those obtained by the LC-MS/MS reference method (Table 2). RSDs lower than 10% were obtained for all samples excluding sample 1. This sample showed RSDs of 9%, 12% and 14 % for the quantifications obtained by the colorimetric and electrochemical MB-based immunoassays and LC-MS/MS analysis, respectively. Since the antibody used for the development of our assay was able to recognise all AZA analogues including the carboxy congeners (Samdal et al., 2015), LC-MS/MS analysis was performed with heated samples. Heating catalyses decarboxylation of AZA-17, AZA-19, AZA-21 and AZA-23 carboxy congeners to AZA-3, AZA-6, AZA-4 and AZA-9, respectively (McCarron et al., 2009 and Kilcoyne et al., 2015b). No significant matrix effects were observed in the LC-MS/MS analysis. Again, CRFs of the AZA analogues were applied to the individual contents determined by LC-MS/MS to better

understand the correlation between approaches. AZAs quantifications obtained by the colorimetric (y = 1.112 x + 32, R^2 = 0.993) and electrochemical (y = 1.174 x - 71, R^2 = 0.998) approaches were in good correlation with LC-MS/MS (Fig. 4). However, although samples with a lower AZA content (samples 1, 2 and 3) showed an excellent 1:1 correlation, a slight overestimation by the MB-based immunoassay was observed in samples with higher AZA content. Taking into account that more than 30 AZA analogues have been described, the MB-based immunoassay could be detecting the presence of other minor AZA analogues that were not targeted in the LC-MS/MS analysis. The presence of other lipophilic toxins different from AZAs was also determined by LC-MS/MS, with OA and DTX-2 concentrations well above the regulatory limit in samples 1, 2 and 3 (Table S2). As quantifications of these samples did not show significant differences between the results determined by the MB-based immunoassay and those provided by LC-MS/MS, the lack of interference from other lipophilic toxins other than AZA analogues was again demonstrated, in this case with naturally-contaminated samples.

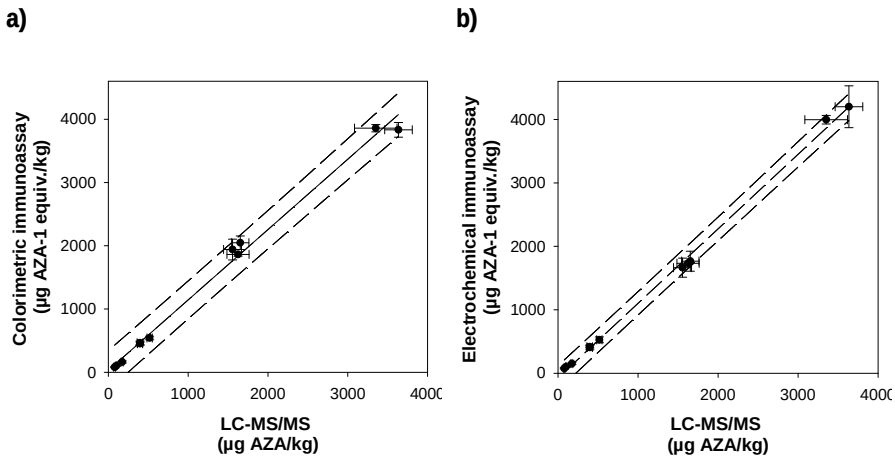

Fig. 4. Linear regressions for the correlations between sample quantifications by the colorimetric **(a)** or electrochemical (Approach 2) **(b)** immunoassay and sample quantifications by LC-MS/MS analysis. Dashed lines represent the prediction intervals of 95%.

Table 2. AZA content (µg AZA/kg mussel) of 11 contaminated mussel tissue extracts from the routine monitoring program in Ireland and comparison between quantifications provided by LC-MS/MS and those provided by the colorimetric and electrochemical (Approach 2) MB-based immunoassays.

	LC-MS/MS											MB-based immunoasay	
	AZA-1	AZA-2	AZA-3	AZA-4	AZA-5	AZA-6	AZA-7	AZA-8	AZA-9	AZA-10	∑ *AZAs (applying CRFs)*	**Colorimetric** *AZA-1 equiv.*	**Electrochemical** *AZA-1 equiv.*
S#1	24	5	15	nd	nd	3	nd	nd	nd	nd	77	80	77
S#2	33	10	19	nd	nd	2	nd	nd	nd	nd	99	100	101
S#3	49	19	31	nd	1	7	nd	2	nd	nd	173	163	151
S#4	148	35	55	3	6	16	nd	1	1	3	396	465	416
S#5	144	59	80	13	5	12	nd	6	1	2	516	542	527
S#6	128	45	66	3	4	10	nd	5	nd	nd	397	452	407
S#7	370	125	216	81	23	44	2	21	19	6	1624	1863	1733
S#8	425	139	189	77	17	35	4	21	16	4	1555	1940	1664
S#9	573	164	174	71	13	37	2	20	17	3	1653	2048	1766
S#10	798	258	480	142	32	101	2	46	32	7	3352	3859	3997
S#11	1524	414	309	132	33	64	10	49	38	9	3636	3833	4201

nd: not detected

4. Conclusions

Colorimetric and electrochemical MB-based direct immunoassays for detection of AZAs, using MBs as antibody immobilisation supports and AZA-HRP as a tracer, have been described. The MB-based immunoassay exhibits excellent analytical performance in terms of sensitivity, selectivity, wide range of quantifiable analyte concentrations, precision, robustness and inter-assay reproducibility. The high specificity of the assay provides a tool able to recognise all regulated AZAs but also a broad range of other toxic AZA analogues, which is complementary to the LC-MS/MS regulatory method.

Assay protocol times were optimised to achieve a rapid screening and quantification method, with the entire assay being completed in just 15 min. Only the sample and the tracer need to be added to perform the competition (step 1) and the enzyme substrate to measure the response (step 2). Additionally, no evaporation of the extracts is required, altogether providing a short and easy-to-perform protocol that does not require highly trained or qualified personnel.

The high accuracy obtained in the determination of AZAs content in mussel samples, with no matrix effects being observed, clearly demonstrates that the use of magnetic immunocomplexes is a valuable strategy in immunoassays for the detection of AZAs in shellfish. Merging the advantages of this approach with the benefits that electrode arrays bestows, the developed analytical tools fulfils all the requirements for its straightforward integration in food safety programs: a user-friendly, rapid, cost-effective and precise high-throughput system able to specifically detect the desired analytes below the regulatory limit in complex matrices. The present work not only reports the first electrochemical immunoassay for AZA detection, but also constitutes a clear demonstration that simple approaches can result in powerful analytical tools.

Acknowledgments

The research leading to these results has received funding from the European Union's Seventh Framework Programme (FP7/2007-2013) under grant agreement no 311820 and under the *Sea Change* strategy (PBA/AF/08/001(01) with the support of the Marine Institute and the Marine Research Sub-Programme of the National Development Plan 2007–2013, co-financed under the European Regional Development Fund. The publication reflects the views only of the author, and the European Union cannot be held responsible for any use which may be made of the information contained therein. The authors acknowledge financial support from CERCA Programme / Generalitat de Catalunya. Sandra Leonardo acknowledges scholarship from IRTA-Universitat Rovira i Virgili-Banco Santander (2013PIPF URV-IRTA-BS-01).

References

Braña-Magdalena, A., Lehane, M., Krys, S., Luisa-Fernández, M., Furey, A., James, K.J., 2003. Toxicon 42, 105-108.

European Commission. Regulation (EU) No 853/2004 of 29 April 2004 laying down specific hygiene rules for on the hygiene of foodstuffs. Off. J. Eur. Union 2011, L139, 55-205.

European Commission. Regulation (EU) No 15/2011 of 10 January 2011 amending Regulation (EC) No 2074/2005 as regards recognised testing methods for detecting marine biotoxins in live bivalve molluscs. Off. J. Eur. Union 2011, L6, 3-6.

Frederick, M.O., Janda, K.D., Nicolau, K.C., Dickerson, T.J., 2009. Chembiochem. 10, 1625-1629.

Forsyth, C.J., Xu, J., Nguyen, S.T., Samdal, I.A., Briggs, L.R., Rundberget, T., Sandvik, M., Miles, C.O., 2006. J. Am. Chem. Soc. 128, 15114-15116.

García-Altares, M., Diogène, J., De la Iglesia, P., 2013. J. Chromatogr. A 1275, 48-60.

Gerssen, A., Mulder, P.J.P., McElhinney, M.A, de Boer, J., 2009. J. Chromatogr. A 1216, 1421-1430.

Hermanson, G.T., 2008. Bioconjugate Techniques, second ed. Academic Press, London.

Hess, P., McCarron, P., Krock, B., Kilcoyne, J., Miles, C.O., 2014. Azaspiracids: chemistry, biosynthesis, metabolism, and detection, in: Botana, L.M. (Ed.), Seafood and Freshwater Toxins. Pharmacology, Physiology, and Detection. CRC Press, Boca Raton, FL, pp. 799-822.

James, K.J, Furey, A., Lehane, M., Ramstad, H., Aune, T., Hovgaard, P., Morris, S., Higman, W., Satake, M., Yasumoto, T., 2002. Toxicon 40, 909-915.

Krock, B., Tillmann, U., Voβ, D., Koch, B.P., Salas, R., Witt, M., Potvin, É., Jeong, H.J., 2012. Toxicon 60, 830-839.

Kilcoyne, J., Keogh, A., Clancy, G., Leblanc, P., Burton, I., Quilliam, M. A., Hess, P., and Miles, C. O., 2012. J. Agric. Food Chem. 60, 2447-2455.

Kilcoyne, J., Twiner, M.J., McCarron, P., Crain, S., Giddings, S.D., Foley, B., Rise, F., Hess, P., Wilkins, A.L., Miles, C.O., 2015a. J. Agric. Food Chem. 63, 5083-5091.

Kilcoyne, J., McCarron, P., Hess, P., Miles, C.O., 2015b. J. Agric. Food Chem. 63, 10980-10987.

Laschi, S., Centi, S., Mascini, M., 2011. Bioanal. Rev. 3: 11-25.

López-Rivera, A., O'Callaghan, K., Moriarty, M., O'Driscoll, D., Hamilton, B., Lehane, M., James, K.J., Furey, A., 2010. Toxicon 55, 692-701.

McCarron, P., Kilcoyne, J., Miles, C.O., Hess, P., 2009. J. Agric. Food Chem. 57, 160-169.

McMahon, T., Silke, J., 1996. Harmful Algae News 14, 2.

Rodríguez, L.P., Vilariño, N., Louzao, M.C., Dickerson, T.J., Nicolaou, K.C., Frederick, M.O., Botana, L.M., 2014. Anal. Biochem. 447, 58-63.

Reverté, L., de la Iglesia, P., del Río, V., Campbell, K., Elliott, C. T, Kwatsu, K., Katikou, P., Diogène, J., Campàs, M., 2015. Anal. Chem. 87, 10839-10847.

Samdal, I.A., Løvberg, K.E., Briggs, L.Y., Kilcoyne, J., Xu, J., Forsyth, C.J., Miles, C.O., 2015. J. Agric. Food Chem. 63, 7855-7861.

Tillmann, U., Elbrächter, M., Krock, B., John, U., Cembella, A.D., 2009. Eur. J. Phycol. 44, 63-79.

Twiner, M., Rehmann, N., Hess, P., Doucette, G.J., 2008. Mar. Drugs 6, 39-72.

Supplementary Information

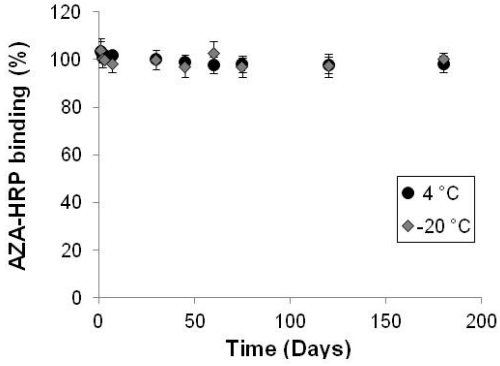

Fig. S1. Storage stability of anti-AZA PAb-MB conjugates.

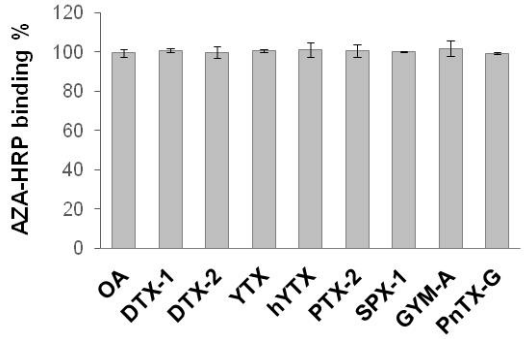

Fig. S2. Study of interferences: response to 100 µg/L of potentially interfering lipophilic marine toxins.

Table S1. Impurities in the AZA-4–10 standards.

Standard	Component	% (total purity)	Concentration (µg/mL)	
			Std	Total AZAs
AZA-4	AZA-4	**98.5**	**1.1**	**1.1**
	37-*epi*-AZA-4	1.5		
AZA-5	AZA-5	**94.5**	**1.1**	**1.2**
	AZA *m/z* 826	1.7		
	AZA-7	1.6		
	37-*epi*- AZA-5	2.2		
AZA-6	AZA-6	**96.5**	**1.2**	**1.4**
	37-*epi*- AZA-6	3.5		
AZA-7	AZA-7	**63.0**	**1.1**	**1.5**
	AZA-5	13.6		
	AZA *m/z* 826	20.4		
	37-*epi*- AZA-7	3.0		
AZA-8	AZA-8	**86.0**	**1.1**	**1.3**
	AZA *m/z* 826	5.6		
	37-*epi*- AZA-8	8.6		
AZA-9	AZA-9	**86.2**	**1.8**	**2.1**
	AZA-26	11.5		
	37-*epi*- AZA-9	2.3		
AZA-10	AZA-10	**95.2**	**0.8**	**0.8**
	AZA-11	4.8		
	37-*epi*- AZA-10	?		

Table S2. Other lipophilic marine toxins (µg toxin/kg mussel) of 11 AZA-contaminated raw mussel samples from the routine monitoring program determined by LC-MS/MS analysis.

	OA	**DTX-1**	**DTX-2**	**YTX**	**45-OH-YTX**	**hYTX**	**45-OH-hYTX**	**PTX-2**	**PTX-1**	**SPX-1**	**GYM-A**	**PnTX-G**
MR	803.5>2	817.5>2	803.5>2	570.4>4	578.4>4	577.4>4	585.4>4	876.5>2	892.5>2	692.5>4	508.4>4	694.5>6
M1	55.2	55.2	55.2	67.4	67.4	74.4	74.4	13.3	13.3	44.2	90.4	76.4
MR	803.5>1	817.5>1	803.5>1	570.4>3	578.4>3	577.4>4	585.4>4	876.5>8	892.5>8	692.5>4	508.4>3	694.5>1
M2	13.1	13.1	13.1	96.4	96.4	03.4	03.4	23.5	21.5	26.3	92.4	64.5
S#1	94	nd	1280	nd	nd	nd	nd	39	nd	12	nd	1
S#2	309	nd	2059	nd	nd	nd	nd	48	nd	12	nd	nd
S#3	122	nd	885	nd	nd	nd	nd	23	nd	11	nd	1
S#4	15	nd	3	nd	nd	nd	nd	nd	nd	12	nd	1
S#5	nd	nd	nd	nd	nd	nd	nd	3	nd	12	nd	7
S#6	nd	nd	nd	nd	nd	nd	nd	nd	nd	nd	nd	1
S#7	12	nd	85	nd	nd	nd	nd	nd	nd	12	nd	2
S#8	15	nd	62	nd	nd	nd	nd	nd	nd	12	nd	1
S#9	nd	nd	2	nd	nd	nd	nd	nd	nd	58	nd	3
S#10	60	nd	18	nd	nd	nd	nd	nd	nd	nd	nd	2
S#11	nd	nd	nd	nd	nd	nd	nd	nd	nd	63	nd	6

nd: not detected; *: LC-MS/MS values under LOQ (µg/kg) are semi-quantitative and should be regarded only as indicative of detection.

Detection of azaspiracids in mussels using electrochemical immunosensors for fast screening in monitoring programs

Sandra Leonardo[a], Jane Kilcoyne[b], Ingunn A. Samdal[c], Christopher O. Miles[c,d], Ciara K. O'Sullivan[e,f], Jorge Diogène[a], Mònica Campàs[a]

[a]*IRTA, Ctra. Poble Nou, km. 5.5, 43540 Sant Carles de la Ràpita, Spain*
[b]*Marine Institute, Rinville, Oranmore, County Galway H91 R673, Ireland*
[c]*Norwegian Veterinary Institute, P.O. Box 750 Sentrum, N-0106 Oslo, Norway*
[d]*National Research Council Canada, 1411 Oxford St., Halifax, Nova Scotia, B3H 3Z1, Canada*
[e]*Departament d'Enginyeria Química, Universitat Rovira i Virgili, Av. Països Catalans, 26, 43007 Tarragona, Spain*
[f]*Institució Catalana de Recerca i Estudis Avançats, Pg. Lluís Companys, 23, 08010 Barcelona, Spain*

Abstract

Given the widespread occurrence of azaspiracids (AZAs), it is clearly necessary to advance in simple and low-cost methods for the rapid detection of these marine toxins in order to protect seafood consumers. To address this need, electrochemical immunosensors for the detection of AZAs based on a competitive direct immunoassay using peroxidase-labelled AZA as a tracer were developed. An anti-AZA polyclonal antibody was immobilised in a controlled and stable manner on protein G or avidin-coated electrodes. Experimental conditions were first optimised using colorimetric immunoassays on microtitre plates, providing intermediate products already applicable to the accurate detection of AZAs. Then, transfer of the protein G and avidin–biotin interaction-based immunoassays to 8-electrode arrays provided compact and miniaturised devices for the high-throughput detection of AZAs. The low amounts of immunoreagents required as well as the potential for reusability of the avidin–biotin interaction-based immunosensors represented significant economic savings as well as a contribution to sustainability. The electrochemical immunosensors enabled the quantification of all regulated AZAs below the regulatory limit, as well as a broad range of other toxic AZA analogues (from 63 ± 3 to 2841 ± 247 µg AZA-1 equiv./kg for the protein G-based immunosensor and from 46 ± 2 to 3079 ± 358 µg AZA-1 equiv./kg for the avidin–biotin interaction-based immunosensor). The good agreement between the results obtained by the immunosensors and LC-MS/MS in the analysis of naturally contaminated mussel samples demonstrated the easy implementation of

electrochemical immunosensors for routine analysis of AZAs in food safety monitoring programs.

1. Introduction

Harmful algal blooms (HABs) and their associated marine toxins pose a serious threat to human health and are an economic concern for the shellfish industry. Among many different groups of marine toxins of microalgal origin are azaspiracids (AZAs). AZAs were first identified in 1998 from contaminated mussels from Ireland that had caused a poisoning outbreak in The Netherlands in the mid-1990s [1]. Since then, AZAs have been particularly problematic in Ireland, but they have also been reported in phytoplankton and/or shellfish around the world including the US [2], China [3], Japan [4], Chile [5, 6] and Argentina [7]. In Europe, AZAs have been found in several countries adjacent to the North Sea such as Norway, Denmark, UK and Sweden [8-10]. AZAs have also been found in the Atlantic coast of other European countries including France, Portugal and Spain [11-15], in the Atlantic coast of NW Africa [16], as well as in countries of the Mediterranean Sea [17].

The AZA group includes more than 40 analogues, which are either produced by phytoplankton of the genera *Azadinium* and *Amphidoma*, through biotransformation in shellfish, or as by-products resulting from storage or cooking of AZA-contaminated shellfish [18]. However, only AZA-1–3 are currently regulated by the European Commission, with 160 µg AZA-1 equiv./kg being the maximum permitted level in shellfish meat [19].

Although current reference chemical methods are highly specific and sensitive, they require the use of sophisticated equipment and trained personnel, being expensive and relatively slow to perform. Thus, there is a need for easy-to-use, rapid, inexpensive and accurate devices for the detection of AZAs in shellfish in monitoring programs. Biosensors have the potential to address this need and, among them, electrochemical biosensors stand out for several reasons: their inherently high sensitivities, low cost, possibility for miniaturisation of electrodes and potentiostats, compatibility with microfluidics systems and automation and subsequent simplification of the protocols [20]. Likewise, the high specificity and selectivity of antibodies (Abs) positions immunosensors as highly attractive candidates for the rapid screening of marine toxins.

Nonetheless, the lack of commercially available anti-AZA Abs has hindered the development of immunosensors, as well as immunoassays, for the detection of AZAs. To date, only a monoclonal antibody (MAb) raised using AZA-1 [21] and a polyclonal antibody (PAb) raised using a synthetic fragment of AZA [22] have been

reported. While the MAb was used in the development of a flow fluorimetry-based immunoassay [23], the anti-AZA PAb has been used in the development of an enzyme-linked immunosorbent assay (ELISA) [24] and an electrochemical immunoassay using magnetic beads as immunorecognition supports [25].

Another crucial step in the development of immunoassays and immunosensors is the immobilisation of the Ab on a solid support. To achieve full functionality, the conformation of the Abs should not be altered and their binding sites should remain accessible after immobilisation. Moreover, in the development of electrochemical biosensors, the immobilisation procedure should ensure a close proximity between the label and the transducer in order to obtain an efficient electron transfer. Bioaffinity immobilisation, mainly based on the avidin–biotin interaction and the affinity of protein A/G for immunoglobulins (IgGs), provides an attractive method for the controlled and stable surface-tethering of antibodies. In our previous work [25], the anti-AZA PAb was immobilised on protein G-coated magnetic beads and a competitive step using peroxidase-labelled AZA (AZA–HRP) was performed. The use of magnetic beads facilitated performance of the assay in suspension, thus allowing rapid assay kinetics, but mass transfer limitations were observed when the immunocomplexes were subsequently anchored on the electrode surface to perform electrochemical detection. In the present work, the anti-AZA PAb is immobilised on the electrode surface by means of protein G, or, alternatively, through the avidin–biotin interaction, with the aim of overcoming the drawbacks associated with the packed distribution of magnetic beads on the electrode surface and allowing a controlled and homogenous immobilisation of the antibody directly on the transducer surface. The immobilisation of the Ab directly on the transducer surface provides more compact and automated devices, since all reactions are performed on the electrode array, with possible signal enhancement since the enzyme product is concentrated closer to the transducer surface.

Colorimetric immunoassays were first developed on microtitre plates and used for protocol optimisation and assay characterisation. Their suitability for AZAs screening and quantification in mussels was also demonstrated. Protein G and avidin–biotin interaction-based immunoassays were then transferred to electrode arrays to develop the corresponding competitive electrochemical immunosensors. With the aim of further improving the economic saving represented by the use of the immunosensors, their reusability was explored. The immunosensors were applied to the determination of AZAs in a mussel certified reference material (CRM) and in mussel samples obtained from the Irish monitoring program. To the best of our knowledge, this work describes the first immunosensors for AZAs detection and guarantees their implementation in routine monitoring programs.

2. Materials and methods

2.1. Reagents and solutions

Protein G from *Streptococcus* sp., avidin from egg white, sodium carbonate, sodium bicarbonate, potassium phosphate monobasic, potassium chloride, Tween–20, bovine serum albumin (BSA) and 3,3'-5,5'-tetramethylbenzidine (TMB) liquid substrate were purchased from Sigma–Aldrich (Madrid, Spain). Milli-Q water (Millipore, Bedford, USA) was used to prepare solutions.

Certified reference materials (CRMs) of AZA-1–3, Zero-Mus and AZA-Mus were obtained from the National Research Council of Canada (NRC, Halifax, NS, Canada). Reference materials (RMs) of AZA-4–10 were prepared as described by Kilcoyne et al. [26].

HRP (Type VI-A) from Sigma–Aldrich (Oslo, Norway) was conjugated to purified AZA-1 [27] using standard procedures for covalent linking of small molecules to enzymes [28]. Antiserum AgR367-11b (anti-AZA PAb) was obtained after 11 immunisations with two different haptens as described in Samdal et al. [24].

Biotin labelling of the anti-AZA PAb was performed with EZ-Link^{TM} NHS–PEG$_4$–Biotin from Thermo Fisher (Barcelona, Spain) following the manufacturer's manual. Unreacted NHS–PEG$_4$–Biotin was removed by Zeba Spin Desalting Colums (7 kDa MWCO, 2 mL) from Thermo Fisher.

2.2. Equipment

Colorimetric measurements were performed with a Microplate Reader KC4 from BIO-TEK Instruments, Inc. (Winooski, VT, USA). Gen5 software was used to collect and evaluate data.

An array of eight screen-printed carbon electrodes (DRP-8X110) and a boxed connector (DRP-CAST8X) were provided by Dropsens S.L. (Oviedo, Spain). The array consists of 8 carbon working electrodes of 2.5 mm in diameter, each with its own carbon counter electrode and silver reference electrode. Amperometric measurements were performed with a PalmSens potentiostat connected to an 8-channel multiplexer (MUX8) (Houte, The Netherlands). Data were collected and evaluated with PalmSens PC software.

2.3. Raw and heat-treated mussel tissues

AZA-Mus CRM (NRC, Halifax, NS, Canada) prepared from naturally contaminated mussel (*Mytilus edulis*) tissues and AZA-contaminated raw mussel samples (*M.*

edulis) from the routine monitoring program in Ireland, were selected for analysis. Zero-Mus CRM (*M. edulis*) (NRC, Halifax, NS, Canada) was used to evaluate matrix effects.

Mussels were shucked and homogenised with an Ultra Turrax homogenizer. A three-step extraction with MeOH (10 mL) was performed on AZA-Mus and Zero-Mus homogenised tissues (1 g) according to Gerssen et al. [29], using a protocol that was intra-laboratory validated by García-Altares et al. [30]. A vortex-mixer MS2 Minishaker (IKA Labortechnik, Staufen, Germany) and a centrifuge Jouan MR 23i (Thermo Fisher Scientific Inc., Waltham, MA, USA) were used. Crude extracts were filtered through polytetrafluoroethylene (PTFE) 0.2-µm membrane syringe filters. Thus, AZA-Mus and Zero-Mus extracts at a matrix concentration of 100 mg/mL were obtained.

Extraction of the Irish AZA-contaminated raw mussel samples was performed by a two-step extraction with MeOH (25 mL) as follows. Homogenised tissue samples were weighed (2 g) into 50-mL centrifuge tubes and extracted by vortex mixing for 1 min with 9 mL of MeOH, centrifuged at 3950 *g* (5 min), and the supernatants decanted into 25-mL volumetric flasks. The pellets were further extracted using an Ultra Turrax for 1 min with an additional 9 mL of MeOH, centrifuged at 3950 *g* (5 min), and the supernatants decanted into the same 25-mL volumetric flasks, which were brought to volume with MeOH. A portion (10 mL) of each extract was transferred into sealed centrifuge tubes and placed for 10 min in a water bath heated to 90 °C to decarboxylate carboxylated AZAs [31, 32]. The raw and heat-treated samples were then passed through Whatman 0.2-µm cellulose acetate filters into HPLC vials for analysis. Heated and raw mussel extracts were obtained at a matrix concentration of 80 mg/mL. All samples were stored at -20 °C until analysis.

2.4. Colorimetric immunoassays protocol

Colorimetric immunoassays were carried out on 96-well microtitre plates. Microtitre wells were incubated with 50 µL of 10 µg/mL protein G or 1 µg/mL avidin in 0.1 M carbonate buffer, pH 9.6, for 1 h. The anti-AZA PAb or biotinylated PAb was then immobilised on the protein G or avidin-coated plates, respectively, by the addition of 50 µL of the corresponding antibody dilution (from 1/10000 to 1/80000 for protocol optimisation and 1/40000 for the final competition assay) in PBS–Tween (0.1 M PBS, pH 7.2, with 0.05% v/v Tween–20) for 1 h. Blocking was then carried out using 100 µL of PBS–Tween containing 2% w/v BSA for 1 h. Subsequently, the competition step was performed using 25 µL of AZA-1 standard solutions (from 0.20 µg/L to 100 µg/L) or natural samples at different dilutions in PBS–Tween and 25 µL of different dilutions of AZA–HRP (from 1/800 to 1/3200 for protocol

optimisation and 1/1600 for the final competition assay) for 30 min. Finally, 100 µL of TMB liquid substrate was added, and 10 min later the absorbance was read at 620 nm. After each step, wells were rinsed three times with 100 µL PBS–Tween. During incubations, microtitre plates were placed on a plate shaker. All reactions were carried out at room temperature.

2.5. Electrochemical immunosensors protocol

The immunosensor assay protocols were essentially the same as the colorimetric immunoassays except for adjustments to the volumes for 8-electrode arrays and diffences in the detection step. Volumes of 10 µL were applied to each working electrode (5 µL of standard or sample dilution plus 5 µL of AZA–HRP in the competition step), and the blocking step was performed by immersion of the electrode arrays in PBS–Tween containing 2% w/v BSA. To perform the electrochemical measurement, 10 µL of TMB was added to each electrode and incubated for 10 min and, finally, the TMB reduction current was measured by applying –0.2 V vs. Ag for 0.5 s. After each step, the electrode arrays were rinsed with PBS–Tween and dried. All reactions were carried out at room temperature.

For the regeneration of the electrochemical immunosensors, the electrode arrays were rinsed with PBS–Tween after the electrochemical measurement and immersed in glycine buffer, pH 2.7, for 30 min. The immunosensors were then rinsed again with PBS–Tween and stored at 4 °C until use.

2.6. LC-MS/MS analysis

For LC-MS/MS analysis of AZA analogues, a Waters Acquity UPLC coupled to a Xevo G2-S QToF monitoring in MS^e mode (*m/z* 100–1200) was used with leucine enkephalin as the reference compound. The cone voltage was 40 V, collision energy was 50 V, the cone and desolvation gas flows were set at 100 and 1000 L/h, respectively, and the source temperature was 120 °C. Analytical separation was performed on an Acquity UPLC BEH C18 (50 × 2.1 mm, 1.7 µm) column (Waters). Binary gradient elution was used, with phase A consisting of H_2O and phase B of CH_3CN (95%) in H_2O (both containing 2 mM ammonium formate and 50 mM formic acid). The gradient was from 30–90% B over 5 min at 0.3 mL/min, held for 0.5 min, and returned to the initial conditions and held for 1 min to equilibrate the system. The injection volume was 2 µL and the column and sample temperatures were 25 °C and 6 °C, respectively. AZA-1–3 were quantified relative to CRMs while AZA-4–10 were quantified with RMs [26]. Matrix interferences were assessed using single point matrix matched standards for AZA-1–6 and AZA-8, using a blank *M. edulis*

tissue. An aliquot (2 g) of tissue was extracted as described above, this time making the solution up to a final volume of 20 mL. The matrix-matched standard was prepared by adding 1.25 mL of an AZA-1–6 and AZA-8 stock solution in MeOH to 1 mL of the filtered (Whatmann, 0.2 µm, cellulose acetate filter) blank tissue extract. In parallel, a MeOH standard was prepared by adding 1.25 mL of the same AZA-1–6 and AZA-8 stock solution to 1 mL of MeOH.

2.7. Data analysis

Measurements were performed in triplicate for the colorimetric immunoassays and electrochemical immunosensors and in duplicate for LC-MS/MS analysis. The immunoassay calibration curves were fitted using a sigmoidal logistic four-parameter equation. Linear regression was used to evaluate the correlation between AZA-1 equivalent concentrations in naturally contaminated mussel samples determined with the colorimetric immunoassays or the electrochemical immunosensors and the values obtained from the LC-MS/MS analyses. To evaluate differences between approaches, data were first tested for normality. To compare values from two different groups, the paired *t*-test was used for normally distributed data sets, while Wilcoxon matched-pairs signed-ranks was used for non-normally distributed data. One-way ANOVA was performed to compare the values obtained in the analysis of the mussel samples by the colorimetric immunoassays, electrochemical immunosensors and LC-MS/MS analysis. Differences were considered statistically significant at the 0.05 level. SigmaStat 3.1 was used for statistical analysis.

3. Results and discussion

3.1. Colorimetric immunoassays

Microtitre plates were coated with protein G or avidin by passive adsorption, taking advantage of the hydrophobic interactions and the electrostatic forces generated between the negatively charged proteins and the positively charged microplates in alkaline conditions. The anti-AZA PAb was then immobilised on the coated plates by means of the affinity of the protein G to the Fc region of the antibody or through the strong avidin–biotin interaction following antibody biotinylation (Fig. 1). Both bioaffinity interactions provided the stable immobilisation of the PAb, while retaining its biological activity. However, while the use of protein G favoured the optimum orientation of the antibody to achieve optimal antigen binding without requiring any chemical modification, the avidin–biotin interaction required biotin

labelling of the primary amines of the PAb, typically distributed on the exterior of the entire antibody, which did not ensure the correct orientation of the antibody.

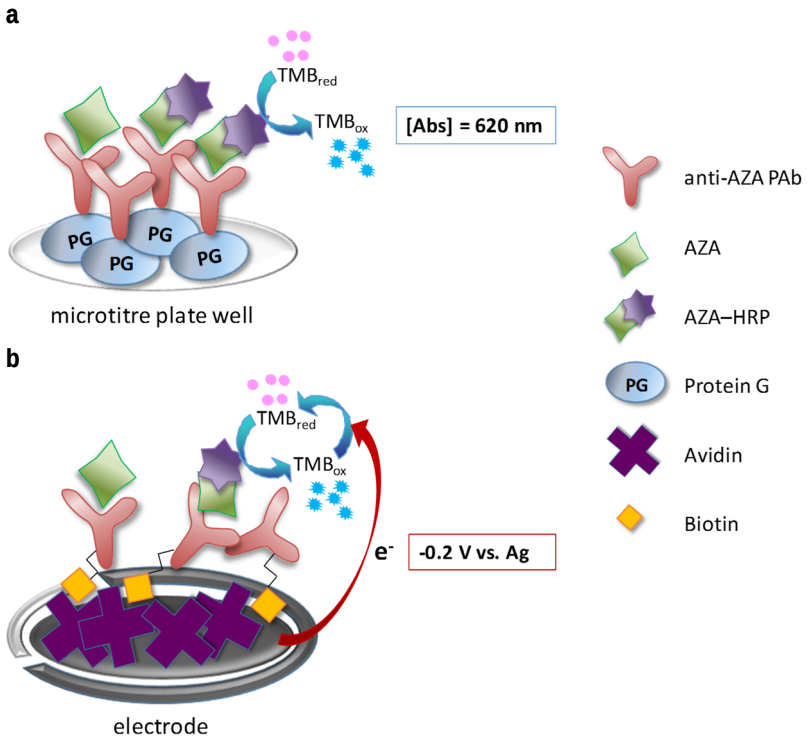

Fig. 1. Schematic representation of the immunoassays and immunosensors configurations achieved by the anti-AZA PAb immobilisation based on **(a)** protein G or **(b)** avidin–biotin affinity interaction on **(a)** microtitre plate wells and **(b)** electrodes, as examples.

Checkerboard titrations and competitive immunoassays were performed to determine if the antibody immobilisation was successful and to establish the optimum PAb and AZA–HRP concentrations. The absorbance values obtained showed expected trends according to antibody and AZA–HRP tracer concentrations. Lo

wer absorbance values were obtained when the antibody was immobilised through the avidin–biotin interaction. Increasing the amount of avidin on the plate did not improve the immobilisation yield of the biotinylated antibody. Nevertheless, the lower absorbance values achieved in this configuration are not unexpected taking

into account the biotinylation yield, which may not reach 100%, the non-optimally oriented immobilisation of the PAb and/or the possibility of biotinylation and immobilisation of other molecules containing primary amines present in the antiserum.

Both immobilisation strategies provided very low non-specific adsorption values of the AZA–HRP. Calibration curves demonstrated competition of free AZA-1 with AZA–HRP for PAb binding. Calibration curves were background-corrected with respect to the controls with no AZA-HRP and fitted to the sigmoidal logistic four-parameter equation:

$$y = y_0 + \frac{a}{1 + (\frac{x}{x_0})^b}$$

where a and y_0 are the asymptotic maximum and minimum values, respectively, x_0 is the x value at the inflection point and b is the slope at the inflection point. Greater sensitivities were achieved with decreasing concentrations of antibody and tracer. Consequently, 1/40000 PAb and 1/1600 AZA–HRP dilutions were selected as a compromise between low antibody/tracer loading and sufficiently high absorbance values. Figure 2 shows the calibration curves for the optimised protein G and avidin-biotin interaction-based immunoassays. In table 1, limits of detection (LODs), established as the 10% inhibition coefficient (IC_{10}) and working ranges (between IC_{20} and IC_{80}) are presented together with the equations and the corresponding R^2 values. Differences between the two approaches were not significant (t=0.292, P=0.774). In comparison with the competitive colorimetric immunoassay previously reported by our group [25], where magnetic beads were used as antibody immobilisation supports, it was possible to use lower antiserum and tracer concentrations, which could explain the lower LODs achieved in these approaches.

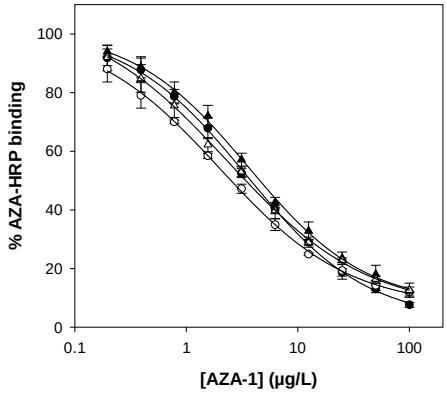

Figure 2. Colorimetric calibration curves for AZA-1 obtained using the protein G-based immunoassay (black) and the avidin–biotin interaction-based immunoassay (white) in buffer (circle) and in 20 mg/mL mussel matrix with 20% MeOH (triangle).

Table 1. Analytical parameters derived from the sigmoidal logistic four-parameter fitting for the Protein G-based and avidin–biotin interaction-based colorimetric immunoassays and electrochemical immunosensors.

		LOD (IC_{10}) (µg/L)	Working range (IC_{20}–IC_{80}) (µg/L)	Equation	R^2
Colorimetric immunoassays	Protein G	0.28	0.70 – 22.74	$y = 2.05 + \frac{99.49}{1 + (\frac{x}{3.47})^{0.81}}$	0.999
	Avidin–biotin	0.14	0.39 – 22.47	$y = 6.78 + \frac{94.67}{1 + (\frac{x}{2.00})^{0.75}}$	1.000
Electrochemical immunosensors	Protein G	0.61	1.25 – 56.81	$y = -10.07 + \frac{132.19}{1 + (\frac{x}{5.41})^{0.52}}$	0.999
	Avidin–biotin	0.37	0.92 – 61.58	$y = -74.38 + \frac{208.61}{1 + (\frac{x}{32.21})^{0.30}}$	0.999

3.2. Study of matrix effects

Prior to the analysis of mussel samples, AZA-1 calibration curves using a blank certified reference mussel tissue matrix (CRM-Zero-Mus) were performed to evaluate matrix effects on the immunoassays. A matrix concentration of 20 mg/mL mussel matrix was chosen according to the protocol for lipophilic toxins extraction in shellfish (100 mg of matrix in 1 mL of MeOH) and its subsequent dilution to 20% v/v MeOH, a percentage that had been previously demonstrated not to interfere with the assay [25]. No significant differences were observed between the calibration curves performed in buffer and in 20 mg/mL mussel matrix with 20% v/v MeOH, neither in the protein G-based immunoassay ($t=0.24$, $P=0.81$) nor in the immunoassay based on the avidin–biotin interaction ($t=0.32$, $P=0.77$) (Figure 2). Consequently, considering a 20 mg/mL matrix loading, effective LODs of 14 ± 1 µg AZA-1 equiv./kg and 7 ± 2 µg AZA-1 equiv./kg were achieved for the immunoassays developed by means of protein G and avidin–biotin immobilisation, respectively. Both immunoapproaches provided a broad working range, from 35 ± 5 µg AZA-1 equiv./kg to 1137 ± 150 µg AZA-1 equiv./kg in the case of the protein G-based immunoassay and from 20 ± 3 µg AZA-1 equiv./kg to 1124 ± 118 in the case of the immunoassay based on the avidin–biotin interaction. Considering the EC regulatory limit for AZAs of 160 µg/kg, the immunoassays enabled the quantification of mussel samples from far below to far above the regulatory limit without requiring additional sample dilutions.

3.3. Electrochemical immunosensors

After protocol optimisation using the colorimetric immunoassays, both strategies were transferred to 8-electrode arrays to develop the corresponding electrochemical immunosensors (Figure 1). Although reagent concentrations were the same as those selected in the colorimetric immunoassays, the use of lower volumes on the screen-printed electrodes required 5-fold lower amounts of protein G, avidin, anti-AZA PAb and tracer, which represents a substantial economic improvement. After background correction with respect to the controls with no AZA-HRP and fitting the calibration curves to the sigmoidal logistic four-parameter equation, Protein G and avidin–biotin interaction-based immunosensors provided similar analytical performances ($t=0.10$, $P=0.92$) (Table 1, Figure 3). This work presents the first immunosensors for AZAs reported to date, providing user-friendly and compact tools that favour operation with low sample volumes and the performance of multiple measurements in a short time.

Considering a 5-fold sample dilution to 20 mg/mL mussel matrix, as in the colorimetric assays, effective working ranges between 63 ± 3 and 2841 ± 247 µg

AZA-1 equiv./kg for the protein G-based immunosensor and between 46 ± 2 and 3079 ± 358 µg AZA-1 equiv./kg for the avidin–biotin interaction-based immunosensor were calculated, again providing a broad working range that included the EC permitted threshold value.

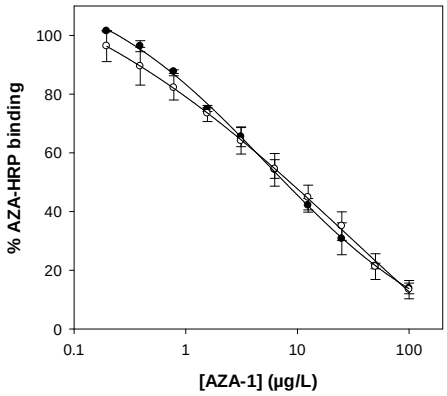

Figure 3. Electrochemical calibration curves for AZA-1 obtained using the protein G-based immunosensor (black) and the avidin–biotin interaction-based immunosensor (white) in buffer.

3.4. Regeneration of the electrochemical immunosensors

Electrochemical immunosensors are commonly developed using disposable screen-printed electrodes due to their low fabrication cost and the possibility of mass production. However, the lack of commercially available anti-AZA antibodies and the time-consuming antibody production process are clear limiting factors in the development of immunosensors for AZAs detection. The feasibility to reuse immunosensors presents expedient advantages regarding these limitations. With this purpose in mind, the possibility to remove the AZAs and the AZA–HRP bound to the PAb, once the competition assay had been performed, while retaining the PAb immobilisation on the electrode surface and its functionality was evaluated.

Antibody-antigen interaction usually occurs at physiological pH and ionic strength, such as in PBS, and can be disrupted by simply raising or lowering the pH or altering the ionic state, ideally releasing the antibody or antigen without irreversibly denaturing or inactivating them. Thus, when immunosensors containing AZA–HRP were immersed in glycine buffer, pH 2.7, for 30 min, only background currents were observed after TMB incubation, indicative of complete AZA–HRP elution from the electrode. A subsequent incubation with AZA–HRP resulted in a response of ~25%

in the protein G-based functionalised electrodes, and a response of ~100% in the avidin–biotin configuration. This 100% response demonstrates that the biotinylated antibody was retained on the avidin-coated electrode retaining its functionality, while the 25% response observed in the protein G approach suggests partial co-elution of the antibody during the elution step in this specific configuration. Responses close to 100% following AZA-HRP incubation were maintained after the regeneration of the functionalised electrodes through the avidin–biotin interaction for 6 consecutive times on 3 different days (Figure 4). These results demonstrate the reusability of the avidin–biotin interaction-based immunosensors and also highlight the storage stability of the immunosensors for at least 3 days. The possibility to reuse and store the immunosensors until use avoids the immobilisation of additional anti-AZA PAb amounts on the electrode surface, as well as simplifies and shortens the protocol assay.

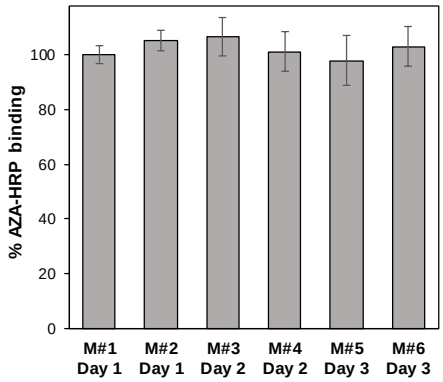

Figure 4. Electrochemical responses of the avidin–biotin interaction-based immunosensors achieved after surface regeneration for 6 consecutive measurements (M#1–M#6) on 3 different days.

3.5. AZAs detection in mussel samples

To demonstrate the applicability of the electrochemical immunosensors as well as the colorimetric immunoassays to the determination of AZAs in shellfish, naturally contaminated mussel (*M. edulis*) samples were analysed using the different approaches.

First, AZAs in a CRM containing AZA-1–3 (certified concentrations) and other analogues (AZA-4–10) (non-certified concentrations) were determined by the protein G and avidin–biotin interaction-based colorimetric immunoassays and electrochemical immunosensors (Table 2). The immunoapproaches provided a

global quantification relative to AZA-1, which was compared with the sum of all different analogues concentrations provided by the NRC. Correlations of 153.4 % and 152.7 % were achieved between the quantifications provided by the protein G and avidin-biotin interaction-based colorimetric immunoassays, respectively, and NRC values. Similar correlations were also obtained in the quantifications provided by the protein G (153.6 %) and avidin-biotin (154.8 %) electrochemical immunosensors. These percentages higher than 100% are not surprising taking into account the different recognition principles between analytical methods. While NRC values are obtained by physicochemical approaches, the immunoapproaches provide responses based on the structural recognition of the toxins by the antibody, which can differ between analogues and the assay configuration [25]. Consequently, the application of cross-reactivity factors (CRFs) to each individual AZA analogue concentration can contribute to better understand the correlation between the different analytical methods. Thus, CRFs that had been previously established in the magnetic bead-based immunoassay [25] –where the same PAb and a similar immunological approach were used– were applied to the individual AZA analogue concentrations provided by the NRC. Following the application of the corresponding CRFs to the certified values, correlations of 101.7% and 101.3% were achieved between the quantifications provided by the protein G and avidin–biotin interaction-based colorimetric immunoassays, respectively, and NRC values. Excellent correlations of 101.9 % and 102.7 % were also obtained in the quantifications provided by the protein G and avidin–biotin electrochemical immunosensors. The obtained results suggest that the PAb recognise all AZA analogues with the same cross-reactivity as in the magnetic bead-based immunoassay and highlight the potential application of all the developed immunoapproaches to the determination of AZAs in mussel samples.

In Ireland, AZAs have been detected in shellfish above the regulatory limit almost every year since the Irish monitoring program was established in 2001 [33]. Raw mussel samples (n=16) from this routine monitoring program containing a wide range of AZAs concentrations were selected for their quantification. From these 16 naturally contaminated samples, 11 had been previously analysed by the magnetic bead-based immunoassay [25]. Five additional mussel samples containing AZA-1, AZA-2 and AZA-3 levels below the established 160 µg equiv./kg regulatory limit were included in the analysis to ensure that the developed immunoassays and immunosensors were able to provide reliable AZA quantifications at low concentrations (Table 1). No differences were observed between the quantifications provided by the protein G and avidin-biotin interaction-based colorimetric immunoassays and electrochemical immunosensors (P=1.00), regardless of whether the values were below (P=0.851) or above (P=0.953) the

regulatory level. Standard deviations lower than 10% were obtained for all samples using both approaches.

Since the PAb used in the development of the immunoapproaches was able to recognise AZA carboxy cogeneres in addition to other AZA analogues, the raw mussel samples analysed were heated to perform LC-MS/MS analysis. Heating catalyses the decarboxylation of AZA carboxy congeners (e.g., AZA-17, AZA-19, AZA-21 and AZA-23) that may be present in the samples to AZA-3, AZA-6, AZA-4 and AZA-9 respectively [31, 32]. AZA quantifications provided by the protein G-based colorimetric immunoassay (y = 1.489 x + 42, R^2 = 0.981) and electrochemical immunosensor (y = 1.604 x + 7, R^2 = 0.990) correlated with those obtained by LC-MS/MS analysis ($p < 0.0001$). The immunoassay (y = 1.574 x + 18, R^2 = 0.990) and the immunosensor (y = 1.582 x + 21, R^2 = 0.977) developed through the avidin–biotin interaction also provided AZA quantifications in correlation with those achieved by the reference method ($p < 0.0001$) (Table 1, Figure 5). Without the application of the CRFs, the trend observed in the analysis of the mussel samples from the Irish monitoring program was similar to the trend obtained in the analysis of the CRM, being the quantifications achieved by the immunoapproaches ~1.5-fold those obtained with the reference method. Following the application of the corresponding CRFs to the individual contents determined by LC-MS/MS, AZA quantifications provided by the protein G-based immunoassay (y = 0.965 x + 14, R^2 = 0.999) and immunosensor (y = 1.035 x - 19, R^2 = 0.999) and the avidin–biotin interaction-based immunoassay (y = 1.016 x - 6, R^2 = 0.998) and immunosensor (y = 1.029 x - 10, R^2 = 0.999) were in excellent agreement with LC-MS/MS values (Table 2, Figure 5), with no significant differences observed between the quantifications achieved by any of the immunoapproaches and LC-MS/MS analysis (P = 1.000).

All these results indicate without doubt that the developed immunoassays and immunosensors are reliable tools for the screening and quantification of AZAs, facilitating not only the detection of all the regulated AZAs below the regulatory limit, but also other toxic analogues in a simple, rapid and cost-effective manner.

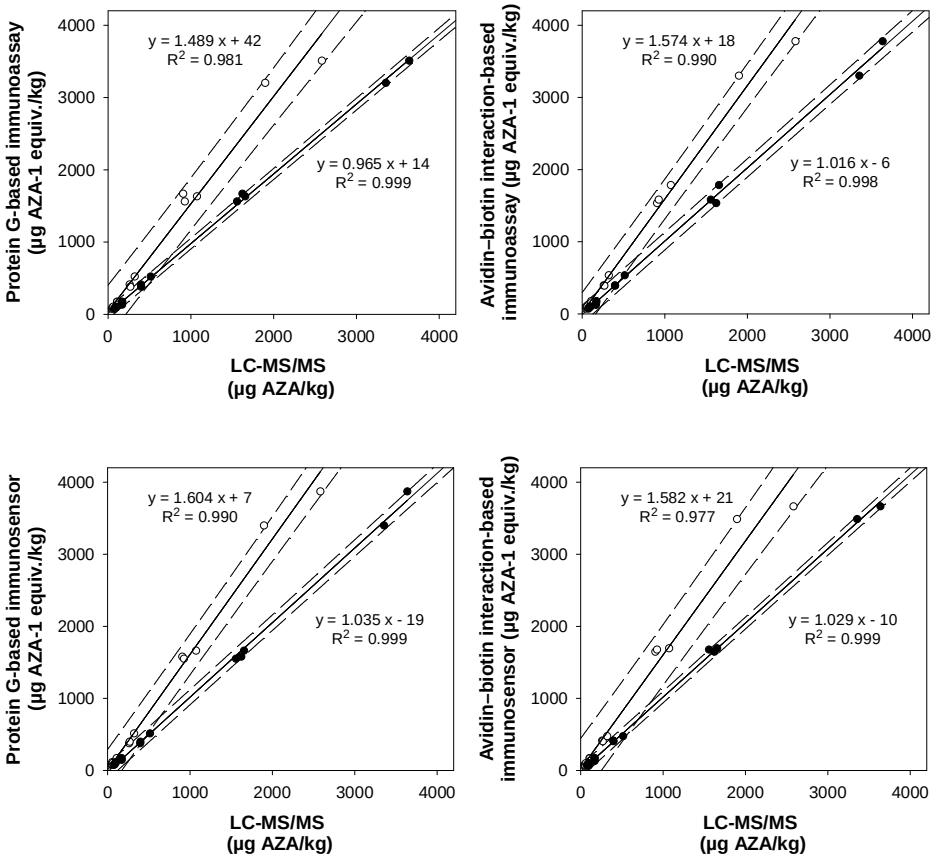

Figure 5. Linear regressions for the correlations between sample quantifications by the colorimetric immunoassays or electrochemical immunosensors and the sum of AZA-1–10 analogues determined by LC-MS/MS analysis, before (white) and after (black) the application of the cross-reactivity factors (CRFs). Dashed lines represent the prediction intervals of 95 %.

Table 2. AZA concentrations (µg AZA/kg mussel) of a mussel certified reference material (CRM) and 16 naturally contaminated mussel tissues from the routine monitoring program in Ireland by LC-MS/MS, the colorimetric immunoassays and the electrochemical immunosensors.

Samples	**LC-MS/MS**												**Colorimetric immunoasays**		**Electrochemical immunosensors**	
	AZA-1	AZA-2	AZA-3	AZA-4	AZA-5	AZA-6	AZA-7	AZA-8	AZA-9	AZA-10	*∑ AZAs*	*AZA-1 equiv. (∑ AZAs applying CRFs)**	**Protein G** *AZA-1 equiv.*	**Avidin-biotin** *AZA-1 equiv.*	**Protein G** *AZA-1 equiv.*	**Avidin-biotin** *AZA-1 equiv.*
CRM	1160	273	211	170	40	90	20	30	40	20	2054	3096	3150	3137	3155	3180
Monitoring																
S#1	24	5	15	nd	nd	3	nd	nd	nd	nd	47	77	77	82	79	66
S#2	22	8	15	nd	nd	3	nd	nd	nd	nd	48	77	79	73	80	76
S#3	28	8	17	nd	nd	2	nd	nd	nd	nd	55	86	94	89	82	86
S#4	21	8	23	nd	nd	3	nd	nd	nd	nd	55	98	95	97	113	65
S#5	33	10	19	nd	nd	2	nd	nd	nd	nd	64	98	105	103	104	100
S#6	49	19	31	nd	1	7	nd	2	nd	nd	109	172	174	177	146	171
S#7	55	19	29	1	1	4	nd	nd	nd	nd	109	165	171	124	159	165
S#8	53	20	31	1	2	4	nd	nd	nd	nd	111	170	133	158	171	130
S#9	128	45	66	3	4	10	nd	5	nd	nd	261	396	412	394	376	414
S#10	148	35	55	3	6	16	nd	1	1	3	268	399	381	391	398	404
S#11	144	59	80	13	5	12	nd	6	1	2	322	515	523	535	513	475
S#12	370	125	216	81	23	44	2	21	19	6	907	1623	1667	1534	1577	1646
S#13	425	139	189	77	17	35	4	21	16	4	927	1558	1561	1582	1550	1676
S#14	573	164	174	71	13	37	2	20	17	3	1074	1656	1631	1784	1661	1694
S#15	798	258	480	142	32	101	2	46	32	7	1898	3356	3202	3301	3399	3488
S#16	1524	414	309	132	33	64	10	49	38	9	2582	3639	3509	3778	3872	3664

*Applied CRFs are: AZA-1 = 1; AZA-2 = 0.76; AZA-3 = 2.73; AZA-4 = 3.83; AZA-5 = 1.39; AZA-6 = 2.70; AZA-7 = 2.00; AZA-8 = 1.85; AZA-9 = 2.69; AZA-10 = 2.17 [25].

4. Conclusions

The immobilisation of the anti-AZA PAb on protein G or avidin-coated supports via bioaffinity interactions has been used to develop immunoassays and immunosensors with excellent analytical performance, thanks to a controlled and stable antibody immobilisation. All approaches showed a broad working range that enabled the quantification of the current regulated AZAs below the regulatory threshold, but also a broad range of other toxic AZA analogues. No matrix effects were observed and no evaporation of the sample extracts was required, resulting in accurate quantifications with simple and rapid protocols. Although both colorimetric immunoassays and electrochemical immunosensors have been demonstrated to be powerful analytical methods for the reliable determination of AZAs, electrochemical immunosensors provide compact and miniaturised devices that pave the way towards the development of portable tools for *in situ* measurements. Moreover, the possibility to use lower amounts of immunoreagents, as well as the feasibility to reuse the avidin-biotin interaction-based immunosensors provide clear advantages in terms of sustainability and cost-effectiveness.

The good results obtained in the analysis of a considerable amount of naturally contaminated mussel samples evidence that electrochemical immunosensors for the detection of AZAs can be effectively implemented as screening tools in routine monitoring programs, as they provide easy-to-handle, rapid and low-cost high-throughput systems for the specific detection of AZAs in complex matrices. For their practical application in current monitoring programs, it is important to keep in mind that the regulatory limit of 160 µg AZA-1 equiv./kg shellfish established by the European Commission only considers AZA-1–3 (including their toxic potential). As a consequence, in samples where more than these three analogues are present, immunoapproaches could provide results that may lead to a closure of a shellfish harvesting area, while LC-MS/MS analysis could not. This fact is not detrimental for immunoapproaches, but helps to better protect consumer health. Taking this in mind, we propose to establish a “positive”, “negative” but also a “suspicious” range to classify samples according to their AZA content. In the case of a “positive” result, a preventive closure of the shellfish harvesting area will be recommended to protect the consumer health and the sample will be analysed by LC-MS/MS to confirm the result. In the case of a “suspicious” sample, analysis by LC-MS/MS will help to determine the decision to undertake. By combining screening and confirmatory methods a faster and cost-effective system for marine toxin control in shellfish will be clearly achieved.

Acknowledgments

The research leading to these results has received funding under the *Sea Change* strategy with the support of the Marine Institute and the Marine Research Sub-Programme of the National Development Plan 2007–2013, co-financed under the European Regional Development Fund (ASTOX 2, (PBA/AF/08/001(01)). The publication reflects the views only of the author, and the European Union cannot be held responsible for any use that may be made of the information contained therein. The authors acknowledge financial support from CERCA Programme / Generalitat de Catalunya and Laura Ibañez for her help in the experimental work. Sandra Leonardo acknowledges scholarship from IRTA-Universitat Rovira i Virgili-Banco Santander (2013PIPF URV-IRTA-BS-01).

References

[1] T. McMahon, J. Silke, Winter toxicity of unknown aetiology in mussels, Harmful Algae News, 14(1996).

[2] V.L. Trainer, L. Moore, B.D. Bill, N.G. Adams, N. Harrington, J. Borchert, et al., Diarrhetic shellfish toxins and other lipophilic toxins of human health concern in Washington State, Marine Drugs, 11(2013) 1815-35.

[3] J. Yao, Z. Tan, D. Zhou, M. Guo, L. Xing, S. Yang, Determination of azaspiracid-1 in shellfishes by liquid chromatography with tandem mass spectrometry, Chinese journal of chromatography, 28(2010) 363-7.

[4] R. Ueoka, A. Ito, M. Izumikawa, S. Maeda, M. Takagi, K. Shin-Ya, et al., Isolation of azaspiracid-2 from a marine sponge *Echinoclathria* sp as a potent cytotoxin, Toxicon, 53(2009) 680-4.

[5] G. Alvarez, E. Uribe, P. Avalos, C. Marino, J. Blanco, First identification of azaspiracid and spirolides in *Mesodesma donacium* and *Mulinia edulis* from Northern Chile, Toxicon, 55(2010) 638-41.

[6] A. Lopez-Rivera, K. O'Callaghan, M. Moriarty, D. O'Driscoll, B. Hamilton, M. Lehane, et al., First evidence of azaspiracids (AZAs): A family of lipophilic polyether marine toxins in scallops (*Argopecten purpuratus*) and mussels (*Mytilus chilensis*) collected in two regions of Chile, Toxicon, 55(2010) 692-701.

[7] A.D. Turner, A.B. Goya, Occurrence and profiles of lipophilic toxins in shellfish harvested from Argentina, Toxicon, 102(2015) 32-42.

[8] K.J. James, A. Furey, M. Lehane, H. Ramstad, T. Aune, P. Hovgaard, et al., First evidence of an extensive northern European distribution of azaspiracid poisoning (AZP) toxins in shellfish, Toxicon, 40(2002) 909-15.

[9] T. Torgensen, N.B. Bremnes, T. Rundberget, T. Aune, Structural confirmation and occurrence of azaspiracids in Scandinavian brown crabs (*Cancer pagurus*), Toxicon, 51(2008) 93-101.

[10] B. Krock, U. Tillmann, T.J. Alpermann, D. Voss, O. Zielinski, A.D. Cembella, Phycotoxin composition and distribution in plankton fractions from the German Bight and western Danish coast, Journal of Plankton Research, 35(2013) 1093-108.

[11] Z. Amzil, M. Sibat, F. Royer, V. Savar, First report on azaspiracid and yessotoxin groups detection in French shellfish, Toxicon, 52(2008) 39-48.

[12] P. Vale, R. Bire, P. Hess, Confirmation by LC-MS/MS of azaspiracids in shellfish from the Portuguese north-western coast, Toxicon, 51(2008) 1449-56.

[13] A.B. Magdalena, M. Lehane, S. Krys, M.L. Fernandez, A. Furey, K.J. James, The first identification of azaspiracids in shellfish from France and Spain, Toxicon, 42(2003) 105-8.

[14] U. Tillmann, D. Jaen, L. Fernandez, M. Gottschling, M. Witt, J. Blanco, et al., *Amphidoma languida* (Amphidomatacea, Dinophyceae) with a novel azaspiracid toxin profile identified as the cause of molluscan contamination at the Atlantic coast of southern Spain, Harmful Algae, 62(2017) 113-26.

[15] J. Blanco, F. Arevalo, A. Morono, J. Correa, S. Muniz, C. Marino, et al., Presence of azaspiracids in bivalve molluscs from Northern Spain, Toxicon, 137(2017) 135-43.

[16] H. Taleb, P. Vale, R. Amanhir, A. Benhadouch, R. Sagou, A. Chafik, First detection of azaspiracids in mussels in north west Africa, Journal of Shellfish Research, 25(2006) 1067-70.

[17] R. Rossi, C. Dell'Aversano, B. Kcrock, P. Ciminiello, I. Percopo, U. Tillmann, et al., Mediterranean *Azadinium dexteroporum* (Dinophyceae) produces six novel azaspiracids and azaspiracid-35: a structural study by a multiplatform mass spectrometry approach, Analytical and Bioanalytical Chemistry, 409(2017) 1121-34.

[18] P. Hess, P. McCarron, B. Krock, J. Kilcoyne, C.O. Miles, Azaspiracids: chemistry, biosynthesis, metabolism, and detection, in: L.M. Botana (Ed.), Seafood and Freshwater Toxins. Pharmacology, Physiology, and Detection. CRC Press, Boca Ratom, FL, USA, 2014, pp. 799-822.

[19] European Commission Regulation (EC) No 853/2004 of 29 april 2004 laying down specific hygiene rules for food of animal origin, Official Journal of the European Union L139, 55-205.

[20] S. Leonardo, A. Toldrà, M. Campàs, Trends and prospects on electrochemical biosensors for the detection of marine toxins, in: J. Diogène, M. Campas (Eds.), Recent Advances in the Analysis of Marine Toxins, Comprehensive Analytical Chemistry, 78, 2017, pp. 303-341 .

[21] M.O. Frederick, S.D.L. Marin, K.D. Janda, K.C. Nicolaou, T.J. Dickerson, Monoclonal antibodies with orthogonal azaspiracid epitopes, Chembiochem, 10(2009) 1625-9.

[22] C.J. Forsyth, J. Xu, S.T. Nguyen, I.A. Samdal, L.R. Briggs, T. Rundberget, et al., Antibodies with broad specificity to azaspiracids by use of synthetic haptens, Journal of the American Chemical Society, 128(2006) 15114-6.

[23] L.P. Rodriguez, N. Vilarino, M. Carmen Louzao, T.J. Dickerson, K.C. Nicolaou, M.O. Frederick, et al., Microsphere-based immunoassay for the detection of azaspiracids, Analytical Biochemistry, 447(2014) 58-63.

[24] I.A. Samdal, K.E. Lovberg, L.R. Briggs, J. Kilcoyne, J. Xu, C.J. Forsyth, et al., Development of an ELISA for the Detection of Azaspiracids, Journal of Agricultural and Food Chemistry, 63(2015) 7855-61.

[25] S. Leonardo, M. Rambla-Alegre, I.A. Samdal, C.O. Miles, J. Kilcoyne, J. Diogène, et al., Immunorecognition magnetic supports for the development of an electrochemical immunoassay for azaspiracid detection in mussels, Biosensors & Bioelectronics, 92(2017) 200-6.

[26] J. Kilcoyne, M.J. Twiner, P. McCarron, S. Crain, S.D. Giddings, B. Foley, et al., Structure elucidation, relative LC-MS response and in vitro toxicity of azaspiracids 7-10 isolated from mussels (*Mytilus edulis*), Journal of Agricultural and Food Chemistry, 63(2015) 5083-91.

[27] J. Kilcoyne, A. Keogh, G. Clancy, P. LeBlanc, I. Burton, M.A. Quilliam, et al., Improved isolation procedure for azaspiracids from shellfish, structural elucidation of azaspiracid-6, and stability studies, Journal of Agricultural and Food Chemistry, 60(2012) 2447-55.

[28] G.T. Hermanson, Bioconjugate Techniques, Academic Press, London, 2008.

[29] A. Gerssen, P.P.J. Mulder, M.A. McElhinney, J. de Boer, Liquid chromatography-tandem mass spectrometry method for the detection of marine lipophilic toxins under alkaline conditions, Journal of Chromatography A, 1216(2009) 1421-30.

[30] M. Garcia-Altares, J. Diogene, P. de la Iglesia, The implementation of liquid chromatography tandem mass spectrometry for the official control of lipophilic toxins in seafood: Single-laboratory validation under four chromatographic conditions, Journal of Chromatography A, 1275(2013) 48-60.

[31] P. McCarron, J. Kilcoyne, C.O. Miles, P. Hess, Formation of azaspiracids-3,-4,-6, and-9 via decarboxylation of carboxyazaspiracid metabolites from shellfish, Journal of Agricultural and Food Chemistry, 57(2009) 160-9.

[32] J. Kilcoyne, P. McCarron, P. Hess, C.O. Miles, Effects of heating on proportions of azaspiracids 1-10 in mussels (*Mytilus edulis*) and identification of carboxylated precursors for azaspiracids 5, 10, 13, and 15, Journal of Agricultural and Food Chemistry, 63(2015) 10980-7.

[33] Marine Institute Ireland, Latest shellfish safety data. http://www.marine.ie/Home/site-area/data-services/interactive-maps/latest-shellfish-safety-data/, 2017 (accessed 17.11.17).

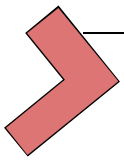

CHAPTER 5

Enzyme biosensors for the detection of biogenic amines

Electrochemical enzyme sensor arrays for the detection of the biogenic amines histamine, putrescine and cadaverine using magnetic beads as immobilisation supports

Sandra Leonardo, Mònica Campàs

IRTA, Carretera de Poble Nou, km 5.5, 43540 Sant Carles de la Ràpita, Spain

Abstract

Electrochemical biosensors based on diamine oxidase (DAO) conjugated to magnetic beads (MBs) are developed for the detection of histamine (Hist), putrescine (Put) and cadaverine (Cad), the most relevant biogenic amines (BAs) related to food safety and quality. DAO-MBs are immobilised on Co(II)-phthalocyanine/carbon and Prussian Blue/carbon electrodes to obtain mono-enzymatic biosensors and on Os-wired HRP-modified carbon electrodes for the development of bi-enzymatic biosensors. The three approaches present a low working potential (+0.4 V, -0.1 V and -0.05 V *vs* Ag, respectively), a linear range of two orders of magnitude (from 0.01 to 1 mM BA), good reproducibility (biosensor variability lower than 10%), high repeatability (up to 8 consecutive measurements), limits of detection in the micromolar range for Hist and in the sub-micromolar range for Put and Cad, and no response from possible interfering compounds. Moreover, DAO-MB conjugates display excellent long-term stability (at least 3 months). The DAO-MB biosensor has been applied to the determination of BAs in spiked and naturally spoiled fish, demonstrating its suitability both as screening tool and for BAs quantification. The use of MBs as supports for enzyme immobilisation is advantageous because the resulting biosensors are simple, fast, stable, affordable, and can be integrated into array platforms. This makes them suitable for high-throughput analysis of BAs in the food industry.

1. Introduction

Biogenic amines (BAs) are low-molecular-weight organic bases mainly produced by microbial decarboxylation of amino acids. BAs may be found in variety of foods, such as fish, meat, cheese, vegetables and wines, as a consequence of inappropriate

processing and storage conditions and subsequent microbial contamination [1, 2]. The most important BAs related with spoilage in food are histamine (Hist), putrescine (Put) and cadaverine (Cad), which can be considered appropriate food freshness indicators. Among them, Hist is considered one of the most relevant due to its biological toxicity, whose harmful effect is enhanced in the presence of Put and Cad, which inhibit the intestinal histamine-metabolizing enzymes [3]. The European Regulation establishes Hist limits of 100 mg/kg (average) and 200 mg/kg (individual) in fishery products from fish species associated with high histidine amounts, while for products which have undergone enzyme maturation treatment in brine, the afore mentioned limits rise to 200 and 400 mg/kg [4]. Nowadays, chromatographic techniques coupled to different instrumentation for the detection are the most commonly used analytical methods for the detection of BAs [5]. However, alternative methods are needed to achieve rapid, accurate, reproducible and low-cost detection. In this direction, some electrochemical biosensors have been reported for BAs detection. Most of them are based on the reaction between amine oxidases and BAs, which generates NH_3 and H_2O_2, the later being subsequently monitored directly, through redox mediators or combined with HRP in order to lower the applied potentials and increase the selectivity of the biosensor.

Regarding enzyme immobilisation, it is well-known that this step is crucial in the development of biosensors. In most of the reported biosensors, amine oxidases have been immobilised directly on electrodes by adsorption, cross-linking [6-10] and/or entrapment into gels, polymers or membranes [11-17]. These methods are simple but, depending on the immobilisation strategy, they may suffer from enzyme leakage, enzyme inactivation or diffusion limitations. Over the last few years, micro/nanomaterials have begun to be explored as biomolecule supports, with the aim to provide advantages in terms of larger electroactive surface area, promoted electron transfer, enhanced electrochemical signals and lower limits of detection (LODs) [18-20]. However, the method used for the immobilisation of the micro/nanomaterial on the electrode certainly plays an important role in the biosensor performance, and techniques such as adsorption or entrapment may also compromise the biosensor performance. The use of magnetic beads (MBs) with diameters in the micro/nanometer range as biomolecule supports allows a stable immobilisation by simply applying a magnetic field, while presenting a large surface area available for biomolecule immobilisation, the possibility to regenerate the electrode surface or the easy integration into microfluidic devices. The combination of functionalised MBs with electrochemical detection constitutes a powerful and efficient strategy for the development of biosensors [21-23]. However, most MB-based electrochemical biosensors reported up to date are based on antibodies or

DNA probes and the use of MBs as enzyme immobilisation supports has been much less explored and still presents some challenges [24].

In this work, diamine oxidase (DAO) has been conjugated to MBs and immobilised on electrodes for the development of electrochemical biosensors for the detection of Hist, Put and Cad. After optimisation of the experimental parameters, the analytical performance of the DAO-MB biosensors has been evaluated. The high storage stability of the conjugates and the possibility to transfer them to multiplexed systems has been demonstrated. The DAO-MB biosensors have been applied to the determination of BAs contents in spiked and naturally spoiled fish samples, demonstrating their promising use as a simple, stable, easy-to-use and inexpensive tool for high-throughput bioanalysis of BAs in routine food industry monitoring programs.

2. Experimental

2.1. Reagents and materials

Diamine oxidase (DAO) from plant (120 U/mL) was supplied by MoLiRom (Roma, Italy, www.molirom.com). Peroxidase from horseradish Type XII (HRP) (250-330 U/mg) was obtained from Sigma-Aldrich (Tres Cantos, Spain, www.sigmaaldrich.com). Horseradish Peroxidase wired with Os-PVP redox polymer (Os-wired HRP) was purchased from from Bioanalytical Systems, Inc. (West Lafayette, USA, www.basinc.com). Dynabeads® M-270 Carboxylic Acid (2 x 10^9 beads/mL) were obtained from Invitrogen by Life Technologies, S.A. (Alcobendas, Spain, www.thermofisher.com).

Histamine dihydrochloride (Hist), putrescine dihydrochloride (Put), cadaverine dihydrochloride (Cad), dopamine hydrochloride (DA), tyramine hydrochloride (TA), L-histidine (His), L-lysine (Lys), L-arginine (Arg), L-tyrosine (Tyr), DL-tryptophan (Trp), hydrogen peroxide 30% solution (H_2O_2), N-(3-dimethylaminopropyl)-N'-ethylcarbodiimide hydrochloride (EDC), N-hydroxysuccinimide (NHS), N-methylphenazonium methyl sulphate (MPMS), 2-(N-morpholino)ethanesulfonic acid hydrate (MES), *o*-dianisidine dihydrochloride (ODA), potassium phosphate monobasic and potassium chloride were supplied by Sigma-Aldrich (Tres Cantos, Spain, www.sigmaaldrich.com). All solutions were prepared using Milli-Q water (Millipore, Bedford, USA, www.merckmillipore.com).

Screen-printed electrodes (carbon DRP-110, single-walled carbon nanotubes/carbon DRP-110SWCNT, graphene/carbon DRP-110GPH, Co-phthalocyanine/carbon DRP-410, Prussian Blue/carbon DRP-710, gold DRP-220AT and an array of eight carbon electrodes DRP-8X110), boxed connectors (DRP-DSC

and DRP-CAST8X) and magnetic supports (DRP-MAGNET and DRP-MAGNET8X) were provided by Dropsens S.L. (Oviedo, Spain, www.dropsens.com). Individual screen-printed carbon electrodes consist of a carbon working electrode (some electrodes are modified with electrochemical mediators or nanomaterials) of 4 mm in diameter, a carbon counter electrode and a silver reference electrode. Individual screen-printed gold electrodes consist of a gold working electrode of 4 mm in diameter, a gold counter electrode and a silver reference electrode. The array consists of 8 carbon working electrodes of 2.5 mm in diameter, each one with its carbon counter electrode and silver reference electrode.

2.2. Conjugation of DAO to MBs

A HulaMixer® Sample Mixer from Invitrogen (Leek, The Netherlands, www.thermofisher.com) was used in the conjugation of DAO to carboxylic acid-modified MBs. Magnetic separation was performed using a Z5342 MagneSphere® Technology Magnetic Separation Stand (for 12 1.5-mL tubes) from Promega (Madrid, Spain, www.promega.com). The protocol was as follows: (1) 100 µL of MB suspension were added to a 1.5-mL tube and washed twice with 100 µL of 25 mM MES, pH 5, for 10 min with vigorous mixing; for the washing steps, the tube was placed on the magnetic separation stand and the washing solutions were removed; (2) 50 µL of 50 mg/mL EDC solution and 50 µL of 50 mg/mL NHS solution (prepared immediately before use in cold 25 mM MES), pH 5.0, were added and incubated for 30 min with slow tilt rotation; (3) the activated MBs were washed twice with 25 mM MES, pH 5.0; (4) 200 µL of DAO (from 1/8 to 1/256 dilution) in 25 mM MES, pH 5.0, were added and incubated for 1 hour with slow tilt rotation; (5) the DAO-MB conjugates were washed three times with 0.1 M potassium phosphate buffer, pH 7.2. All steps were performed at room temperature. For higher MB amounts, volumes were adjusted proportionally.

2.3. Biosensor preparation

10 µL of DAO-MB suspension were placed on Co(II)-phthalocyanine/carbon, Prussian Blue/carbon or Os-wired HRP-modified carbon working electrodes, where modified MBs were trapped with a magnetic support at the back side. The supernatant was then removed. Os-wired HRP-modified carbon electrodes were previously obtained by placing 1 µL of Os-wired HRP stock solution on the DRP-110 working electrode and allowing to dry for 30 min.

DRP-8X110 electrodes were used for multiple analysis (eight samples). In this case, 5 µL of a 1/10 Os-wired HRP dilution from stock solution were placed on each

working electrode and allowed to dry for 30 min. Then, 5 µL of DAO-MB suspension were placed on the working electrodes, modified MBs were trapped with a magnetic support and the supernatant was removed.

2. 4. Storage stability of DAO-MB conjugates

A DAO-MB conjugate pool was prepared, and aliquots were stored at 4 °C and -20 °C without and with 10% of glycerol. The initial activity of the conjugates (reference value) and the activity after 1, 2, 7, 15, 30, 60 and 90 days was measured as explained in section 2.6.

2.5. Fish samples and BAs extraction

Sea bass samples were obtained from Alfacs bay in Ebre Delta (NW Mediterranean Sea). Fish samples were first cleaned and eviscerated, cutting thick slices from back of the pectoral fin, halfway and posterior to the vent. Then, they were blended to obtain a homogenous mixture. Samples were stored at 4 °C and at room temperature (25 °C) during 3 days.

For BAs extraction, 2 g of the homogenized sample were vigorously mixed with 4 mL of phosphate buffer, pH 7.2 for 1 min in a vortex. The mixture was then centrifuged at 4 °C for 10 min at 15,000 rpm and the supernatant was recovered. The procedure was repeated and the two extracts were gathered, adjusting the volume to a final concentration of 25 mg/mL with the same buffer.

2.6. Electrochemical protocols

Cyclic voltammetry and amperometric measurements were performed with an AUTOLAB PGSTAT128N potentiostat (Utrecht, The Netherlands, www.metrohm-autolab.com) and a PalmSens potentiostat connected to an 8-channel multiplexer (MUX8) (Houte, The Netherlands, www.palmsens.com). Data were collected and evaluated by General Purpose Electrochemical System (GPES) and PalmSensPC software. Screen-printed electrodes were horizontally-positioned on the magnetic supports. All measurements were performed at room temperature.

Cyclic voltammetry was used to characterise the response of the DAO-modified electrodes towards BAs in mono-enzymatic and bi-enzymatic configurations. The protocol was as follows: 45 µL of 0.1 M potassium phosphate buffer, 0.1 M KCl, pH 7.2, were placed on the electrode and cyclic voltammograms were recorded between -0.2 and +0.8 V *vs.* Ag (potential window depended on the electrode and

electrochemical transduction approach) at 5 mV/s; 5 µL of 10 mM Hist, Put or Cad solution were then added and, after 10 min, a cyclic voltammogram was recorded again. This protocol, using Co(II)-phthalocyanine/carbon electrodes and 50 mM Hist, was applied for the optimisation of the concentration of DAO to use in the conjugation to MBs.

Amperometry was used to construct the calibration curves, to evaluate the storage stability of DAO-MB conjugates and to determine the BAs content in fish samples. The protocol was as follows: 25 µL of 0.1 M potassium phosphate buffer, 0.1 M KCl, pH 7.2 were placed on the electrode and a potential of +0.4 V (*vs.* Ag) for Co(II)-phthalocyanine/carbon electrodes, -0.1 V (*vs.* Ag) for Prussian Blue/carbon electrodes or +0.05 V (*vs.* Ag) for Os-wired HRP-modified carbon electrodes was applied; the current intensity was recorded for 60 s; 50 µL of sample were then added and, after 10 min, the current was recorded again for 120 s. The difference in current intensity between before and after sample addition was measured. Experiments were performed in triplicate (N = 3). For the BA calibration curves, the samples consisted of Hist, Put or Cad solutions at different concentrations ranging from 1 µM to 4 mM and the three type of electrodes were used. In the study of the DAO-MB storage stability, the sample was 10 mM Put and Prussian Blue/carbon electrodes were used. In the analysis of fish samples, the sample was sea bass extract at 25 mg/mL and Prussian Blue/carbon electrodes were also used.

The amperometric multiplexed detection was used to construct a Hist calibration curve and to perform an interferences study. The protocol was similar to the one with individual electrodes, but adjusting the volumes to the smaller area of the working electrodes of the array. In this case, 20 µL of 0.1 M potassium phosphate buffer, 0.1 M KCl, pH 7.2 were placed on the electrodes and a potential of +0.05 V (*vs.* Ag) was applied; the current intensity was recorded for 60 s; 40 µL of sample were added on each electrode and, after 10 min, the current was recorded again for 120 s. The difference in current intensity between before and after sample addition was measured. Experiments were also performed in triplicate (N = 3). For the Hist calibration curve, concentrations ranging from 1 µM to 4 mM Hist were used. In the study of interferences, 1 mM Hist, His, Lys, Arg, Tyr, Trp, DA or TA were used.

All experiments reported were performed using a different electrode for each measurement. However, consecutive measurements were performed with the same electrode to study the repeatability of the DAO-MB biosensors. In this case, Prussian Blue/carbon electrodes were used and the protocol was as follows: 25 µL of 0.1 M potassium phosphate buffer, 0.1 M KCl, pH 7.2 were placed on the biosensor and a potential of -0.1 V was applied. When the current was stabilised, 50 µL of 1mM Hist were added. Once the current was stabilised again, the difference in current intensity between before and after Hist addition was measured. The

supernatant was then removed and the biosensor was washed with 50 µL of 0.1 M potassium phosphate buffer, 0.1 M KCl, pH 7.2. The same protocol was repeated up to 8 consecutive times. Repeatability studies were performed in quadruplicate (N = 4).

2.7. Colorimetric enzyme assay

For the colorimetric enzyme assay, 100 µL of Hist at concentrations ranging from 0.01 to 1 mM or sea bass extracts at 25 mg/mL were added into microtiter wells containing 20 µL of 5 mg/mL *o*-dianisidine, 20 µL of 0.01 mg/mL HRP and 60 µL of 1/100 DAO dilution or 0.1 M potassium phosphate buffer, pH 7.2. After 15 min incubation with gentle shaking at room temperature, absorbance at 440 nm was measured using a Synergy HT microplate reader (Winooski, United States, www.biotek.com). Assays were performed in duplicate (N = 2).

2.8. Statistical analysis

The linear regression model was used to evaluate the correlation between the expected and the determined Hist equivalent contents in spiked fish samples. In the comparison of the analysis of naturally spoiled fish samples by the electrochemical biosensor and the colorimetric assay, data were first tested for normality. Since data were non-normally distributed, the Wilcoxon matched-pairs signed-ranks test was used to evaluate the differences in the Hist equivalent contents determined by the two methods. SigmaStat 3.1 software package was used for the linear regression and the Wilcoxon matched-pairs signed-ranks test. In both analyses, differences in the results were considered statistically significant at the 0.05 level.

3. Results and discussion

3.1. Optimisation of the DAO-MB biosensors

The detection of Hist, Put and Cad was performed following the strategies shown in Schema I. DAO specifically recognises the biogenic amines, oxidising them and producing H_2O_2 in the enzyme reaction. The H_2O_2 is then detected directly on the electrode surface or through redox mediators (mono-enzymatic biosensor) or through reaction with mediated HRP (bi-enzymatic biosensor). An exhaustive comparison of electrode supports and electrochemical transduction strategies for the detection of H_2O_2 was previously performed. Results are presented in the Supplementary Information. Co(II)-phthalocyanine/carbon and Prussian

Blue/carbon electrodes and Os-wired HRP-modified carbon electrodes were selected for the subsequent development of mono-enzymatic and bi-enzymatic biosensors, respectively.

Although HRP is known to have a higher enzyme activity when working at lower pH, potassium phosphate buffer, pH 7.2, the optimal buffer for DAO enzyme activity, was used. Unlike HRP, which is present in excess, DAO activity may become limiting and thus, it was prioritised regarding the pH.

For the optimisation of DAO concentration to use in the conjugation to MBs, conjugates synthesised with different DAO dilutions were tested on Co(II)-phthalocyanine/carbon electrodes by cyclic voltammetry. The conjugation of DAO to MBs is based on a stable amide bond between the activated carboxylic acid group of the beads and an amine group of the enzyme. The oxidation peak intensity due to the presence of a saturated concentration of Hist was constant from 1/8 to 1/128 DAO dilution, and started to decrease at 1/256 DAO dilution (*results not shown*), suggesting that the 1/128 DAO dilution was enough to completely coat the MBs. As a preventive measure, a 1/100 DAO dilution was chosen for subsequent experiments. This experiment demonstrated not only the efficiency of the immobilisation method, but also the retention of the functionality of the enzyme despite having been immobilised through one of its amine groups.

Schema I. Enzymatic mechanisms and electrochemical transduction strategies of DAO-MB mono- and bi-enzymatic biosensors.

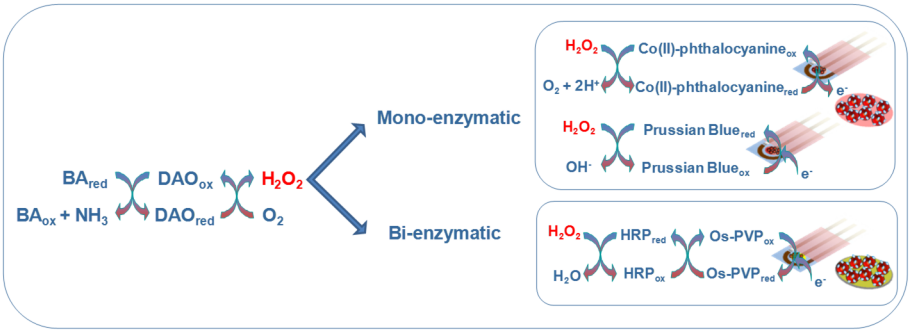

Cyclic voltammetry was performed to compare the response from DAO-MB conjugates to different BAs. Addition of the BA on the mono-enzymatic biosensors incorporating DAO-MB conjugates and Co(II)-phthalocyanine (Figure 1A) and Prussian Blue (Figure 1B) mediators resulted in an increase of the oxidation and reduction current, respectively. A higher affinity of DAO towards Put and Cad

compared with Hist was observed, as it happened when measuring the activity of DAO in solution by the colorimetric assay. Similar results were obtained with the bi-enzymatic biosensor using DAO-MB conjugates on Os-wired HRP-modified carbon electrodes (Fig. 1C). Well-defined osmium oxidation and reduction peaks were observed before BAs addition. In the presence of BAs, bioelectrocatalytic currents were obtained and differences between BAs were clearly observed.

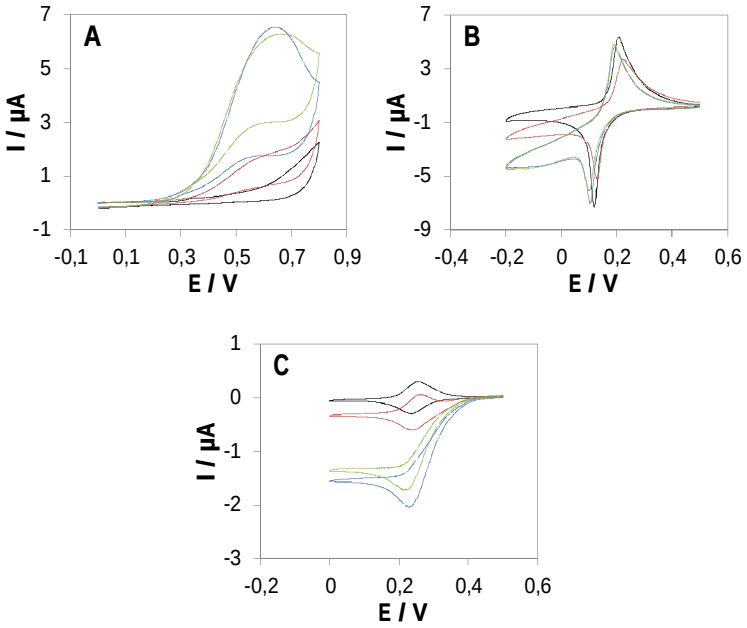

Figure 1. Cyclic voltammograms performed in 0.1 M potassium phosphate buffer, 0.1 M KCl, pH 7.2 at 5 mV/s in the presence of DAO-MB conjugates before (black) and after the addition of 10 mM Hist (red), Put (blue) and Cad (green) using: **(A)** Co(II)-phthalocyanine/carbon; **(B)** Prussian Blue/carbon; and **(C)** Os-wired HRP-modified carbon electrodes.

3.2. Characterisation of the DAO-MB biosensors

Amperometric detection of BAs was performed applying the potentials selected from the characterisation by cyclic voltammetry. For Prussian Blue/carbon and Os-wired HRP-modified carbon electrodes, working potentials of -0.1 V and +0.05 V were chosen, respectively, to guarantee a complete reduction of the mediator oxidised after the BA addition, and thus to obtain high current intensities in amperometry. However, the potential of the oxidation peak with Co(II)-

phthalocyanine/carbon electrodes was too high (+0.6 V) and compromise between high current intensities and interferences avoidance had to be undertaken. Consequently, calibration curves were obtained for Hist, Put and Cad applying +0.4 V to Co-phthalocyanine/carbon electrodes, -0.1 V to Prussian Blue/carbon electrodes and +0.05 V to Os-wired HRP-modified carbon electrodes. The biosensor variability, expressed as the relative standard deviation (RSD) for the triplicate measurements, was always less than 10% in all configurations, showing appropriate intra-day reproducibility. Despite enzyme adsorption generally results in weak immobilisations that could lead to enzyme leaching, the configuration with Os-wired HRP-modified carbon electrodes presented similar biosensor variability than the other configurations. This can be well explained by the high adsorptive properties of the Os-wired HRP due to the presence of the PVP redox polymer.

Table 1 summarises the results obtained from the calibration curves. Analytical parameters were very similar across strategies, with linear measuring ranges from 0.01 up to 1 mM BA. Higher sensitivities and lower LODs (LOD = blank + 3 SD) and limits of quantification (LOQs) (LOQ = blank + 10 SD) were always attained for Put and Cad, as expected from the cyclic voltammetry measurements. However, it should be mentioned that the bi-enzymatic approach presented higher intercept values compared to the mono-enzymatic approaches. This fact may be explained by the presence of Os-wired HRP adsorbed on the modified electrode and a change on the kinetics of the overall enzymatic reaction [25]. Although some works have reported that bi-enzymatic approaches result in a better performance compared to mono-enzymatic approaches [26], in this work the bi-enzymatic biosensor did not present a higher sensitivity. Taking into account the results obtained in the H_2O_2 detection optimisation (*see SME*), we hypothesise that the amount of immobilised redox mediator may be limiting the bioelectrocatalytic current. Nonetheless, the three strategies present enough sensitivity to detect Hist at lower concentrations than the regulation levels and even at much lower concentrations for Put and Cad, as well as high reproducibility, low-cost and rapid detection. Any of the three approaches can be used to conduct the subsequent experiments.

Lower LODs may be attained applying a higher working potential when using Co(II)-phthalocyanine/carbon electrodes, but this can be detrimental because matrix compounds often interfere. In case of electrodes modified with Os-wired HRP, higher amounts of immobilised redox mediator may also improve the LODs, but this would raise the price of the assay. Consequently, although feasible, these improvements in the LOD may compromise the practical applicability. Table 2 summarises the electrochemical biosensors for Hist, Put or Cad detection reported since 2010. As it can be observed, the LODs obtained in this work are similar to those attained with other enzymatic electrochemical biosensors. When comparing the

DAO-MB electrochemical biosensors to the optical biosensor that also uses magnetic beads as DAO immobilisation supports, the LODs obtained are even two orders of magnitude lower [27]. The use of MBs as enzyme immobilisation supports allows the direct modification of the electrode surface in a simple and fast way, and provides high stability to the biosensor.

Due to the low cost, ease construction and high reproducibility, DAO-MB biosensors were originally designed for single use. However, a repeatability study was performed using Prussian Blue electrodes by consecutive 1mM Hist additions. Results demonstrated that the biosensor can be used at least 8 times consecutive without any loss of activity (>95% amperometric response). The possibility to reuse the same biosensor further reduces the cost of the assay and highlights another advantage of the use of MBs in terms of biosensor regeneration.

Table 1. Analytical parameters of the DAO-MB electrochemical biosensors on Co(II)-phthalocyanine/carbon at +0.4 V (*vs.* Ag), Prussian Blue/carbon at -0.1 V (*vs.* Ag) and Os-wired HRP-modified carbon electrodes at +0.5 V (*vs.* Ag) for Hist, Put and Cad determination

		Intercept (nA)	Sensitivity (nA/µM)	LOD (µM)	LOQ (µM)	R^2
Co(II)-phthalocyanine	Hist	6.07	0.13	5.13	49.46	0.998
	Put	5.83	2.11	1.03	3.16	0.999
	Cad	6.22	3.03	0.60	2.07	0.995
Prussian Blue	Hist	7.27	0.57	4.80	38.12	0.995
	Put	7.09	3.22	0.90	6.80	0.997
	Cad	7.93	3.12	0.67	6.70	0.999
Os-wired HRP	Hist	31.70	0.31	4.50	38.48	0.999
	Put	30.07	3.31	0.90	3.90	0.997
	Cad	31.85	2.61	0.47	4.27	0.999

3.3. Storage stability of DAO-MB conjugates

To investigate the possibility to store the DAO-MB conjugates until use, their stability at 4 °C and -20 °C during 90 days was evaluated. Glycerol was added to MB-DAO suspensions to study if the addition of a stabiliser improved the retention of the activity of the conjugates. Amperometric recordings on Prussian Blue/carbon electrodes were constant with time, clearly demonstrating that DAO-MB conjugates were stable for at least 3 months, regardless the temperature and the presence of glycerol (Fig. S3). A high robustness of the conjugates under different storage

conditions was observed (RSD between 3 and 10%, depending on the measurement day). Additionally, the measurements showed an appropriate inter-day reproducibility (RSD = 8%). To the best of our knowledge, the high stability of the DAO-MB conjugates provides the most stable enzymatic electrochemical biosensor for Hist, Put or Cad detection reported in recent years (Table 2).

As observed in previous works [28], the immobilisation of the enzyme on MBs increases the stability of the enzyme activity. The good storage stability of the conjugates demonstrates additional advantages of using MBs as enzyme immobilisation supports in the biosensor development. On the one hand, as there is no need to prepare the conjugates immediately prior the analysis, the protocol is simplified and the assay time is drastically shortened. On the other hand, the ability to use a same conjugate pool for the analysis of different samples on different days provides even higher reproducibility to the system.

3.4. Multiplexed detection

To demonstrate the straightforward integration of the DAO-MBs in a multiplexed system, a calibration curve for Hist was performed using an array of 8 Os-wired HRP-modified carbon screen-printed modified electrodes connected to the potentiostat through an 8-channel multiplexer. The array configuration presented a sensitivity of 0.47 nA/µM, with a linear range from 0.06 mM to 1 mM Hist and an LOD of 8.25 µM. Despite the smaller surface area of the working electrodes of the array compared to the single electrodes (2.5 mm in diameter in front of 4 mm) and the lower amount of DAO-MB conjugates used in this configuration (5 µL in front of 10 µL), the sensitivity is slightly higher (0.47 nA/µM in front of 0.31 nA/µM). However, the LOD is higher than in the single approach (8.25 µM in front of 4.50 µM). This increase in the LOD may be explained by a lower accuracy of the portable PalmSens potentiostat (±0.5%), additionally connected to the 8-channel multiplexer, in comparison with the AUTOLAB PGSTAT128N potentiostat used to measure the single electrodes (±0.2%). Nevertheless, it remains at the same order of magnitude than the previous configurations and it is still low enough to detect Hist at values lower than those established by the European Regulation or other agencies.

The feasibility to use lower amounts of MBs and reduce the cost of the biosensor, together with the possibility to perform multiple measurements in a compact and fast way, makes the use of DAO-MBs on array electrodes clearly suitable for high-throughput analysis of BAs.

3.5. Study of interferences

Histidine (Hist), lysine (Lys), arginine (Arg), tyrosine (Tyr) and tryptophan (Trp) are amino acids involved in the biosynthesis of BAs, and frequently found in fish. Dopamine (DA) and tyramine (TA) are biogenic amines similar to Hist, Put and Cad that may show electrochemical interferences [29, 30]. To ensure the applicability of the developed biosensor to the determination of Hist, Put and Cad content in fish samples, the possible interference from these amino acids as well as DA and TA should be evaluated. As can be seen in Figure 2, all amperometric responses were lower than 6% of the response towards Hist. Results demonstrate that all these related compounds are not detected by the biosensor and thus do not interfere in the determination of BAs contents. Moreover, as this study was conducted with the electrode array, it demonstrates again the suitability of the approach for the analysis of multiple samples.

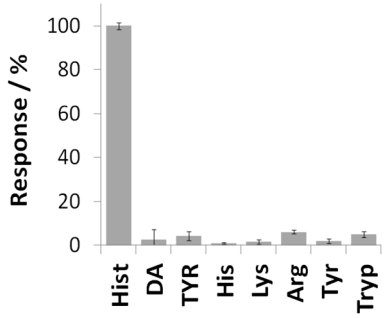

Figure 2. Study of interferences of DAO-MB biosensors using Os-wired HRP-modified carbon electrode arrays. Comparison between 1 mM histamine (Hist) and 1 mM of potentially interfering compounds: histidine (His), lysine (Lys), arginine (Arg), tyrosine (Tyr) and tryptophan (Tryp), dopamine (DA) and tyramine (TA).

3.6. Analysis of fish samples

To evaluate the applicability of the DAO-MB electrochemical biosensor to the determination of BAs contents in fish samples, spike recovery studies and analysis of naturally-spoiled sea bass samples were performed on Prussian Blue/carbon electrodes. In the recovery experiments, different Hist/Put/Cad combinations were spiked and the final BAs contents of the samples were expressed in Hist equivalent contents (Put and Cad concentrations were converted into Hist equivalents by interpolation using the calibration curves). For the calculation of the recovery, the

initial BAs content present in the sample (combination 1) was subtracted. As it can be seen in Table 2, results obtained were satisfactory, recovery being always between 97.0 and 102.2%. Comparing the whole set of combinations, statistical analysis revealed that were not significant differences between the expected and the determined Hist equivalent contents ($y = 0.983x + 1.761$, $R^2 = 0.998$, $p < 0.001$).

DAO-MB biosensors were also used to analyse sea bass samples stored for 3 days at 4 °C and 25 °C to follow natural spoilage (Table 3). As expected, sea bass samples presented low initial BAs contents, which increased with storage time, the effect being much more evident with samples stored at 25 °C. In some samples, BAs were detected at concentrations below the LOQ. Although quantifications at these levels were not accurate and showed high relative standard deviation values, they have been provided to show the increase of BAs concentrations in fish with time and/or under inadequate storage conditions. Concentrations above the LOQ provide relative standard deviations not higher than 10%.

BAs contents determined with the biosensor were compared to those obtained by the colorimetric enzyme assay. Statistical analysis revealed that were not significant differences between the results determined by the amperometric biosensor and those provided by the colorimetric enzyme assay ($W = 53$, $p = 1$). These results demonstrate the applicability of the developed biosensor to the analysis of fish samples and their use as both screening tool at the regulatory level and quantification analysis technique.

Table 2. BAs spiking combinations and recovery percentages from sea bass samples with the DAO-MB electrochemical biosensor using Prussian Blue/carbon electrodes.

Spiking combinations	Hist	Put	Cad	Expected [Hist]eq (µM)	Determined [Hist]eq (µM)	Recovery (%)
1	-	-	-	-	-	-
2	+	-	-	62.50	61.45 ± 0.11	98.3
3	-	+	-	66.01	64.03 ± 0.77	97.0
4	-	-	+	44.86	45.70 ± 0.14	101.9
5	+	+	-	128.51	125.06 ± 0.53	97.3
6	+	-	+	107.36	107.24 ± 0.89	99.9
7	-	+	+	110.86	113.25 ± 0.17	102.2
8	+	+	+	173.36	175.94 ± 0.65	101.5

**The + symbol indicates 62.5 µM for Hist and 15.6 µM for Put and Cad; the - symbol indicates 0.*

Table 3. Hist equivalent contents (mg/kg) in sea bass samples determined by the DAO-MB electrochemical biosensor using Prussian Blue/carbon electrodes and the colorimetric enzyme assay.

	DAO-MB electrochemical biosensor		***Colorimetric enzyme assay***	
0 h	23 ± 10		36 ± 9	
	4° C	25° C	4° C	25° C
24 h	57 ± 17	212 ± 35	89 ± 29	170 ± 9
48 h	149 ± 17	301 ± 28	87 ± 35	425 ± 40
72 h	162 ± 36	1050 ± 110	138 ± 20	1188 ± 16

Table 2. Enzymatic electrochemical biosensors for the determination of Hist, Put or Cad reported since 2010.

Biogenic amines	Enzyme	Immobilisation	Mediator	Potential (mV)	LOD	Stability	Sample	Refs.
Hist, Put, Cad	DAO DAO/HRP	Covalent binding with carboxylic acid groups of magnetic beads	Co(II)-phthalocyanine Prussian Blue Osmium	+400 -100 +50	4.5-5.13 µM Hist 0.90-1.03 µM Put 0.47-0.60 µM Cad	3 months	Sea bass	*This work*
Hist, Put	PUO and HMD	Crosslinking with GA and BSA on SPE	Tetrathiafulvalene	+130 +300	8.1±0.7 µM Hist 10±0.6 µM Put	-	Octopus Zucchini	[6]
Put	PUO	Crosslinking with GA and BSA on SPE	Tetrathiafulvalene	+300	10.1 ±0.6 µM	-	Octopus Zucchini	[7]
Hist	DAO	Entrapment on CeO_2-polyaniline nanoparticles using a Nafion solution	-	-100	48.7 µM	18 days	Prawns	[18]
Hist	DAO/HRP	Immobilisation into a polysulfone/carbon nanotubes/ferrocene membrane	Ferrocene	-50	0.17 µM	1 month	Fish	[11]

(Continued)

Biogenic amines	Enzyme	Immobilisation	Mediator	Potential (mV)	LOD	Stability	Sample	Refs.
Put, Cad	MAO	Crosslinking with GA and BSA on SPE or an array modified with AuNPs	Tetrathiafulvalene	+250	9.9 µM Put 19.9± 0.9 µM Cad	-	Octopus	[8]
Put	MAO	Crosslinking with GA and BSA on SPE	TTF	+250	17.2 µM Put	-	Zucchini Anchovies	[9]
Put, Cad	PSAO	Entrapment into a Nafion membrane	MnO_2	+400	6.8 µM Put 12.6 µM Cad *(Flow injection analysis)*	-	Chicken	[12]
Put, Cad	PSAO	Entrapment into a Nafion membrane	MnO_2	+400	49.6 µM Put 57.1 µM Cad	-	Fish sauce	[13]
Hist	DAO	Entrapment into a photocured poly (2-hydroxyethyl) metacrylate film	Potassium ferricyanide	+350	3.5 µM	-	Prawns	[14]
Put	PUO/HRP	Entrapment into PEGDE	Osmium	+50	5 µM	7-10 days	Beer	[15]
Hist Put	DAO/HRP PUO/HRP	Entrapment into PEGDE	Osmium	-50 and +50	5 µM Hist 5 µM Put	-	Fish Meat	[16]
Put	DAO	Crosslinking on FeO_3 nanoparticles	-	+400	0.65 nM	6 days	-	[19]

(Continued)

Biogenic amines	Enzyme	Immobilisation	Mediator	Potential (mV)	LOD	Stability	Sample	Refs.
Put	DAO	Entrapment into a polyazetine prepolymer	-	+600	1.24 µM	-	Wine Beer	[17]
Hist	MAO/HRP DAO/HRP	Crosslinking on SPE using an aryl diazonium salt	Ferrocene	+250	0.4 µM *(MAO/HRP)* 0.18 µM *(DAO/HRP)*	-	Anchovies	[10]

DAO: diamine oxidase; HMD: histamine deshydrogenase; HRP: horseradish peroxidase; MAO: monoamine oxidase; PSAO: pea seedling amine oxidase; PUO: putrescine oxidase; SPE: screen-printed electrode

4. Conclusions

The present work reports low-cost and easy-to-use amperometric biosensors for BAs determination using MBs as DAO immobilisation supports. This immobilisation technique is simple and efficient, provides stable conjugates and allows direct contact of the enzyme with the analyte without diffusion barriers. Moreover, the immobilisation of DAO on MBs increases the stability of the enzyme activity.

The use of MBs as immobilisation supports allows the direct modification of any type of electrode surface by only placing the electrode on a magnetic support. By this method, Co(II)-phthalocyanine and Prussian Blue mono-enzymatic biosensors and Os-wired HRP-modified bi-enzymatic biosensors have been developed, presenting in all cases LODs for Hist, Put and Cad in the submicromolar to micromolar range, a broad linear range of two orders of magnitude, good reproducibility, high repeatability and no interferences from other related compounds. A clear advantage presented by the use of DAO-MB conjugates over other BAs electrochemical biosensors is their excellent storage stability, which allows having ready-to-use conjugates available any time. This fact, together with their easy transfer to multiplexed systems to perform multiple measurements, reduces the analysis time and drastically simplifies the protocol. Given the demonstrated suitability of the three approaches for monitoring the BAs content, DAO-MBs constitute an excellent tool to foster the applicability of electrochemical biosensors to fast, easy, low-cost and high throughput detection of BAs in the fish industry in particular and in the agro-food sector in general. Efforts focused on the increase of bio/electrocatalytic currents may lead to lower LODs and LOQs, providing more accurate and precise BAs quantifications at lower concentrations. The integration of these DAO-MB biosensors into microfluidics systems may also result in more sensitive and faster analysis devices, which would also be automated and portable.

The described approaches, applied to DAO as enzyme and BAs as analytes, are versatile and can be easily used with other oxidases and target compounds of interest in food control, but also in environmental and medical applications.

Acknowledgements

The authors acknowledge financial support from the Ministerio de Economía y Competitividad through the DIANA (BIO2011-26311) project. The authors also acknowledge Pere Campàs for the gift of sea bass samples. Sandra Leonardo acknowledges scholarship from IRTA – Universitat Rovira i Virgili – Banco Santander (2013PIPF URV-IRTA-BS-01).

References

[1] Santos MHS (1996) Biogenic amines: Their importance in foods. Int. J. Food Microbiol. 29: 213-31.

[2] Chong CY, FA, Russly AR, Jamilah B, Mahyudin NA (2011) The effects of food processing on biogenic amines formation. Int Food Res J 18: 867-876.

[3] Stratton JE, Hutkins RW, Taylor SL (1991) Biogenic-Amines in Cheese and Other Fermented Foods - a Review. J Food Prot 54: 460-470.

[4] Comission Regulation No. 1441/2007 of December 5, 2007. Off. J. Eur. Communities, L139 (2007) 11.82.

[5] Önal A (2007) A review: Current analytical methods for the determination of biogenic amines in foods. Food Chem 103: 1475-1486.

[6] Henao-Escobar W, Del Torno-de Roman L, Domínguez-Renedo O, Alonso-Lomillo MA, Arcos-Martínez MJ (2016) Dual enzymatic biosensor for simultaneous amperometric determination of histamine and putrescine. Food Chem 190: 818-23.

[7] Henao-Escobar W, Domínguez-Renedo O, Alonso-Lomillo MA, Cascalheira JF, Dias-Cabral AC, Arcos-Martínez MJ (2015) Characterization of a Disposable Electrochemical Biosensor Based on Putrescine Oxidase from Micrococcus rubens for the Determination of Putrescine. Electroanal 27: 368-377.

[8] Henao-Escobar W, Domínguez-Renedo O, Alonso-Lomillo MA, Arcos-Martínez MJ (2013) Simultaneous determination of cadaverine and putrescine using a disposable monoamine oxidase based biosensor. Talanta 117: 405-411.

[9] Henao-Escobar W, Domínguez-Renedo O, Alonso-Lomillo MA, Arcos-Martínez MJ (2013) A screen-printed disposable biosensor for selective determination of putrescine. Microchim Acta 180: 687-693.

[10] Alonso-Lomillo MA, Domínguez-Renedo O, Matos P, Arcos-Martínez MJ (2010) Disposable biosensors for determination of biogenic amines. Anal Chim Acta 665: 26-31.

[11] Pérez S, Bartrolí J, Fàbregas E (2013) Amperometric biosensor for the determination of histamine in fish samples. Food Chem 141: 4066-4072.

[12] Telsnig D, Kassarnig V, Zapf C, Leitinger G, Kalcher K, Ortner A (2012) Characterization of an Amperometric Biosensor for the Determination of Biogenic Amines in Flow Injection Analysis. Int J Electrochem Sc 7: 10476-10486.

[13] Telsnig D, Terzic A, Krenn T, Kassarnig V, Kalcher K, Ortner A (2012) Development of a Voltammetric Amine Oxidase-Modified Biosensor for the Determination of Biogenic Amines in Food. Int J Electrochem Sc 7: 6893-6903.

[14] Keow CM, Bakar FA, Salleh AB, Heng LY, Wagiran R, Siddiquee S (2012) Screen-printed histamine biosensors fabricated from the entrapment of diamine oxidase in a photocured poly(HEMA) film. Int J Electrochem Sc 7: 4702-4715.

[15] Bóka B, Adányi N, Szamos J, Virág D, Kiss A (2012) Putrescine biosensor based on putrescine oxidase from Kocuria rosea. Enzyme Microb Tech 51: 258-62.

[16] Bóka B, Adányi N, Virág D, Sebela M, Kiss A (2011) Spoilage detection with biogenic amine biosensors, comparison of different enzyme electrodes. Electroanal 24: 181-186.

[17] Di Fusco M, Federico R, Boffi A, Macone A, Favero G, Mazzei F (2011) Characterization and application of a diamine oxidase from Lathyrus sativus as component of an electrochemical biosensor for the determination of biogenic amines in wine and beer. Anal Bioanal Chem 401: 707-716.

[18] Gumpu MB, Nesakumar N, Sethuraman S, Krishnan UM, Rayappan JBB (2014) Development of electrochemical biosensor with ceria-PANI core-shell nano-interface for the detection of histamine. Sensor Actuat B-Chem 199: 330-338.

[19] Shanmugam S, Thandavan K, Gandhi S, Sethuraman S, Rayappan JBB, Krishnan UM (2011) Development and evaluation of a highly sensitive rapid response enzymatic nanointerfaced biosensor for detection of putrescine. Analyst 136: 5234-5240.

[20] Yang X, Feng B, He X, Li F, Ding Y, Fei J (2013) Carbon nanomaterial based electrochemical sensors for biogenic amines. Microchim Acta 180: 935-956.

[21] Reverté L, Prieto-Simón B, Campàs M (2016) New advances in electrochemical biosensors for the detection of toxins: Nanomaterials, magnetic beads and microfluidic systems. A review. Anal Chim Acta 908: 8-21.

[22] Hasanzadeh M, Shadjou, De la Guardia M (2015) Iron and iron-oxide magnetic nanoparticles as signal-amplification elements in electrochemical biosensing. Trac- Trends Anal Chem 72: 1-9.[23] Pedrero M, Campuzano S, Pingarrón JM (2012) Magnetic beads-based electrochemical sensors applied to the detection and quantification of bioterrorism/biohazard agents. Electroanal 24: 470-482.

[24] Shi X, Gu W, Li B, Chen N, Zhao K, Xian Y (2014) Enzymatic biosensors based on the use of metal oxide nanoparticles. Microchim Acta 181: 1-22.

[25] Lindgren A, Ruzgas T, Gorton L, Csöregi E, Ardila GB, Sakharov IY, Gazaryan IG (2000) Biosensors based on novel peroxidases with improved properties in direct and mediated electron transfer. Biosens Bioelectron 15: 491-4971.

[26] Gu M, Wang J, Tu Y, Di J (2010) Fabrication of reagentless glucose biosensors: A comparison of mono-enzyme GOD and bienzyme GOD-HRP systems. Sensor Actuat B-Chem 148: 486-491.

[27] Pospiskova K, Safarik I, Sebela M, Kuncová G (2013) Magnetic particles-based biosensor for biogenic amines using an optical oxygen sensor as a transducer. Microchim Acta 180: 311-318.

[28] Garibo D, Devic E, Marty JL, Diogène J, Unzueta I, Blazquez M, Campàs M (2012) Conjugation of genetically engineered protein phosphatases to magnetic particles for okadaic acid detection. J Biotech 157: 89-95.

[29] Shangavi BJ, Wolfbeis OS, Hirsch T, Swami NS (2015) Nanomaterial-based electrochemical sensing of neurological drugs and neurotransmitters. Microchim Acta 182: 1-41.

[30] Enache TA, Oliveira-Brett AM (2011) Phenol and *para*-substituted phenols electrochemical oxidation pathways. J Electroanal Chem 655: 9-16.

Supplementary Information

Electrochemical protocol for optimisation of the H_2O_2 detection

Cyclic voltammetry was used to characterise the response of the electrodes towards H_2O_2 (for the subsequent development of mono-enzymatic biosensors). The protocol was as follows: 45 µL of 0.1 M potassium phosphate buffer, 0.1 M KCl, pH 7.2, were placed on the screen-printed electrode and a cyclic voltammogram was recorded between -0.2 and +0.8 V *vs.* Ag (potential window depended on the electrode and the electrochemical transduction approach) at 5 mV/s; 5 µL of 10 mM H_2O_2 solution were then added and cyclic voltammograms were recorded again.

Cyclic voltammetry was also used to characterise the response of the HRP-modified electrodes towards H_2O_2 (for the subsequent development of bi-enzymatic biosensors). The protocol was as follows: 1 µL of 2 mg/mL HRP solution in water or Os-wired HRP stock solution was placed on the DRP-110 working electrode and allowed to dry for 30 min. When using HRP, 45 µL of 0.5 mM N-methylphenazonium methyl sulphate (MPMS) in 0.1 M potassium phosphate buffer, 0.1 M KCl, pH 7.2, were then placed on the screen-printed electrode and a cyclic voltammogram was recorded between 0 and -0.4 V at 5 mV/s; 5 µL of 10 mM H_2O_2 solution were then added and, after 1 min, a cyclic voltammogram was recorded again. When using Os-wired HRP, 45 µL of 0.1 M potassium phosphate buffer, 0.1 M KCl, pH 7.2, were placed on the screen-printed electrode and a cyclic voltammogram was recorded between +0.5 and 0 V at 5 mV/s; 5 µL of 10 mM H_2O_2 solution were then added and, after 1 min, a cyclic voltammogram was recorded again.

Optimisation of the H_2O_2 detection

Several electrochemical strategies for the detection of H_2O_2, either directly (on carbon, single-walled carbon nanotubes/carbon, graphene/carbon and gold electrodes), through immobilised redox mediators (on Co(II)-phthalocyanine/carbon, Prussian Blue/carbon) or by HRP-modified electrodes, have been tested previous the use of DAO-MB conjugates for the subsequent development of mono-enzymatic and bi-enzymatic biosensors for BAs detection. The aim of this work was seek the most sensitive and optimal detection for a BAs amperometric biosensor based on the use of magnetic beads as DAO immobilisation supports.

First, the direct detection of H_2O_2 on different electrodes was investigated. As expected, cyclic voltammograms of carbon, single-walled carbon

nanotubes/carbon, graphene/carbon and gold screen-printed electrodes did not show any redox peak in the potential range from 0 to +0.8 V (*results not shown*). The H_2O_2 addition did not cause any effect on carbon electrodes, but resulted in an increase of the oxidation current starting at +0.4 V on single-walled carbon nanotubes/carbon electrodes, graphene/carbon and gold electrodes (Fig. S1A).

Inorganic redox mediators were added to the electrochemical transduction strategy to investigate if it was possible to detect H_2O_2 at lower working potentials and thus avoid possible electrochemical interferences. The cyclic voltammetry of Co(II)-phthalocyanine/carbon electrodes did not show any oxidation or reduction peak (Fig. S1B, black line), but the addition of H_2O_2 resulted in the chemical reduction of the immobilised mediator (from Co^{3+} to Co^{2+}) and the subsequent electrochemical re-oxidation, which started at +0.2 V and showed a peak at +0.6 V (Fig. S1B, red line). Compared to the carbon-based materials and gold, much lower potentials can be applied to measure H_2O_2 when using Co(II)-phthalocyanine, obtaining higher current intensities. The cyclic voltammetry of Prussian Blue/carbon electrodes showed well-defined oxidation and reduction peaks, with a midpoint redox potential of +0.12 V and a peak-to-peak separation of 100 mV (Fig. S1C, black line). The addition of H_2O_2 resulted in the chemical oxidation of the immobilised mediator (from Fe^{2+} to Fe^{3+}) and the subsequent increase in the reduction current (Fig. S1C, red line). Current intensities obtained were comparable to those attained using Co(II)-phthalocyanine/carbon electrodes.

The detection of H_2O_2 on different HRP-modified electrodes was then investigated for the subsequent development of bi-enzymatic biosensors. In this case, the transduction strategy was based on the enzymatic reaction between HRP and its substrate, H_2O_2, and the subsequent mediated bioelectrocatalysis. First trials were performed using the redox mediator MPMS in solution and HRP adsorbed on screen-printed carbon electrodes. Before H_2O_2 addition, MPMS showed an oxidation and a reduction peak, with a midpoint redox potential of -0.15 V and a peak-to-peak separation of 60 mV (Fig. S2A, black line). After H_2O_2 addition, an increase in the reduction peak current and a decrease in the oxidation peak current were observed (Fig. S2A, red line). This effect is certainly due to the bioelectrocatalysis, and not to the direct H_2O_2 reduction on the electrode, since no response was observed in the controls without HRP. Otherwise, the bioelectrocatalytic currents from HRP adsorbed on Prussian Blue/carbon electrodes were also recorded. Results did not shown significant differences compared to the configurations without HRP (*results not shown*).

The last configuration incorporated Os-wired HRP. The electrical wiring of HRP with Os-polyvinylpyridine (Os-PVP) redox polymer favours the electron transfer from the redox centre of the enzyme to its periphery and, if it is immobilised, to the electrode

[1]. When adsorbing the wired enzyme on the electrode, the osmium showed well-defined oxidation and reduction peaks, with a midpoint redox potential of +0.23 V and a peak-to-peak separation of 20 mV (Fig. S1E, black line). Since osmium complexes have particularly high self-exchange rates and, additionally, PVP polymer relays the electrons via the osmium centres to the electrode [2], the lower current intensity of the redox peaks compared to those of MPMS in solution (Fig. S2B, black line) were attributed to a lower amount of immobilised Os redox mediator. In the presence of H_20_2, the Os oxidation peak completely disappeared and a bioelectrocatalytic reduction current was observed (Fig. S2B, red line). Although the current intensity of the reduction peak increased, it did not reached a steady-state plateau. The use of a twice higher amount of Os-wired HRP did not substantially increase the reduction current neither resulted in a steady-state plateau.

At this stage, three electrode supports were selected for the subsequent detection of BAs based on the attained current intensities: Co(II)-phthalocyanine/carbon and Prussian Blue/carbon electrodes for the development of mono-enzymatic biosensors, and Os-wired HRP-modified carbon electrodes for the development of a bi-enzymatic biosensor. Single-walled carbon nanotubes/carbon, graphene/carbon and gold electrodes showed H_2O_2 oxidation currents but at potentials too high for the subsequent development of biosensors. On the contrary, the use of Co(II)-phthalocyanine and Prussian Blue redox mediators resulted in well-defined redox peaks of higher current intensities and at lower potentials.

Each configuration presents advantages and limitations. Whereas in the mono-enzymatic approaches, Co(II)-phthalocyanine/carbon and Prussian Blue/carbon electrodes are commercially available and ready to use, the bi-enzymatic approaches require the immobilisation of HRP, step that increases the experimental procedure time. Moreover, the HRP immobilisation may increase the variability among electrodes due to possible enzyme leaking. Nevertheless, the use of a bi-enzymatic approach may increase the sensitivity and selectivity, and decrease the limit of detection (LOD) [3]. In fact, the current intensities attained when using HRP were slightly higher than in the mono-enzymatic approaches with immobilised mediators. Regarding the choice of redox mediator in the bi-enzymatic approach, immobilised Os was preferred to free diffusing MPMS because HRP wiring directly connects the enzyme with the electrode, which may also increase the sensitivity and decrease the LOD [4].

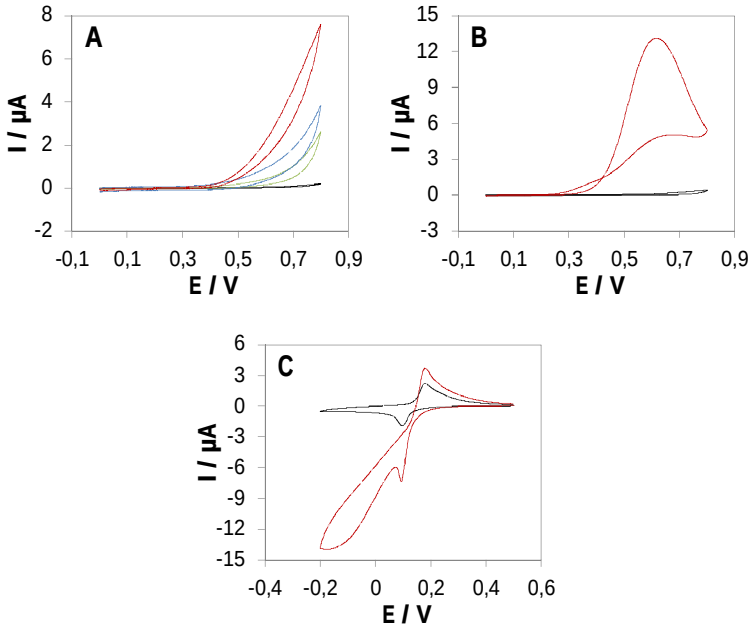

Fig. S1. Cyclic voltammograms performed in 0.1 M potassium phosphate buffer, 0.1 M KCl, pH 7.2 at 5 mV/s for: **(A)** carbon (black), single-walled carbon nanotubes (green), graphene/carbon (blue) and gold (red) electrodes after the addition of 10 mM H_2O_2 (cyclic voltammograms before H_2O_2 addition were always lower than carbon electrodes after H_2O_2 addition and are not shown for clarity); **(B)** Co(II)-phthalocyanine/carbon electrodes before (black) and after (red) the addition of 10 mM H_2O_2; **(C)** Prussian Blue/carbon electrodes before (black) and after (red) the addition of 10 mM H_2O_2.

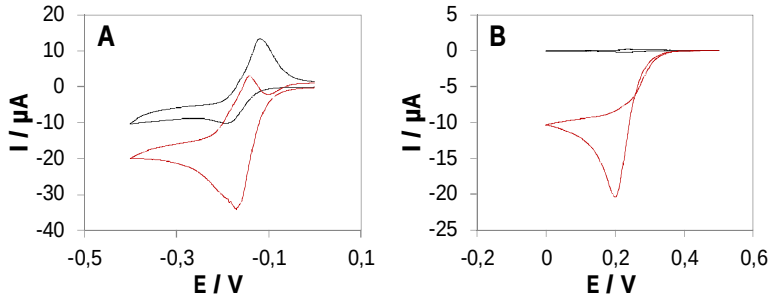

Fig. S2. Cyclic voltammograms performed in 0.1 M potassium phosphate buffer, 0.1 M KCl, pH 7.2 at 5 mV/s for: **(A)** HRP-modified carbon electrodes by adsorption in the presence of N-methylphenazonium methyl sulphate (MPMS) in solution before (black) and after (red) the addition of 10 mM H_2O_2; and **(B)** Os-wired HRP-modified carbon electrodes by adsorption before (black) and after (red) the addition of 10 mM H_2O_2.

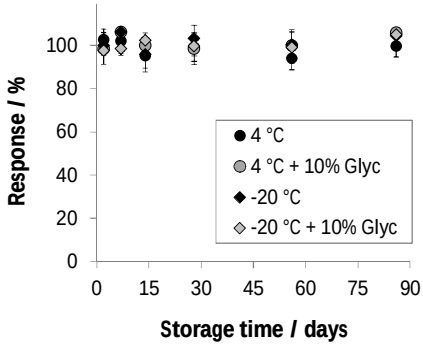

Fig. S3 Storage stability of DAO-MB conjugates

References

[1] Heller A (1992) Electrical connection of enzyme redox centers to electrodes. J Phys Chem 96: 3579-87.

[2] Ohara TJ (1995) Osmium bipyridyl redox polymers used in enzyme electrodes. Platinum Metals Rev 39: 54-62.

[3] Gu M, Wang J, Tu Y, Di J (2010) Fabrication of reagentless glucose biosensors: A comparison of mono-enzyme GOD and bienzyme GOD-HRP systems. Sensor Actuat B-Chem 148: 486-491.

[4] Vreeke M, Maidan R, Heller A (1992) Hydrogen peroxide and β-nicotinamide adenine dinucleotide sensing amperometric electrodes based on electrical connection of horseradish peroxidase redox centers to electrodes through a three-dimensional electron relaying polymer network. Anal Chem 64: 3084-3090.

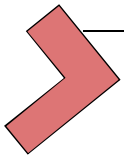

CHAPTER 6

Diatoms as natural nanostructured supports for the development of biosensors

Past, present and future of diatoms in biosensing

Sandra Leonardo[a], Beatriz Prieto-Simón[b], Mònica Campàs[a]

[a]*IRTA, Carretera Poble Nou km. 5.5, 43540 Sant Carles de la Ràpita (Tarragona), Spain*
[b]*ARC Centre of Excellence in Convergent Bio-Nano Science and Technology, Future Industries Institute, University of South Australia, SA 5095, Australia*

Abstract

Diatoms possess natural nanostructures and unique properties of great interest in nanotechnological applications. Among them, their use as nanostructured supports in biosensing platforms, although still in its childhood, is promising. Herein, the works focused on the immobilisation of diatom frustules, the modification of their composition and chemical features, and their functionalisation with biomolecules, are reviewed. The preservation of the three-dimensional nanostructure is almost always pursued and thus, processes are carried out under strict control. Additionally, high immobilisation yields, appropriate spatial distributions, modification or coating with specific components and oriented immobilisation of biomolecules, are also sought. The biocompatibility of diatom frustules, together with the nanofeatures, and the wide variety of processing methods, indicate that their exploitation in biosensing is imminent.

1. Introduction

The unique properties of diatoms led in 1988 to a new interdisciplinary area of research called diatom nanotechnology [1]. The interest of biologists and materials scientists on exploiting this intricate three-dimensional hierarchically nanostructured material as building blocks for the next generation of nanodevices has been continuously growing since then [2-9]. Diatoms are single cell microalgae with a silica (SiO_2) shell called frustule, which possesses a nanoporous pattern of unparalleled diversity far beyond the possibilities of current micro- and nanofabrication techniques. Even though still being under research, it is commonly accepted that these precise silica micro- and nanostructures have evolved to suit diatoms functionality. Such is the case of their biophotonic properties, which have been related to their capacity to guide light as a way to help photosynthesis [10].

Nature is a continuous source of inspiration for the design of advanced biomaterials at the nanoscale and thus diatom frustules are an excellent example of platforms

able to feature multiple functions. Diatoms can be modified to incorporate nanoparticles or biomolecules with different functionalities, and their composition and morphology can be easily tuned, overcoming some of the challenges involved in the production of nanomaterials. Their mechanical strength, high surface area and porous three-dimensional micro- and nanopatterns, open up a wealth of possibilities in terms of nanoengineering new attractive functional materials, maximising the potential of ancient nanochemistry based on using glass as a host for functional nanoparticles (e.g. the Lycurgus Cup) [7].

Compared to other recent reviews [11-15], this survey aims to describe the protocols used in each of the three fundamental steps (immobilisation, modification and biofunctionalisation) addressed to rationally design the use of diatoms as building blocks in biosensing systems. We describe in detail the methods used to assemble diatoms onto solid supports, to modify their properties by using physical, chemical or culture methods producing composite frustules or replicas, and/or to functionalise them with biomolecules. Most of the works described below are summarised in Table 1. The exploitation of the knowledge acquired on the advantages and limitations of these fundamental steps will provide researchers with the capacity to harness the unique properties of diatom frustules to rationally design diatom-based building blocks for biosensing applications.

2. Diatom immobilisation

Methods for the immobilisation of diatom frustules on transducers are needed to ensure the exploitation of these natural nanostructures for biosensing purposes. The nature of the substrate may constrain the method to use, which will dictate the diatom orientation, immobilisation yield and spatial distribution that can be achieved. Although it may depend on the application, morphological integrity of the frustules is usually sought, and thus, high pressure or temperature should be avoided. Figure 1 represents some of the methods used for diatom immobilisation, which are described below.

Most of the immobilisation methods used are based on the modification of either cleaned diatom frustules or immobilisation solid support for the subsequent assembling. As an exception, Umemura et al. [16] first cultured the diatoms on a mica surface treated with 3-aminopropyltriethoxysilane (APTES) and then baked the surface to remove the organic components of the diatom cells adhered to the surface.

Wang et al. [17] modified a glass substrate with a polyelectrolyte multilayer by inkjet printing for the subsequent immobilisation of diatom frustules by electrostatic

attraction between the final positively charged layer and the silanol groups of the frustules (Fig. 1A). Two centric diatoms were immobilised, *Coscinodiscus wailesii* and *Cyclotella* sp., being 200 µm and 10 µm in diameter, respectively. Tailoring the diameter of the positively charged multilayer dots to 200 µm, deposition of only one diatom frustule per dot was achieved. Several hundreds of the small *Cyclotella* frustules were deposited as a monolayer onto dots of equal size.

Lin et al. [18] used a more sophisticated technique for the site-directed immobilisation of only one diatom frustule onto a specific spot. After coating the gold microelectrode chip with polylysine, an individual *Coscinodiscus wailesii* frustule was micro-manipulated by a positioner and attached onto the chip. Since the *Coscinodiscus* frustule was rather large, it completely covered the gold sensing site, comprised of a 25-µm diameter working electrode and a 125-µm diameter counter electrode. It is important to note that by covering the whole sensing area the nanoscale pores of the frustule structure mimicked arrays of nanowells, which were used as biosensor platforms for the electrochemical detection of cardiovascular biomarker proteins, as explained in detail in section 4.

Conventional Si-O-Si bonding techniques have also been explored to immobilise diatoms onto Si-based substrates, either directly [19, 20] or through polymers such as poly(dimethylsiloxane) (PDMS) [21, 22] and ethylene-vinyl acetate (EVA) [22, 23] (Fig. 1B). The combined use of these polymers with photoresists and photolithography techniques provides microarrays of defined activated patterns where diatoms are specifically immobilised. The process usually requires energy supply in the form of pressure [19, 20], ultraviolet light [21] or heat [22, 23]. The incorporation of a catalyst like HCl allows the bonding of diatoms under more gentle conditions [19, 20]. Once bonded, diatom frustules retain their physical and chemical properties, such as their photoluminescence that allowed their use as gas-sensors [19], or their three-dimensional nanoporous structure that was used as a mask to obtain nanogold pillar arrays for surface-enhanced Raman scattering (SERS) detection [20]. Combining photolithography and frustule flotation, multi-layer diatom arrays have been formed packaging *Nitzschia soratensis* into *Coscinodiscus argus* frustules. These arrays enhanced the fluorescent intensity from a fluorescein isothiocyanate-labelled anti-IgG antibody after binding to the immobilised IgG, as explained in section 4 [23].

Recently, Chandrasekaran et al. [24] reduced diatom frustules from SiO_2 to Si by magnesiothermic conversion to allow their functionalisation via hydrosilylation with allyl mercaptan. Thiolated diatom frustules were subsequently self assembled on gold-plated glass slides (Fig. 1C). To achieve high diatom immobilisation yields, five consecutive immobilisation cycles were performed. These nanostructured surfaces worked as photoelectrodes for current generation from solar energy.

So far, only a few immobilisation techniques, tailored to the unique properties of diatoms, have demonstrated to be effective for diatom-based device manufacturing. Furthermore, they usually require sophisticated instrumentation, multi-step processes or drastic experimental conditions that may affect diatoms 3D structure. Simple, fast and efficient methods for stable diatom immobilisation onto several supports are highly desired for the development of biosensors.

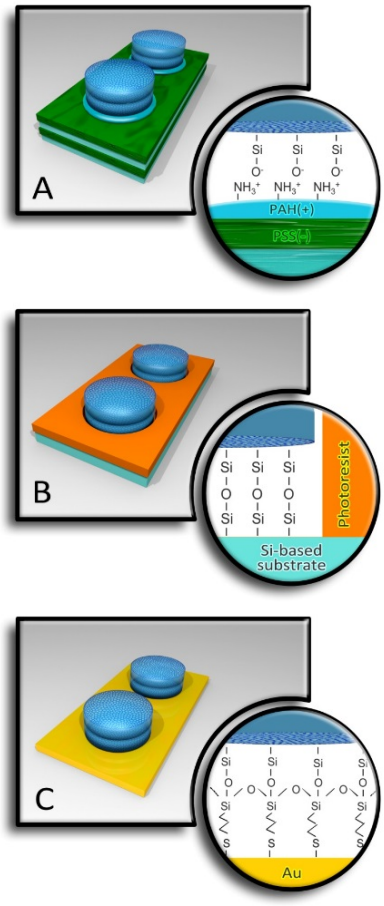

Figure 1. Diatom immobilisation methods based on electrostatic interactions (A), Si-O-Si bonding techniques (B), and self assembly on gold substrates (C).

Table 1. Immobilisation, modification and bio/functionalisation of diatom frustules and their applications.

Diatom	Immobilisation	Modification	Bio/functionalisation	Application	Ref.
Coscinodiscus wailesii *Cyclotella*	Layer-by-layer electrostatic interaction	-	-	-	[17]
Cymbella perpusilla	Si-O-Si bonding onto glass assisted by HF and pressure	-	-	-	[19]
Coscinodiscus decrescens	Si-O-Si bonding onto Si assisted by HF and pressure	-	-	Nanogold pillar arrays for SERS detection	[20]
Coscinodiscus *Navicula* *Nitschia*	Si-O-Si bonding onto glass/PDMS assisted by UV	-	-	-	[21]
Nitzschia soratensis *Coscinodiscus argus*	Si-O-Si bonding onto glass/EVA and glass/PDMS assisted by UV and heat	-	Silane/IgG	Fluroescence detection	[22]
Cymbella perpusilla *Coscinodiscus argus* *Nitzschia dubia*	Si-O-Si bonding onto glass/EVA assisted by UV and heat	-	-	Fluorescence spectroscopy	[23]
Aulacoseira	Self assembly on gold-plated electrode	Thiols *via* magnesiothermic reduction and hydrosilylation	-	Photoelectrodes	[24]
Aulacoseira	-	MgO *via* magnesiothermic reduction	-	-	[25]
Aulacoseira	-	Si *via* magnesiothermic reduction	-	NO sensing	[26]

(Continued)

Diatom	Immobilisation	Modification	Bio/functionalisation	Application	Ref.
Aulacoseira	-	Si *via* magnesiothermic reduction	-	Drug delivery	[27]
Aulacoseira	-	TiO_2 *via* gas/solid displacement reactions	-	-	[28]
Aulacoseira	-	ZrO_2 *via* gas/solid displacement reactions	-	-	[29]
Aulacoseira	-	Zn_2SiO_4 *via* combined use of displacement reactions and coating methods	-	-	[30]
Aulacoseira	-	$BaTiO_3$ *via* combined use of displacement reactions and coating methods	-	-	[31]
Aulacoseira	-	Ag, Au or Pd *via* combined use of displacement reactions and coating methods	-	-	[32]
Aulacoseira	-	C, or Pt/C *via* combined use of displacement reactions and coating methods	-	Electrocatalytic oxygen reduction	[33]
Aulacoseira	-	C or Au *via* combined use of displacement reactions and coating methods	Amino-dendrimers/proteamine/GOx	Glucose catalysis	[34]
Diatomaceous earth	-	Zeolites *via* hydrothermal growth	-	Water filtration	[35]
Diatomaceous earth	-	Zeolites *via* layer-by-layer	-	-	[36]
Diatomaceous earth	-	Zeolites *via* vapour-phase transport	-	-	[37]
Coscinodiscus Melosira Navicula	-	MnO_2 *via* template-assisted hydrothermal process	-	Supercapacitors	[38]

(Continued)

Diatom	Immobilisation	Modification	Bio/functionalisation	Application	Ref.
Synedra *Thalassiosira* *Coscinodiscus*	-	Ag *via* thermal evaporation		SERS substrates	[39]
Thalassiosira eccentrica	-	Au *via* thermal evaporation	-	Localised surface plasmon resonance	[40]
Centric diatom *Coscinodiscus* *Thalassiosira eccentrica*	-	TiO_2 *via* atomic layer deposition	-	-	[41]
Aulacoseira	-	TiO_2 *via* proteamine-mediated layer-by-layer	-	H_2 sensor	[42]
Diatomaceous earth	-	Ag *via in situ* nanoparticle synthesis	-	-	[43]
Diatomaceous earth	-	Au *via* electroless deposition	-	4-NP catalysis	[44]
Synedra *Navicula*		Au *via* DNA hybridisation	Silane/crosslinker/DNA	DNA hybridisation Au nanoparticle assembly	[45]
Pinnularia	Adsorption onto glass	Ag *via* self assembly	-	SERS detection of rhodamine 6G	[46]
Pinnularia	Adsorption onto glass	Ag *via* self assembly	Silane/Ag NP/IgG	SERS detection of DTNB-labelled anti-IgG	[47]
Eucampia zodiacus	-	Ag, Pt and Au *via* layer-by-layer or covalent binding	-	SERS, catalysis and SEM improvement	[48]
Diatomaceous earth	-	Polyaniline *via* polymerisation	-	-	[49]
Diatomaceous earth	-	Epoxy-based polymer *via* polymerisation	-	-	[50]
Thalassiosia weissflogii		Polymer *via* grafting and polymerisation	-	-	[51]

(Continued)

Diatom	Immobilisation	Modification	Bio/functionalisation	Application	Ref.
Aulacoseira	-	Polymer *via* grafting and polymerisation	Silane/polymer/levofloxacin	Drug delivery	[52]
Fresh water diatoms	-	PVP-Au *via* adsorption	-	Au nanoparticle assembly	[53]
Aulacoseira	-	ZrO_2 *via* sol-gel process	-	-	[54]
Aulacoseira	-	SnO_2 *via* sol-gel process	-	NO sensor	[55]
Aulacoseira	-	Fe_3O_4 *via* sol-gel process	-	As removal from water	[56]
Aulacoseira	-	Au, Cu, Au/Cu, CuO or Ni-P *via* layer-by-layer and electroless deposition	-	-	[57]
Aulacoseira *Coscinodiscus asteromphalus* *Amphora* *Navicula ramossisima* *Skeletonema*	-	Au *via* layer-by-layer and electroless deposition	-	-	[58]
	-	GO *via* direct esterification	-	Electrochemical detection of cationic biomolecules	[59]
Diatomaceous earth *Aulacoseira*	-	GO *via* covalent or electrostatic interaction	Silane/GO/indomethacin	Drug delivery	[60]
Diatomaceous earth	-	Amino groups via silanisation and GO *via* immersion, followed by freeze-drying for aerogel composite formation	-	Hg^{2+} removal from water	[61]
Diatomaceous earth	-	C *via* sucrose polymerisation and carbonisation	-	-	[62] [63]
Diatomaceous earth	-	Fe_3O_4 nanoparticles *via* electrostatic interaction	Fe_3O_4/dopamine/indomethacin	Drug delivery	[64]

(Continued)

Diatom	Immobilisation	Modification	Bio/functionalisation	Application	Ref.
Diatomaceous earth	-	Fe_3O_4 nanoparticles *via* HSA-mediated electrostatic interaction	Fe_3O_4/HSA-dopamine/drug mimic	Drug delivery Tumor imaging	[65]
Nitzschia frustulum	-	Si-Ge *via* culture method	-	-	[66] [67]
Pinnularia		Si-Ge *via* culture method		-	[68] [69]
Pinnularia	-	TiO_2 *via* culture method	-	-	[70]
Coscinodiscus wailesii	-	-	Silane/crosslinker/protein A/MAb	Fluorescence detection of rhodamine-labelled antigen	[73]
Coscinodiscus concinnus	-	-	Silane/crosslinker/protein A/MAb	Photoluminescence detection of antigen	[74]
Coscinodiscus wailesii	-	-	Silane/crosslinker/anti-IgY	Tubulin detection Antigen discrimination Immunoprecipitation	[75]
Cyclotella sp.	-		Silane/crosslinker/IgG	Photoluminescence detection of antigen	[76]
Fresh water diatoms	-	-	Silane/crosslinker/tyrosinase	Phenolic compounds removal from wastewater	[77]

3. Diatom modification

The silica shell of diatoms provides them a perfectly ordered, symmetrical and 3D structure, with thermal and mechanical stability, biocompatibility and unique optical properties. However, their poor electrical properties make difficult their use in electrochemical biosensors. SiO_2-based diatom frustules can be converted into new materials with additional attractive features, such as high electrical conductivity, catalytic activity and/or optical properties that can be exploited in the development of electrochemical as well as optical biosensors.

Several approaches have been used to change the composition of diatom frustules while preserving their 3D morphologies. These processes, referred collectively as BaSIC (Bioclastic and Shape-preserving Inorganic Conversion), merge the attractive characteristics of nature with the chemical versatility of synthetic processes, providing a promising route towards mass production of nanostructured devices with complex 3D shapes and tailored chemistries. Changes in diatom composition include the direct processing of frustules, where frustules made of a new material are directly prepared by means of displacement reactions, or the use of frustules as templates, where coating methods are performed to produce composite frustules. If the coating is continuous and rigid, but does not fill or coat the nanopores, frustules can be selectively removed (e.g. by selective dissolution) to yield a replica with the desired composition. This replica retains the 3D features of the starting diatom template and features new material properties. In other cases, coating methods are used to replicate the pore patterns of the diatom frustules and obtain inverse replicas with the same multi-level pore and nanoscale precision as the original frustules.

Nevertheless, although most described works focus on preserving the three-dimensional structure of the frustules as much as possible, the ability to control and modify the pore size and morphology of the frustules, in addition to the chemical composition, can bestow the potential to tailor structural, photonic, absorptive, diffusion and mechanical properties of diatom frustules to suit particular applications. With this aim, the controlled modification of diatoms morphology has also been explored.

This section is divided into different methods that allow the modification of the properties of the frustules, specially their chemical composition, which include gas/silica displacement reactions, coatings, combination of both and culture methods that exploit the composition of the culture medium as a parameter to tune diatom features. Figure 2 represents bare and coated diatoms, as well as replicas and inverse replicas obtained by means of these processes.

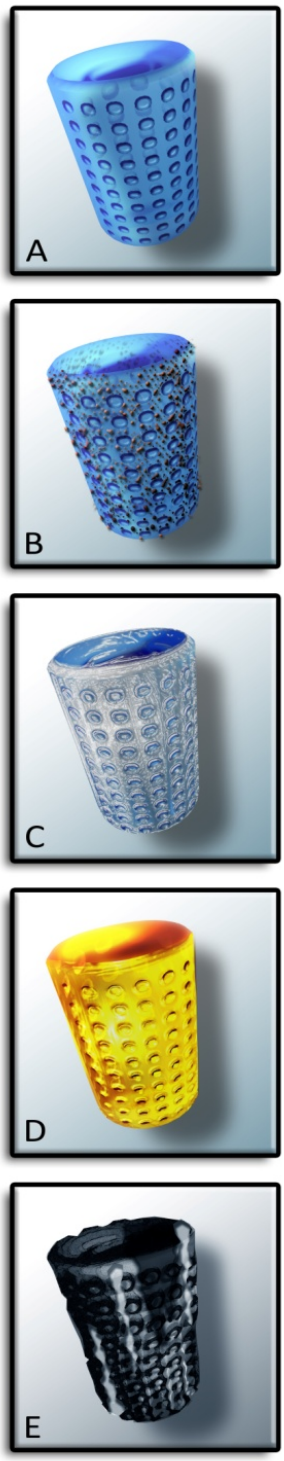

Figure 2. Bare diatom (A), diatom coated with nanoparticles (B), diatom coated with a polymer (C), gold replica (D), and carbon inverse replica (E).

3.1. Gas/solid displacement reactions

Gas/SiO_2 displacement reactions were used to convert SiO_2-based diatom frustules into new material replicas retaining their natural morphology. Solid SiO_2 coming from diatom frustules was transformed into solid MgO and Si, by placing the frustules in an atmosphere of Mg gas at 900 °C for 4 h (magnesiothermic reduction) [25]. Mg from MgO/Si-bearing replicas was further dissolved to obtain new Si replicas of frustules [24, 26, 27]. These Si replicas have been used for different applications, e.g. as impedance sensors for the detection of gaseous NO [26], as nanostructured photoelectrodes for current generation from solar energy [24] and as degradable drug microcarriers [27].

Using a different gas/SiO_2 displacement reaction, SiO_2-based diatom frustules were also converted into a new TiO_2 nanocrystalline material [28]. Going further, ZrO_2 replicas were produced by series of gas/solid displacement reactions, first converting frustules into MgO replicas and then exposing them to $ZrCl_4$ gas to form ZrO_2 by a metathetic displacement reaction [29].

3.2. Combined use of displacement reactions and coating methods

In some cases, the composition of the native frustule may not be chemically compatible with a desired coating material. Displacement reactions are then needed prior to the coating. By this method, new frustules composed of Zn_2SiO_4 [30], $BaTiO_3$ [31], Ag, Au, Pd [32], C or Pt/C [33] were obtained. Further, C replicas were converted into porous Au-bearing replicas by a series of electroless metal deposition reactions [34]. In this case, the excellent catalytic activity was clearly appreciated when used as glucose oxidase (GOx) immobilisation supports in a flow system.

3.3. Coating methods

Gas/solid displacement reactions are very effective to obtain diatomaceous replicas which retain the 3D features of the frustules, but they are limited to gaseous reactants capable of reducing SiO_2 or converting SiO_2 into a halide product. Here, other approaches based on coating the frustules with metal nanoparticles or thin films, polymers, carbon-based materials and/or magnetic nanoparticles are reported, providing both composites and replicas with new properties that promote their use in multiple applications.

3.3.1. Coating with metals

The first works focused on coating diatoms were performed with zeolites. Deposition and growth of zeolites on diatoms was achieved by different approaches: hydrothermal growth [35], layer-by-layer [36] and vapour-phase transport [37]. During the hydrothermal treatment, zeolite crystals may overgrowth and block the submicron pores of the diatomite (fossilised remains of diatoms). The layer-by-layer technique allows easy control of the coating thickness and composition, but the zeolite content in the final samples is very low. The vapour-phase transport better preserves the porosity of the frustules, the zeolite content reaching values even higher than 50%. Zeolitisation of diatomite provides materials with ion exchange and catalytic properties.

MnO_2 replicas coming from three different diatom species have been synthesised by a template-assisted hydrothermal process [38]. The purified diatom material was dispersed into a $KMnO_4$ solution and then maintained at 160 °C for 24 h. The SiO_2 cores were then removed with NaOH. Although pores of certain diatom genera were blocked using this method, the replicas showed excellent electrochemical properties, such as high specific capacitance, and good cyclability and rate capability, demonstrating a promising application as supercapacitors.

Otherwise, thermal evaporation of Ti and Ag onto a diatom-coated substrate provided Ag-coated diatoms, which were subsequently converted to Ag diatom replicas by removing the SiO_2 frustule and the Ti layer via HF treatment [39]. Using the same method, Au was evaporated over a silicon wafer with deposited diatoms [40]. The metal condensed inside the pores, resulting in inverse Au replicas after mechanically stripping off the diatom frustules jointly with the wafer.

The incorporation of metals into diatom structures has also been performed to modify the pore size and morphology of diatoms. The work presented by Losic et al. [41] is a clear example. Here, ultrathin films of TiO_2 were deposited on two centric diatom species by atomic layer deposition. By increasing the number of deposition cycles, the thickness of TiO_2 films increased and, consequently, the size of the sieve pores was reduced from 43 to less than 5 nm. This enables to tune the reduction of the pores while preserving the original 3D shape and geometry, providing scope to enhance the potential filtering properties of frustule membranes, and to retain the unique surface chemistry provided by the TiO_2 coating.

A special approach to obtain TiO_2-frustules was based on the iterative exposition to a silica-binding, titania-forming protein (protamine) and an aqueous titania precursor to generate a conformal and continuous TiO_2 coating on the biosilica template. Upon organic pyrolysis and SiO_2 dissolution with NaOH, TiO_2 replicas were

obtained [42]. This TiO_2 coating allowed the sensitive electrochemical detection of hydrogen.

Diatom frustules have also been decorated with metal nanoparticles by *in situ* synthesis. Toster et al. [43] immersed frustules into an $AgNO_3$ solution and added NaOH to facilitate the reduction process and the subsequent synthesis of Ag_2O nanoparticles (10 to 20 nm in size) on the diatom surface, which were then readily reduced by glucose. Ag-coated frustules were further immersed into an Au plating solution to obtain Au replicas, after removal of the silica by HF, with excellent catalytic properties, as demonstrated in the reduction of 4-nitrophenol (4-NP) to 4-aminophenol (4-AP) in the presence of $NaBH_4$ [44].

A particular case is that in which thiolated DNA was immobilised on amino-silanised diatom frustules through a hetero-bifunctional crosslinker and then hybridised with a complementary DNA strand bearing 13-nm Au nanoparticles [45]. Up to seven nanoparticle layers were added by iterative cycles of nanoparticle assembling and sequence-specific hybridisation process, with no aggregation phenomena being observed.

The importance of the use of diatom frustules modified with metal nanoparticles as biosensor materials has been previously demonstrated by several authors. As an example, Ren et al. [46] proved the self-ordered deposition of Ag nanoparticles onto the frustules and inside their pores by exposing amino-functionalised *Pinnularia* sp. diatoms to an Ag colloidal suspension. This configuration allowed the SERS detection of the model compound rhodamine 6G with four times higher intensity than when using glass as a substrate. The same group used the diatom frustules decorated with the self-assembled Ag nanoparticles in a SERS sandwich immunoassay and attained a detection limit of 10 pg/mL of mouse IgG, two orders of magnitude better than that obtained on flat glass substrates [47]. Another work demonstrated that the attachment of Ag, Au and Pt nanoparticles on diatom frustules improved sensitivity in SERS and quality in SEM imaging, and also catalysed the redox reaction between hexacyanoferrate (III) and thiosulfate [48]. With this in mind, there is no doubt that coating of diatoms frustules with metal nanoparticles is of high interest for the development of both optical and electrochemical biosensors.

3.3.2. Coating with polymers

Polymers have been used to coat diatom frustules, providing thermal, mechanical or conductive properties among others. Li et al. [49] obtained polyaniline-coated frustules by oxidative polymerisation. The polyaniline was bound to the diatom

surface by hydrogen bonds between the electronegative surface of the frustule and amine groups from polyaniline. Results indicated that the coated frustules only contained 8% of polymer, but it was enough to provide conductivity to the diatoms. Polymeric frustule replicas were generated by Gaddis and Sandhage [50], who immersed diatom frustules into polymer solutions to afterwards evaporate the solvent and remove the silica by HF.

Grafting methods have been used to introduce a hyperbranched copolymer onto the diatom surface [51, 52]. Diatoms were first modified with 2-bromoisobutyril bromide for the grafting of the copolymer. Subsequent cross-linking of the vinyl groups of the co-polymer generated a rigid and stable coating, which allowed silica removal by incubation in KOH [51]. Recently, surface-initiated atom transfer radical polymerisation has been employed to graft thermo-responsive copolymers of oligo(ethyleneglycol)methacrylates from the surface of diatom frustules [52]. The application of the resulting composites for temperature-controlled drug delivery was demonstrated.

Although polymer-coated diatoms have only been applied to drug delivery, the approach has huge potential in biosensors to provide diatoms with tailored electrical properties and enhanced electron transfer.

3.3.3. Coating with polymers/metals

Diatoms have been coated with Au nanoparticles by immersing the frustules into a poly(vinylpyridine) (PVP) solution and then exposing the polymer-coated diatoms to an $HAuCl_4$ solution [53]. Au nanoparticles (10 to 50 nm in size) were regiospecifically assembled taking advantage of the interaction between the pyridyl groups of PVP with metals and the wettability/dewettability nature of PVP according to the pH. Whereas under acidic conditions the PVP swelled favouring the formation of a PVP film on the diatom surface and the subsequent growth of Au nanoparticles randomly distributed on the frustule, basic conditions resulted in the PVP film to dewet the surface and relocate on the pores, where Au nanoparticles were then synthesised.

Another combination of polymerisation process and metal incorporation has been reported by Zhao et al. [54]. Here, a sol-gel process with a zirconium alkoxide-bearing solution was performed to coat the frustules with a metal thin layer. After SiO_2 dissolution by immersion into a NaOH solution, the subsequent nanocrysalline ZrO_2 replicas were obtained.

Previous functional groups density enrichment of the native frustule surface has been demonstrated to improve the coating process by ensuring the continuity of

the film. Surface hydroxyl amplification was performed through a sequential deposition of silanes and hyperbranched multi-layers of acrylate/amine, followed by the addition of hydroxyl-rich amines [55, 56]. The subsequent sol-gel process with a metal solution yielded a thin conformal coating of nanocrystalline SnO_2 [55] or Fe_3O_4 [56]. SnO_2-coated frustules were used as NO gas detectors, while Fe_3O_4-coated frustules were demonstrated to exhibit high specific adsorption for As(V) and As(III) ions in a circulating filter system. Binding of metal chloride catalysts to the intermediate amine groups obtained during the polyacrylate/polyamine deposition also enabled the rapid electroless deposition of different thin coatings on the frustules [57, 58]. SiO_2 dissolution of the frustules by HF yielded monolithic (Au, Cu), multilayer (Au/Cu) and homogeneous multicomponent (Ni-P, CuO) replicas. As an example of use, Au replicas showed extraordinary optical transmission arising from the combined effects of the quasi-periodic hexagonal porous structure inherited from the diatom frustule and the gold chemistry [58].

3.3.4. Coating with carbon-based materials

The broad range of physical and chemical properties of carbon nanomaterials is responsible for the increasing interest in their incorporation into biosensor configurations. Among them, graphene attracts special attention due to its excellent electrical conductivity. Regarding this, graphene oxide (GO) was bound to diatom SiO_2 via direct esterification reaction [59]. Electrochemical measurements by cyclic voltammetry revealed that GO-diatom SiO_2 has a negatively charged surface and can be used as an electrode. Similarly, Kumeria et al. [60] fabricated nano-hybrid materials through covalent coupling or electrostatic interactions between GO sheets and amino-silanised diatomaceous earth. The composites showed interesting photoluminescence properties with promising biosensing applications. Additionally, their application to load indomethacin (IMC), a poorly water-soluble drug used as a model, and sustain its pH-sensitive release was demonstrated. In a recent work, graphene-diatom aerogels have been obtained by freeze-drying, with high efficiency for mercury removal from water [61].

The production of carbon inverse replicas has also been pursued. The void spaces of the SiO_2 template were filled with sucrose by impregnation, which was then polymerised and carbonised. SiO_2 was finally dissolved with a NaOH solution, obtaining a negative structure of the frustules produced in carbon [62, 63]. Changes in the pore architecture were observed with repeated sucrose impregnation.

Carbon-coated diatoms and carbon inverse replicas have not been applied to the development of biosensors yet. Nevertheless, taking into account the considerable number of reported biosensors integrating carbon nanomaterials (mainly carbon

nanotubes, graphene and GO) and nanoporous structures, it is safe to say that this application will be explored soon.

3.3.5. Coating with magnetic nanoparticles

Diatoms have also been modified with magnetic nanoparticles to confer magnetic properties. Dopamine (DOPA)-modified Fe_3O_4 nanoparticles (20 nm in diameter) were assembled onto the diatom surface by electrostatic interactions [64]. DOPA was used because it forms a stable and robust cationic anchor on the surface of Fe_3O_4 and because its primary amine can be used as the reaction site to covalently immobilise biomolecules of interest, as it was demonstrated by the labelling of diatoms with fluorescein isothiocyanate (FITC). The application of DOPA/Fe_3O_4-functionalised diatoms as magnetically guided drug delivery microcarriers was demonstrated by the loading of IMC into the diatoms and the subsequent sustained release over 2 weeks. Going a step further, Todd et al. [65] used similar magnetic nanoparticle-modified diatoms as drug carriers *in vitro* and *in vivo* using murine breast cancer cells and mice, respectively. Several dyes (drug mimics) were used to demonstrate by means of the imaging technology the multiple applications of magnetic diatoms.

Regarding biosensing applications, although not yet tested, diatoms coated with magnetic nanoparticles are conductive to be easily captured on the transducer by an external magnetic field, as well as to be used for immunomagnetic purification and concentration procedures.

3.4. Culture methods

Diatom cultivation can also be explored as a relevant step in the micro- and nanofabrication of structures based on diatom SiO_2, tuning their structure, chemical composition and pore size by changing the culture medium. Regarding this, Rorrer's research group demonstrated that the addition of $Ge(OH)_4$ or GeO_2 in the culture medium resulted in the biosynthesis of nanostructured Si-Ge oxides in the frustules of the diatom *Nitzschia frustulum* [66, 67] and *Pinnularia* sp. [68, 69]. Ge-doped diatom frustules showed electroluminescence and photoluminescence properties [67, 69]. In another work, $Ti(OH)_4$ was added to the medium and incorporated into diatoms, with no detrimental effects on cell growth and frustule morphology [70]. Townley et al. [71] reported that the presence of $NiSO_4$ in the culture increased twice the size of the pores of *Coscinodiscus wailesii* and quenched the intrinsic photoluminescence of the amorphous SiO_2. Finally, the addition of $HAuCl_4$ into the culture medium also resulted in the synthesis of Au nanoparticles, which were

associated with the diatom frustules but also with extracellular polysaccharides excreted by the diatom cells [72]. These methods can be used not only to coat diatom frustules with nanomaterials, but also to synthesise such nanomaterials in a simple, effective, low-cost and environmentally friendly way.

4. Diatom biofunctionalisation

Diatoms feature large surface area and pore volume thanks to their high porosity, which favour high ratios of encapsulated or immobilised sensing molecules per diatom, reducing times and lowering detection limits. Because of the biocompatible nature of SiO_2, in principle any type of biomolecule can be conjugated to diatom frustules. Almost all immobilisation protocols start with an acidic activation followed by a chemical reaction with silanes that contain functional groups for the subsequent biomolecule conjugation. Figure 3 summarises different strategies to functionalise diatom frustules with oligonucleotides, antibodies or enzymes.

As previously mentioned, Rosi et al. [45] used an amino-terminated silane to introduce amine groups on the diatom surface, which were afterwards coupled to a fluorophore-labelled thiolated DNA by using a heterobifunctional crosslinking agent (Fig. 3A). Fluorescence measurements demonstrated the covalent immobilisation of DNA onto the surface of the frustules. These oligonucleotides were then used as templates for the assembly of Au nanoparticles, which had been previously functionalised with complementary DNA strands. This work anticipated the possible use of functionalised diatoms in DNA sensing systems as well as in SERS measurements.

Diatom frustules have also been functionalised with antibodies. Amino-silanised *Coscinodiscus wailesii* frustules were coupled to protein A using glutaraldehyde as a crosslinker [73, 74]. Herein, a murine monoclonal antibody with specific reactivity towards human thymocytes was bound through its Fc region to protein A, providing oriented immobilisation and thus free access to antigen-binding domains. Fluorescence [73] and photoluminescence [74] measurements demonstrated that the antibodies linked to the SiO_2 surface retain their binding affinity. Townley et al. [75] also coupled antibodies to amino-silanised diatoms using two different strategies. In the first approach, a heterobifunctional crosslinker with an *N*-hydroxysuccinimide (NHS) ester and a photoactivatable nitrophenyl azide was used to link a rabbit anti-IgY antibody to the amino-silanised diatom. Nevertheless, to provide site-specific antibody immobilisation and retain its biological activity, a second strategy focused on the antibody attachment via the carbohydrate moieties on the Fc region of mouse anti-tubulin antibodies was approached. Upon oxidation of the hydroxyl groups of the sugar residue to form aldehydes, the antibody was

bound to the amino groups of the diatom surface, reaction favoured by the addition of $NaBH_4$. In both approaches, HRP-labelled secondary antibody was added, and a subsequent chemiluminescence enzyme reaction demonstrated that the immobilisation process was successful. Furthermore, the frustule surface was used to tether two different antibodies, a rabbit serum and a purified IgY, which were then incubated with Cy5-conjugated anti-rabbit antibody and FITC-conjugated anti-IgY and detected by confocal microscopy. This work demonstrated that different antibodies can be successfully attached and detected on the surface of a single diatom, providing a cheap and disposable system to discriminate between antigens. An alternative exploitation proposed in this work was based on the use of rat anti-tubulin antibodies bound to diatom silica for immunoprecipitation. The technique allows the selective precipitation of tubulin from a complex mixture that can be brought out of the solution thanks to the solid phase matrix that provides the frustule. As a last example, Gale et al. [76] functionalised *Cyclotella* sp. diatom frustules with rabbit IgG by covalent binding to amine groups on the silanised frustules through a succinimidyl crosslinking agent (Fig. 3B). The nucleophilic IgG antibody intensified the intrinsic blue photoluminescence of diatom biosilica by a factor of 6, which was further increased by a factor of 3 when goat anti-rabbit IgG was added (no increase was observed when goat anti-human IgG was used). The *N. soratensis* diatoms of the array described in section 2 were also functionalised with rabbit IgG by silanisation of the frustule surfaces [23]. After incubation with fluorescent secondary anti-rabbit IgG, the multi-layer *C. argus – N. soratensis* array produced an enhancement effect on the fluorescence intensity, at least 2.7 times stronger than those configurations with only one type of diatom frustules.

Diatom micro and nanopores were interestingly explored as nanowells of a sensing platform [18]. Here, two biotinylated monoclonal antibodies against two cardiovascular biomarkers proteins (C-reactive protein and myeloperoxidase) were bound not to the frustule, but to the streptavidin-modified gold surface at the base of the nanowells formed by the immobilisation of *Coscinodiscus wailesii* onto an electrode. To detect antibody-antigen interactions, changes in the impedance were recorded. The use of nanopores as nanowells enhanced diffusion of fluids providing faster response times and higher sensitivities in the simultaneous detection of both biomarkers.

Enzymes are another example of biomolecules that have been bound to diatom silica. Tyrosinase was immobilised by covalent binding on amino-silanised frustules activated with glutaraldehyde, providing high stability to the enzyme [77] (Fig. 3C). The obtained biosilica was applied to the enzymatic removal of phenolic compounds from wastewater.

Although the biofunctionalisation methods described above are based on the chemical attachment of biomolecules to diatom frustules, Kröger's research group explored a different approach for protein immobilisation based on genetic manipulation of the biological SiO_2-forming machinery [78, 79]. Their approach was based on the incorporation and expression of fusion proteins, consisting on silaffins and enzymes, in the genome of the diatoms. The process allowed the immobilisation of both monomeric simple enzymes, such as the bacterial enzyme hydroxylaminobenzene mutase [78], and other enzymes with more complex activity requirements, such as β-glucuronidase, glucose oxidase, galactose oxidase and horseradish peroxidase, in the small diatom *Thalassiosira pseudonana* [79] . In principle, such process could also provide the direct expression of antibodies or other functional biomolecules onto the nanostructured biosilica during diatom cell wall biosynthesis, resulting in novel functional materials. However, although it can result in more stable conjugates, it is difficult to compete with the simplicity and the broad possibilities offered by the tethering of biomolecules *in vitro*.

The review demonstrates the feasibility to modify diatoms with biomolecules, that retain their functionality upon conjugation. The use of these conjugates in biosensing will certainly contribute to greatly enhance analytical performance of the final devices and thus this is a field of research that deserves further work.

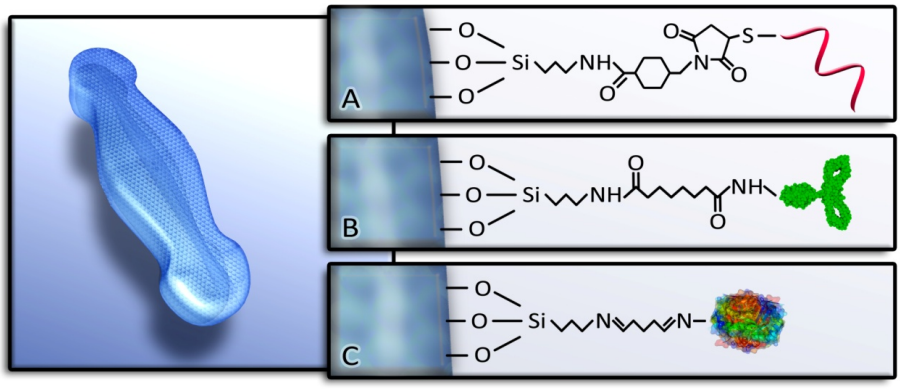

Figure 3. Diatom biofunctionalisation with an oligonucleotide (A), an antibody (B), and an enzyme (C).

5. Conclusions

The use of diatoms as building blocks of biosensor platforms is an incipient and still poorly explored niche. Although a few examples can be found in the literature, more effort is required to boost the advantages rendered by combining the tailored immobilisation, modification and biofunctionalisation of diatom frustules.

The diatom immobilisation method should maintain the nanofeatures of the frustules, while providing a high immobilisation yield, a correct orientation and an appropriate spatial distribution over the support. Gentle conditions are preferred, since high pressure or temperature may disrupt the 3D nanostructure. Our group is working on an electrochemical method to address diatom frustules towards specific array sites by means of gold electrodeposition. Preliminary results have demonstrated the addressed immobilisation of diatoms of different genera (*Coscinodiscus* and *Grammatophora*) on carbon and gold electrodes produced by screen-printing and photolithography techniques.

Much more exhaustive is the work aimed at tailoring the composition of diatom frustules to confer them specific properties. Again, the morphology should be preserved and thus, a strict control of the process is necessary. Gas/solid displacement reactions, coating with metals, polymers, carbon-based materials and magnetic nanoparticles, and combinations of both have been described. Incorporation of metal salts into the medium during the diatom culture has also been carried out to a minor extent. As a result, composites of new materials and replicas or inverse replicas are obtained. The wide variety of materials that have been produced provides a solid foundation to achieve any desired modification.

Due to the reactive Si-OH groups that coat the frustule, a variety of moieties can be introduced on the diatoms through well-established chemistries that facilitate the tethering of biomolecules. Mainly antibodies, but also oligonucleotides and enzymes, have been linked to diatoms, almost always through silanisation of the frustules and subsequent chemical binding. The site-specific immobilisation of biomolecules on the frustules has been pursued in some cases to preserve their functionality.

The large surface area of diatom frustules with their porous hierarchical nanostructure makes them a promising platform for the development of biosensors, enhancing the diffusion of species through the highly branched network of micro and nanopores and thus increasing the sensing sensitivity. Additionally, diatom frustules can act as physical filters and decrease the matrix effects in practical applications. The wide variety of diatom shapes, sizes and geometries bestows a great flexibility in the design of biosensors and advantages in terms of easiness and rapidity of analysis, low-cost and eco-sustainability.

Summarising, recent advances in frustules immobilisation, modification and functionalisation have provided successful outcomes, and now emphasis should be focused on merging the advantages of the three processes in order to make a qualitative leap forward to the use of diatoms as natural nanostructured supports in biosensing platforms.

Acknowledgements

The authors acknowledge financial support from the *Ministerio de Economía y Competitividad* through the DIANA (BIO2011-26311) and the SEASENSING (BIO2014-56024-C2-2-R) projects. The authors also acknowledge Marc Cirera (www.science.marccirera.com) for the illustrations. Sandra Leonardo acknowledges scholarship from IRTA – Universitat Rovira i Virgili – Banco Santander.

References

[1] R. Gordon, B.D. Aguda, Diatom morphogenesis - Natural fractal fabrication of a complex microstructure, in: G. Harris, C. Walker (Eds.), Proceedings of the Annual International Conference of the IEEE Engineering in Medicine and Biology Society, Part 1/4: Cardiology and Imaging, New Orleans, 1988, pp. 273-274.

[2] R.W. Drum, R. Gordon, Star trek replicators and diatom nanotechnology, Trends Biotechnol., 21 (2003) 325-328.

[3] R.R. Naik, M.O. Stone, Integrating biomimetics, Mater. Today, 8 (2005) 18-26.

[4] P.J. Lopez, J. Descles, A.E. Allen, C. Bowler, Prospects in diatom research, Curr. Opin. Biotech., 16 (2005) 180-186.

[5] A.R. Parker, H.E. Townley, Biomimetics of photonic nanostructures, Nat. Nanotechnol., 2 (2007) 347-353.

[6] I.C. Gebeshuber, Biotribology inspires new technologies, Nano Today, 2 (2007) 30-37.

[7] N.J. Halas, Nanoscience under glass: The versatile chemistry of silica nanostructures, ACS Nano, 2 (2008) 179-183.

[8] R. Gordon, D. Losic, M.A. Tiffany, S.S. Nagy, F.A.S. Sterrenburg, The glass menagerie: Diatoms for novel applications in nanotechnology, Trends Biotechnol., 27 (2009) 116-127.

[9] D. Losic, J.G. Mitchell, N.H. Voelcker, Diatomaceous lessons in nanotechnology and advanced materials, Adv. Mater., 21 (2009) 1-12.

[10] N. Nassif, J. Livage, From diatoms to silica-based biohybrids, Chem. Soc. Rev., 40 (2011) 849-859.

[11] T. Fuhrmann, S. Landwehr, M. El Rharbi-Kucki, M. Sumper, Diatoms as living photonic crystals, Appl. Phys. B-Lasers Opt., 78 (2004) 257-260.

[12] W.R. Yang, P.J. Lopez, G. Rosengarten, Diatoms: Self assembled silica nanostructures, and templates for bio/chemical sensors and biomimetic membranes, Analyst, 136 (2011) 42-53.

[13] J.E.N. Dolatabadi, M. de la Guardia, Applications of diatoms and silica nanotechnology in biosensing, drug and gene delivery, and formation of complex metal nanostructures, TRAC-Trends Anal. Chem., 30 (2011) 1538-1548.

[14] Y. Wang, J. Cai, Y.G. Jiang, X.G. Jiang, D.Y. Zhang, Preparation of biosilica structures from frustules of diatoms and their applications: Current state and perspectives, Appl. Microbiol. Biotechnol., 97 (2013) 453-460.

[15] C. Jeffryes, S.N. Agathos, G. Rorrer, Biogenic nanomaterilas from photosynthetic microorganisms, Curr. Opin. Biotechnol., 33 (2015), 23-31.

[16] K. Umemura, Y. Noguchi, T. Ichinose, Y. Hirose, R. Kuroda, S. Mayama, Diatom cells grown and baked on a functionalized mica surface, J. Biol. Phys., 34 (2008) 189-196.

[17] W. Wang, T. Gutu, D.K. Gale, J. Jiao, G.L. Rorrer, C.H. Chang, Self-assembly of nanostructured diatom microshells into patterned arrays assisted by polyelectrolyte multilayer deposition and inkjet printing, J. Am. Chem. Soc., 131 (2009) 4178-4179.

[18] K.C. Lin, V. Kunduru, M. Bothara, K. Rege, S. Prasad, B.L. Ramakrishna, Biogenic nanoporous silica-based sensor for enhanced electrochemical detection of cardiovascular biomarkers proteins, Biosens. Bioelectron., 25 (2010) 2336-2342.

[19] D.Y. Zhang, J.F. Pan, J. Cai, Y. Wang, Y.G. Jiang, X.G. Jiang, Hydrofluoric acid-assisted bonding of diatoms with SiO_2-based substrates for microsystem application, J. Micromech. Microeng., 22 (2012).

[20] J.F. Pan, Y. Wang, J. Cai, A.B. Li, H.Y. Zhang, Y.G. Jiang, D.Y. Zhang, Bonding of diatom frustules and Si substrates assisted by hydrofluoric acid, New J. Chem., 38 (2014) 206-212.

[21] Y. Wang, J.F. Pan, J. Cai, A.B. Li, M.L. Chen, D.Y. Zhang, Assembling and patterning of diatom frustules onto PDMS substrates using photoassisted chemical bonding, Chem. Lett., 40 (2011) 1354-1356.

[22] A.B. Li, J. Cai, J.F. Pan, Y. Wang, Y. Yue, D.Y. Zhang, Multi-layer hierarchical array fabricated with diatom frustules for highly sensitive bio-detection applications, J. Micromech. Microeng., 24 (2014).

[23] J.F. Pan, J. Cai, D.Y. Zhang, Y. Wang, Y.G. Jiang, Micro-arraying of nanostructured diatom microshells on glass substrate using ethylene-vinyl acetate copolymer and photolithography technology for fluorescence spectroscopy application, Physica E, 44 (2012) 1585-1591.

[24] S. Chandrasekaran, M.J. Sweetman, K. Kant, W. Skinner, D. Losic, T. Nann, N.H. Voelcker, Silicon diatom frustules as nanostructured photoelectrodes, Chem. Commun, 50 (2014) 10441-10444.

[25] K.H. Sandhage, M.B. Dickerson, P.M. Huseman, M.A. Caranna, J.D. Clifton, T.A. Bull, T.J. Heibel, W.R. Overton, M.E.A. Schoenwaelder, Novel, bioclastic route to self-assembled, 3D, chemically tailored meso/nanostructures: Shape-preserving reactive conversion of biosilica (diatom) microshells, Adv. Mater., 14 (2002) 429-433.

[26] Z.H. Bao, M.R. Weatherspoon, S. Shian, Y. Cai, P.D. Graham, S.M. Allan, G. Ahmad, M.B. Dickerson, B.C. Church, Z.T. Kang, H.W. Abernathy, C.J. Summers, M.L. Liu, K.H. Sandhage, Chemical reduction of three-dimensional silica micro-assemblies into microporous silicon replicas, Nature, 446 (2007) 172-175.

[27] S. Maher, M. Alsawat, T. Kumeria, D. Fathalla, G. Fetih, A. Santos, F. Habib, D. Losic, Luminescent silicon diatom replicas: Self-reporting and degradable drug carriers with biologically derived shape for sustained delivery of therapeutics, Adv. Funct. Mater., 25 (2015) 5107-5116.

[28] R.R. Unocic, F.M. Zalar, P.M. Sarosi, Y. Cai, K.H. Sandhage, Anatase assemblies from algae: Coupling biological self-assembly of 3-D nanoparticle structures with synthetic reaction chemistry, Chem. Commun., (2004) 796-797.

[29] S. Shian, Y. Cai, M.R. Weatherspoon, S.M. Allan, K.H. Sandhage, Three-dimensional assemblies of zirconia nanocrystals via shape-preserving reactive conversion of diatom microshells, J. Am. Ceram. Soc., 89 (2006) 694-698.

[30] Y. Cai, K.H. Sandhage, Zn_2Sio_4-coated microparticles with biologically-controlled 3D shapes, Phys. Status Solidi A, 202 (2005) 105-107.

[31] M.R. Weatherspoon, S.M. Allan, E. Hunt, Y. Cai, K.H. Sandhage, Sol-gel synthesis on self-replicating single-cell scaffolds: applying complex chemistries to nature's 3-D nanostructured templates, Chem. Comm., 651 (2005) 651-653.

[32] Z.H. Bao, E.M. Ernst, S. Yoo, K.H. Sandhage, Syntheses of porous self-supporting metal-nanoparticle assemblies with 3D morphologies inherited from biosilica templates (diatom frustules), Adv. Mater., 21 (2009) 474-478.

[33] Z.H. Bao, M.K. Song, S.C. Davis, Y. Cai, M.L. Liu, K.H. Sandhage, High surface area, micro/mesoporous carbon particles with selectable 3-D biogenic morphologies for tailored catalysis, filtration, or adsorption, Energ. Environmen. Sci., 4 (2011) 3980-3984.

[34] S.C. Davis, V.C. Sheppard, G. Begum, Y. Cai, Y.N. Fang, J.D. Berrigan, N. Kroger, K.H. Sandhage, Rapid flow-through biocatalysis with high surface area, enzyme-loaded carbon and gold-bearing diatom frustule replicas, Adv. Funct. Mater., 23 (2013) 4611-4620.

[35] M.W. Anderson, S.M. Holmes, N. Hanif, C.S. Cundy, Hierarchical pore structures through diatom zeolitization, Angew. Chem. Int. Ed., 39 (2000) 2707-2710.

[36] Y.J. Wang, Y. Tang, X.D. Wang, A.G. Dong, W. Shan, Z. Gao, Fabrication of hierarchically structured zeolites through layer-by-layer assembly of zeolite nanocrystals on diatom templates, Chem. Lett., (2001) 1118-1119.

[37] Y.J. Wang, Y. Tang, X.D. Wang, W. Shan, A.G. Dong, N. Ren, Z. Gao, Fabrication of hierarchical structured zeolitic materials through vapor-phase transforming of the seeded diatomite, Chem. Lett., (2002) 862-863.

[38] F. Li, Y. Xing, M. Huang, K.L. Li, T.T. Yu, Y.X. Zhang, D. Losic, MnO_2 nanostructures with three-dimensional (3D) morphology replicated from diatoms for high-performance supercapacitors, J. Mater. Chem. A, 3 (2015) 7855-7861.

[39] E.K. Payne, N.L. Rosi, C. Xue, C.A. Mirkin, Sacrificial biological templates for the formation of nanostructured metallic microshells, Angew. Chem. Int. Ed., 44 (2005) 5064-5067.

[40] D. Losic, J.G. Mitchell, N.H. Voelcker, Fabrication of gold nanostructures by templating from porous diatom frustules, New J. Chem., 30 (2006) 908-914.

[41] D. Losic, G. Triani, P.J. Evans, A. Atanacio, J.G. Mitchell, N.H. Voelcker, Controlled pore structure modification of diatoms by atomic layer deposition of tio2, J. Mater. Chem., 16 (2006) 4029-4034.

[42] Y.N. Fang, Q.Z. Wu, M.B. Dickerson, Y. Cai, S. Shian, J.D. Berrigan, N. Poulsen, N. Kroger, K.H. Sandhage, Protein-mediated layer-by-layer syntheses of freestanding microscale titania structures with biologically assembled 3-D morphologies, Chem. Mater., 21 (2009) 5704-5710.

[43] J. Toster, Q.L. Zhou, N.M. Smith, K.S. Iyer, F. Rosei, C.L. Raston, In situ coating of diatom frustules with silver nanoparticles, Green Chem., 15 (2013) 2060-2063.

[44] Y. Yu, J. Addai-Mensah, D. Losic, Synthesis of self-supporting gold microstructures with three-dimensional morphologies by direct replication of diatom templates, Langmuir, 26 (2010) 14068-14072.

[45] N.L. Rosi, C.S. Thaxton, C.A. Mirkin, Control of nanoparticle assembly by using DNA-modified diatom templates, Angew. Chem. Int. Ed., 43 (2004) 5500-5503.

[46] F. Ren, J. Campbell, X. Wang, G.L. Rorrer, A.X. Wang, Enhancing surface plasmon resonances of metallic nanoparticles by diatom biosilica, Opt. Express, 21 (2013) 15308-154313.

[47] J. Yang, L. Zhen, F. Ren, J. Campbdell, G.L. Rorrer, A.X. Wang, Ultra-sensitive immunoassay biosensors using hybrid plasmonic-biosilica nanostructured materials, J. Biophotonics, 8 (2015) 659-667.

[48] A. Jantschke, A.K. Hermann, V. Lesnyak, A. Eychmüller, E. Brunner, Decoration of diatom biosilica with noble metal and semiconductor nanoparticles (<10 nm): Assembly, characterization, and applications, Chem. Asian. J., 7 (2012) 85-90.

[49] X.W. Li, C.Q. Bian, W. Chen, J.B. He, Z.Q. Wang, N. Xu, G. Xue, Polyaniline on surface modification of diatomite: A novel way to obtain conducting diatomite fillers, Appl. Surf. Sci., 207 (2003) 378-383.

[50] C.S. Gaddis, K.H. Sandhage, Freestanding microscale 3D polymeric structures with biologically-derived shapes and nanoscale features, J. Mater. Res., 19 (2004) 2541-2545.

[51] J. O'Connor, Y. Lang, J.H. Chao, H.L. Cao, L. Collins, B.J. Rodriguez, P. Dockery, D.P. Finn, W.X. Wang, A. Pandit, Nano-structured polymer-silica composite derived from a marine diatom via deactivation enhanced atom transfer radical polymerization grafting, Small, 10 (2014) 469-473.

[52] R.B. Vasani, D. Losic, A. Cavallaro, N.H. Voelcker, Fabrication of stimulus-responsive diatom biosilica microcapsules for antibiotic drug delivery, J. Mater. Chem. B, 3 (2015) 4325-4329.

[53] J. Toster, K.S. Iyer, R. Burtovyy, S.S.O. Burgess, I.A. Luzinov, C.L. Raston, Regiospecific assembly of gold nanoparticles around the pores of diatoms: Toward three-dimensional nanoarrays, J. Am. Chem. Soc., 131 (2009) 8356-8357.

[54] J.P. Zhao, C.S. Gaddis, Y. Cai, K.H. Sandhage, Free-standing microscale structures of nanocrystalline zirconia with biologically replicable three-dimensional shapes, J. Mater. Res., 20 (2005) 282-287.

[55] M.R. Weatherspoon, M.B. Dickerson, G. Wang, Y. Cai, S. Shian, S.C. Jones, S.R. Marder, K.H. Sandhage, Thin, conformal, and continuous SnO_2 coatings on three-dimensional biosilica templates through hydroxy-group amplification and layer-by-layer alkoxide deposition, Angew. Chem. Int. Ed., 46 (2007) 5724-5727.

[56] G.J. Wang, Y.N. Fang, P. Kim, A. Hayek, M.R. Weatherspoon, J.W. Perry, K.H. Sandhage, S.R. Marder, S.C. Jones, Layer-by-layer dendritic growth of hyperbranched thin films for surface sol-gel syntheses of conformal, functional, nanocrystalline oxide coatings on complex 3D (bio)silica templates, Adv. Funct. Mater., 19 (2009) 2768-2776.

[57] Y.N. Fang, J.D. Berrigan, Y. Cai, S.R. Marder, K.H. Sandhage, Syntheses of nanostructured cu- and ni-based micro-assemblies with selectable 3-D hierarchical biogenic morphologies, J. Mater. Chem., 22 (2012) 1305-1312.

[58] Y.N. Fang, V.W. Chen, Y. Cai, J.D. Berrigan, S.R. Marder, J.W. Perry, K.H. Sandhage, Biologically enabled syntheses of freestanding metallic structures possessing subwavelength pore arrays for extraordinary (surface plasmon-mediated) infrared transmission, Adv. Funct. Mater., 22 (2012) 2550-2559.

[59] J.Q. Dalagan, E.P. Enriquez, L.J. Li, Simultaneous functionalization and reduction of graphene oxide with diatom silica, J. Mater. Sci., 48 (2013) 3415-3421.

[60] T. Kumeria, M. Bariana, T. Altalhi, M. Kurkuri, C.T. Gibson, W.R. Yang, D. Losic, Graphene oxide decorated diatom silica particles as new nano-hybrids: Towards smart natural drug microcarriers, J. Mater. Chem. B, 1 (2013) 6302-6311.

[61] S. Kabiri, D.N.H. Tran, S. Azari, D. Losic, Graphene-diatom silica aerogels for efficient removal of mercury ions from water, ACS Appl. Mater. Interfaces, 7 (2015) 11815-11823.

[62] S.M. Holmes, B.E. Graniel-Garcia, P. Foran, P. Hill, E.P.L. Roberts, B.H. Sakakini, J.M. Newton, A novel porous carbon based on diatomaceous earth, Chem. Commun., (2006) 2662-2663.

[63] X. Cai, G.S. Zhu, W.W. Zhang, H.Y. Zhao, C. Wang, S.L. Qiu, Y. Wei, Diatom-templated synthesis of ordered meso/macroporous hierarchical materials, Eur. J. of Inorg. Chem., (2006) 3641-3645.

[64] D. Losic, Y. Yu, M.S. Aw, S. Simovic, B. Thierry, J. Addai-Mensah, Surface functionalisation of diatoms with dopamine modified iron-oxide nanoparticles: Toward magnetically guided drug microcarriers with biologically derived morphologies, Chem. Commun., 46 (2010) 6323-6325.

[65] T. Todd, Z.P. Zhen, W. Tang, H.M. Chen, G. Wang, Y.J. Chuang, K. Deaton, Z.W. Pan, J. Xie, Iron oxide nanoparticle encapsulated diatoms for magnetic delivery of small molecules to tumors, Nanoscale, 6 (2014) 2073-2076.

[66] G.L. Rorrer, C. Chang, S. Liu, C. Jeffryes, J. Jiao, J.A. Hedberg, Biosynthesis of silicon-germanium oxide nanocomposites by the marine diatom *Nitzschia frustulum*, J. Nanosci. Nanotechnol., 5 (2005) 41-49.

[67] T. Qin, T. Gutu, J. Jiao, C.H. Chang, G.L. Rorrer, Biological fabrication of photoluminescent nanocomb structures by metabolic incorporation of germanium into the biosilica of the diatom *Nitzschia frustulum*, ACS Nano, 2 (2008) 1296-1304.

[68] C. Jeffryes, T. Gutu, J. Jiao, G.L. Rorrer, Two-stage photobioreactor process for the metabolic insertion of nanostructured germanium into the silica microstructure of the diatom *Pinnularia* sp., Mater. Sci. Eng. C-Bio. S., 28 (2008) 107-118.

[69] C. Jeffryes, R. Solanki, Y. Rangineni, W. Wang, C.H. Chang, G.L. Rorrer, Electroluminescence and photoluminescence from nanostructured diatom frustules containing metabolically inserted germanium, Adv. Mater., 20 (2008) 2633-2637.

[70] C. Jeffryes, T. Gutu, J. Jiao, G.L. Rorrer, Metabolic insertion of nanostructured TiO_2 into the patterned biosilica of the diatom *Pinnularia* sp. by a two-stage bioreactor cultivation process, ACS Nano, 2 (2008) 2103-2112.

[71] H.E. Townley, K.L. Woon, F.P. Payne, H. White-Cooper, A.R. Parker, Modification of the physical and optical properties of the frustule of the diatom *Coscinodiscus wailesii* by nickel sulfate, Nanotechnology, 18 (2007).

[72] A. Schrofel, G. Kratosova, M. Bohunicka, E. Dobrocka, I. Vavra, Biosynthesis of gold nanoparticles using diatoms-silica-gold and EPS-gold bionanocomposite formation, J. Nanopart. Res., 13 (2011) 3207-3216.

[73] L. De Stefano, A. Larnberti, L. Rotiroti, M. De Stefano, Interfacing the nanostructured biosilica microshells of the marine diatom *Coscinodiscus wailesii* with biological matter, Acta Biomater., 4 (2008) 126-130.

[74] L. De Stefano, L. Rotiroti, M. De Stefano, A. Lamberti, S. Lettieri, A. Setaro, P. Maddalena, Marine diatoms as optical biosensors, Biosens. Bioelectron., 24 (2009) 1580-1584.

[75] H.E. Townley, A.R. Parker, H. White-Cooper, Exploitation of diatom frustules for nanotechnology: Tethering active biomolecules, Adv. Funct. Mater., 18 (2008) 369-374.

[76] D.K. Gale, T. Gutu, J. Jiao, C.H. Chang, G.L. Rorrer, Photoluminescence detection of biomolecules by antibody-functionalized diatom biosilica, Adv. Funct. Mater., 19 (2009) 926-933.

[77] G. Bayramoglu, A. Akbulut, M.Y. Arica, Immobilization of tyrosinase on modified diatom biosilica: Enzymatic removal of phenolic compounds from aqueous solution, J. Hazard. Mater., 244 (2013) 528-536.

[78] N. Poulsen, C. Berne, J. Spain, N. Kroger, Silica immobilization of an enzyme through genetic engineering of the diatom *Thalassiosira pseudonana*, Angew. Chem. Int. Ed., 46 (2007) 1843-1846.

[79] V.C. Sheppard, A. Scheffel, N. Poulsen, N. Kroger, Live diatom silica immobilization of multimeric and redox-active enzymes, Appl. Environ. Microb., 78 (2012) 211-218

Addressed immobilization of biofunctionalized diatoms on electrodes by gold electrodeposition

Sandra Leonardo[a], Diana Garibo[a], Margarita Fernández-Tejedor[a], Ciara K. O'Sullivan[b,c], Mònica Campàs[a]

[a]*IRTA, Carretera de Poble Nou, km 5.5, 43540 Sant Carles de la Ràpita, Spain*
[b]*Nanobiotechnology and Bioanalysis Group, Department of Chemical Engineering, Universitat Rovira i Virgili, 43007 Tarragona, Spain*
[c]*Institució Catalana de Recerca i Estudis Avançats, Passeig Lluís Companys 23, 08010 Barcelona, Spain*

Abstract

Diatoms are single cell microalgae with a silica shell (frustule), which possess a micro/nanoporous pattern of unparalleled diversity far beyond the possibilities of current micro- and nanofabrication techniques. To explore diatoms as natural three-dimensional nanostructured supports in sensing and biosensing devices, a simple, rapid and stable method to immobilize diatoms via gold electrodeposition is described. In this process, gold microstructures are formed, immobilizing diatoms by entrapment or crossing their nanopores. Varying the applied potential, time and $HAuCl_4$ concentration, gold deposits of different morphologies and roughness are obtained, thereby determining the diatom immobilization process. Optical and scanning electron microscopy (SEM) have been used to characterize diatom immobilization yields, the morphology of the gold microstructures, and the morphological integrity of diatoms. Cyclic voltammetry (CV) has been performed to characterize the gold deposits and to demonstrate the enhanced electrocatalytic activity of the gold-diatom electrodes. Electro-addressed immobilization of different diatoms on specific bands of interdigitated electrode arrays has been achieved, highlighting the potential application of diatoms for site-specific immobilization on microarrays. The feasibility to combine tailored immobilization with diatom biofunctionalization has also been demonstrated. Antibody-functionalized diatoms were immobilized on electrodes retaining their ability to detect its cognate antigen. The reported method exploits the natural three-dimensional nanostructures of diatoms together with their easy modification with biomolecules and the simplicity of gold electrodeposition to produce micro/nanostructured and highly electrocatalytic electrodes, providing low-cost

and eco-friendly platforms and arrays with potential application in biosensing devices.

1. Introduction

The potential applications of micro/nanoscale materials in electronics, optics, mechanics, catalysis and biotechnology has been widely reported. However, the synthesis of nanomaterials with a range of chemical compositions, sizes, and high monodispersity is still limited to high-cost and sophisticated techniques.

Biological materials are a promising alternative to existing fabrication technologies, and diatoms, one of the most abundant unicellular microalgae found in aquatic environments, are among the most remarkable examples. Diatoms have rigid cell walls of silica, called frustules, with pores ranging from nanometers to micrometers, perfectly ordered and arranged in a radial (centric diatoms) or bilateral (pennate diatoms) symmetry [1, 2]. Because of their large surface area, high and ordered pore and channel density, thermal and mechanical stability, optical properties and biocompatibility, diatoms have recently attracted extensive attention in nanotechnology applications, such as drug delivery, nanofiltration systems, photocatalysis, nanofabrication, nanocomputers or computer nanocomponents, nanofluidics and biophotonics [3-11]. Additionally, diatoms present reactive Si-OH groups that coat the frustules, facilitating their chemical modification through well-established chemistries. Thus, their use as nanostructured supports in biosensing platforms has also been pursued [12-17].

Nevertheless, the use of diatoms as building blocks in biosensor platforms is still an incipient and poorly explored niche. A crucial step is the immobilization of diatoms on supports. To date, only a few immobilization techniques have been demonstrated to be effective and most of them require sophisticated instrumentation, multi-step processes or extreme experimental conditions that may affect the three-dimensional nanostructure of diatoms [18-23]. New methods that allow the immobilization of diatoms onto different surfaces in a simple, stable and low-cost way without compromising their structure are thus highly desired. Some more works reporting diatom biofunctionalization have been described. Mainly antibodies, but also oligonucleotides and enzymes, have been linked to diatoms. However, in order to truly foster the use of diatoms as nanostructured supports in biosensing devices, a combination of tailored immobilization and diatom biofunctionalization is required [24].

Gold electrodeposition on electrodes allows the formation of micro/nanostructured metal films with excellent properties, such as high conductivity, chemical stability

and large surface area, in a facile, rapid, efficient and cost-effective manner. Moreover, by carefully varying the experimental parameters (e.g. electrode surface and pre-treatment, electrochemical method, applied potentials, electrodeposition time, gold concentration, pH, media composition and presence of additives), films with different morphologies and roughness can be tailor-made [25-38]. Exploiting these properties, gold micro/nanostructures have found widespread application in catalysis, electronics, bio/sensors, nanofabrication and surface-enhanced Raman spectroscopy (SERS) [26, 29, 33, 34, 36-41].

In this work, we propose a method for diatom immobilization on screen-printed electrodes by means of gold electrodeposition. Gold microstructures with controlled roughness and morphology are formed and, simultaneously, diatoms are anchored on the electrode surface. Optical microscopy and/or scanning electron microscopy (SEM) have been used to characterize the diatom immobilization yields, the morphology of the gold microstructures, and the morphological integrity of diatoms after immobilization. Gold deposits have also been characterized using cyclic voltammetry. Micro/nanostructuring of electrodes is achieved by diatom features in the micro and nanometer range and gold microstructures, providing enhanced electrocatalytic activities as demonstrated by the electrochemical oxidation of hydrogen peroxide. Furthermore, site-specific electro-addressing facilitated the immobilization of different diatoms on specific bands of an interdigitated electrode, presenting an interesting approach for microarray fabrication. Finally, the possibility of immobilizing biofunctionalized diatoms retaining their functionality has been demonstrated, supplying a wide range of possibilities for biosensors.

2. Experimental

2.1. Reagents and materials

Gold (III) chloride 30% ($HAuCl_4$), formaldehyde 37%, sulfuric acid (H_2SO_4), acetic acid, hydrogen peroxide 30% (H_2O_2), (3-aminopropyl)triethoxysilane (APTES), glutaraldehyde (GA), protein G from *Streptococcus*, bovine serum albumin (BSA), 3,3'-5,5'-Tetramethylbenzidine (TMB) liquid substrate system for ELISA, N-methylphenazinium methyl sulfate (MPMS), Guillard's medium (f/2), potassium phosphate monobasic, potassium phosphate dibasic, sodium carbonate and sodium bicarbonate were supplied by Sigma-Aldrich (Tres Cantos, Madrid, Spain).

Mouse monoclonal antibody (mAb) against microcystin-LR (MC-LR) (MC10E7) was provided by Enzo Life Sciences (Lausen, Liestal, Switzerland). MC-LR-horseradish peroxidase (MC-LR-HRP) was purchased from Prof. W.W. Carmichael's laboratory

(Wright State University, Dayton, Ohio, USA). Milli-Q water (Millipore, Bedford, New Hampshire, USA) was used to prepare solutions. Screen-printed carbon electrodes (DRP-110), with carbon working and counter electrodes and silver reference electrode (working electrode of 4 mm in diameter), and screen-printed gold interdigitated electrodes (DRP-SCA 200) (bands and gaps of 200 µm in width) were purchased from Dropsens (Oviedo, Spain). External Ag/AgCl reference electrode was obtained from Microelectrodes, Inc. (Bedford, New Hampshire, USA).

2.2. Equipment

Amperometric electrodeposition and cyclic voltammetry (CV) and amperometric measurements were performed using an AUTOLAB PGSTAT128N potentiostat (Metrohm Autolab, Utrecht, The Netherlands). Data were collected by General Purpose Electrochemical System (GPES) software. Gold nano/microstructures and diatom immobilizations were characterized using optical microscopy (Leica DMLB and Leica M165 C) (Leica Microsistemas, Barcelona, Spain) and scanning electronic microscopy (SEM) (Jeol JSM-6400) (Jeol Ltd, Akishima, Tokio, Japan). A Synergy HT microplate reader (Biotek, Winooski, Vermont, USA) was used in the colorimetric characterization of biofunctionalized diatoms.

2.3. Diatom cultures

Coscinodiscus wailesii CCMP 2513 was obtained from the Provasoli-Guillard National Center for Marine Algae and Microbiota (East Boothbay, Maine, USA). *Coscinodiscus* sp. and *Grammatophora* sp. were isolated from the southern Catalan coast (North Western Mediterranean Sea). The strains were cultured in non-treated cell culture flasks containing Guillard's medium (f/2) at 20 °C under a light:dark 12:12 regime with cool-white fluorescent light. Growth potentiality was maintained through regular sub-culturing techniques. The cultures were upscaled to 400 mL, and the growth was stopped at the end of the exponential phase using 2% formaldehyde:acetic acid (1:1) as a fixative. Diatom cultures were harvested by gravity filtration through a 5-µm Sefar Nitex mesh (Sefar Maissa, Cardedeu, Barcelona, Spain) mounted on a Sterifil 500 filter holder (Merck chemicals & Life Science, Madrid, Spain) and re-suspended in 0.2-µm filtered seawater. Organic matter was removed by adding the equal volume of hydrogen peroxide 30% for 12-24h and heated to 100 °C for 4 h. Cleaned frustules were placed on 50 mL plastic tubes and concentrated using gravity filtration. The supernatant was removed and diatom frustules were re-suspended in milli-Q water up to 40 mL, mixed vigorously and concentrated again using gravity filtration. The same washing procedure was

repeated twice. Finally, the supernatant was removed leaving 5 mL of diatom aqueous suspension in the tubes.

2.4. Diatom immobilization and characterization

Diatom aqueous suspensions (10 µL) and 0.8 or 0.2 M $HAuCl_4$ in phosphate buffer (pH 7.2) (30 µL) were placed on the horizontally-positioned screen-printed carbon electrodes, and different potentials (ranging from -1 V to +1 V *vs.* Ag) were applied for varying durations (150, 300, 600 and 1200 s). Electrodes were then rinsed with water. Gold microstructures and diatom immobilizations were characterized using optical microscopy and SEM. CVs between -0.2 and +1.2 V (*vs.* Ag) at 50 mV/s in a 0.1 M H_2S0_4 solution were performed to characterize the amount of electrodeposited gold. CVs between 0 and +0.4 V at 10 mV/s in a 2 mM H_20_2 solution characterized the electrocatalytic activity for hydrogen peroxide oxidation.

Amperometry was used to construct an H_20_2 calibration curve with electrodes where diatom frustules were immobilized in the presence of 0.6 M $HAuCl_4$ solution and by the application of -2 V (*vs.* Ag) for 300 s. The sensor protocol was as follows: 40 µL of 0.1 M phosphate buffer (pH 7.2) were placed on the horizontally-positioned electrode and a potential of +0.4 V (*vs.* Ag) was applied. The current intensity was recorded for 60 s. Subsequently, 20 µL of H_2O_2 (at concentrations ranging from 0 to 1600 mM) were added and the current intensity was recorded again for 60 s. The difference in current intensity before and after H_2O_2 addition was measured. The experiment was performed in triplicate.

Electro-addressed immobilization of different diatoms on specific bands of interdigitated electrode arrays was performed as follows: *Grammatophora* sp. aqueous suspension (40 µL) and 4.8 M $HAuCl_4$ stock solution (30 µL) were placed on the horizontally-positioned screen-printed gold interdigitated electrode array and -2.5 V (*vs.* Ag/AgCl) were applied for 1200 s on one of the two electrodes. An external Ag/AgCl reference electrode was used. The array was then rinsed with water. Once dried, the same procedure was performed using *Coscinodiscus* sp. and applying the same potential on the other electrode. The array was rinsed with water again. The selective immobilization of diatoms was characterized using optical microscopy.

2.5. Diatom biofunctionalization and characterization

A *Coscinodiscus* sp. diatom suspension (200 µL) was incubated in a 10% v/v APTES in water:methanol (1:1) for 2 h. The silanized diatom suspension was incubated in 2.5% v/v glutaraldehyde (GA) in 0.1 M phosphate buffer (pH 7.2) for 30 min,

followed by incubation in 20 µg/mL of Protein G in 0.1 M carbonate buffer (pH 9.6) overnight. Diatom frustules were then incubated in a 1/500 dilution of 1 mg/mL monoclonal antibody against MC-LR (anti-MC-LR mAb) in 0.1 M potassium phosphate buffer (pH 7.2) overnight. Once biofunctionalized, the *Coscinodiscus* sp. diatom suspension was incubated in 2% w/v BSA in 0.1 M phosphate buffer (pH 7.2) for 1 h as a blocking step. Finally, a 1/37,500 dilution of MC-LR-HRP in 0.1 M potassium phosphate buffer (pH 7.2) was added and allowed to interact for 30 min. Three washing steps were performed in water:methanol (1:1) after the silanization step and in 0.1 M potassium phosphate buffer (pH 7.2) after the other steps, and by centrifugation at 12,500 rpm for 15 min. All steps were performed at room temperature.

Colorimetry was used to characterize the biofunctionalization of diatoms with anti-MC mAb and the subsequent affinity interaction with MC-LR-HRP. Diatom suspensions (25 µL) were placed into microtiter plate wells and 125 µL of TMB were then added. After a 10 min incubation, the absorbance was read at 620 nm. Non-biofunctionalized *Coscinodiscus* sp. diatom suspension was used as a control. The assay was performed in triplicate. To evaluate differences between biofunctionalized and non-biofunctionalized diatom responses, statistical analysis was performed applying the paired *t* test. Differences in the results were considered statistically significant at the 0.05 level. Prior to analysis, data were tested for normality.

2.6. Biofunctionalized diatom immobilization and characterization

Biofunctionalized and non-biofunctionalized *Coscinodiscus* sp. diatom suspensions (10 µL) were immobilized in the presence of 0.8 M $HAuCl_4$ in phosphate buffer (pH 7.2) (30 µL) placed on the horizontally-positioned screen-printed carbon electrodes and -1 V (*vs.* Ag) was applied for 150 s. Electrodes were then rinsed with water and a blocking step was performed with 2% w/v BSA in 0.1 M phosphate buffer (pH 7.2) for 1 h. Subsequently, gold-diatom electrodes were incubated in a 1/1,000 dilution of MC-LR-HRP in 0.1 M potassium phosphate buffer (pH 7.2) for 30 min. The electrodes were then rinsed with 0.1 M phosphate buffer (pH 7.2). All steps were performed at room temperature.

Amperometry was used to characterize the immobilization of diatoms biofunctionalized with anti-MC mAb and the subsequent affinity interaction with MC-LR-HRP. The protocol was as follows: 45 µL of 0.5 mM MPMS in 100 mM acetate buffer containing 300 mM NaCl (pH 5), were placed on the horizontally-positioned electrode and a potential of -0.15 V (*vs.* Ag) was applied. The current intensity was recorded for 60 s. Subsequently, 5 µL of 10 mM H_2O_2 were added and following a

10-minute incubation, the current intensity was recorded again for 60 s. The difference in current intensity before and after H_2O_2 addition was measured. The experiment was performed in triplicate. To evaluate differences between biofunctionalized and non-biofunctionalized diatom responses, statistical analysis was performed applying the paired *t* test. Differences in the results were considered statistically significant at the 0.05 level. Prior to analysis, data were tested for normality.

3. Results and discussion

Three different marine diatoms were used in the work reported: *Coscinodiscus* sp. and *Coscinodiscus wailesii*, centric diatoms of approximately 50 µm and 200 µm in diameter, respectively, and *Grammatophora* sp., a pennate diatom of approximately 50 µm in length and 6 µm in width. Following cultivation, harvesting and removal of the organic matter, diatom frustules were immobilized via gold electrodeposition on screen-printed carbon electrodes. In this process, gold ions from tetrachloroauric acid are reduced to metallic gold according to the following single three-electron reaction [26, 43]:

$$AuCl_4^-{}_{(aq)} + 3e^- \rightarrow Au_{(s)} + 4Cl^-{}_{(aq)}$$

Metallic gold is electrodeposited on the electrode surface, assisting the immobilization of diatom frustules previously placed on the horizontally-positioned electrode. Electrodeposition was performed under different experimental conditions: applied potential (ranging from -1 V to +1 V *vs.* Ag), time (150, 300, 600 and 1200 s) and $HAuCl_4$ concentration (0.6 and 0.15 M). Varying these experimental conditions, different gold nano/microstructures and diatom immobilization yields were obtained. The different gold morphologies observed under different operating conditions suggest different nucleation and growth rates, as has been previously described [27, 33, 37-39]. Nevertheless, neither the addition of diatom frustules nor the different species of diatoms used, significantly modified the morphology of the gold deposits.

3.1. Morphological characterization by optical microscopy

Figure 1 shows the images obtained using optical microscopy of gold-assisted *Coscinodiscus* sp. immobilization on screen-printed carbon electrodes using 0.6 M $HAuCl_4$ at different applied potentials and times. While the electrodeposition at the most negative potential (-1 V *vs.* Ag) produced a very thick and rough gold layer, the thickness and roughness decreased as the applied potential reached positive

potentials (Figure 1 a-d). In fact, at -0.2 V (*vs.* Ag) microspheres were clearly observed. Higher diatom immobilization yields were achieved at more negative potentials, although the diatom films were less ordered, with frustules with different orientations and heights.

The use of different diatom species did not alter the morphology of the gold deposits, and whilst no *C. wailesii* were observed at positive potentials, some *Coscinodiscus* sp. and *Grammatophora* sp. were obtained. The immobilization yield was higher when using *Grammatophora* sp., probably due to its lower surface area. This fact indicates that although the size and the shape of the frustules do not modify the morphology of gold deposits, they have an influence on the diatom immobilization process and yield.

Longer electrodeposition times produced a higher density of the gold deposits with a gradual augmentation of the microsphere size and even aggregate formation, increasing the diatom immobilization yields (Figure 1 e-h). The same size augmentation effect was observed with other gold morphologies, obtained when applying other potentials (e.g. leaf-like structures obtained at -1 V *vs.* Ag, *see below*).

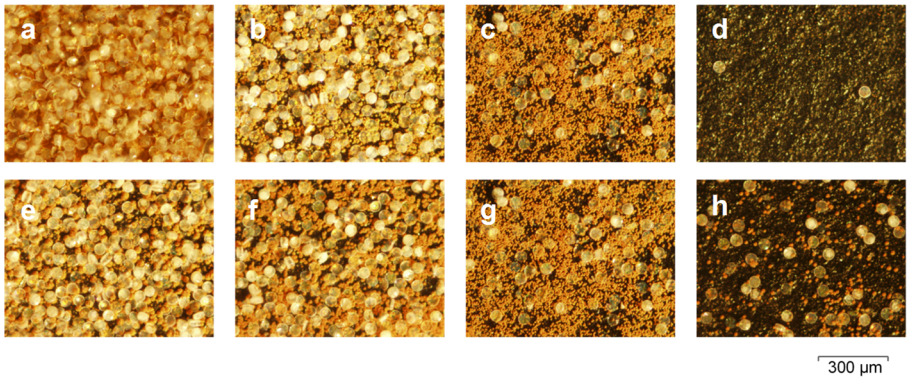

Figure 1. Optical microscopy images of screen-printed carbon electrodes containing *Coscinodiscus* sp. immobilized in the presence of 0.6 M $HAuCl_4$ and by the application of -1 V (a), -0.5 V (b), -0.2 V (c) and +0.2 V (d) (*vs.* Ag) for 5 min, and by the application of -0.2 V (*vs.* Ag) for 1,200 s (e), 600 s (f), 300 s (g) and 150 s (h).

It was thus observed that both the electrodeposition potential and time affect the gold morphology as well as diatom immobilization orientation and yield. Whereas the application of milder potentials provides more ordered diatom films, higher immobilization yields are obtained at more negative potentials. Similarly, whereas the application of longer times provides higher immobilization yields, diatom films

are more ordered at shorter times. It is also necessary to mention that electrodepositions performed at positive potentials and short times drastically decrease the diatom immobilization yield, and that electrodepositions performed at negative potentials and very long times result in fragile large microstructures that detach from the electrode surface.

3.2. Morphological characterization by scanning electron microscopy (SEM)

In order to elucidate a better understanding of the diatom immobilization processes and investigate the morphological integrity of the immobilized frustules, electrodes with *C. wailesii* and *Grammatophora* sp. were characterized by SEM. Figure 2 shows the SEM images of gold-assisted diatom immobilization on screen-printed carbon electrodes by using 0.6 M $HAuCl_4$ at negative applied potentials for 300 s. The gold electrodeposition at the lowest applied potential (-1 V *vs.* Ag) produced a film of dendritic microstructures of different size, some of them even forming huge leaf-like structures up to 100 μm in length. However, when applying -0.5 V (*vs.* Ag), gold was electrodeposited forming microspheres mainly of 15-20 μm in diameter but also with some smaller ones (around 7-11 μm), principally randomly spaced but some of them merging together and forming aggregates. By shifting the potential to -0.2 V (*vs.* Ag), the same microspheres were observed, but in a much lower density. From the SEM images, it is safe to affirm that the morphological integrity of the diatoms has not been affected by the process and that diatoms should be in contact with electrodeposited gold microstructures in order to be immobilized. Moreover, it is important to highlight that, as diatom modification is not needed to achieve its immobilization and most part of diatom surface is not covered by gold, the diatom surface is still available for bio/functionalization through its Si-OH reactive groups.

The use of a lower gold chloride concentration (0.15 M $HAuCl_4$) also resulted in diatom immobilization, but to a lower extent. As can be observed in Figure 3, the gold structures achieved at -1 V (*vs.* Ag) and -0.5 V (*vs.* Ag) were completely different than when using a higher gold chloride concentration with some electrode areas not achieving complete gold coverage. The lower gold amount electrodeposited at -0.2 V (*vs.* Ag) was not enough to perform SEM without metallic pre-treatment, as performed with the other electrodes surfaces characterized. It is interesting to note that the electrodepositions performed at -1 V (*vs.* Ag) using 0.2 M $HAuCl_4$ showed mixed microstructures with two kinds of populations, leaf-like structures (up to 6 μm in length) and small microspheres (0.3-1.2 μm in diameter). Upon application of -0.5 V (*vs.* Ag), unlike Figures 2b and 2e (where electrodepositions were performed

at a higher gold concentration), a gold thin layer with no microspheres and only leaf-like structures (until 20 μm in length) was observed.

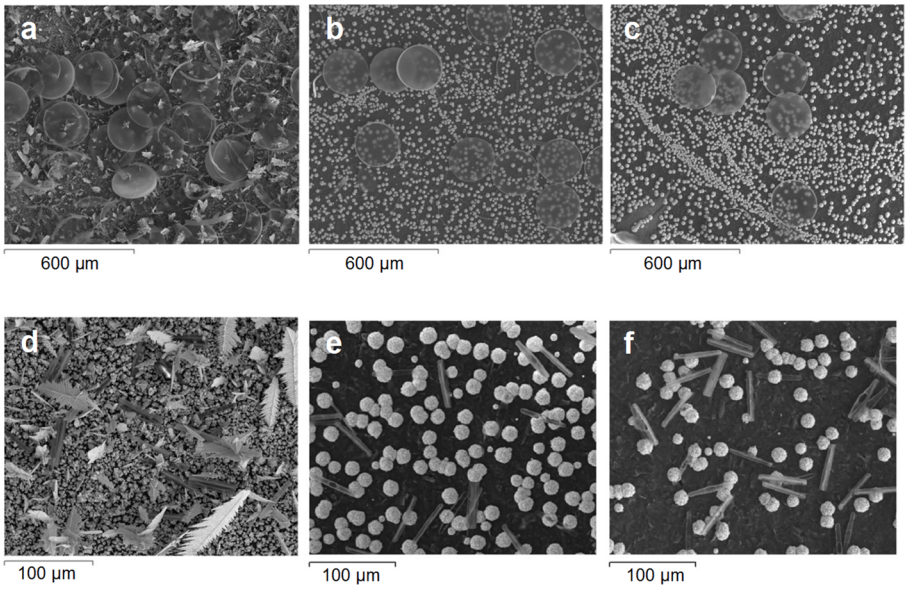

Figure 2. SEM images of screen-printed carbon electrodes containing *Coscinodiscus wailesii* (a, b, c) and *Grammatophora* sp. (d, e, f) immobilized in the presence of 0.6 M $HAuCl_4$ and by the application of -1 V (a, d), -0.5 V (b, e) and -0.2 V (c, f) (*vs.* Ag) for 300 s.

The reduction of gold ions to metallic gold and the morphology and size of the subsequently formed microstructures are strongly dependent on the material [29] and the surface morphology of the electrode [31, 36]. Consequently, local facets present on the electrode may lead to a preferential nucleation and growth of specific sites. Additionally, the application of very negative potentials generates hydrogen bubbles due to the reduction of water, which could inhibit the growth of gold on randomly distributed sites and favor the growth on the most accessible sites [37], leading to the formation of structures such as the leaf-like structures.

SEM images at higher magnification factors were taken in order to elucidate the process of diatom immobilization. Figure 4 shows *C. wailesii* immobilized in the presence of leaf-like structures and microspheres. As can be observed, gold was able to grow through the diatom micropores, crossing the frustules without affecting their nanostructure. It is postulated that this gold transition assists diatom immobilization. When immobilizing *Grammatophora* sp., gold growth through the

nanopores was also observed and, additionally, dendritic leaf-like structures adopted conformations that embraced diatoms, retaining them on the electrode surface (Figure 5).

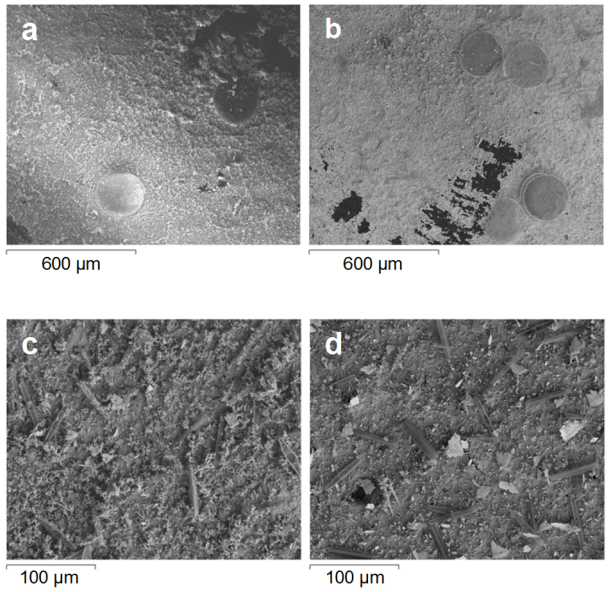

Figure 3. SEM images of screen-printed carbon electrodes containing *Coscinodiscus wailesii* (a,b) and *Grammatophora* sp. (c, d) immobilized in the presence of 0.15 M $HAuCl_4$ and by the application of -1 V (a, c) and -0.5 V (b, d) (*vs*. Ag) for 300 s.

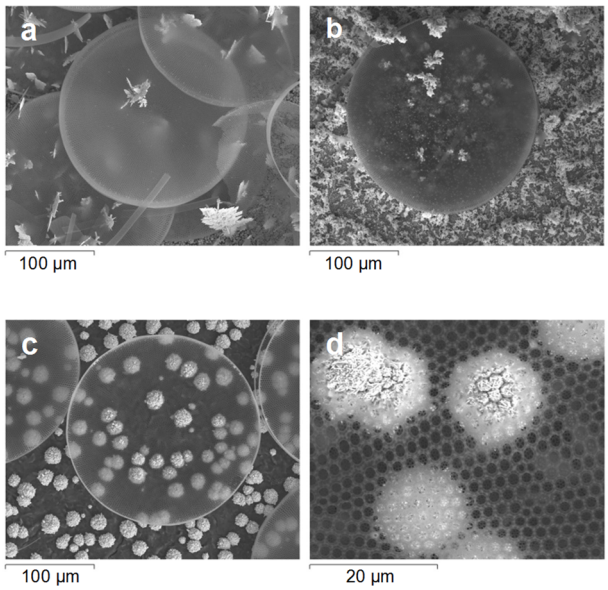

Figure 4. SEM images of screen-printed carbon electrodes containing *Coscinodiscus wailesii* immobilized using a 0.6 M $HAuCl_4$ solution at -1 V (*vs*. Ag) (a), a 0.2 M $HAuCl_4$ solution and by the application of -1 V (*vs*. Ag) (b) and a 0.8 M $HAuCl_4$ solution at -0.5 V (*vs*. Ag) (c, d) for 300 s.

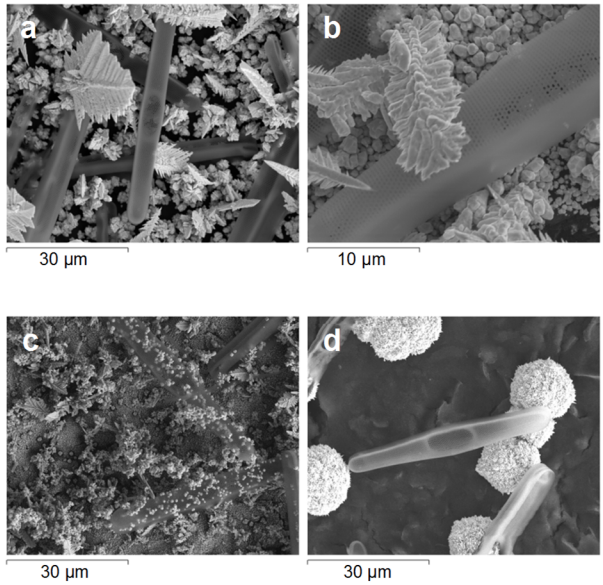

Figure 5. SEM images of screen-printed carbon electrodes containing *Grammatophora* sp. immobilized using a 0.6 M $HAuCl_4$ solution and by the application of -1 V (*vs*. Ag) (a, b), a 0.2 M $HAuCl_4$ solution at -1 V (*vs*. Ag) (c) and a 0.8 M $HAuCl_4$ solution at -0.5 V (*vs*. Ag) (d) for 300 s.

3.3. Electrochemical characterization of gold deposits

Cyclic voltammograms (CVs) between -0.2 and +1.2 V (*vs.* Ag) at 50 mV/s in a 0.1 M H_2SO_4 solution were performed to characterize the amount of gold electrodeposited on the screen-printed carbon electrodes during the diatom immobilization process. In Figure 6, the CVs for the electrodes where *Coscinodiscus* sp. frustules were immobilized (in the presence of 0.6 M $HAuCl_4$ solution and by the application of -1, -0.5, -0.2 and +0.2 V *vs.* Ag for 300 s) are plotted as an example. When applying -1, -0.5 and -0.2 V (*vs.* Ag), the CVs showed two anodic peaks at +1.0 and +0.8 V (*vs.* Ag) and a cathodic peak at around +0.6 V (*vs.* Ag), which indicate the formation of different gold oxides on the forward scan and their subsequent reduction on the backward scan. As expected, higher current intensities were observed when more negative potentials were applied due to the higher amount of electrodeposited gold. When applying +0.2 V (*vs.* Ag), oxidation and reduction peaks were non-significant. Results were similar when immobilizing *C. wailesii* and *Grammatophora* sp. frustules or when electrodepositing gold in the absence on diatoms (*results not*

shown). We can conclude that the presence of diatoms on the electrode does not significantly influence the amount of electrodeposited gold.

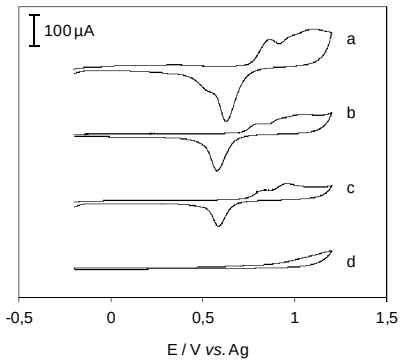

Figure 6. Cyclic voltammograms performed in 0.1 M H_2S0_4 at 50 mV/s of screen-printed carbon electrodes containing *Coscinodiscus* sp. immobilized using a 0.6 M $HAuCl_4$ solution and by the application of -1 V (a), -0.5 V (b), -0.2 V (c) and +0.2 V (d) (*vs*. Ag) for 300 s.

3.4. Electrocatalytic activity for hydrogen peroxide oxidation

Micro/nanostructuration of surface electrodes provides high surface-to-volume ratios that may enhance electrochemical signals and provide improved electrocatalytic properties. It is known that gold materials have catalytic activity for the electrochemical oxidation of hydrogen peroxide [44]. In this work, the electrocatalytic activity of the gold-diatom surfaces was evaluated for the oxidation of hydrogen peroxide. CVs were performed between 0 and +0.4 V (*vs.* Ag) at 10 mV/s in a 2 mM H_20_2 solution. In Figure 7a, the CVs for the hydrogen peroxide oxidation with electrodes where *Grammatophora* sp. frustules were immobilized (in the presence of 0.6 M $HAuCl_4$ solution and by the application of -1, -0.5, -0.2 and +0.2 V *vs.* Ag for 300 s) can be observed. Whereas no significant responses were observed with the electrode where electrodeposition had been performed at +0.2 V (*vs.* Ag) (results were no significantly different to those obtained with bare carbon screen-printed electrodes), oxidation current intensities substantially increased when -0.2, -0.5 and -1.0 V (*vs.* Ag) were applied. The oxidation reaction is more favorable at the gold-diatom electrodes with higher amount of gold deposit, indicating that the gold-diatom films exhibit good electrocatalytic activity. Despite the fact that the diatom silica is a semiconductor silicon oxide-based material and therefore diatom immobilization on the electrode may limit electron transfer, no differences in the electrocatalytic activity were observed when immobilizing

different diatom frustules or when electrodepositing gold in the absence of diatoms. An H_2O_2 calibration curve was performed with electrodes with gold electrodeposited at –1 V (*vs.* Ag) for 300 s (Figure 7b). As it can be observed, the gold-diatom modified electrode exhibits a limit of detection (S/N = 3) of 0.01 mM and an excellent linear response until 133 mM H_2O_2. This makes gold-diatom nanostructured electrodes desirable supports for the development of biosensors where oxidoreductases are used as biorecognition molecules or labels.

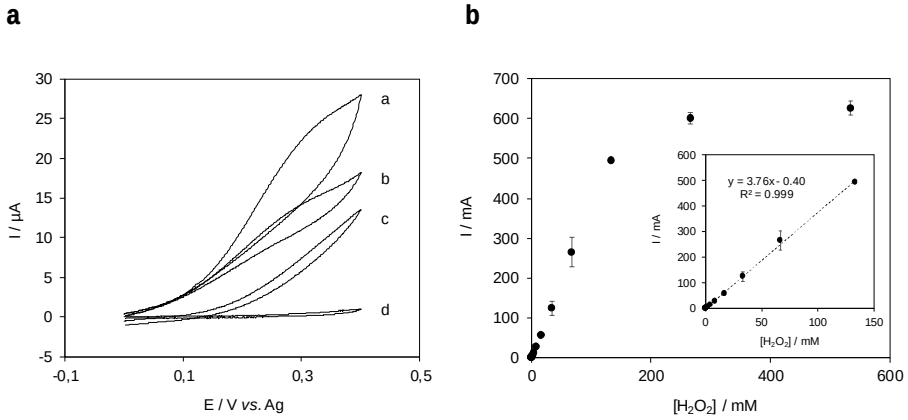

Figure 7. (a) Cyclic voltammograms performed in 2 mM H_2O_2 at 10 mV/s of electrodes containing *Grammatophora* sp. immobilized using a 0.6 M $HAuCl_4$ solution and by the application of -1 V (a), -0.5 V (b), -0.2 V (c) and +0.2 V (d) (*vs*. Ag) for 300 s. **(b)** H_2O_2 calibration curve on gold-diatom electrodes.

3.5. Addressed diatom immobilization on interdigitated electrodes

Screen-printed gold interdigitated electrodes were used as supports to investigate the possibility of exploiting the electro-addressed immobilization of diatoms in microarray fabrication. As can be observed in Figure 8, *Coscinodiscus* sp. and *Grammatophora* sp. were selectively immobilized on different bands of the interdigitated electrode array by applying a consecutive negative potential to each working electrode after a washing step in the presence of the gold-diatom solution. The two consecutive electro-addressing steps did not disrupt the immobilization process of the two different diatoms, and no cross-immobilization was observed between the bands. This proof of concept demonstrates that this method could be an interesting approach for microarray fabrication.

On the other hand, as the immobilization approach has been demonstrated to be successful on both screen-printed carbon electrodes and screen-printed gold

interdigitated electrodes, it is safe to affirm that, by carefully adjusting the electrodeposition conditions, diatom immobilization on electrodes of different material, geometry and size is possible.

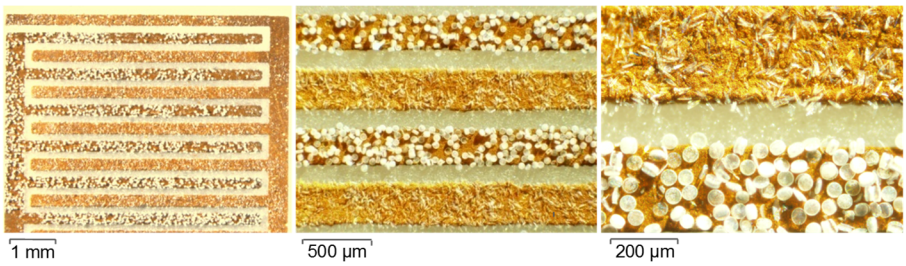

Figure 8. Optical microscopy images of *Grammatophora* sp. and *Coscinodiscus* sp immobilized on specific bands of screen-printed gold interdigitated electrodes in the presence of 3.6 M $HAuCl_4$ and by the application of -2.5 V (*vs*. Ag/AgCl) for 1200 s.

3.6. Immobilization of biofunctionalized diatoms

To foster the use of diatoms as building blocks in biosensor platforms, their biofunctionalization and the retention of the functionality once immobilized are required. Anti-MC-LR mAb was used as a model biorecognition molecule. Microcystins (MCs) are one of the most commonly found toxins produced by freshwater cyanobacteria and their presence in drinking water supplies poses a serious threat to animal and human health. In order to ensure water quality and to protect human health, the World Health Organization (WHO) proposed a provisional maximum permitted level of 1 µg/L of MC-LR in drinking water [45]. The anti-MC-LR mAb is able to recognize all microcystins (MCs) variants containing an arginine at position 4. The previous biofunctionalization of diatoms with Protein G facilitated the immobilization of the mAb without requiring chemical modification and proffering an optimal orientation on the diatom frustule, avoiding possible steric effects. To demonstrate the successful biofunctionalization of diatoms with anti-MC-LR mAb, as well as the avidity of the antibody once immobilized on the frustule, an MC-LR-horseradish peroxidase (MC-LR-HRP) conjugate was used. Colorimetric detection of the HRP label was used to demonstrate that the antibodies were linked to the diatom frustule and were able to recognize the MC-LR-HRP conjugate (Figure 9). Significant differences were observed between non-biofunctionalized (controls) and biofunctionalized diatoms ($t = 14.044$, $p < 0.001$), demonstrating that the non-specific adsorption was almost negligible (< 10%).

To demonstrate the feasibility of combining the tailored immobilization with diatom biofunctionalization, anti-MC-LR mAb biofunctionalized diatoms were immobilized on the electrodes via gold electrodeposition (Figure 10). MC-LR-HRP conjugate was used to show that biofunctionalized diatoms were able to recognize the antigen once immobilized on the support. In this case, MPMS was used as an HRP redox mediator to record electrochemical currents. Although non-specific adsorption values were observed from non-biofunctionalized diatoms (controls) (19%), the differences in electrochemical currents achieved were high enough to demonstrate that diatoms still retained their biofunctionality after immobilization ($t = 11.708$, $p < 0.001$) (Figure 9). Furthermore, despite the presence of $HAuCl_4$ or the application of a negative potential during the immobilization process, the antibody retained its biological activity.

More work focused on increasing the bioelectrocatalytic currents (e.g. improving the diatom biofunctionalization process to provide higher biomolecule immobilization yields) is required prior to performing a competition step between MC-LR and the MC-LR-HRP tracer and obtain a convenient calibration curve. Nevertheless, the results obtained so far anticipate the potential applicability of diatoms in biosensing and the great possibilities offered by the effective, rapid and facile immobilization method reported herein.

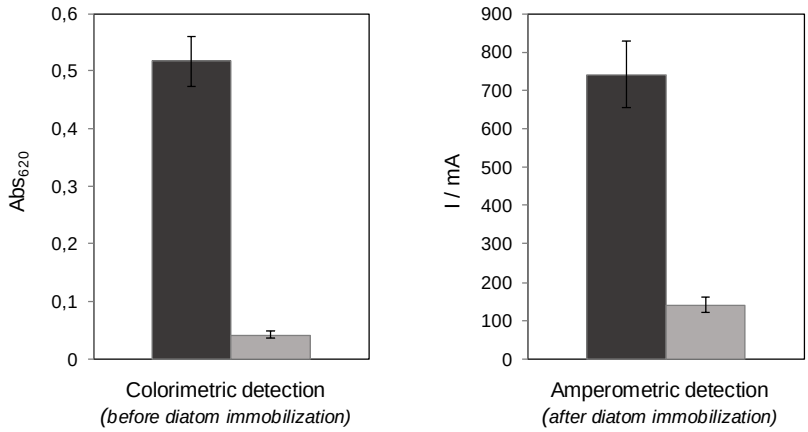

Figure 9. Colorimetric (diatoms in suspension) and amperometric (diatoms immobilized on electrodes) MC-LR-HRP detection after incubation with biofunctionalized (dark grey) and non-biofunctionalized (light grey) diatoms.

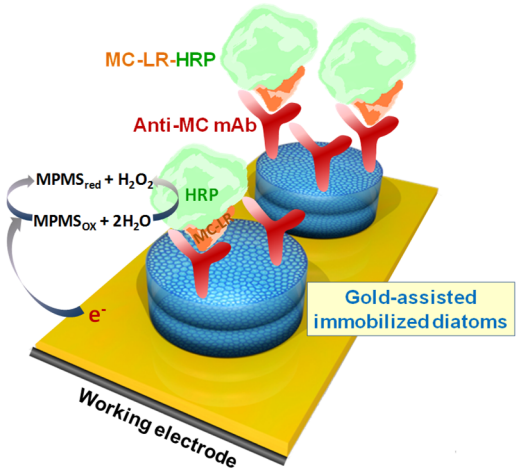

Figure 10. Schematic representation of the antibody-functionalized diatoms immobilized via gold electrodeposition on a carbon working electrode and the subsequent electrochemical detection of the enzyme-labelled antigen.

4. Conclusions

This work details a facile, rapid, efficient and cost-effective method to functionalize electrodes with micro/nanostructures derived from diatom frustules and gold deposits. Stable and addressed diatom immobilization was achieved by means of gold electrodeposition, via a process that generates gold-diatom films with features in the micrometer range. The electrodeposition applied potential, time and gold concentration determine the roughness and morphology of the gold deposits, and therefore, the diatom immobilization orientation and yield. Two processes could explain diatom immobilization on the electrodes: gold crossing through the diatom pores and/or diatom embracing by gold microstructures. The immobilization method has been shown to be successful with diatoms of different sizes and shapes and different electrode sizes and materials, demonstrating that it is generic and in principle applicable to any diatom and electrode. Hence, this method provides three-dimensional micro/nanostructures without the requirement for sophisticated fabrication techniques and is only limited by the resolution of the method used to produce electrodes and the diatom size.

Gold electrodeposition not only allows the immobilization of diatoms on electrodes but also confers excellent properties to the final gold-diatom electrodes, as demonstrated by the highly efficient electrocatalytic activity for hydrogen peroxide sensing. Although gold-diatom films are initially proposed as supports for the development of electrochemical sensors, the optical properties of gold and silicon-

oxide diatom frustules suggest the possible applicability of gold-diatom films in optical sensing devices.

The combination of the electro-addressed immobilization of different diatoms on specific bands of interdigitated electrode arrays with the facile diatom biofunctionalization highlights the possibility to develop miniaturized biosensing devices for the detection of multiple target analytes in complex samples. This fast, selective and low-cost method is fully compatible with the mass production processes and the microelectronics industry, providing sensitive and eco-friendly platforms with potential applications in the development of biosensing systems highly suitable for applications such as diagnostics, environmental monitoring and food quality and safety control.

Acknowledgements

The authors acknowledge financial support from the *Ministerio de Economía y Competitividad* through the DIANA and SEASENSING projects (BIO2011-26311 and BIO2014-56024-C2-2-R) and from CERCA Programme / Generalitat de Catalunya. Sandra Leonardo acknowledges scholarship from IRTA-URV-BANCO SANTANDER. The authors acknowledge O. Carnicer and P. Hardy for diatom isolation and Marc Cirera (www.sience.marccirera.com) for his help on the illustration.

References

[1] Werner D 1977 *The Biology of Diatoms* (Oxford: Blackwell Scientific Publications)

[2] Round F E, Crawford R M and Mann D G 1990 *The Diatoms, Biology & Morphology of the Genera* (Cambridge: Cambridge University Press)

[3] Parkinson J and Gordon R 1999 Beyond micromachining: the potential of diatoms *Trends Biotechnol.* **17** 190-196

[4] Drum R W and Gordon R 2003 Star trek replicators and diatom nanotechnology *Trends Biotechnol.* **21** 325-328

[5] Lopez P J, Desclés J, Allen A E and Bowler C 2005 Prospects in diatom research *Curr. Opin. Biotechnol.* **16** 180-186

[6] Naik R R and Stone M O 2008 Integrating biomimetics, *Mater. Today* **8** 18-26

[7] Gebeshuber I C 2007 Biotribology inspires new technologies *Nano Today* **2** 30-37

[8] Gordon R, Losic D, Tiffany M A, Nagy S S and Sterrenburg F A S 2009 The Glass Menangerie: Diatoms for novel applications in nanotechnology *Trends Biotechnol.* **27** 116-127

[9] Losic D, Mitchell J G and Voelcker N H 2009 Diatomaceous lessons in manotechnology and advanced materials *Adv. Mater.* **21** 2947-2958

[10] Dolatabadi J E N and De la Guardia M 2011 Applications of diatoms and silica nanotechnology in biosensing, drug and gene delivery, and formation of complex metal nanostructures *Trends Anal. Chem.* **30** 1538-1547

[11] Yang W, Lopez P J and Rosengarten G 2011 Diatoms: self assembled silica nanostructures, and templates for bio/chemical sensors and biomimetic membranes *Analyst* **136** 42-53

[12] Townley H E, Parker A R and White-Cooper H 2008 Exploitation of diatom frustules for nanotechnology: tethering active biomolecules *Adv. Funct. Mater.* **18** 369-374

[13] Rosi N L, Thaxton S and Mirkin C A 2004 Control of nanoparticle assembly by using DNA-modified diatom templates *Angew. Chem. Int. Ed.* **43** 2004 5500-5503

[14] Setaro A, Lettieri S, Maddalena P and De Stefano L 2007 Highly sensitie optochemical gas detection by luminescent marine diatoms *Appl. Phys. Lett.* **91** 051921

[15] De Stefano L, Lamberti A, Rotiroti L and De Stefano M 2008 Interfacing the nanostructured biosilica microshells of the marine diatom *Coscinodiscus wailessi* with biological matter *Acta Biomater.* **4** 126-130

[16] Gale D K, Gutu T, Jiao J, Chang C H and Rorrer G L 2009 Photoluminescence detection of biomolecules by antibody-functionalized diatom biosilica *Adv. Funct. Mater.* **19** 926-933

[17] Bayramoglu G, Akbulut A and Africa M Y 2013 Immobilization of tyrosinase on modified diatom biosilica: enzymatic removal of phenolic compounds from aqueous solution *J. Hazard. Mater.* **244** 528-536

[18] Rea I, Terracciano M, Chandrasekaran S, Voelcker N H, Dardano P, Martucci N M, Lamberti A and De Stefano L 2016 Bioengineered silicon diatoms: adding photonic features to a nanostructured semiconductive material for biomolecular sensing *Nanoscale Res. Lett.* doi: 10.1186/s11671-016-1624-1.

[19] Wang W, Gutu T, Gale D K, Jiao J, Rorrer G L and Chang C H 2009 Self-assembly of nanostructured diatom microshells into patterned arrays assisted by polyelectrolyte multilayer deposition and inkjet printing *J. Am. Chem. Soc.* **131** 4178-4179

[20] Wang Y, Pan J, Cai J, Li A, Chen M and Zhang D 2011 Assembling and patterning of diatom frustules onto PDMS substrates using photoassisted chemical bonding *Chem. Lett.* **40** 1354-1356

[21] Pan J, Cai J, Zhang D, Wang Y and Jiang Y 2012 Micro-arraying of nanostructured diatom microshells on glass substrate using ethylene-vinyl acetate copolymer and photolithography technology for fluorescence spectroscopy applications *Physica E* **44** 1585-1591

[22] Zhang D, Pan J, Cai J, Wang Y, Jiang Y and Jiang X Hydrofluoric acid-assisted bonding of diatoms with SiO_2-based substrates for microsystem application *J. Micromech. Microeng.* **22** 035021

[23] Li A, Cai J, Pan J, Wang Y, Yue Y and Zhang D 2014 Multi-layer hierarchical array fabricated with diatom frustules for highly sensitive bio-detection applications *J. Micromech. Microeng.* **24** 025014

[24] Chandrasekaran S, Sweetman M J, Kant K, Skinner W, Losic D, Nann T and Voelcker N H 2014 Silicon diatom frustules as nanostructures photoelectrodes *Chem. Commun.* **50** 10441-10444

[25] Leonardo S, Prieto-Simón B and Campàs M 2016 Past, present and future of diatoms in biosensing *Trends Anal. Chem.* **79** 276-285

[26] Holt K B, Sabin G, Compton R G, Foord J S and Marken F 2002 Reduction of tetrachloroaurate(III) at boron-doped diamond electrodes: gold deposition versus gold colloid formation *Electroanal*. **14** 797-803
[27] El-Deab M S, Sotomura T and Ohsaka T 2005 Morphological selection of gold nanoparticles electrodeposited on various substrates *J. Elecrochem. Soc.* **152** 730-737
[28] Jiang Y, Wang Z, Yu X, Shi F, Xu H and Zhang X 2005 Self-assembled monolayers of dendron thiols for electrodeposition of gold nanostructures: toward fabrication of superhydrophobic/superhydrophilic surfaces and pH-responsive surfaces *Langmuir* **21** 1986-1990.
[29] Aldous L, Silvester D S, Villagra'n C, Pitner W R, Compton R G, Lagunas M C and Hardacre C 2006 Electrochemical studies of fold and chloride in ionic liquids *New J. Chem* **30** 1576-1583
[30] Tian Y, Liu H, Zhao G and Tatsuma T 2006 shape-controlled electrodeposition of gold nanostructures *J. Phys. Chem. B* **110** 23478-23481
[31] Praig V G, Piret G, Manesse M, Castel X, Boukherroub R, Szunerits S 2008 Seed-mediated electrochemical growth of gold nanostructures on indium tin oxide thin films *Electrochim. Acta* **53** 7838-7844
[32] Zhang H, Xu J J and Chen H Y 2008 Shape-controlled gold nanoarchitectures: synthesis, superhydrophobicity, and electrocatalytic properties *J. Phys. Chem. C* **112** 13886-13892
[33] Huang X J, Yarimaga O, Kim J H and Choi Y K 2009 Substrate surface roughness-dependent 3-D complex nanoarchitectures of gold particles from directed electrodeposition *J. Mater. Chem.* **19** 478-483
[34] Bechelany M, Brodard P, Elias J, Brioude A, Michler J and Philippe L 2010 Simple synthetic route for SERS-active gold nanoparticles substrate with controlled shape and organization *Langmuir* **26** 14364-14371
[35] Elias J, Brodard P, Vemoojj M G C, Michler J and Philippe L 2011 Gold flails by electrochemical deposition: the role of gelatin *Electrochim. Acta* **56** 1485-1489
[36] Monzon L M A, Byrne F and Coey J M D 2011 Gold electrodeposition in organic media *J. Electroanal. Chem.* **657** 54-60
[37] Elias J, Gizowska M, Brodard P, Widmer R, deHazan Y, Graule T, Michler J and Philippe L 2012 Electrodeposition of gold thin films with controlled morphologies and their applications in electrocatalysis and SERS *Nanotechnology* **23** 255705
[38] Hezard T, Fajerwerg K, Evrard D, Collière V, Behra P and Gros P 2012 Influence of the gold nanoparticles electrodeposition method on Hg(II) trace electrochemical detection *Electrochim. Acta* **73** 15-22
[39] Gotti G, Fajerwerg K, Evrard D and Gros P 2014 Electrodeposited gold nanoparticles on glassy carbon: correlation between nanoparticles characteristics and oxygen reduction kinetics in neutral media *Electrochim. Acta* **128** 412-419
[40] Kim J H, Huang X J and Choi Y K Controlled synthesis of gold nanocomplex arrays by a combined top-down and bottom-up approach and their electrochemical behavior *J. Phys. Chem. C* **112** 12747-12753
[41] Kim J H, Kang T, Yoo S M, Lee S Y, Kim B and Choi Y K 2009 A well-ordered flower-like gold nanostructure for integrated sensors via surface-enhanced Raman scattering *Nanotechnology* **20** 235302

[42] Zhang R, and Olin H 2014 Porous gold films – A short review on recent progress *Materials* **7** 3834-3854
[43] Komsiyska L and Staikov G 2008 Electrocrystallization of Au nanoparticles on glassy carbon from $HClO_4$ solution containing $[AuCl_4]^-$ *Electrochim. Acta* **54** 168-172
[44] Zeis R, Lei T, Sieradzki K, Snyder J and Erlebacher J 2008 Catalytic reduction of oxygen and hydrogen peroxide by nanoporous gold *J. Catal.* **253** 132-138
[45] WHO 1998 *Guidelines for Drinking Water-Water Quality* (Geneva: World Health Organisation)

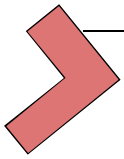

CHAPTER 7

General discussion

Colorimetric biochemical assays and electrochemical biosensors prospects in seafood safety

Biochemical assays and/or electrochemical biosensors for the detection of the marine toxins okadaic acid (OA) and dinohysistoxins (DTXs), tetrodotoxins (TTXs) and azaspiracids (AZAs) as well as the biogenic amines (BAs) histamine, putrescine and cadaverine, have been developed. Colorimetric assays are sometimes presented as a previous step for the subsequent development of electrochemical biosensors, but their suitability as powerful analytical tools by themselves has been widely demonstrated in this thesis. Colorimetric assays are usually performed in a standard microtitre plate format allowing easy handling of samples and high assay throughput. In addition, these type of assays are easy to perform, relatively rapid, and are amenable to automation. In recent years, biosensors have raised much interest in the field of seafood safety because they can analyse turbid samples, can be portable and even perform on-line monitoring. Ideally, for a biosensor to be useful, it should be sensitive, selective, precise, rapid, inexpensive, miniaturised and automated, allow *in situ* analysis and are able to handle small sample volumes. Electrochemical biosensors for the detection of AZAs and BAs presented herein clearly are powerful devices with potential application in seafood safety monitoring, as it has been demonstrated in the analysis of naturally contaminated shellfish and fish samples. Although the developed biosensors benefit from some of the advantages provided by electrochemistry, such as low cost and miniaturisation of electrodes and potentiostats or the possibility to handle small sample volumes, there are still some general technical barriers, such as cost consideration and performance issues that need to be solved to truly harness the potential provided by biosensors.

A key factor when implementing analytical devices is the sample preparation and analyte extraction previous to the analysis. When analysing complex matrices such as seafood, this process tends to be tedious and time-consuming, and thus, it is the limiting factor for analytical devices that pursue a rapid high sample throughput. Consequently, solutions for simplifying, automating, and speeding up sample preparation without compromising the assay performance are particularly beneficial because they can provide savings in time and money and lead to an increased analysis rate. Moreover, interfering substances, which may be co-extracted with the analyte, should be excluded. The extraction process and sample preparation is dependent on the analyte, the sample matrix and the method of analysis. Compared to instrumental analytical methods, antibody-based assays can

afford more simplified sample preparation procedures, in some cases avoiding additional purification or evaporation steps as demonstrated in the case of the detection of TTXs in shellfish and urine samples by the maleimide-based immunoassay (Chapter 3). Although optimisation of the sample extraction process has not been addressed in detail in this thesis, it is evident that future work should focus on improving sample preparation and extraction protocols to truly implement biosensors as rapid analysis tools for *in situ* analysis.

Analytical requirements depend on the final applicability of the analytical methods. Thus, in some cases, an improvement in the selectivity and sensitivity of biosensors and bioanalytical assays may be of interest, while in others the response time or the possibility to regenerate the interaction surface, for example, can play an important role. In this sense, recent advances in biotechnology and nanotechnology are contributing to the modernisation and an acclaimed improvement of the applicability of this type of bioanalytical device. A general statement is accepted attributing significantly improved performance to biosensors based on bionanotechnological approaches (e.g. lower limits of detection (LODs) or higher sensitivities). Nevertheless, proper evaluation of the improvement achieved with these novel biosensors is not always possible, since comparison of equivalent systems is often difficult to perform. The global evaluation of the system, considering a broad range of parameters including the conventional ones (LOD, sensitivity and working range) but also additional features such as the stability of the biosensor, the possibility of regeneration, the cost, the time needed to perform the assay or the ease of handling, is required to be addressed if the integration of micro/nanomaterials is worthwhile or if it only adds sophistication to the configuration.

The use of magnetic beads (MBs) with diameters in the micro/nanometre range as biomolecule supports allows a stable immobilisation by simply applying a magnetic field, while presenting a large surface area available for biomolecule immobilisation or improved assay kinetics. Additional advantages are provided depending on the analytical approach. In the case of the enzyme biosensors for the detection of BAs, the immobilisation of the enzyme on the MBs increases the stability of the enzyme activity. Moreover, higher enzyme immobilisation yields as a result of larger surface areas can result in higher responses and lower LODs. In contrast, when performing competitive assays, as in the development of the immunoassays for the detection of AZAs, the increase in the surface area is not as relevant, as greater sensitivity is usually achieved with decreasing concentrations of immobilised antibody. In this case, the use of MBs as immobilisation supports provides advantages in terms of improved washing steps and subsequent reduction of matrix effects as well as conferring high stability, reproducibility, robustness and, especially, rapidity to the

assay. The transition from MB-based colorimetric assays to MB-electrochemical biosensors is straightforward and only requires the immobilisation of the functionalised MBs on magnetised electrodes and the electrochemical measurement. Although the combination of MBs with electrochemical detection constitutes a powerful strategy for the development of biosensors, providing some advantages such as the possibility to regenerate the electrode surface or the easy integration into microfluidic devices, mass transfer limitations have been observed when anchoring the immunocomplexes on the electrode surface to perform electrochemical detection. To a certain extent, the immobilisation of the functionalised MBs on the electrode surface for the development of biosensors can be contradictory if we keep in mind that some of the benefits provided by the use of MBs resulting from the possibility to perform the assay in suspension. In the case of the development of immunoassays and immunosensors for the detection of AZAs, sensitivities were slightly improved when immobilising the antibody directly on the transducer surface by means of bioaffinity interactions. The lower immunoreagent concentrations needed and the avoidance of the MBs provided economic savings in comparison with the MB-based immunoassays. Nevertheless, the MB-based immunoassays could be performed in just 15 min, while the assays based on the direct immobilisation of the antibody on the transducer required more than 3 hours to be completed.

Exploring biomaterials, such as diatoms, as natural nanostructured supports in the development of biosensors represents an important breakthrough in the achievement of low-cost and eco-friendly nanomaterial-based devices, overcoming some of the challenges of current high-cost and sophisticated micro/nanofabrication techniques. This thesis contributes to making a leap forward to the use of diatoms as natural nanostructured supports in biosensing platforms, proposing a new simple, rapid, addressed and cost-effective method to immobilise biofunctionalised diatoms on electrodes by means of gold electrodeposition. Although the potential use of diatoms as building blocks in electrochemical biosensing platforms is demonstrated, more work focused on merging the advances made on diatom immobilisation, modification and biofunctionalisation in an effective and reproducible way is required to take advantage of the unique features of diatoms in biosensing. Furthermore, the electro-addressed immobilisation of diatoms on specific sites of electrode arrays is an interesting approach for microarray fabrication. In combination with the facile diatom biofunctionalisation, the feasibility to specifically immobilise functionalised diatoms with different biorecognition molecules on electrode arrays opens the possibility to develop miniaturised biosensing devices for the detection of multiple target analytes. The

development of multiplexed assays provides an inherent considerable economic and time reduction in the field of biosensors.

Antibodies are the most commonly used biorecognition molecules in the development of biochemical assays and biosensors in seafood safety, specifically in the field of marine toxins. The biorecognition event between the antibody and the molecule of interest is based on a structural recognition. Thus, antibodies can have the ability to recognise structurally related molecules other than the target analyte, but not necessarily with the same cross-reactivity. This cross-reactivity can be advantageous or not, depending on whether the purpose is to detect the whole family of molecules or just a specific one. Some of the antibodies produced for specific groups of marine toxins can detect several toxin analogues within that toxin family. In those situations where several toxic analogues are present in a sample, it is important to consider that different toxicities among toxin analogues may influence the estimation of the potential risk that the group of toxins may pose. Ideally, a biochemical assay should be able to recognise the toxic analogues according to their individual toxicity and provide a global quantification equivalent to the total toxicity. Consequently, the development of biorecognition molecules able to recognise the different related molecules proportional to their specific toxicity would be desirable to achieve pseudofunctional assays. However, this is not straightforward, and, in the field of marine toxins, the lack of information and data available further hinders this.

When developing new analytical methods, results are compared with those obtained by current reference analysis methods, which usually are instrumental analytical methods. These methods focus on the identification and quantification of individual analytes according to their structure and physicochemical properties and are extremely selective and specific. Again taking marine toxins as an example, instrumental analytical methods are very interesting approaches when all toxin analogues are known and the toxicity of each analogue has been reported, i.e, their toxic equivalency factors (TEFs) in relation to a reference toxin have been established. Once instrumental analysis provides the concentration of the toxin analogues present in the sample, the availability of TEFs allows an estimation of the overall toxic potential of the combination of the toxins present in a given sample, which is expressed according to a reference toxin. If some analogues are not known, are not targeted in the analysis, or if some of their TEFs are not available, analytical instrumentation may have a limitation to correctly estimate the potential risk of a sample according to its toxin profile. Assays implementing recognition molecules are less specific than analytical methods, but on the other hand, may be suitable to obtain a composite toxicity of the sample, even if they may not provide information regarding the individual concentration of each analogue. The idea of providing a

global quantification of the sample is not only interesting in the case of immunoassays and immunosensors for the detection of marine toxins (such as the OA-group toxins, TTXs and AZAs, which have been addressed in this thesis), but also provides an interesting approach in the analysis of BAs using enzymatic assays. Since histamine is the only regulated biogenic amine in seafood, conventional analysis is only addressed to its detection. Nonetheless, its harmful effects have been demonstrated to be enhanced in the presence of putrescine and cadaverine, thus, the detection of these additional biogenic amines together with histamine is highly desirable to protect human health [1].

Nowadays, biochemical assays and biosensors are considered effective screening tools to be used in combination with confirmatory instrumental analysis methods for the analysis of suspicious samples to obtain unequivocal identification and quantification of the analyte of interest. At best, assays implementing biorecognition molecules can offer good sensitivity, robustness, inexpensive analysis, high throughput, and speed of analysis with generally less complicated sample preparation protocols compared to confirmatory methods. The most appropriate method to be implemented in the identification and quantification of the analyte/s of interest has to be selected according to the type of analyte and matrix sample, the purpose of the analysis (e.g. official control or research), as well as the specificity and sensitivity of the method, the cost, the time of the analysis, the number of samples to be managed, the required equipment or the need for trained personnel to perform the analysis. Furthermore, to be applicable to routine screening, biochemical methods, regardless of the chosen assay format, have to be validated with appropriate sample matrices. In this sense, this thesis has addressed the application of the developed assays and biosensors to the analysis of different matrix samples, demonstrating their potential application in seafood safety in almost all the food chain.

Immunoassays for the detection of OA have been used to monitor the presence of diarrhetic shellfish poisoning (DSP) toxins in seawater. Specifically, the analysis has been conducted using the particulate fraction of seawater, thus, OA detected mainly corresponded to the toxin present in phytoplankton cells. The concentration of OA in the particulate fraction has been previously demonstrated to temporally correlate with the concentration of OA in mussels [2], thus, the detection of OA in seawater using immunoassays do not provide a good early warning tool. Alternative strategies that would allow the detection of marine toxins prior to the contamination of shellfish would be beneficial to mitigate the risk for human health and avoid economic losses to the seafood industry. Nevertheless, the determination of toxin concentration in the particulate fraction of seawater provides a viable alternative to the monitoring of *Dinophysis* levels or the presence of DSP toxins in

shellfish. Moreover, the applicability of the immunoassays to the analysis of mussel samples has also been demonstrated.

Shellfish matrices have also been analysed for the detection of TTX. The work focused on the development of a maleimide-based enzyme-linked immunosorbent assay for the detection of TTXs in oysters and mussels perfectly highlights the complexity addressed when working with natural matrices instead of buffer. Oyster and mussel samples, that one could consider need to be processed in a similar way, provided surprisingly different results and required alternative sample preparation. This provides a clear demonstration of the importance to perform matrix effects studies for any of the matrices to be analysed before the implementation of the analytical methods. The determination and application of correction factors (CFs) to TTX contents provided by the immunoassay overcomes the matrix effects in the analysis of shellfish samples, providing effective limits of detection in good agreement with the level of 44 µg TTX equiv./kg shellfish meat [3], which has been considered not to result in adverse effects in humans by the European Food Safety Authority (EFSA). Nonetheless, recent risk assessment studies based on experimental animal data suggest that this maximum concentration should be increased to 200 TTX equiv./kg shellfish meat [4]. The availability of new analytical methods that enable quantifications of TTXs in different matrices in an easy, rapid and cost-effective way will help to provide more data related to the occurrence of TTXs for further risk assessment studies and regulatory decision making. The immunoassay for the detection of TTXs has also been applied to the analysis of human urine samples derived from a puffer fish poisoning incident. In this case, only a simple dilution was required for the analysis of the samples by the maleimide-based enzyme-linked immunosorbent assay. Biochemical assays for the detection of marine toxins have been demonstrated to be applicable in almost all the stages of seafood safety, but the range of fields in which they can be applied is practically unlimited, including public health, forensic science or environmental studies to mention a few.

Colorimetric and electrochemical assays and biosensors for the detection of AZAs in mussels have been demonstrated to be powerful screening tools that can be easily implemented in routine monitoring programs. All immunoapproaches show a broad working range that enable the quantification of AZA-1–3, whose presence in raw shellfish meat is regulated by the European Commission, but there is also a broad range of other toxic analogues and carboxy congeners that are not considered in the current legislation [5]. For their implementation as screening tools in monitoring programs, it is important to keep in mind that the regulatory limit of 160 µg AZA-1 equivalents/kg shellfish only considers AZA-1–3 (including their toxic potential). As a consequence, in samples where more than these three analogues are present,

immunoapproches could provide results that may lead to a closure of a shellfish harvesting area, while LC-MS/MS analysis could not. This fact is not detrimental for immunoapproaches, but helps to better protect consumer health. Although AZA-1–3 are the most abundant analogues in most samples, one cannot discard that other AZA analogues may pose problems (even moreso if we take into account that some of them may suffer decarboxylation after shellfish cooking and be converted to other AZA analogues including AZA-3) [6-7]. For the use of the immunoapproaches as screening tools in monitoring programs, a "positive", "negative" but also a "suspicious" range has to be established. In the case of "negative" samples, shellfish can be consumed without posing a threat to consumers. On the contrary, when a "suspicious" or "positive" result is obtained, a preventive closure of the shellfish harvesting area will be recommended to protect consumer health and the sample will be further analysed by LC-MS/MS to discard or confirm the result. By combining screening and confirmatory methods a faster and more cost-effective system for seafood control will be achieved.

BAs in fish can be considered as a marker of freshness. Considerable amounts of some BAs can appear during fish storage under certain conditions depending on the handling of the raw material, packaging conditions or storage temperature and time. The possibility to carry out a rapid and *in situ* analysis is of major relevance in this case. Thus, the development of biosensors for the detection of BAs plays an important role to achieve this purpose. In addition to fish, BAs are also found in other food products as meat, cheese, wine or beer [8], therefore, the application of these biosensors is not only limited to seafood and can be further expanded to other sectors. Otherwise, histamine is a BA involved in the local responses of the immune system. It has a fundamental role in allergic reactions and is believed to regulate the release of gastric acid in the stomach and intestinal motility, to act as a neurotransmitter in the central nervous system and to regulate the sleep biological rhythm and the control of appetite [9]. Thus, the application of electrochemical biosensors to the detection of BAs in human body fluids could contribute to assess and study cases of inflammation, allergies or sleep-wake regulation, among many others, thus providing an important impact in the field of human health.

Although further validation and inter-laboratory studies should be performed to take colorimetric biochemical assays and electrochemical biosensors to the market, the future of these alternative methods looks bright, especially when time issues related to sample preparation will be solved. By merging the advances made on interdisciplinary areas such as bioengineering, surface biochemistry or electrical engineering and promoting technology transfer, seafood industry and marine monitoring programs, as well as the agri-food, biosanitary, pharmaceutical and environmental sectors in general, will benefit from increasingly simple, sensitive,

compact, automated, reliable and low-cost devices that will allow multi-sample analysis in very short times.

References

[1] P. Visciano, M. Schirone, R. Tofalo, G. Suzzi, Histamine poisoning an control measures in fish and fishery products, Frontiers in Microbiology 5 (2014) doi: 10.3389/fmicb.2014.00500.

[2] M. García-Altares, A. Casanova, M. Fernández-Tejedor, J. Diogène, P. de la Iglesia, Bloom of Dinophysis spp. dominated by D. sacculus and its related diarrhetic shellfish poisoning (DSP) outbreak in Alfacs Bay (Catalonia, NW Mediterranean Sea): identification of DSP toxins in phytoplankton, shellfish and passive samples, Regional Studies of Marine Science 6 (2016) 19-28.

[3] EFSA (European Food Safety Authority), Risks for public health related to the presence of tetrodotoxin (TTX) and TTX analogues in marine bivalves and gastropods, EFSA J. 15 (4) (2017) 4752.

[4]E.E.J. Kasteel, R.H.S. Westerink, Comparison of the acute inhibitory effects of Tetrodotoxin (TTX) in rat and human neuronal networks for fish assessment purposes, Toxicology Letters 270 (2017) 12–16.

[5] European Commission Regulation (EC) No 853/2004 of 29 april 2004 laying down specific hygiene rules for food of animal origin, Official Journal of the European Union L139, 55-205.

[6] P. McCarron, J. Kilcoyne, C.O. Miles, P. Hess, Formation of azaspiracids-3,-4,-6, and-9 via decarboxylation of carboxyazaspiracid metabolites from shellfish, Journal of Agricultural and Food Chemistry, 57(2009) 160-169.

[7] J. Kilcoyne, P. McCarron, P. Hess, C.O. Miles, Effects of heating on proportions of azaspiracids 1-10 in mussels (*Mytilus edulis*) and identification of carboxylated precursors for azaspiracids 5, 10, 13, and 15, Journal of Agricultural and Food Chemistry, 63(2015) 10980-10987.

[8] M.H.S. Santos, Biogenic amines: Their importance in foods, International Journal of Food Microbiology 29 (1996) 213-231.

[9] M.S. Repka-Ramirez, J.N. Baraniuk, Histamine in health and disease, Clinical Allergy and Immunology 17 (2002) 1-25.

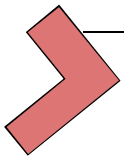

CHAPTER 8

Conclusions

Conclusive remarks

To really take advantage of the multiple benefits that colorimetric biochemical assays and electrochemical biosensors provide in the field of seafood safety, the most appropriate approach in each situation should be selected according to the target analyte and the matrix sample, the analytical performance of the method, the purpose of the analysis and the available resources.

The use of self-assembled monolayers (SAMs) as building blocks in the development of colorimetric immunoassays provides a stable, ordered and optimally oriented immobilisation of the immunospecies. Okadaic acid (OA) has been immobilised on self-assembled monothiols and dithiols for the development of an immunoassay for the detection of diarrhetic shellfish poisoning (DSP) toxins. Although the use of monothiols and dithiols provides colorimetric immunoassays with similar analytical performance, the use of monothiols such as cysteamine considerably decreases the cost of the assay. In the case of the development of a SAM-based immunoassay for the detection of tetrodotoxins (TTXs) by replacing carboxylate-dithiols by cysteamine, the use of monothiols for the SAM formation enabled reductions in the assay time in addition to cost savings.

Both monothiol and dithiol SAM-based immunoassays for OA detection have been successfully applied to the analysis of OA content in the particulate fraction of seawater samples from different locations and also to a mussel sample containing OA, dinophysistoxin-1 (DTX-1) and dinophysistoxin-2 (DTX-2) certified contents. The correlation between *Dinophysis* cells and OA content in seawater has been evaluated, demonstrating that OA detection in the particulate fraction of seawater by the SAM-based immunoassays constitutes a viable alternative to the current monitoring of *Dinophysis* levels. On the other hand, the cysteamine SAM-based immunoassay for the detection of TTXs has been applied to the analysis of oyster and mussel samples, attaining a sensitivity in good agreement with the concentration of TTX that is considered not to result in adverse effects in humans. Matrix effects and toxin recovery values have been shown to strongly depend on the shellfish type and the sample treatment. The determination and application of correction factors (CFs) to the toxin contents provided by the immunoassays overcomes the matrix effects in the analysis of natural samples. The applicability of the TTX immunoassay to the analysis of human urine samples derived from a puffer fish poisoning incident has also been demonstrated, contributing to the confirmation of TTXs as the causative agent of the intoxication. Both shellfish and urine samples can be rapidly processed and analysed by the immunoassay without

the requirement of sample clean-up, which is a clear advantage over LC-MS/MS where solid phase extraction (SPE) is usually required. Results obtained by the immunoassays and LC-MS/MS show an excellent correlation, demonstrating the applicability of the immunoassays as screening tools and the complementarity of the techniques based on different recognition principles.

The establishment of cross-reactivity factors (CRFs) in the development of immunoassays helps to better understand the comparison between the quantifications provided by the immunochemical tools and those obtained by LC-MS/MS in the determination of toxin content in samples with multiple analogues. In the development of magnetic bead (MB)-based immunoassays for azaspiracids (AZAs) detection and their subsequent validation by comparison with LC-MS/MS, CRFs for AZA-2–10 (with respect to AZA-1) have been established. In these immunoassays, MBs are used as antibody supports and peroxidase-labelled AZA as a tracer. The combination of the functionalised MBs with electrode arrays enables the electrochemical detection of all regulated AZAs but also other toxic AZA analogues and possible AZA derivatives. After applying the CRFs to the individual contents of AZA analogues determined by LC-MS/MS analysis, an excellent correlation between LC-MS/MS values and the quantifications obtained by the immunoassays has been achieved in the analysis of naturally contaminated mussel samples. Excellent analytical performance has also been achieved in the development of electrochemical immunosensors for the detection of AZAs by the direct immobilisation of the antibody on protein G or avidin-coated electrodes. Bioaffinity interactions allow a stable and controlled immobilisation of the antibody. As a matter of fact, the strong avidin–biotin interaction has enabled the reusability of the avidin–biotin interaction-based immunoassays. Together with the low amounts of immunoreagents required, it represents significant economic savings as well as a contribution to sustainability in the development of electrochemical biosensors.

The use of MBs as immobilisation supports provides large surface areas available for biomolecule immobilisation and improves assay kinetics. A clear example is that the MB based-immunoassays for AZAs detection only requires 15 min to be completed. Moreover, both the anti-AZA PAb-MB conjugates for the development of the immunoassays for AZAs detection as well as the diamine oxidase (DAO)-MB conjugates used for the development of electrochemical biosensors for the detection of biogenic amines, have been demonstrated to have excellent storage stability, which allows the provision of ready-to-use conjugates. This property enables the reduction of analysis time and facilitates protocol simplification. In the case of the enzyme biosensors, enzyme binding on the magnetic beads provides stability to the enzyme activity, as well as, demonstrates the strong covalent linkage

between the diamine oxidase and the magnetic beads. The immobilisation of DAO-MB conjugates on any type of electrode surface, by simply placing the electrode over a magnet, has enabled the provision of different approaches for the electrochemical monitoring of biogenic amines in fish. Through the favourable application of electrochemical biosensors for the analysis of different analytes and in different matrices, the potential of electrochemical biosensors as rapid, cost-effective, compact and easy-to-use screening tools in the field of seafood safety has been highlighted.

The exploitation of diatoms as natural nanostructured supports opens a new range of possibilities in the development of biosensors. In this thesis, a method for the addressed diatom immobilisation on screen-printed electrodes by means of gold electrodeposition has been proposed, with the aim to harness the unique properties of diatoms as building blocks in the development of electrochemical biosensors. Gold electrodeposition not only allows the immobilisation of the diatoms on electrodes but also confers excellent electrocatalytic activity to the final gold-diatom electrodes. The feasibility to combine tailored immobilisation with diatom biofunctionalisation provides an interesting approach for microarray fabrication and brings us closer to future biosensor arrays, which will be addressed to the detection of multiple target analytes in complex samples in one single analysis.

Personally, I expect that the experimental design presented throughout this thesis, including several steps such as the study of matrix effects or the application of cross-reactivity factors, the analytical methods developed and the several examples provided regarding their application, serve beyond the writing of this thesis and help to the implementation of these powerful analytical devices to daily life food safety monitoring but also to research programs, which are the origin of the establishment of food safety regulations. The application of the biochemical devices presented herein is not only limited to the field of food safety but also to many other sectors such as environmental monitoring or biomedical diagnostics. For instance, immunoassays and immunosensors for marine toxins can be applicable to the analysis of seawater (as it has been demonstrated in the case of the SAM-based immunoassays for OA detection), which is of great interest for researchers aiming to study harmful algal blooms and toxin dynamics. In the same way, biosensors for the detection of BAs can be used to the analysis of human body fluids to help to confirm a diagnosis of anaphylaxis, or mastocytosis, among many other disorders related with elevated histamine levels in blood or urine. Furthermore, given that the described approaches are versatile and can be easily used with other biorecognition molecules and target compounds, one can envisage that the applications of colorimetric biochemical assays are practically unlimited.

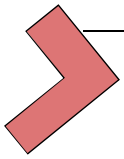

ANNEX

Biosensors for the detection of emerging marine toxins

Sandra Leonardo, Laia Reverté, Jorge Diogène, Mònica Campàs

IRTA, Carretera de Poble Nou, km 5.5, 43540 Sant Carles de la Ràpita, Spain

Abstract

Emerging marine toxins present in the environment are relevant for food safety issues. Researchers are currently putting special emphasis on the development of biosensors for their detection. Due to their structural complexity and the difficulty to produce the corresponding biorecognition molecules, the development of assays and biosensors for their detection has become a challenge. Compared to traditional detection techniques, biosensors can provide advantages in terms of sensitivity, specificity, design versatility, portability and multiplexed configurations. This chapter provides a critical overview of the immunosensors, receptor-based biosensors, cell-based biosensors and aptasensors that have been developed for the detection of palytoxins (PlTXs), brevetoxins (PbTXs) and tetrodotoxins (TTXs). Although only few biosensors for these emerging marine toxins have been described to date, the chapter reflects the promising advances made in this field.

1. Introduction

Marine toxins are secondary metabolites some of which can be produced by microalgae of the groups of dinoflagellates and diatoms. The specific role these toxins may play in the microalgae that produce them is not clear. These toxins often enter the food webs and may ultimately reach humans through food consumption or direct exposure to marine water, causing different illnesses.

As some virus, bacteria, fungi and protozoa, some marine toxins, such as saxitoxins (STXs) and tetrodotoxins (TTXs), can be considered as potential chemical warfare agents (Anderson 2012 and Kruger et al. 2014). Nevertheless, reported poisoning incidents related with marine toxins have only been due, to the best of our knowledge, to accidental ingestion of contaminated seafood or direct exposure to marine water. In a “fictive world” (movies, books) everything is plausible, including the use of marine toxins as potential weapons. In the “real world”, STX, which is a potent neurotoxin produced by several species of marine dinoflagellates (e.g.

Alexandrium minutum, A. catenella, Gymnodynium catenatum), is included in the list of chemical weapons described by the Organisation for the Prohibition of Chemical Weapons (OPCW 2015). However, although being extremely potent, marine toxins seem not to be presently considered as practical weapons, probably due to the difficulty or cost to produce them in comparison with other chemical weapons. Still, as one may understand, this analysis may only be speculative since probably very little information would be available in case these toxins were presently being used as chemical weapons.

Some marine toxins are quite well described according to their structure, mechanism of action, potency and geographical distribution. This is the case for Amnesic Shellfish Poisoning (ASP, e.g. domoic acid, DA), Diarrheic Shellfish Poisoning (DSP, e.g. okadaic acid, OA) and Paralytic Shellfish Poisoning (PSP, e.g. STX) toxins for which international regulations exist that set up maximum permitted levels in food and define the official methodologies to detect them.

Nonetheless, many marine toxins are presently considered, with a certain degree of subjectivity, as "emerging" toxins including those recently discovered (e.g. pinnatoxins), those that may have recently appeared in certain areas (e.g. ciguatoxins – CTXs recently identified in fish from the Canary Islands), or those that are not yet regulated because not enough information is available regarding their toxicity or distribution (e.g. palytoxins – PlTXs, brevetoxins – PbTXs and cyclic imines – CIs), and those for which regulation exists but additional toxicological information is required (e.g. azaspiracids, AZAs) (Reverté et al. 2014).

The little information and data available for some emerging marine toxins, their structural complexity and the scarcity of standards have compromised the development of methodologies for their detection. The development of biosensors requires stable biorecognition molecules such as enzymes, receptors or antibodies that will unequivocally detect the analyte. In some cases biorecognition molecules for marine toxins have not been produced and this limits the number of biosensors developed. Nevertheless, marine toxins are nowadays awaking interest in the biosensors world, possibly due to their importance in food safety and environmental monitoring and this opens new applicability fields for biosensors.

In this chapter, we present a detailed overview of the biosensors that have been developed for the detection of PlTXs, PbTXs and TTXs. CTXs and CIs (spirolides, gymnodimines, pinnatoxins and pteriatoxins), although also of concern as reflected in the Scientific Opinions on marine biotoxins in shellfish of the European Food Safety Authority (EFSA) Panel on Contaminants in the Food Chain (EFSA 2010a and EFSA 2010b), have not been included since no biosensors have been reported to date.

2. Biosensors for palytoxins

Palytoxin (PlTX)-group toxins are complex polyhydroxylated compounds with lipophilic and hydrophilic areas (Fig. 1). They have been isolated from marine zoanthids (soft corals) of the genus *Palythoa* and are also found in benthic dinoflagellates of the genus *Ostreopsis*. PlTX-group toxins have been identified as the toxins responsible for clupeotoxism, a form of ichthyosarchotoxism caused by sardines, and are also found in seafood (fish, shellfish, gastropods or echinoderms) from Japan, Vietnam, Philippines, Malaysia, Singapore, Indonesia, Micronesia, Australia, New Zealand, Hawaii, Cook Islands, French Polynesia, Brazil, Mexico, the Caribbean sea, Madagascar, Reunion Island and the Mediterranean sea (Aligizaki et al. 2011 and Reverté et al. 2014). Apart from the contamination with PlTX-group toxins of seafood intended for human consumption, outbreaks of *Ostreopsis* spp. have been implicated in respiratory, dermatological and ophthalmologic symptoms in coastal human populations in the Mediterranean (Pfannkuchen et al. 2012 and Barroso et al. 2008). However, the available toxicological information is limited and the signs and symptoms are not well-defined. Currently there are no regulations on PlTX-group toxins in shellfish, either in the European Union (EU) (EFSA 2009) or in other regions of the world. Nevertheless, the National Reference Laboratories for Marine Biotoxins (NRLMB) have proposed a provisional limit of 250 µg/kg in shellfish (CRLMB 2005).

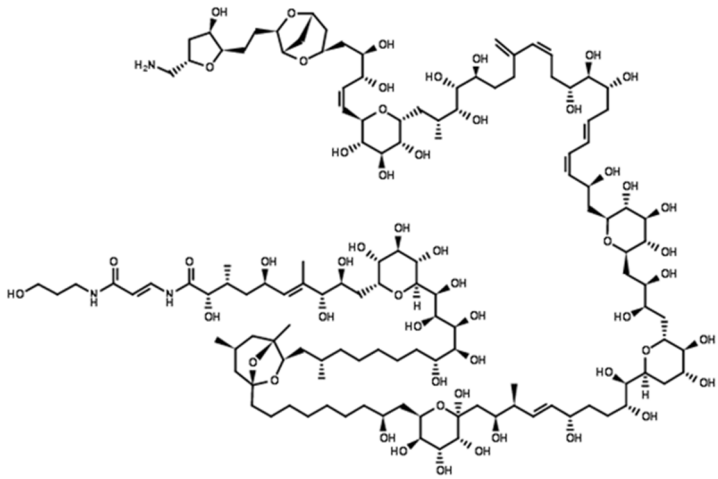

Fig. 1. Palytoxin structure.

2.1. Immunosensors for palytoxins

The relatively large size of PlTX makes easy the antibody (Ab) production via animal immunization, thereby simplifying the development of immunoassays and immunosensors. Optical surface plasmon resonance (SPR) biosensors offer the capability of Ab characterization and then incorporation of these bioreceptors into rapid, sensitive assays on the same platform. An SPR biosensor based on a direct format has been developed for the detection of PlTX (Yakes et al. 2011a). After characterization of monoclonal antibody (MAb) kinetics and optimisation of the experimental parameters, the appropriate performance of the optical immunosensor was demonstrated by performing standard curves for PlTX in buffer as well as in seafood matrices. The limits of detection (LODs) obtained were 0.52, 2.8 and 1.4 ng/mL for PlTX in buffer, grouper and clam samples, respectively, which highlight the need of matrix matching for accurate determination of toxin concentration.

A substantial matrix effect was also observed in the development of a multiplexed SPR immunosensor for the detection of PlTX, STX, OA and DA (Campbell et al. 2014). Regarding PlTX, the toxin was immobilised onto the chip surface of a flow cell using the carbodiimide reaction to covalently link the amine group of the PlTX molecule to activated carboxylic groups of the chip. The low amount of antibody and toxin available – note that there are no commercial antibodies and that PlTX-group toxins standards are not always available – did not allow to perform exhaustive optimisation studies and validate the assay. Nevertheless, the work clearly demonstrated the applicability of SPR multichannel systems to multiple toxin detection on a single bioanalytical sensing platform. Additionally, the analysis was fast (it required less than one hour to analyse four toxin classes per sample) and simple (a single multi-toxin extraction procedure was used). Multiplexed and miniaturised devices pave the way towards the development of compact and automated tools for high-throughput sample analysis in a fast and expensive way, and additionally facilitate to move analyses to places away from laboratories, such as harvesting sites.

Regarding electrochemical biosensors, a highly sensitive biosensor for the detection of PlTX-group toxins based on a sandwich format and electrochemiluminescence detection has been described (Zamolo et al. 2012) (Fig. 2). The immunosensor incorporated doubly carboxyl-functionalised multi-walled carbon nanotubes (MWCNTs), the groups on the sidewalls being used to conjugate capture anti-PlTX MAb and those on the tips being used to immobilize it on the surface of an optically transparent electrode coated by an electrochemical polymer layer. The electrochemiluminescent detection was performed by labelling the detection anti-PlTX polyclonal antibody (PAb) with a ruthenium complex. The use of CNTs

increased the amount of immobilised MAb and favoured the electron transfer, providing specific and sensitive electrochemiluminescent immunosensors with an LOD as low as 0.07 ng/mL of PITX. The applicability of the immunosensor was demonstrated by the analysis of PITX-spiked mussels and microalgae samples. Low matrix effects were observed due to the modification of the electrode with CNTs, which minimised the non-specific adsorption, and the electrochemiluminescent transduction strategy.

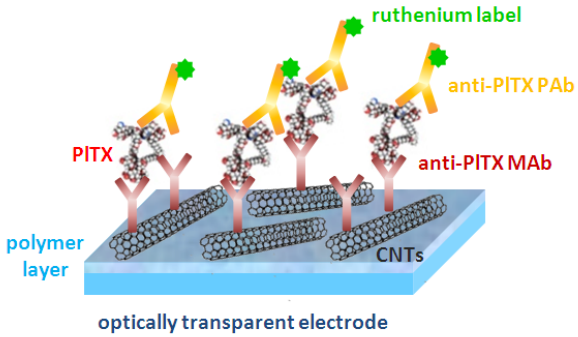

Fig. 2. Scheme of the electrochemiluminescence immunosensor for the detection of palytoxin.

2.2. Receptor-based biosensor for palytoxins

Other biosensors for PITX-group toxins are based on their mechanism of action. PITX binds to the Na^+/K^+-ATPase in the cell membrane, inhibiting its activity and converting it into a permanently open ion channel (Hilgemann 2003). As a consequence, a rapid sodium influx and potassium efflux from cell is produced, triggering with this a plethora of secondary effects. An optical SPR biosensor for the detection of PITX based on its affinity towards Na^+/K^+-ATPase has been reported (Alfonso et al. 2014). In this work, the Na^+/K^+-ATPase pump was immobilised on the SPR chip via thiol coupling, and the PITX binding was afterwards recorded in real time. The developed biosensor showed a very low LOD (3.73 pg) and it was applied to the analysis of PITX-group toxins in *Ostreopsis siamensis* cultures, which demonstrated the viability of the approach. It is interesting to mention that a previous work had tried to immobilise the Na^+/K^+-ATPase pump on the SPR sensor by amine coupling but this kind of immobilisation prevented PITX-group toxin from binding. Amine coupling is usually easy and effective because most macromolecules contain many groups that can participate in the reaction. However, in some cases, these reactive groups can be located near or on the active site of the macromolecule

and the immobilisation process can result in conformational changes and loss of biological activity, as it seemed to occur when immobilising the Na^+/K^+-ATPase pump.

2.3. Cell-based electrochemical assay for palytoxins

Haemolysis assays for the detection of PlTX-group toxins are also based on the capacity of the toxins to interact with the Na^+/K^+-ATPase of erythrocytes and its conversion into a non-specific cation channel. Ion imbalance in red blood cells results in their haemolysis. Samples pre-treated with ouabain, a glycoside which inhibits the Na^+/K^+-ATPase pump, are used as a control to ensure the specificity of the assay towards PlTX; the presence of ouabain will reduce the haemolytic activity of PlTXs, while it will have no effect on the haemolytic effect of other haemolytic compounds. Haemolysis is usually detected by spectrophotometry, but it is interesting to describe the work performed by Volpe and co-workers (2014). These authors combined the haemolysis of sheep erythrocytes by PlTX-group toxins with the electrochemical measurement of the lactate dehydrogenase (LDH) released in the culture supernatant after cell disruption. The LDH activity was measured by adding NADH/pyruvate as enzyme substrates and PMS^+. The later reacted with the remaining NADH to produce PMSH, which reacted with the redox mediator hexacyanoferrate(III) to produce hexacyanoferrate(II). Oxidation of hexacyanoferrate(II) was then performed on the electrode surface of a strip of eight screen-printed electrodes (SPEs). The LOD depended on the haemolysis time, being 0.007 and 0.16 ng/mL for 24 and 4 h, respectively. The necessity to use matrix-standard calibration curves for accurate analysis of PlTX was observed when applying the electrochemical assay to the analysis of PlTX-spiked samples.

3. Biosensors for brevetoxins

Brevetoxin (PbTX)-group toxins are lipid-soluble cyclic polyether compounds (Fig. 3). They are primarily produced by the dinoflagellate *Karenia brevis* (formerly *Ptychodiscus brevis*, Pb giving name to the acronym PbTX) and can accumulate in shellfish and fish. PbTX-group toxins seem to be limited to the Gulf of Mexico, the east coast of USA, and the New Zealand Hauraki Gulf region. These toxins cause neurotoxic shellfish poisoning (NSP), with symptoms such as nausea, vomiting, diarrhoea, paraesthesia, cramps, bronchoconstriction, paralysis, seizures and coma, and dermal or inhalation exposure can result in irritant effects. Moreover, they are potentially carcinogenic. However, the toxicological database for PbTX-group toxins is limited. As a consequence, currently there are no regulatory limits for PbTX-group

toxins in shellfish or fish in Europe (EFSA 2010c). Nevertheless, maximum permitted levels have been established in USA (20 mouse units (MUs)/100 g or 0.8 mg PbTX-2 equivalents/kg fish) (US FDA 2001), New Zealand and Australia (20 MUs/100 g, analogue not specified) (NZFSA 2006 and FSANZ 2010). The discovery of new PbTX-group toxin producing algae and the apparent trend towards expansion of algal bloom distribution, suggest that PbTX-group toxins could emerge in Europe and their analysis in shellfish and fish should be considered. Further information is needed to better characterize the oral toxicity of PbTX-group toxins and their relative potencies.

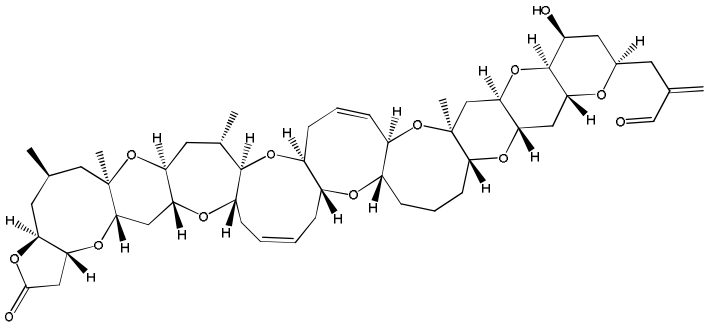

Fig. 3. Brevetoxin-1 structure.

3.1. Immunosensors for brevetoxins

PbTX is a low-molecular weight toxin with very few functional groups available for cross-linking, and this usually hinders its immobilisation to develop immunosensors. The first biosensor for PbTX was reported on 1993 (Carter et al. 1993). PbTX-3-bovine serum albumin (PbTX-3-BSA) conjugates were prepared to immobilise the toxin on a membrane through the lysine moiety of BSA. Free and immobilised PbTX-3 competed for glucose oxidase (GOx)-labelled anti-PbTX-3 Ab. Finally, the H_20_2 produced by the addition of β-D-glucose was detected amperometrically. Some years after, Kreuzer and co-workers (2002) developed electrochemical immunosensors to detect different marine toxins (PbTX, OA, DA and TTX). PbTX-3-BSA conjugates were prepared via carbodiimide reaction to immobilise the toxin on the SPE surface. Nevertheless, the hydroxyl group of PbTX-3 (the only functional group available) had to be modified to make the molecule more active for coupling to BSA via carbodiimide chemistry. Once the conjugates were immobilised on the electrode surface, a competition step between immobilised and free toxin in solution for the labelled primary Ab was performed. Amperometric detection of *p*-aminophenyl phosphate produced by the enzyme label, alkaline phosphatase (ALP),

was used to measure the recognition event. Sensitivity problems were observed, which were attributed to the difficulties in the conjugate synthesis and the low amount of toxin available.

The immobilisation of biomolecules on the electrode is a crucial step in the development of electrochemical immunosensors. Usually, the sensitivity of immunosensors can be improved by the control of the amount and orientation of antigens/Abs immobilised on the electrode, which have to be able to retain their biological activity. Dendrimers are hyperbranched polymers precisely engineered to carry molecules encapsulated in their interior void spaces or attached to their surface. A sensitive electrochemical immunosensor for PbTX was developed exploiting dendrimers as toxin immobilisation nanostructured supports (Tang et al. 2011). Au NPs were simultaneously synthesised and encapsulated into amine-terminated poly(amidoamine) dendrimers, providing AuNP-PAADS conjugates that were afterwards absorbed on ester-modified gold electrodes. PbTX-2-BSA conjugates were then immobilised on the nanostructured surface. Free and immobilised PbTX-2 competed for the horseradish peroxidase (HRP)-labelled anti-PbTX-2 MAb and the immunosensor response was measured using *o*-phenylendiamine and H_2O_2. An LOD of 0.01 ng/mL was obtained, which is much lower than the LOD for the immunosensor without Au NPs or dendrimers (0.5 and 0.1 ng/mL, respectively). As demonstrated, the use of the 3D-newtwork of AuNP-PDAAs greatly increased the amount of immobilised PbTX-2-BSA and improved the conductivity of the immunosensing interface, therefore enhancing the sensitivity of the electrochemical immunosensor.

Enzyme labels, usually HRP or ALP, are widely used and well-explored in the development of immunosensors. Nevertheless, these strategies usually require an enzyme substrate and its bioactivity can decrease when the biomolecules are exposed to reactive groups and harsh reaction conditions. To tackle this issue, other electroactive species such as thionine or guanine/adenine nucleobases can be used as indicators, as well as various nanomaterials, including quantum dots (QDs), metal nanoparticles and metal ions. Chen's research group explored the use of magnetic beads to covalently immobilise anti-PbTX-2 MAb and use them as immunosensing probes for the capture of PbTX-2 (Tang et al. 2012) (Fig. 4). The recognition element was prepared by chemical modification of PbTX-2-BSA conjugates with guanine-assembled graphene nanoribbons (GGNRs). Guanine was used as label, since it can be oxidised in the presence of $Ru(bpy)_2^{3+}$. The catalytic oxidation was electrochemically detected after the competition step and entrapment of the magnetic immunocomplex on a carbon paste electrode by a magnet. The LOD of the magneto-controlled electrochemical immunoassay was 1 pg/mL of PbTX-2 and its applicability was demonstrated by the analysis of spiked mussel, clam and cockle

samples, providing similar results than those obtained with a commercial ELISA kit for PbTX-2 determination. The same research group also explored the use of metal nanoclusters as labels (Zhang et al. 2012). In this work, magnetic beads were used to co-immobilise anti-PbTX-2 and anti-dinophysistoxin-1 (anti-DTX-1) MAbs by epoxy-amine reaction. Cadmium nanoclusters (CdNC) and copper nanoclusters (CuNC) were linked to PbTX-2-BSA and DTX-1-BSA, respectively, and used as distinguishable signal tags. On the basis of the competitive-type immunoassay format, the magnetic immunocomplexes were collected onto a magnetic detection cell and the electrochemical signals were simultaneously recorded at different peak potentials using square wave anodic stripping voltammetry (SWASV). The multiplexed immunosensor was able to discriminate between PbTX-2 and DTX-1 toxins without any interference. The LODs obtained were 1.8 ng/mL and 2.2 ng/mL for PbTX-2 and DTX-1, respectively. The method featured unbiased identification of negative and positive samples, as was demonstrated by the analysis of 12 spiked mussel, clam and cockle samples containing both marine toxins and the comparison with the commercial PbTX-2 ELISA kit.

Another enzyme-free electrochemical immunoassay for PbTX-2 has been recently developed using a mesoporous carbon-enriched palladium nanostructure (MSC-PdNS) as a label due to its peroxidase mimic activity (Lin et al. 2015). In this configuration, PbTX-2-BSA was immobilised onto a nanogold-functionalised carbon electrode through the affinity between cysteine or lysine residue of BSA and gold. Afterwards, free PbTX-2 present in the sample competed with immobilised PbTX-2-BSA for the MSC-PdNS-labelled MAb, and the resulting catalytic current in the presence of H_2O_2 and thionine mediator was recorded. The electrochemical immunosensor showed an LOD of 5 pg/mL and was successfully applied to the analysis of spiked mussel samples, providing results in good correlation with the PbTX-2 ELISA kit.

Quartz crystal microbalance (QCM) has also been used for the detection of small molecules such as PbTX-2 (Tang et al. 2013). The QCM sensors measure the resonant frequency by the standard oscillation technique. The immunosensor is based on the immobilisation of dextran onto the quartz crystal coated with graphene and the following binding of the capture anti-PbTX-2 MAb to concanavalin A (ConA) *via* biotin-streptavidin interaction. The anti-PbTX-2 MAb-ConA immunocomplex is bound to dextran through the affinity between dextran and ConA. Gold nanoparticles functionalised with glucoamylase and PbTX-2-BSA conjugates compete with free PbTX-2 for the binding to the immobilised MAb. In the absence of free PbTX-2, amylopectin is hydrolysed by the glucoamylase to glucose, which displaces the anti-PbTX-2 MAb-ConA immunocomplex from the graphene-coated crystal surface, leading to a large change in the frequency of the

immunosensor. The presence of free PbTX-2 decreased this effect. An LOD as low as 0.6 pg/mL of PbTX-2 was attained and the applicability of the QCM immunosensor was demonstrated by the analysis of a large number of spiked mussel, clam and cockle samples. Results were in good agreement with those obtained by the commercial ELISA kit.

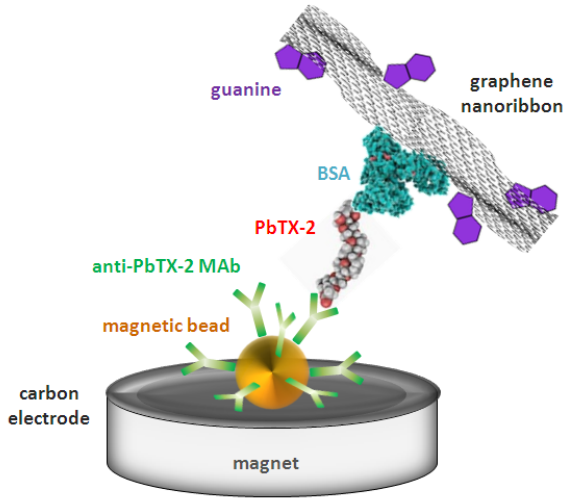

Fig. 4. Scheme of the magneto-controlled electrochemical immunosensor for the detection of brevetoxin-2.

3.2. Aptasensor for brevetoxins

Aptamers are single stranded DNA (ssDNA) or RNA oligonucleotides that were proposed two decades ago as stable, reproducible and low-cost bioreceptors to replace antibodies in assays and biosensors. In this regard, an electrochemical biosensor for the detection of PbTX-2 using aptamers has been developed (Eissa et al. 2015). After obtaining several aptamers, the aptamer with the highest binding activity was selected using fluorescence and electrochemical impedance spectroscopy. Then, the corresponding impedimetric label-free competitive biosensor for PbTX-2 was developed. The competition was established between PbTX-2 immobilised on the gold surface and free PbTX-2 in solution in the presence of a fixed amount of aptamer. PbTX-2 had been covalently linked to the gold surfaced through a cysteamine self-assembled monolayer. An LOD of 106 pg/mL was achieved, and a high degree of cross reactivity of the aptamer towards other PbTX-group toxins was observed. The applicability of the aptasensor was

demonstrated by the detection of PbTX-2 in spiked shellfish samples, which showed high recovery percentages.

3.3. Phosphodiesterase inhibition-based sensor for brevetoxins

As previously mentioned, SPR is used either to study interactions or to quantify relevant molecules. However, SPR systems show low sensitivity to small molecules. Inhibition detection and sandwich protocols can be implemented in this case to solve this inconvenient. To this purpose, a SPR-based method for the detection of ladder-shaped polyether compounds (PbTX-2 among them) has been reported (Mouri et al. 2009). The ability of these molecules to inhibit the interaction of desulfo-yessotoxin to phosphodiesterase II was used to design an indirect assay able to detect several toxins. In the case of PbTX-2, inhibition was achieved in the µM range. However, this assay was not tested in shellfish matrixes and the data point to a lack of specificity, since toxins from different groups can be detected, including the marine toxins yessotoxins.

3.4. Cell-based sensors for brevetoxins

PbTX-group toxins bind with high affinity to receptor site 5 of the α subunit within voltage-gated sodium channels (VGSCs) present in cell membranes. Binding of PbTX to VGSCs leads to channel activation, uncontrolled Na^+ influx into the cells and depolarization phase of action potential in excitable cells, such as cardiomyocytes and neurons. With this in mind, some biosensors based on the use of cardiomyocytes (Wang et al. 2015a) or neuronal networks (Kulagina et al. 2006) for the detection of PbTX-group toxins have been described. Since STX also binds to VGNCs on a different site of the α subunit, both biosensors have been used to detect these two marine toxins. In contrast to PbTX, STX is a potent and selective inhibitor of VGSCs, which produces a blockage of action potentials. In both works, the excitable cells have been cultured on the surface of a microelectrode array (MEA) and the changes in the electrophysiologic parameters in the presence of the toxins have been recorded. The cardiomyocyte-based biosensor consisted of a label-free and real-time wireless 8-channel recording system, which dynamically monitor the multi-site electrical activity of the cardiomyocyte network. This biosensor attained an LOD of 1.55 ng/mL of PbTX-2 within 5 min and it was able to discriminate between STX and PbTX-2. This biosensor is a clear example that the development of portable and remote devices with a real-time detection is possible but still incipient. On the other hand, the work reported by Kulagina and co-workers (2006) demonstrated the utility to use a neuronal network biosensor for the detection of

important neurotoxins in algal samples, with only a minimum sample preparation being required. This biosensor provided an LOD for PbTX-3 of 0.30 ng/mL in buffer and 0.43 ng/mL in the presence of 25-fold-diluted seawater. Although the two biosensors described could be used to classify potential neurotoxins due to their signature effects on electrophysiological parameters, it is important to note that this generic detection approach will neither fully identify nor quantify the individual toxins. Nevertheless, it is a complementary tool to other structure-based assays able to detect biologically active mixtures and provides an integrative overview

4. Biosensors for tetrodotoxins

Tetrodotoxin (TTX)-group toxins are low-molecular-weight compounds consisting of a guanidinium moiety connected to a highly oxygenated carbon skeleton that possesses a 2,4-dioxaadamantane portion (Fig. 5). TTX-group toxins are usually found in puffer fish, and are produced by endo-symbiotic bacteria that naturally inhabit the gut of the animal. These toxins have also been found in gastropods, newts crabs, frogs, sea slugs, star fishes, blue-ringed octopuses and ribbon worms. Previously they were reported only in Japan, but later on they have also been found in Korea, Taiwan, China, Thailand, Bangladesh, India, Australia, New Zealand, Hawaii, USA, Madagascar, Norway, Israel, Egypt, Greece and Spain (gastropod caught in Portugal). TTX is a potent neurotoxin, which acts as a sodium channel blocker. Some symptoms of poisoning are tingling of the tongue and lips, headache, vomiting, muscle weakness, ataxia and even death (Bane et al. 2014). In Japan the regulatory limit for TTX in food is 2 mg/kg, while in the USA a zero level has been established. No regulation specific for this toxin exists in Europe, although the commercialization of tetraodontidae is forbidden.

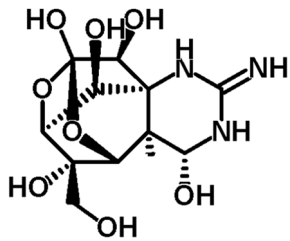

Fig. 5. Tetrodotoxin structure.

4.1. Immunosensors for tetrodotoxins

Most of the existing biosensors for the detection of TTX are based on the use of specific Abs as biorecognition molecules. However, the production of Abs has been hindered by the small size of this toxin. In regard to this, TTX needs to be conjugated to protein carriers to immunize the animals but also to develop the corresponding immunoassays and/or immunosensors.

A few works exploit the use of TTX conjugates in direct competitive immunoassays for the subsequent transfer to SPEs to develop the corresponding electrochemical immunosensors (Neagu et al. 2006 and Kreuzer et al. 2002). Following the same procedure used to develop the electrochemical immunosensor for PbTX in section 3.1 (Kreuzer et al. 2002), TTX has been conjugated to BSA, and the conjugates have been then immobilised on SPEs for the subsequent competition step. In the other work, TTX has been conjugated to the ALP enzyme, the conjugate being used in this case as a tracer (Neagu et al. 2006). The approach using the tracer provided an LOD of 1 ng/mL. In the work of Kreuzer and collaborators (2002), the use of TTX-BSA coater together with a primary Ab labelled with the ALP enzyme, allowed to obtain the lowest LOD ever reported for TTX (0.016 ng/mL). In this case, it is important to mention that the use of a labelled primary Ab is an advantage compared to the use of a secondary Ab, since it improves the performance of the biosensor and decreases the analysis time.

Several optical SPR immunosensors have been reported for TTX. Due to the small size of TTX, most of them are based on the immobilization of the toxin on gold SPR chips and the subsequent competition step. In the first works, the immobilization of TTX was performed through mixed self-assembled monolayers (SAMs) of hydroxy- and amino-terminated oligo-ethylene glycol alkanethiols (OEG-ATs) (Yakes et al. 2011b, Taylor et al. 2008, Taylor et al. 2011 and Vaisocherová et al. 2011). While the amino-terminated OEG-ATs were used to covalently link the TTX to the surface through formaldehyde, hydroxy-OEG-ATs were used as spacer molecules to avoid cross-linking between amino-OEG-ATs. The use of SAMs provides an oriented TTX immobilization and the ethylene glycol molecules minimize the non-specific adsorption of proteins onto the surface of the chip. All these immunosensors attained similar LODs, ranging from 0.3 to 3.4 ng/mL of TTX in buffer. Recently, Campbell and co-workers (2013) have proposed the direct TTX immobilization on carboxymethylated chips. Although in this approach TTX is not oriented as properly as when using SAMs, it simplifies and shortens the experimental protocol, still retaining the performance of the biosensor (LOD ≤ 0.2 ng/mL) (Fig. 6). The applicability of the SPR immunosensors to the analysis of naturally-contaminated samples has been demonstrated in several matrixes: puffer fish (Yakes et al. 2011b,

Taylor et al. 2011 and Vaisocherová et al. 2011), sea snail (Campbell et al. 2013), human urine (Taylor et al. 2011), milk and apple juice (Yakes et al. 2011b).

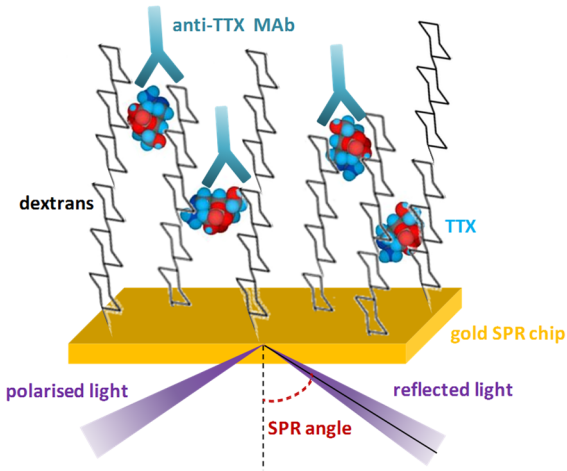

Fig. 6 .Scheme of the optical SPR immunosensor for the detection of tetrodotoxin.

Although, as previously mentioned, the detection of small molecules by SPR usually requires the immobilization of the antigen, Yakes and co-workers (2014) have proposed the immobilization of the Ab on the chip and the subsequent non-competitive detection of TTX. This new configuration provided an LOD of 0.09 ng/mL, even lower than in the previous SPR immunosensors. This has been possible thanks to the advances in SPR instrumentation, including higher signal-to-noise ratio, improved fluidics with stronger vacuum pumps and higher number of antibody sites on the chips, advantages that could benefit the detection of other small analytes.

4.2. Aptasensor for tetrodotoxins

An electrochemical aptasensor for the detection of TTX has been recently proposed (Fomo et al. 2015). In this work, glassy carbon electrodes were modified with poly(4-styrenesolfonic acid)-doped polyaniline films (PSSA/PANI) by electropolymerisation. Afterwards, an amino-terminated aptamer against TTX was covalently immobilised on the PANI/PSSA films via glutaraldehyde cross-linking. The detection of TTX was assessed by electrochemical impedance according to the charge transfer resistance of the PSSA/PANI film, providing an LOD of 0.199 ng/mL. This low LOD was attained

thanks to the ordered monolayer of conductive PANI/PSSA films which improved the electron transfer.

4.3. Cell-based sensors for tetrodotoxins

Apart from the antibody-based methods, cell-based biosensors also deserve to be mentioned since they provide realistic models mimicking the original tissue, information which is usually complementary to that obtained from immunosensors. These cell-based methods are based on the mechanism of action of TTX, which is able to selectively inhibit sodium channels, blocking both nerve and muscular action potentials. Following this principle, some biosensors have been reported (Cheun et al. 1996, Pancrazio et al. 2003, Charkhkar et al. 2012, Wang et al. 2015b). In the simplest approach, Cheun and co-workers (1996) developed a biosensor consisting of a sodium electrode covered with frog bladder membrane integrated within a flow cell. TTX concentration was measured from the inhibition ratio of the sensor peak output by patch clam recording, the lowest amount detected being 86 fg. The application of this biosensor to the analysis of puffer fish was successfully achieved and results were in agreement with those obtained by MBA.

Aiming at the development of compact and multiplexed devices, portable microelectrode arrays incorporating cultured neuronal networks for the detection of TTX have been reported (Pancrazzio et al. 2003 and Charkhkar et al. 2012). In these works, spinal cord cells cultured on gold electrodes were exposed to TTX and extracellular potentials from these cells were recorded, providing an IC_{50} of 0.95 ng/mL of TTX. Following the same biorecognition principle but a different measurement technique, a cardiomyocyte-based impedance biosensor has been recently developed for both TTX and STX, because of their common mechanism of action (Wang et al. 2015b). In this case, cardiomyocyte cells growth and beating status after TTX treatment were measured on 96-well gold electrodes plates by impedance recording. Although the LOD is higher than in other methods described for the detection of TTX (89 ng/mL vs 0.087 ng/mL for TTX and STX, respectively), this novel real-time and label-free impedimetric biosensor platform is versatile and could be applied to the detection of other neurotoxic molecules.

5. Conclusions and perspectives

In the past years, a few biosensors for the detection of PlTXs, PbTXs and TTXs have been described. Most of them are immunosensors, but some cell-based sensors, a receptor-based biosensor for PlTX, and even aptasensors for PbTXs and TTXs and an inhibition-based sensor for PbTXs have also been recently reported, showing a

breakthrough in the development of biosensors for the detection of emerging marine toxins. This is not the case for other emerging toxins such as CTXs and CIs, for which no biosensors have been described yet. Nevertheless, given the numerous possibilities in the development of biosensors (e.g. different transduction strategies, biorecognition molecules and configurations) and the multiple advantages they offer (e.g. simplicity, rapidity, low-cost, sensitivity, multiple toxin detection and portability), it is safe to say that the future of biosensors for the detection of most marine toxins is assured.

In the field of immunosensors for the detection of emerging marine toxins, it is important to keep in mind the difficulty in some cases to obtain the recognition antibodies, since they are not always commercially available and they can be difficult to produce due to the small size of some marine toxins. It is important to mention that the interaction of toxins with antibodies is based on a structural recognition, thus not necessarily related to their toxicity. However, antibodies are robust biorecognition molecules, with high affinity and sensitivity towards their analytes, sometimes being able to detect different analogues of the same group of toxins. Additionally, their easy handling and manipulation allow their integration into different assay formats, offering a wide range of possibilities and configurations using several detection methods.

Aptasensors have been proposed to avoid some of the drawbacks associated with the development of immunosensors, such as the complicated *in vivo* production of antibodies. Aptasensors for PbTX and TTX have been described, demonstrating that the aptamer-based detection methods are promising. Nonetheless, it is necessary to note that the development of aptamers still require the use of toxin standards, which are not always available.

Receptor-based and cell-based biosensors provide a signal related with the toxicity of the toxins. In that sense, these biosensors have the advantage to better reflect the toxic effects that these toxins may cause to *in vivo* models, contrarily to structural-based sensors. However, these approaches do not allow identifying or discriminating compounds different from the target toxins but that share the same mechanism of action. Moreover, cell-based biosensors imply the use of “live” material, a factor that may increase variability in the response.

Biosensors can be considered as effective screening tools to be used in combination with confirmatory instrumental analysis methods to achieve highly specific, sensitive and fast routine monitoring of emerging marine toxins. Research on biosensor development for marine toxins should be focused on elucidating or better describing the mechanisms of action of emerging marine toxins, producing biorecognition molecules, and validating the biosensing systems with naturally-

contaminated samples in order to promote their implementation. To really foster the use of biosensors in food safety and environmental monitoring, compact analysis devices, sensitive, robust, reliable and easy to handle even by non-trained personal are desired. The use of biosensors to detect and quantify emerging marine toxins is being achieved, but the implementation of such devices in daily life still requires a lot of effort. Nevertheless, progress in this area is very fast and, provided the scientific community will focus not only on the development of the bioanalytical systems but also on their validation, biosensors for emerging marine toxins could soon be implemented in routine analysis.

Acknowledgements

The authors acknowledge financial support from the European Union Seventh Framework Programme (FP7/2007-2013) through the ECsafeSEAFOOD project (grant agreement n° 311820) and from the Ministerio de Economía y Competitividad (MINECO) through the DIANA (BIO2011-26311) and the SEASENSING (BIO2014-56024-C2-2-R) projects. Sandra Leonardo and Laia Reverté acknowledge IRTA – Universitat Rovira i Virgili – Banco Santander and the ECsafeSEAFOOD project, respectively, for their PhD grants.

References

Alfonso A, Pazos MJ, Fernández-Araujo A et al (2014) Surface plasmon resonance biosensor method for palytoxin detection based on Na^+, K^+-ATPase affinity. Toxins 6:96-107

Aligizaki K, Katikou P, Milandri A et al (2011) Occurrence of palytoxin-group toxins in seafood and future strategies to complement the present state of art. Toxicon 57:390-399

Anderson PD (2012) Bioterrorism: Toxins as weapons. J Pharm Pract 25:121-129

Bane V, Lehane M, Dikshit M et al (2014) Tetrodotoxin: chemistry, toxicity, source, distribution and detection. Toxins 6:693-755

Barroso GP, Rueda P, Parron CT et al (2008) An epidemic outbreak with respiratory symptoms in the province of Almeria (Spain) due to toxic microalgae exposure]. Gac Sanit 22(6):578–84.

Campbell K, Barnes P, Haughey SA et al (2013) Development and single laboratory validation of an optical biosensor assay for tetrodotoxin detection as a tool to combat emerging risks in European seafood. Anal Bioanal Chem 405:7753-7763

Campbell K, McNamee SE, Huet AC et al (2014) Evolving to the optoelectronic mouse for phycotoxin analysis in shellfish. Anal Bioanal Chem 406:6867-6881

Carter RM, Poli MA, Pesavento M et al (1993) Immunoelectrochemical biosensors for detection of saxitoxin and brevetoxin. Immunomethods 3(2): 128-133.

Charkhkar H, Knaack GL, Gnade BE et al (2012) Development and demonstration of a disposable low-cost microelectrode array for cultured neuronal network recording. Sensor Actuat B-Chem 161:655-660

Cheun B, Endo H, Hayashi T et al (1996) Development of an ultra high sensitive tissue biosensor for determination of swellfish poisoning, tetrodotoxin. Biosens Bioelectron 11:1185-1191

CRLMB (2005) Report on toxicology working group meeting. CRLMB: Cesenatico, Italy, 24–25 October 2005; p 24-25

Eissa S, Siaj M, Zoroub M (2015) Aptamer-based competitive electrochemical biosensor for brevetoxin-2. Biosens Bioelectron 69:148-154

EFSA (2009) Scientific opinion on marine biotoxins in shellfish – Palytoxin group. EFSA J 7(12):1393

EFSA (2010a) Scientific opinion on marine biotoxins in shellfish – Emerging toxins: Ciguatoxin group. EFSA J 8(6):1627

EFSA (2010b) Scientific opinion on marine biotoxins in shellfish: Cyclic imines (spirolides, gymnodimines, pinnatoxins and pteriatoxins). EFSA J 8(6):1628

EFSA (2010c) Scientific opinion on marine biotoxins in shellfish-Emerging toxins: Brevetoxin group. EFSA J 8(7):1677

Fomo G, Waryo TT, Sunday CE et al (2015) Aptameric recognition-modulated electroactivity of poly(4-styrenesolfonic acid)-doped polyaniline films for single-shot detection of tetrodotoxin. Sensors 15:22547-22560

FSANZ (Food Standards Australia New Zealand) (2010). Food standard code, incorporating amendments up to and including amendment 116, standard 4.1.1, primary production and processing standards, preliminary provisisons, Standard 1.4.1, contaminants and natural toxicants, issue 111. http://www.foodstandards.gov.au/_srcfiles/Standard_1_4_1_Contaminants_v113.pdf. Accessed 29 October 2015.

Hilgemann DW (2003) From a pump to a pore: how palytoxin opens the gates. Proc. Natl. Acad. Sci. USA 100:386-388

Kreuzer MP, Pravda M, O'Sullivan CK et al (2002) Novel electrochemical immunosensors for seafood toxin analysis. Toxicon 40:1267-1274

Kruger CL, Reddy CS, Conze DB et al (2014) Food safety and foodborne toxicants. In: Hayes W, Kruger C L (ed) Hayes' principles and methods of toxicology, 6th edn. Boca Raton, FL: CRC Press, p 621-675

Kulagina NV, Mikulski CM, Gray S et al (2006) Detection of marine toxins, brevetoxin-3 and saxitoxin, in seawater using neuronal networks. Environ Sci Technol 40:578-583

Lin Y, Zhou Q, Lin Y et al (2012) Mesoporous carbon-enriched palladium nanostructures with redox activity for enzyme-free electrochemical immunoassay of brevetoxin B. Anal Chim Acta 887:67-74

Mouri R, Oishi T, Torikai K et al (2009) Surface plasmon resonance-based detection of ladder-shaped polyethers by inhibition detection method. Bioorg med Chem Lett 19:2824-2828

Neagu D, Micheli L, Palleschi G (2006) Study of a toxin-alkaline phosphatase conjugate for the development of an immunosensor for tetrodotoxin determination. Anal Bioanal Chem 385:1068-1074

NZFSA (New Zealand Food Safety Authority) (2006) Animal products (specification for bivalve molluscan shellfish. http://www.nzfsa.govt.nz/animalproducts/legislation/notices/animal-materialproduct/shellfish/bmsrcsspecv-16_2_signed.pdf. Accessed 29 October 2015.

OPCW (2015) Toxins. Potential chemical weapons from living organisms. http://www.opcw.org/about-chemical-weapons/types-of-chemical-agent/toxins/. Accessed 28 October 2015

Pancrazio J, Gray SA, Shubin YS et al (2003) A portable microelectrode array recording system incorporating cultured neuronal networks for neurotoxin detection. Biosens Bioelectron 18:1339-1347

Pfannkuchen M, Godrijan J, Pfannkuchen DM (2012) Toxin-producing *Ostreopsis* cf. *ovata* are likely to bloom undetected along coastal areas. Environ Sci Technol 46:5574-5582

Reverté L, Soliño L, Carnicer O et al (2014) Alternative methods for the detection of emerging marine toxins: biosensors, biochemical assays and cell-based assays. Mar Drugs 12:5719-5763

Tang D, Tang J, Su B et al (2011) Gold nanoparticles-decorated amine-terminated poly(amidoamine) dendrimer for sensitive electrochemical immunoassay of brevetoxins in food samples. Biosens Bioelectron 26:2090-2096

Tang D, Zhang B, Tang J et al (2013) Displacement-type quartz crystal microbalance immunosensing platform for ultrasensitive monitoring of small molecular toxins. Anal Chem 85:6958-6966

Tang J, Hou L, Tang D et al (2012) Magneto-controlled electrochemical immunoassay of brevetoxin B in seafood based on guanine-functionalized graphene nanoribbons. Biosens Bioelectron 38:86-93

Taylor AD, Ladd J, Etheridge S et al (2008) Quantitative detection of tetrodotoxin (TTX) by a surface plasmon resonance (SPR) sensor. Sensor Actuat B-Chem 130:120-128

Taylor AD, Vaisocherová H, Deeds J et al (2011) Tetrodotoxin detection by a surface plasmon resonance sensor in pufferfish matrices and urine. J Sens doi:10.1155/2011/601704

US FDA (United States Food and Drug Administration) (2001) Fish and fisheries products hazards and controls guidance, 3rd edn. appendix 5 - FDA & EPA Safety levels in regulations and guidance. http://www.fda.gov/Food/GuidanceComplianceRegulatoryInformation/GuidanceDocuments/Seafood/ucm091782.htm. Accessed 29 October 2015.

Vaisocherová H, Taylor AD, Jiang S et al (2011) Surface plasmon resonance biosensor for determination of tetrodotoxin: Prevalidation study. J AOAC Int 94:596-604

Volpe G, Cozzi L, Migliorelli D et al (2014) Development of a haemolytic-enzymatic assay with mediated amperometric detection for palytoxin analysis: application to mussels. Anal Bioanal Chem 406:2399-2410

Wang Q, Fang J, Cao D et al (2015a) An improved functional assay for rapid detection of marine toxins, saxitoxin and brevetoxin using a portable cardiomyocyte-based potential biosensor. Biosens Bioelectron 72:10-17

Wang Q, Su K, Hu L et al (2015b) A novel and functional assay for pharmacological effects of marine toxins, saxitoxin and tetrodotoxin by cardiomyocyte-based impedance biosensor. Sensor Actuat B-Chem 209:828-837

Yakes B J, Deeds J, White K et al (2011b) Evaluation of surface plasmon resonance biosensors for detection of tetrodotoxin in food matrices and comparison to analytical methods. J Agric Food Chem 59:839-846

Yakes B, DeGrasse S, Poli M et al (2011a) Antibody characterization and immunoassays for palytoxin using an SPR biosensor. Anal Bioanal Chem 400:2865-2869

Yakes B, Kanyuck K, DeGrasse SL (2014) First report of a direct surface plasmon resonance immunosensor for a small molecule seafood toxin. Anal Chem 86: 9251-9255

Zamolo VA, Valenti G, Venturelli E et al (2012) Highly sensitive electrochemiluminescent nanobiosensor for the detection of palytoxin. ACS Nano 6:7989-7997

Zhang B, Hou L, Tang D et al (2012) Simultaneous multiplexed stripping voltammetric monitoring of marine toxins in seafood based on distinguishable metal nanocluster-labeled molecular tags. J Agric Food Chem 60:8974-8982

UNIVERSITAT ROVIRA I VIRGILI
DEVELOPMENT AND APPLICATION OF COLORIMETRIC ASSAYS AND ELECTROCHEMICAL BIOSENSORS IN SEAFOOD SAFETY
Sandra Leonardo Benet

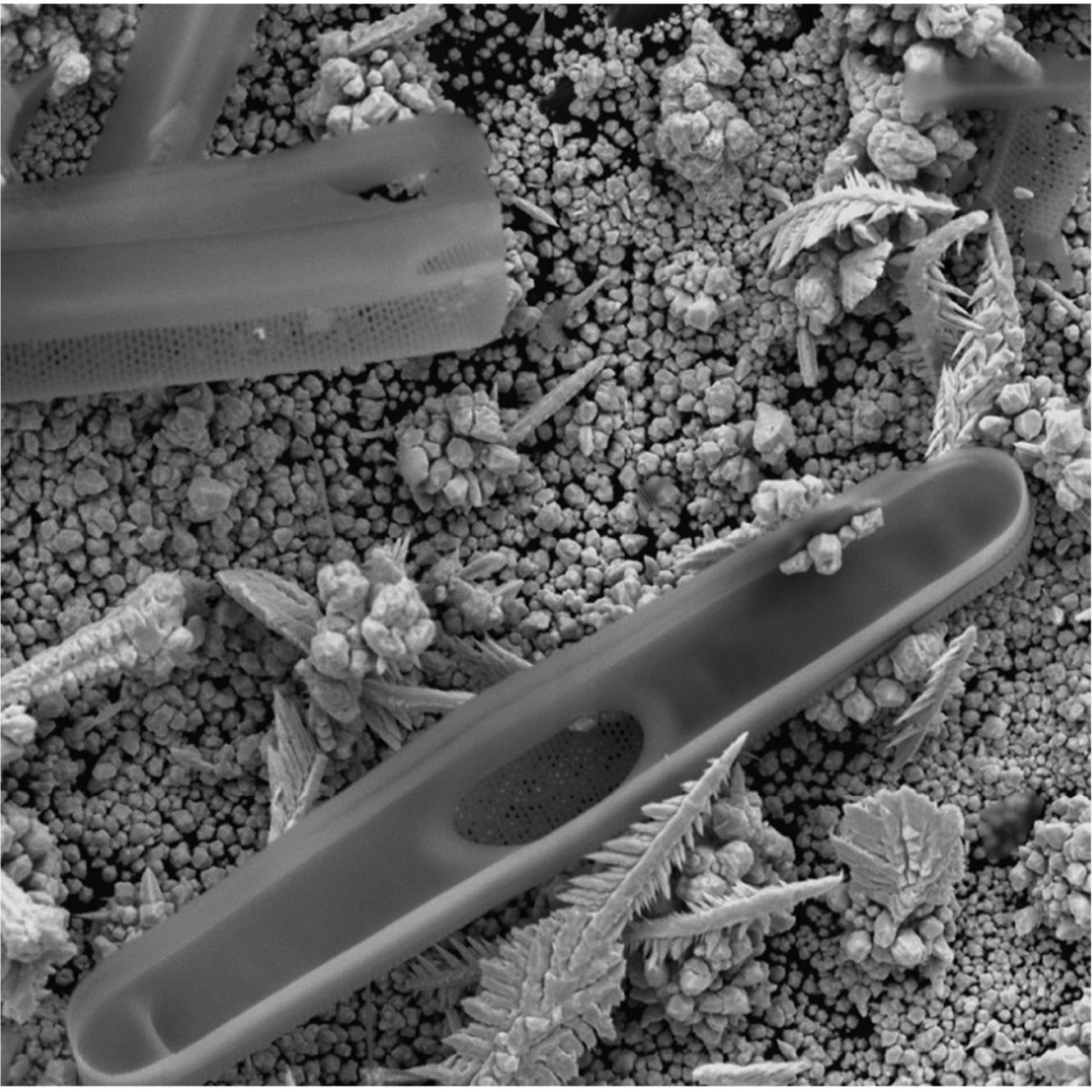

IRTA
RECERCA | TECNOLOGIA AGROALIMENTÀRIES

UNIVERSITAT ROVIRA i VIRGILI

Santander